Final report

Particulate matter formation potential of gas-phase emissions over Germany

by:

Ruud Janssen, Leon Geers, Richard Kranenburg,
Peter Coenen, Martijn Schaap

TNO, Utrecht

Umwelt Bundesamt

Final report

Particulate matter formation potential of gas-phase emissions over Germany

by
Ruud Janssen, Leon Geers, Richard Kranenburg,
Peter Coenen, Martijn Schaap

TNO, Utrecht

Imprint

Abstract: Particulate matter formation potential of gas-phase emissions over Germany

Particulate matter (PM) is the air pollutant that is responsible for the highest burden of disease in Germany and other European countries. Therefore, measures are needed to reduce its ambient concentrations, but a large proportion of PM is not emitted directly: it is formed from gaseous precursors in the atmosphere. Hence, there is an urgent need to assess the contribution of gaseous emissions to the concentration of secondary inorganic and organic aerosol particles (SIA and SOA, respectively). The main objective of this project is to derive factors for the PM formation potential of gaseous emissions in order to assess the consequences of emission reductions for the atmospheric PM load and the derived exposure.

For this purpose, the *formation factor (FF)* is applied. It indicates the change in concentration of a certain PM component resulting from a change in its (precursor) emissions. The *intake factor (IF)* was applied to assess the change of population exposure of a certain PM component resulting from changes in its (precursor) emissions. The report also discusses the reasoning to use this approach compared to other methodologies to quantify PM formation from gaseous precursors.

LOTOS-EUROS is used as the chemical transport model (CTM) to describe the formation, transport and removal from the atmosphere of (secondary) particulate matter. The most important pathways of SIA formation are known. For organic aerosol, the level of process understanding is relatively low, although a lot of progress has been made over the last years. With LOTOS-EUROS, we performed reference simulations for SIA and OA, yielding annual mean SIA concentration of 5.5 µg/m^3 and annual mean OA concentration of 1 µg/m^3 OA over Germany in 2018. Nitrate and primary organic aerosol (POA) appear to contribute the largest mass fraction to SIA and OA levels across Germany, respectively. POA concentrations are underestimated despite the inclusion of condensable PM emissions. Based on these reference runs, emission reduction scenarios were performed for (precursor) species and specific sectors. SIA and OA concentrations were found to be most sensitive to reductions in Agriculture and Residential Combustion, respectively. The species that mostly account for these reductions are NH_3 for Agriculture and POA for Residential combustion. The species reduction scenarios gave FFs for SIA of about 0.001 µg m^{-3} kTon^{-1}, against about 0.006 µg m^{-3} kTon^{-1} for SOA. As for PPM this number is about 0.01 µg m^{-3} kTon^{-1}, this means that 1 kTon of NO_x emissions from a certain sector leads to a roughly tenfold smaller PM formation than 1 kTon of PPM emission. Calculated SIA intake factors for all precursors (NO_x, SO_2, and NH_3) were around 0.3 x 10^{-6} kg/kg, versus 4 x 10^{-6} kg/kg for OA, which is in line with the literature. Further, we found that the FF and IF are not very sensitive to model resolution at the resolutions that we applied in this study (7x7 versus 2x2 km^2) and interannual variability.

Finally, a toolkit was developed to enable FF and IF calculations from simulation data and to estimate the SIA formation potential for alternative emission reduction scenarios without using the results of the CTM directly.

Kurzbeschreibung: Bewertung des Feinstaubbildungspotenziales gasförmiger Emissionen für Deutschland

Feinstaub (PM) ist der Luftschadstoff, der in Deutschland und anderen europäischen Ländern für die höchste Krankheitslast verantwortlich ist. Deshalb sind Maßnahmen erforderlich, um die Feinstaubkonzentration in der Luft zu senken. Ein großer Teil des Feinstaubs wird jedoch nicht direkt emittiert, sondern aus gasförmigen Vorläufersubstanzen in der Atmosphäre gebildet. Daher ist es dringend notwendig, den Beitrag gasförmiger Emissionen (NO_x, SO_2, NH_3 und organische Stoffen) zur Konzentration sekundärer anorganischer und organischer

Aerosolpartikel (SIA bzw. SOA) zu ermitteln. Das Hauptziel dieses Projekts ist es, Faktoren für das PM-Bildungspotenzial gasförmiger Emissionen abzuleiten, um die Folgen von Emissionsminderungen für die atmosphärische PM-Belastung und die daraus abgeleitete Exposition zu bewerten.

Zu diesem Zweck wird der Bildungsfaktor (FF) verwendet. Er gibt die Veränderung der Konzentration einer bestimmten PM-Komponente an, die sich aus einer Veränderung ihrer (Vorläufer-)Emissionen ergibt. Der Aufnahmefaktor (IF) wurde angewandt, um die Veränderung der Exposition der Bevölkerung gegenüber einer bestimmten PM-Komponente aufgrund von Veränderungen ihrer (Vorläufer-)Emissionen zu bewerten. In dem Bericht werden auch die Gründe für die Verwendung dieses Ansatzes im Vergleich zu anderen Methoden zur Quantifizierung der PM-Bildung aus gasförmigen Vorläufersubstanzen erörtert.

LOTOS-EUROS wird als chemisches Transportmodell (CTM) verwendet, um die Bildung, den Transport und den Abtransport von (sekundärem) Feinstaub aus der Atmosphäre zu beschreiben. Die wichtigsten Wege der SIA-Bildung sind bekannt. Für organisches Aerosol ist das Prozessverständnis relativ gering, obwohl in den letzten Jahren große Fortschritte gemacht wurden.

Mit LOTOS-EUROS haben wir Referenzsimulationen für SIA und OA durchgeführt, die im Jahresmittel eine SIA-Konzentration von 5,5 µg/m^{-3} und eine OA-Konzentration von 1 µg/m^{-3} OA über Deutschland im Jahr 2018 ergaben. Nitrat und primäres organisches Aerosol (POA) tragen in ganz Deutschland den größten Massenanteil zur SIA- bzw. OA-Konzentration bei. Die POA-Konzentrationen werden trotz der Einbeziehung der kondensierbaren PM-Emissionen unterschätzt.

Auf der Grundlage dieser Referenzläufe wurden Emissionsminderungsszenarien für (Vorläufer-)Substanzen und bestimmte Sektoren durchgeführt. Es wurde festgestellt, dass die SIA- und OA-Konzentrationen am empfindlichsten auf Emissionsminderungen in der Landwirtschaft bzw. bei der Verbrennung in Haushalten reagieren. Die Substanzen, die am stärksten für diese Verringerungen verantwortlich sind, sind NH_3 in der Landwirtschaft und POA bei der Verbrennung in Wohngebäuden.

Die Reduktionsszenarien ergaben FFs für SIA von etwa 0,001 µg m^{-3} kt^{-1}, für SOA dagegen von etwa 0,006 µg m^{-3} kt^{-1}. Für PPM liegt diese Zahl bei etwa 0,01 µg m^{-3} kt^{-1}. Das bedeutet, dass 1 kt NO_X-Emissionen aus einem bestimmten Sektor zu einer etwa zehnmal geringeren PM-Bildung führt als 1 kt PPM-Emission. Die berechneten SIA-Aufnahmefaktoren für alle Vorläuferstoffe (NO_X, SO_2 und NH_3) lagen bei etwa 0,3 x 10^{-6} kg/kg gegenüber 4 x 10^{-6} kg/kg für OA, was mit der Literatur übereinstimmt. Außerdem haben wir festgestellt, dass die FF und IF bei den in dieser Studie verwendeten Auflösungen (7x7 km^2 gegenüber 2x2 km^2) und der interannuellen Variabilität nicht sehr empfindlich auf die Modellauflösung reagieren.

Schließlich wurde ein Toolkit entwickelt, um FF- und IF-Berechnungen aus Simulationsdaten zu ermöglichen und das SIA-Bildungspotenzial für alternative Emissionsminderungsszenarien abzuschätzen, ohne die Ergebnisse des CTM direkt zu verwenden.

Table of content

List of figures

List of tables

List of acronyms

API	Application Programming Interface
aSOA	SOA from Anthropogenic NMVOC
bSOA	SOA from Biogenic NMVOC
CTM	Chemical Transport Model
EU	European Union
FF	Formation Factor
HDV	Heavy Duty Vehicles
IF	Intake Factor
IVOC	Intermediate Volatility Organic Compound
LDV	Light Duty Vehicles (in this study including passenger cars)
LE	LOTOS-EUROS
MSECV	Mean Squared Error of Cross-Validation
NEC	National Emissions reduction Commitments
NMVOC	Non-methane Volatile Organic Compound
OA	Organic Aerosol
OC	Organic Carbon
PLS(R)	Partial Least Squares (Regression)
PM	Particulate Matter
POA	Primary Organic Aerosol
PPM	Primary Particulate Matter
RWC	Residential Wood Combustion
SIA	Secondary Inorganic Aerosol
siSOA	SOA from SVOC and IVOC
SOA	Secondary Organic Aerosol
SPM	Secondary Particulate Matter
SVOC	Semi-volatile Organic Compound
VBS	Volatility Basis Set
VOC	Volatile Organic Compound

Summary

Aim of the project

Particulate matter (as $PM_{2.5}$ or PM_{10}) is the air pollutant that is responsible for the highest burden of disease attributed to air pollution in Germany as well as in other European countries. Therefore, measures to reduce the ambient concentrations of particulate matter are of particular importance. Such measures usually start on the emission side. It is crucial to reduce emissions in an efficient manner and to optimise the measures in a way that maximises health benefits. A major challenge in prioritizing mitigation options, however, is that a large proportion of PM is not emitted directly, but is formed from gaseous precursors in the atmosphere. Therefore, there is an urgent need to assess the contribution of gaseous emissions to the concentration of secondary inorganic aerosol and organic aerosol particles (SIA and OA, respectively) in Germany. This quantification requires the use of a chemical transport model (CTM), which includes the emissions of all relevant gases, their chemical transformation, mixing in the atmosphere and the removal of these gases and their reaction products. The main objective of this project is to derive factors for the PM formation potential of gaseous emissions in order to assess the consequences of emission reductions, of both gaseous precursors and directly emitted PM, for the atmospheric PM load and for the derived exposure over Germany. These factors are then applied in a toolkit that enables the estimation of the effect of emission reduction scenarios of gaseous precursors on SIA concentration without the need for additional CTM simulations. This project has been performed by TNO, starting in October 2019 and ending in October 2022.

To achieve this main objective several research questions have been defined:

► What is the current understanding of the processes that cause the formation and concentration of secondary aerosols in the atmosphere?

► How well does TNO's CTM LOTOS-EUROS capture these processes compared to the state of the process knowledge, and compared to observations and other models?

► What is the most appropriate indicator of the PM formation potential of gaseous emissions?

► To what extent do emission reductions of gaseous precursors affect the concentration of particulate matter in the atmosphere over Germany? Do these factors differ depending on the emitting sector and compound? And what effects do these reductions have on PM exposure?

► What effects do spatial and temporal variations in emissions have on the PM formation potential? How sensitive are the obtained PM reduction factors to uncertainties in model processes and parameters, to meteorological variations, and to the resolution of the model?

► What are the requirements for a screening tool that can effectively support the mitigation of PM pollution?

There are two factors relevant in this research: formation of PM and exposure to PM. The first step in this project was to search the literature for indicators that could be applied in the calculation of the formation and intake (i.e. the amount of PM inhaled by the population) of PM from gaseous precursors. The goal of the literature study was to identify the different available approaches, and to choose the most appropriate one to be applied in this project. We chose to use the Formation Factor (FF) as the indicator for the conversion from gaseous emissions to secondary PM (Van Zelm et al., 2008; Thunis and Clappier, 2014). The FF is a variable that quantifies the relationship between emissions of a pollutant (or pollutant precursor) and the

concentration of a pollutant. For primary PM, this relationship between emission and concentration is linear: an emission reduction leads to a concentration reduction that is proportional to that emission reduction. For secondary PM, however, the relation is non-linear, because of the role of chemistry and deposition of the precursors. As the indicator for exposure, we adopted the intake factor (IF) from Van Zelm et al. (2008). The IF is calculated by multiplying the FF by the volume of air breathed in by the population in a given area and can be interpreted as the mass of PM inhaled per mass emitted PM (precursor).

The quantification of both FF and IF require the use of a CTM. The CTM takes into account the emissions of all relevant gases, their chemical transformations and mixing in the atmosphere and the removal of these gases and their reaction products. The LOTOS-EUROS CTM enabled us to derive the relationships between emissions of precursors and primary PM, and the modelled concentration. With the LOTOS-EUROS labelling technique it was also possible to quantify emission source contributions from various sectors and/or regions within Germany.

Primary PM factors

Even though primary PM is emitted in particulate form already, there are several factors that determine the relationship between its emission and concentration for a region and/or sector, and therefore its formation factor (FF). These factors include the emission height, temporal emission variability, meteorological conditions. The intake factor (IF) of primary PM is further affected by the degree of spatial co-location of population centres and emissions. To gain insight in these factors, which play a role for secondary PM as well, we first calculated the FF and the IF for primary PM from labelled LOTOS EUROS model simulations. The first aim was to answer two questions for primary PM:

► In how far do the formation factors vary between sectors and regions?

► How do these formation factors translate into the population intake factor?

We answer these questions through labelled model simulations in which the emissions of 30 sectors and regions (or combinations thereof) are traced. The results of simulations of primary PM concentrations over a period of 4 years (2015-2018) at a resolution of 7x7 km^2 have been analysed. In addition, a simulation for a 1 year period (2015) at a high resolution of 2x2 km^2 was performed. Although the absolute emissions and source contributions vary largely between sectors, the formation factor shows a relatively even distribution between the labeled sources. Residential combustion has the highest FF, which can be attributed to the above average emissions during cold and stable conditions in winter which do not favor dilution. Other sectors that show high FF for the different federal states all have emissions close to ground level. The FFs for large plants in the industrial and power sectors are systematically lower than those of the surface emission source sectors, because the emissions occur above the mixing layer for a substantial part of the year. The IF for residential combustion is the highest, followed by road transport – light duty vehicles and passenger cars. Both sectors emit close to where people live, which leads to these high IFs. In contrast, the IFs for the agriculture-related labels are low, because this mostly takes place in remote regions. The difference in FF and IF between the 7x7 km^2 and 2x2 km^2 resolution simulations is low (<5%), which indicates that the coarser resolution suffices for the calculation of robust indicators on an annual basis. Moreover, the calculated interannual variability in FF and IF is low over all labels, and caused by differences in meteorology.

Secondary PM – formation (SIA)

Secondary inorganic aerosol (SIA) and organic aerosol (OA) formation includes processes of formation, chemical transformation, transport and removal from the atmosphere. Secondary inorganic aerosols (SIA) are aerosols that are produced in the atmosphere from reactions involving primary or secondary inorganic gases (Ansari and Pandis, 1998). Salts of ammonium (NH_4^+), nitrates (NO_3^-) and sulfates (SO_4^{2-}), form the major part of SIA composition (Putaud et al., 2010). They are formed by oxidation of NO_x and SO_2 to nitric and sulfuric acid, respectively, and subsequent neutralization by ammonia. Several reaction pathways in both gas and aqueous phases contribute to the formation of the acids. The efficiency of the reaction pathways is controlled by the availability of the reactants, temperature and relative humidity, as well as pH for aqueous phase reactions.

While ammonium sulphate is non-volatile, ammonium nitrate is a semi-volatile component (Nenes et al., 1999). The latter will maintain an equilibrium with its gaseous counterparts. At high temperatures, i.e. in summer, much more ammonia will be needed to arrive at the same ammonium nitrate concentration than in winter. Therefore, ammonium nitrate concentrations show a strong seasonal signature in most regions, including Germany. For sulphate, current models report an underestimation compared to observed particulate sulphate concentrations in Europe, China and North-America, possibly due to missing SO_2 oxidation pathways.

Dry deposition is the direct removal of atmospheric gases and particles by vegetation, soils, or surface waters (Fowler et al., 2007). The dry deposition flux of trace gases depends on the surface concentrations and the dry deposition velocity. Note that for ammonia the surface-atmosphere exchange is bi-directional, i.e. NH_3 can be re-emitted from surfaces into the atmosphere. Further, the dry deposition velocities of NH_3 and SO_2 are connected (Fowler et al., 2001), because the pH of the fluids in the system determines the rate in which either gas is dissolved. This pH dependence also affects the wet deposition of these gases.

Emission reductions of precursor gases may lead to shifts in the chemical regimes which affect the formation, residence time and removal of sulphur and nitrogen compounds (Banzhaf et al., 2013). This can result in a non-linear response of the SIA concentrations in the atmosphere (Fagerli and Aas, 2008). The impact of the complex interactions varies seasonally and regionally over Europe with changing emission regime. Among emission changes of SO_2, NO_x and NH_3, responses to NH_3 emission changes show the largest non-linear behavior (Tarrasón et al., 2005).

Secondary PM – formation (OA)

Organic aerosol comprises all particulate matter in the atmosphere that consists of organic molecules. The most common way of grouping the many individual compounds that exist is based on their volatility. For the definition of non-methane volatile organic compounds (NMVOC), semi-volatile organic compounds (SVOC) and intermediate volatility organic compounds (IVOC), we refer to the naming convention for atmospheric organic aerosol as suggested by Murphy et al. (2014). Primary organic aerosol (POA) is organic material that is emitted as aerosol under atmospheric conditions, but partly evaporates after emission. So POA is semi-volatile, but how much of it will evaporate depends on the atmospheric conditions. SOA, in contrast, is the organic aerosol that is formed in the atmosphere from a VOC after one or more generations of oxidation. Therefore, it includes OA formed from both NMVOCs, such as toluene and monoterpenes, which have traditionally been seen as SOA precursors, as well as the SVOC and IVOC that originate from the evaporation of POA.

SOA is formed from two main categories of organic compounds that are separate species in emission inventories: 1) the part of the POA emissions (which themselves are a fraction of $PM_{2.5}$

emissions) that enters the gas phase after emission as primary SVOC, 2) NMVOC, which are completely in the gas phase just after emission. In addition, IVOC are not routinely included in emission inventories, but are usually added to models as a fixed faction of the POA emissions. SVOC, IVOC and NMVOC are subject to oxidation in the atmosphere and subsequently form products with lower volatilities. These secondary S/IVOC species will then partition between the gas and the particulate phase. Organic compounds in the atmosphere can occur in the gas and in the particle phase and move from one phase to the other due to several chemical and physical processes (Safieddine et al., 2017), with an atmospheric lifetime between days and weeks. The fate of the S/IVOC depends on the phase to which it partitions. In the gas-phase it will be subject to oxidation, mainly by the OH radical (Ma et al., 2017; Shrivastava et al., 2008). Dry and wet deposition are other important loss processes for SVOC. Wet deposition is the most efficient deposition mechanism for SOA (Knote et al., 2015), while dry deposition only has a minor effect. With regard to the sources of OA over Europe, the picture that emerges from the literature is that biogenic and residential wood combustion (RWC) emissions are the main sources of OA in summer and winter, respectively. Road transport forms a minor contribution overall, but may be important in urban areas. In terms of the potential for reducing OA concentrations over Europe, the semi-volatile POA emissions seem the most promising, especially those from RWC.

Secondary PM factors

We ran with LOTOS-EUROS to determine the formation and intake factors for secondary PM, including a set of more advanced emission datasets than in the simulation that we used for the primary PM. The main reason for using new emission datasets is the recent availability of datasets that include the emission of condensable species, which can form a significant contribution to modelled (in)organic aerosol. For the European domain, this concerns the CAMS 5.1 REF2 emission dataset for the year 2018, which includes condensables from RWC. For Germany, we use a recently developed GRETA dataset (year 2018, submission 2022) that includes condensables from all sources. IVOC emissions are added to that, using an approach that is commonly used in CTM calculations of SOA formation: by assuming that IVOC scale with semi-volatile POA emissions by a factor 1.5 for all sectors.

LOTOS-EUROS includes modules that represent the formation of secondary PM: the thermodynamic SIA module ISORROPIA-II (Fountoukis and Nenes, 2007) scheme is applied to calculate the temperature and relative humidity dependent thermodynamic equilibrium between gaseous nitric acid, sulphuric acid, ammonia and particulate ammonium nitrate and ammonium sulphate and aerosol water. The Volatility Basis Set (VBS; Donahue et al., 2006) describes the formation of OA through pas/particle partitioning. It accounts for the formation of SOA from NMVOCs and semi-volatile POA.

Annual mean modelled concentrations of sulfate, nitrate and ammonium and its precursors across in the Reference simulation show that the gradients of the SIA compounds are much smaller than those of their primary emitted precursors. This is explained by the effect of atmospheric chemistry involved in SIA formation and the time scale at which this takes place. Nitrate contributes the largest mass fraction to SIA levels across Germany. Nitrate concentrations do not peak in the regions with the largest NO_x emissions, but in those with the largest ammonia concentrations. The reason is found in the semi-volatile nature of ammonium nitrate: with a larger ammonia concentration a larger amount of nitric acid is driven into the aerosol phase. Ammonium neutralizes both sulfate and nitrate leading to a field that shows a large correspondence with the nitrate concentration levels, albeit with less distinct gradients.

SIA over Germany consists of an amount of ammonium sulphate and almost 5 times as much ammonium nitrate. Without accounting for interdependencies, sulphate source contributions are dominated by Industry and Energy, nitrate concentrations are attributed to Traffic (~1/3 of the part originating from Germany) and comparable shares from Energy, Industry, Agriculture and Natural sources. Ammonium originates from ammonia, almost exclusively produced in Agriculture as mentioned.

To enable assessment of the effects of emission reductions on the average concentrations of SIA, a number of simulations were performed for different reduction scenarios. Emission reductions in a single sector may impact the formation of SIA in another sector. For example, when agricultural ammonia emissions are reduced by 40%, the pH dependencies in the formation of sulfate may change, impacting the amount of SO_2 converted into sulphate from the energy sector. Hence, to investigate the sensitivity of the SIA concentrations, the sector dependent formation factors and the cross sector dependencies the following scenarios were performed:

► Precursor reductions: 20, 40 and 60% reduction for NO_x, SO_2, and NH_3 in all sectors

► Sector reductions: three sets of 20, 40, 60% reductions of all emissions originating from a single sector, i.e. Traffic, Residential combustion and Agriculture

► NEC scenario: what are the formation factors for each sector under a realistic emission reduction scenario?

In each scenario the labelling approach was used to track the contribution of a sector in that scenario. The modelled concentration distributions were averaged to a mean value over the whole country for the year 2018. The emission distributions were integrated over the country and the same period to arrive at total annual emission numbers.

The species reduction scenarios show that the main effect of reducing the precursor is on their respective products (viz. NO_x to $NO^-_{3,a}$, SO_2 to $SO^{2-}_{4,a}$ and NH_3 to $NH^+_{4,a\,f}$). The same relative reduction on NO_x and NH_3 has a larger impact than the reduction in SO_2 emission, which reflects the lower importance of sulphate in the total SIA mass. Surprisingly, the reduction of NO_x and NH_3 have an almost equal effect on the sum of the domestic SIA concentration. This seems to be a double effect, since the reduction in either of them also reduces the other. Most likely, this strong correlation is caused by the volatility of ammonium nitrate. For each reduction scenario the FFs for all sectors were calculated and compared. Regions of high nitrate concentrations line up with regions of high ammonia emissions due to the semi-volatile nature of ammonium nitrate. This, combined with the fact that ammonium nitrate is the predominant constituent of SIA in Germany, explains the higher formation factor for SIA/NH_3 (in Agriculture, mainly emitting NH_3), compared to SIA/NO_x (in Traffic, mainly emitting NO_x).

Simulations where reductions are effected for all species in a whole sector provide the possibility to investigate the overall effect of sector wide reductions and it shows the effect of reductions in one sector on concentrations of SIA generated in another sector. However, care should be taken in analysing these data. Because the reductions are effected on *all species* emitted in the sector, the formation factor of SIA over a single emitted species can be misleading since it is not the only species that is reduced. A third way to look at the consistency in formation factors is to compare the FFs in a relevant future scenario to those calculated for the present day. For this purpose we took existing NEC scenario calculations in which the emissions of all European countries were scaled to their respective ceiling in 2030. The FFs formation factors of SIA on its precursors are similar to the factors presented for the single species reduction scenarios, except for SIA/SO_2 which is approximately twice as high. This may have to do with the

fact that the NEC scenario is a complex combination of different reduction measures for all emissions in many sectors and the non-linear effects of the SIA formation mechanism. Finally, as a precursor to the investigation of health effects of the intake of SIA species, the total annual intake and intake factors were calculated. The overall picture of the intake factors is that they look very similar to the formation factors. This is most likely caused by the fact that the same concentrations are used for both calculations, but the IF is weighted by population density. Hence, in the IF calculation densely populated areas are emphasized.

The simulations of the OA show that both semi-volatile POA and NMVOC emissions contribute to anthropogenic OA formation. The yearly mean modelled concentration of total OA across Germany is about 1 µg m^{-3}. POA forms about half of the OA concentration with 0.52 µg m^{-3}. POA is formed mainly in winter when its emissions have a maximum and when atmospheric mixing is suppressed. Originating from the same emission sources as POA is siSOA, but its contribution is about a factor of 3 lower. This is due to the fact that most POA emissions take place in winter when photochemistry is slow, which prohibits the oxidation of the semi-volatile organic vapors which lead to SOA formation, and when temperatures are low, which favors the partitioning of the semi-volatile emissions to the particle phase. Anthropogenic SOA, which is formed by the oxidation of NMVOC contributes only a small part of the total OA over Germany (0.04 µg m^{-3}), due to the inefficient conversion of its precursors, the anthropogenic NMVOC. The contribution of biogenic SOA is significant on the annual average (0.26 µg m^{-3}), but shows a clear peak in summer when it is the dominant OA contributor over Germany. This suggests that there is a significant part of OA which cannot (or only indirectly) be controlled by emission reduction policies. As for the validation of these results, the model shows an underestimation by a factor ~5 compared to organic carbon observations at the few monitoring stations that are available for OA and its precursors.

To enable assessment of the effects of emission reductions on the average concentrations of OA, a number of simulations were performed with different reduction scenarios for anthropogenic POA and NMVOC emissions. Further, there are specific sectors which emit large quantities of POA, so reducing emissions from these sectors has potentially a strong effect on OA concentration reductions. Therefore, we performed the following set of simulations:

► Precursor reductions: 20, 40 and 60% reduction of POA and NMVOC emissions in all sectors

► Sector reductions: 20, 40, 60% reductions of all emissions originating from a single sector, i.e. Residential combustion and Traffic

The outcomes of the reduction scenarios show that reducing POA emissions is more effective for reducing OA concentrations than reducing NMVOC emissions. For instance, a POA emission reduction of 20% leads to a decrease of total OA by 8% (POA concentration decreases by 14% and siSOA by 4%). NMVOC reductions only have a minor influence on total OA concentrations (for instance, a 20% emission reduction leads to a 0.3% OA concentration reduction), resulting from a small decrease in aSOA concentration. In the sector reduction scenarios, the effects of reducing Residential combustion and Traffic emissions are very similar to the species reduction scenarios, since Residential combustion emissions mainly consist of POA and Traffic emissions of NMVOC. The FF for OA/POA has a value of over 0.006 µg m^{-3} kTon^{-1}, which is high compared to that of other species. This is caused by the fact that POA formation results from a fast physical process, i.e. gas/particle partitioning of SVOCs. The FF of OA/NMVOC is about 2 orders of magnitude lower than that of OA/POA. This further illustrates the limited role that NMVOC play in OA formation over Germany as a whole. OA/POA formation factors for Residential combustion emission reductions are about 0.009 µg m^{-3} kTon^{-1}. In the Reference scenario, the total annual

intake of OA is about 440 kg for the German population as a whole. The IFs of OA/POA for the three POA reduction scenarios have values of about 4.2-4.4 x 10^{-6}.

SIA Toolkit

Based on these simulations, we developed a toolkit for the assessment of the sensitivity of SIA formation over Germany to emission reductions. The main objective of this toolkit is to provide calculations of the impact of emission reduction scenario of choice on PM concentrations without using the results of the CTM directly. In addition, in the toolkit an assessment is made of the conditions under which the calculated factors are valid.

Conclusions and recommendations

This report deals with the contribution of gaseous emissions to the concentration of secondary inorganic and organic aerosol particles (SIA and OA, respectively) over Germany. As indicator of the conversion of precursors to PM, we applied the formation factor, and as indictors of population exposure we applied the intake factor. The formation of secondary (in)organic aerosols has been investigated and documented. For PPM, we find a FF of about 0.01 $\mu g\ m^{-3}$ $kTon^{-1}$. For SIA this number is about 0.001 $\mu g\ m^{-3}\ kTon^{-1}$, and for OA about 0.006 $\mu g\ m^{-3}\ kTon^{-1}$. Reducing emissions from Agriculture appears the most effective pathway to reduce SIA concentrations, while for OA the reduction of emissions from the Residential combustion sector is the most effective.

SIA intake factors for all precursors (NO_x, SO_2, and NH_3) were around 0.3 x 10^{-6} kg/kg. For OA, the intake factor is around 4 x 10^{-6} kg/kg. These values are in the same order of magnitude as those in the literature.

Recommendations for future research on this topic include improved dynamic emission modelling for sectors such as agriculture and traffic and refinement of spatial resolution for certain subsectors. Also, validation of the PM source apportionment with experimental data is recommended. Simulations of sulphate could benefit from the inclusion of recent insights on SO_2 oxidation pathways into models, while for organic aerosol the process understanding on e.g. semi-volatile emission and gas-phase ageing needs to be improved. Also, the scarcity of observational data forms a challenge for representing the latter in models. Emission datasets that include condensables are not yet available for multiple years, which currently hinders the evaluation of the interannual variability of the FF of SIA and OA. Finally, FF and IF are presented here as countrywide data. For better support of state-level policies, simulations which label the concentrations, FF and IF per federal state are highly recommended.

Zusammenfassung

Ziel des Projekts

Feinstaub (als PM$_{2,5}$ oder PM$_{10}$) ist der Luftschadstoff, der sowohl in Deutschland als auch in anderen europäischen Ländern für die höchste Krankheitslast aufgrund von Luftverschmutzung verantwortlich ist. Daher sind Maßnahmen zur Reduzierung der Feinstaubkonzentration in der Luft von besonderer Bedeutung. Solche Maßnahmen fangen in der Regel auf der Emissionsseite an. Es ist von entscheidender Bedeutung, die Emissionen auf effiziente Weise zu reduzieren und die Maßnahmen so zu optimieren, dass der Nutzen für die Gesundheit maximiert wird. Eine große Herausforderung bei der Priorisierung von Minderungsoptionen ist jedoch, dass ein großer Teil des Feinstaubs nicht direkt emittiert wird, sondern sich aus gasförmigen Vorläufern in der Atmosphäre bildet. Daher ist es dringend erforderlich, den Beitrag gasförmiger Emissionen zur Konzentration sekundärer anorganischer Aerosol- und organischer Aerosolpartikel (SIA bzw. OA) in Deutschland zu bewerten. Diese Quantifizierung erfordert den Einsatz eines chemischen Transportmodells (CTM), das die Emissionen aller relevanten Gase, ihre chemische Umwandlung, die Vermischung in der Atmosphäre und den Abtransport dieser Gase und ihrer Reaktionsprodukte berücksichtigt. Das Hauptziel dieses Projekts ist die Ableitung von Faktoren für das Feinstaubbildungspotenzial gasförmiger Emissionen, um die Folgen von Emissionsminderungen sowohl bei gasförmigen Vorläufersubstanzen als auch bei direkt emittiertem Feinstaub für die atmosphärische Feinstaubbelastung und die daraus abgeleitete Exposition über Deutschland zu bewerten. Diese Faktoren werden dann in einem Toolkit angewandt, das die Abschätzung der Auswirkungen von Emissionsminderungsszenarien für gasförmige Vorläufersubstanzen auf die SIA-Konzentration ermöglicht, ohne dass zusätzliche CTM-Simulationen erforderlich sind. Dieses Projekt wurde von TNO durchgeführt mit Anfang im Oktober 2019 und Ende im Oktober 2022.

Um dieses Hauptziel zu erreichen, wurden mehrere Forschungsfragen definiert:

► Wie ist der aktuelle Kenntnisstand über die Prozesse, die die Bildung und Konzentration von sekundären Aerosolen in der Atmosphäre verursachen?

► Wie gut erfasst das TNO-CTM LOTOS-EUROS diese Prozesse im Vergleich zum Stand des Prozesswissens und im Vergleich zu Beobachtungen und anderen Modellen?

► Welches ist der geeignetste Indikator für das PM-Bildungspotenzial von gasförmigen Emissionen?

► Inwieweit beeinflussen Emissionsminderungen von gasförmigen Vorläufersubstanzen die Konzentration von Feinstaub in der Atmosphäre über Deutschland? Unterscheiden sich diese Faktoren je nach emittierendem Sektor und Verbindung? Und welche Auswirkungen haben diese Reduzierungen auf die Feinstaubbelastung?

► Welche Auswirkungen haben räumliche und zeitliche Schwankungen der Emissionen auf das PM-Bildungspotenzial? Wie empfindlich reagieren die ermittelten PM-Reduktionsfaktoren auf Unsicherheiten bei Modellprozessen und -parametern, auf meteorologische Schwankungen und auf die Auflösung des Modells?

► Was sind die Anforderungen an ein Screening-Tool, das die Minderung der PM-Belastung wirksam unterstützen kann?

Für diese Forschung sind zwei Faktoren relevant: die Entstehung von Feinstaub und die Exposition gegenüber Feinstaub. Der erste Schritt in diesem Projekt bestand darin, in der

Literatur nach Indikatoren zu suchen, die bei der Berechnung der Bildung und Aufnahme (d.h. der Menge an PM, die von der Bevölkerung eingeatmet wird) von PM aus gasförmigen Vorläufersubstanzen verwendet werden können. Das Ziel der Literaturstudie war es, die verschiedenen verfügbaren Ansätze zu identifizieren und den für dieses Projekt am besten geeigneten auszuwählen. Wir haben uns für den Formationsfaktor (FF) als Indikator für die Umwandlung von gasförmigen Emissionen in sekundäre PM entschieden (Van Zelm et al., 2008; Thunis und Clappier, 2014). Der FF ist eine Variable, die das Verhältnis zwischen den Emissionen eines Schadstoffs (oder eines Schadstoffvorläufers) und der Konzentration eines Schadstoffs quantifiziert. Bei primärem Feinstaub ist diese Beziehung zwischen Emission und Konzentration linear: eine Emissionsreduzierung führt zu einer Konzentrationsreduzierung, die proportional zu dieser Emissionsreduzierung ist. Bei sekundärem Feinstaub ist die Beziehung jedoch nicht linear, da die Chemie und die Ablagerung der Vorläuferstoffe eine Rolle spielen. Als Indikator für die Exposition haben wir den Aufnahmefaktor (IF) von Van Zelm et al. (2008) übernommen. Der IF wird berechnet, indem der FF mit dem Volumen der von der Bevölkerung in einem bestimmten Gebiet eingeatmeten Luft multipliziert wird und könnte als die Masse des eingeatmeten PM pro Masse des emittierten PM (Vorläufer) interpretiert werden.

Die Quantifizierung sowohl der FF als auch der IF erfordert die Verwendung eines CTM. Das CTM berücksichtigt die Emissionen aller relevanten Gase, ihre chemische Umwandlung und Vermischung in der Atmosphäre sowie die Entfernung dieser Gase und ihrer Reaktionsprodukte. Die LOTOS-EUROS-CTM ermöglichte es uns, die Zusammenhang zwischen den Emissionen von Vorläufern und primärem Feinstaub und der modellierten Konzentration abzuleiten. Mit der LOTOS-EUROS-Kennzeichnungstechnik war es auch möglich, die Beiträge der Emissionsquellen aus verschiedenen Sektoren und/oder Regionen in Deutschland zu quantifizieren.

Primäre PM-Faktoren

Obwohl primärer Feinstaub bereits in Form von Partikeln emittiert wird, gibt es mehrere Faktoren, die das Verhältnis zwischen seiner Emission und seiner Konzentration für eine Region und/oder einen Sektor und damit seinen Bildungsfaktor (FF) bestimmen. Zu diesen Faktoren gehören die Emissionshöhe, die zeitliche Variabilität der Emissionen und die meteorologischen Bedingungen. Der Aufnahmefaktor (IF) von primärem Feinstaub wird außerdem durch das Ausmaß der räumlichen Zusammenlagerung von Bevölkerungszentren und Emissionen beeinflusst. Um einen Einblick in diese Faktoren zu erhalten, die auch bei sekundärem Feinstaub eine Rolle spielen, haben wir zunächst den FF und den IF für primären Feinstaub aus gekennzeichneten LOTOS-EUROS-Modellsimulationen berechnet. Das erste Ziel bestand darin, zwei Fragen für primäre PM zu beantworten:

► Inwieweit variieren die Bildungsfaktoren zwischen Sektoren und Regionen?

► Wie setzen sich diese Bildungsfaktoren in den Aufnahmefaktor für die Bevölkerung um?

Wir beantworten diese Fragen durch gekennzeichnete Modellsimulationen, in denen die Emissionen von 30 Sektoren und Regionen (oder Kombinationen davon) nachverfolgt werden. Dafür wurden die Ergebnisse der Simulationen der primären PM-Konzentrationen über einen Zeitraum von 4 Jahren (2015-2018) mit einer Auflösung von 7x7 km² analysiert. Darüber hinaus wurde eine Simulation für einen Zeitraum von 1 Jahr (2015) mit einer hohen Auflösung von 2x2 km² durchgeführt. Obwohl die absoluten Emissionen und Quellenbeiträge zwischen den Sektoren stark variieren, zeigt der Bildungsfaktor eine relativ gleichmäßige Verteilung zwischen den gekennzeichneten Quellen. Der Hausbrand weist den höchsten FF auf, was auf die überdurchschnittlichen Emissionen während der kalten und stabilen Bedingungen im Winter zurückzuführen ist, die eine Verdünnung nicht begünstigen. Andere Sektoren, die hohe FF für

die verschiedenen Bundesländer aufweisen, haben alle Emissionen in Bodennähe. Die FFs für Großanlagen im Industrie- und Energiesektor sind systematisch niedriger als die der Sektoren mit oberirdischen Emissionsquellen, da die Emissionen während eines großen Teils des Jahres oberhalb der Mischungsschicht stattfinden. Der IF für den Hausbrand ist am höchsten, gefolgt vom Straßenverkehr - leichte Nutzfahrzeuge und PKW. Beide Sektoren emittieren in der Nähe der Wohnorte, was zu diesen hohen IFs führt. Im Gegensatz dazu sind die IFs für die landwirtschaftlichen Labels niedrig, da diese meist in abgelegenen Regionen stattfinden. Der Unterschied in FF und IF zwischen den Simulationen mit einer Auflösung von 7x7 km^2 und 2x2 km^2 ist gering (<5%), was darauf hindeutet, dass die gröbere Auflösung für die Berechnung robuster Indikatoren auf Jahresbasis ausreicht. Darüber hinaus ist die berechnete interannuelle Variabilität in FF und IF über alle Labels gering und durch Unterschiede in der Meteorologie verursacht.

Sekundäre PM - Bildung (SIA)

Die Bildung sekundärer anorganischer Aerosole (SIA) und organischer Aerosole (OA) umfasst Prozesse der Bildung, der chemischen Umwandlung, des Transports und der Entfernung aus der Atmosphäre. Sekundäre anorganische Aerosole (SIA) sind Aerosole, die in der Atmosphäre durch Reaktionen mit primären oder sekundären anorganischen Gasen entstehen (Ansari und Pandis, 1998). Salze von Ammonium (NH_4^+), Nitraten (NO_3^-) und Sulfaten (SO_4^{2-}) bilden den größten Teil der SIA-Zusammensetzung (Putaud et al., 2010). Sie werden durch die Oxidation von NO_X und SO_2 zu Salpetersäure bzw. Schwefelsäure und die anschließende Neutralisierung durch Ammoniak gebildet. Mehrere Reaktionswege sowohl in der Gas- als auch in der wässrigen Phase tragen zur Bildung der Säuren bei. Die Effizienz der Reaktionswege wird durch die Verfügbarkeit der Reaktanten, die Temperatur und die relative Luftfeuchtigkeit sowie den pH-Wert bei Reaktionen in der wässrigen Phase gesteuert.

Während Ammoniumsulfat nicht flüchtig ist, ist Ammoniumnitrat eine halbflüchtige Komponente (Nenes et al., 1999). Letzteres wird ein Gleichgewicht mit seinen gasförmigen Gegenteilen aufrechterhalten. Bei hohen Temperaturen, d.h. im Sommer, wird viel mehr Ammoniak benötigt, um die gleiche Ammoniumnitratkonzentration zu erreichen wie im Winter. Daher weisen die Ammoniumnitratkonzentrationen in den meisten Regionen, auch in Deutschland, eine starke saisonale Signatur auf. Bei Sulfat zeigen die aktuellen Modelle eine Unterschätzung im Vergleich zu den beobachteten Sulfatpartikelkonzentrationen in Europa, China und Nordamerika, was möglicherweise auf fehlende SO_2-Oxidationswege zurückzuführen ist.

Die trockene Deposition ist die direkte Entfernung von atmosphärischen Gasen und Partikeln durch Vegetation, Böden oder Oberflächengewässer (Fowler et al., 2007). Der Fluss der trockenen Deposition von Spurengasen hängt von den Oberflächenkonzentrationen und der Geschwindigkeit der trockenen Deposition ab. Es ist zu beachten, dass der Austausch zwischen Oberfläche und Atmosphäre bei Ammoniak bidirektional ist, d.h. NH_3 kann von Oberflächen wieder in die Atmosphäre emittiert werden. Außerdem hängen die Geschwindigkeiten der trockenen Deposition von NH_3 und SO_2 zusammen (Fowler et al., 2001), da der pH-Wert der Flüssigkeiten im System die Geschwindigkeit bestimmt, mit der sich eines der beiden Gase auflöst. Diese pH-Abhängigkeit wirkt sich auch auf die nasse Deposition dieser Gase aus.

Die Verringerung der Emissionen von Vorläufergasen kann zu Verschiebungen im chemischen Regime führen, die sich auf die Bildung, die Verweilzeit und den Abbau von Schwefel- und Stickstoffverbindungen auswirken. Dies kann zu einer nichtlinearen Reaktion der SIA-Konzentrationen in der Atmosphäre führen (Fagerli und Aas, 2008). Die Auswirkungen der komplexen Wechselwirkungen variieren saisonal und regional über Europa mit wechselnden

Emissionsregimen. Von den Änderungen der SO_2-, NO_x- und NH_3-Emissionen zeigen die Reaktionen das stärkste nichtlineare Verhalten auf Änderungen der NH_3-Emissionen (Tarrasón et al., 2005).

Sekundäre PM - Bildung (OA)

Organisches Aerosol umfasst alle Feinstaubpartikel in der Atmosphäre, die aus organischen Molekülen bestehen. Die gebräuchlichste Methode zur Gruppierung der vielen einzelnen Verbindungen, die es gibt, basiert auf ihrer Flüchtigkeit. Für die Definition von flüchtigen organischen Verbindungen ohne Methan (NMVOC), halbflüchtigen organischen Verbindungen (SVOC) und mittelflüchtigen organischen Verbindungen (IVOC) beziehen wir uns auf die von Murphy et al. (2014) vorgeschlagene Namenskonvention für atmosphärisches organisches Aerosol. Primäres organisches Aerosol (POA) ist organisches Material, das unter atmosphärischen Bedingungen als Aerosol emittiert wird, aber nach der Emission teilweise verdunstet. POA ist also halbflüchtig, aber wie viel davon verdunstet, hängt von den atmosphärischen Bedingungen ab. SOA hingegen ist das organische Aerosol, das sich in der Atmosphäre aus einem VOC nach einer oder mehreren Generationen der Oxidation bildet. Daher umfasst SOA sowohl Reaktionsprodukte von NMVOCs wie Toluol und Monoterpene, die traditionell als SOA-Vorläufer angesehen werden, als auch SVOC und IVOC, die aus der Verdunstung von POA stammen.

SOA wird aus zwei Hauptkategorien von organischen Verbindungen gebildet, die in Emissionsinventare als separate Spezies geführt werden: 1) dem Teil der POA-Emissionen (die ihrerseits einen Teil der $PM_{2,5}$-Emissionen ausmachen), der nach der Emission als primäre SVOC in die Gasphase gelangt, 2) NMVOC, die sich unmittelbar nach der Emission vollständig in der Gasphase befinden. Darüber hinaus werden IVOC nicht routinemäßig in Emissionsinventare aufgenommen, sondern in der Regel als fester Bestandteil der POA-Emissionen in die Modelle aufgenommen. SVOC, IVOC und NMVOC unterliegen der Oxidation in der Atmosphäre und bilden anschließend Produkte mit geringerer Flüchtigkeit. Diese sekundären S/IVOC-Spezies werden dann zwischen der Gas- und der Partikelphase verteilt. Organische Verbindungen können in der Atmosphäre sowohl in der Gas- als auch in der Partikelphase vorkommen und aufgrund verschiedener chemischer und physikalischer Prozesse von einer Phase in die andere übergehen (Safieddine et al., 2017), wobei die atmosphärische Lebensdauer zwischen Tagen und Wochen liegt. Das Schicksal der S/IVOC hängt von der Phase ab, in die sie sich verteilen. In der Gasphase unterliegt es der Oxidation, hauptsächlich durch das OH-Radikal (Ma et al., 2017; Shrivastava et al., 2008). Trockene und nasse Deposition sind weitere wichtige Verlustprozesse für SVOC. Die nasse Deposition ist der effizienteste Depositionsmechanismus für SOA (Knote et al., 2015), während die trockene Deposition nur einen geringen Effekt hat. Was die Quellen von SOA über Europa betrifft, so ergibt sich aus der Literatur das Bild, dass biogene Emissionen und Emissionen aus der Verbrennung von Holz in Haushalten (RWC) im Sommer bzw. im Winter die Hauptquellen von SOA sind. Der Straßenverkehr trägt insgesamt nur geringfügig dazu bei, kann aber in städtischen Gebieten von Bedeutung sein. Was das Potenzial zur Verringerung der OA-Konzentrationen über Europa angeht, so scheinen die halbflüchtigen POA-Emissionen am vielversprechendsten zu sein, insbesondere die von RWC.

Sekundäre PM-Faktoren

Wir haben LOTOS-EUROS verwendet, um die Faktoren für die Bildung und Aufnahme von sekundärem Feinstaub zu bestimmen, einschließlich einer Reihe von fortschrittlicheren Emissionsdaten als in der Simulation, die wir für den primären Feinstaub verwendet haben. Der Hauptgrund für die Verwendung neuer Emissionsdatensätze ist die neuere Verfügbarkeit von Datensätzen, die die Emission kondensierbarer Spezies einschließen, die einen erheblichen

Beitrag zum modellierten (in)organischen Aerosol leisten können. Für den europäischen Bereich betrifft dies den CAMS 5.1 REF2 Emissionsdatensatz für das Jahr 2018, der kondensierbare Stoffe aus RWC enthält. Für Deutschland verwenden wir einen kürzlich entwickelten GRETA-Datensatz (Jahr 2018, Submission 2022), der kondensierbare Stoffe aus allen Quellen enthält. Die IVOC-Emissionen werden dazu addiert, wobei ein Ansatz verwendet wird, der üblicherweise in CTM-Berechnungen der SOA-Bildung verwendet wird: Es wird angenommen, dass IVOC mit den halbflüchtigen POA-Emissionen um den Faktor 1,5 für alle Sektoren skalieren.

LOTOS-EUROS enthält Module, die die Bildung von sekundärem Feinstaub darstellen: Das thermodynamische SIA-Modul ISORROPIA-II (Fountoukis und Nenes, 2007) wird zur Berechnung des von der Temperatur und der relativen Luftfeuchtigkeit abhängigen thermodynamischen Gleichgewichts zwischen gasförmiger Salpetersäure, Schwefelsäure, Ammoniak und partikelförmigem Ammoniumnitrat und Ammoniumsulfat sowie Aerosolwasser verwendet. Das Volatility Basis Set (VBS; Donahue et al., 2006) beschreibt die Bildung von SOA durch die Verteilung von Gas und Partikeln. Es berücksichtigt die Bildung von SOA aus NMVOCs und halbflüchtigen POA.

Die modellierten Jahresmittelwerte der Konzentrationen von Sulfat, Nitrat und Ammonium und deren Vorläufern in der Referenzsimulation zeigen, dass die Gradienten der SIA-Verbindungen viel kleiner sind als die ihrer primär emittierten Vorläufer. Dies lässt sich durch die Auswirkungen der atmosphärischen Chemie erklären, die an der SIA-Bildung beteiligt ist, sowie durch die Zeitskala, in der diese stattfindet. Nitrat trägt den größten Massenanteil zur SIA-Konzentration in Deutschland bei. Die Nitratkonzentrationen erreichen ihren Höhepunkt nicht in den Regionen mit den größten NO_X-Emissionen, sondern in denen mit den höchsten Ammoniakkonzentrationen. Der Grund dafür liegt in der halbflüchtigen Natur von Ammoniumnitrat: Mit einer höheren Ammoniakkonzentration wird eine größere Menge an Salpetersäure in die Aerosolphase getrieben. Ammonium neutralisiert sowohl Sulfat als auch Nitrat, was zu einem Konzentrationsfeld führt, das eine große Übereinstimmung mit den Nitratkonzentrationen aufweist, wenn auch mit weniger ausgeprägten Gradienten.

SIA über Deutschland besteht aus einer Menge Ammoniumsulfat und fast 5 Mal so viel Ammoniumnitrat. Ohne Berücksichtigung der gegenseitigen Abhängigkeiten werden die Beiträge der Sulfatquellen von der Industrie und der Energie dominiert, während die Nitratkonzentrationen dem Verkehr (~1/3 des aus Deutschland stammenden Anteils) und vergleichbaren Anteilen aus Energie, Industrie, Landwirtschaft und natürlichen Quellen zugeschrieben werden. Ammonium stammt von Ammoniak ab, das wie erwähnt fast ausschließlich in der Landwirtschaft produziert wird.

Um die Auswirkungen von Emissionsminderungen auf die durchschnittlichen SIA-Konzentrationen beurteilen zu können, wurde eine Reihe von Simulationen für verschiedene Minderungsszenarien durchgeführt. Emissionsminderungen in einem einzelnen Sektor können sich auf die Bildung von SIA in einem anderen Sektor auswirken. Wenn beispielsweise die Ammoniakemissionen in der Landwirtschaft um 40% gesenkt werden, können sich die pH-Abhängigkeiten bei der Bildung von Sulfat ändern, was sich auf die Menge an SO_2 auswirkt, die im Energiesektor in Sulfat umgewandelt wird. Um die Empfindlichkeit der SIA-Konzentrationen, der Sektor abhängigen Bildungsfaktoren und der sektorübergreifenden Abhängigkeiten zu untersuchen, wurden daher die folgenden Szenarien durchgeführt:

► Reduzierung der Vorläuferstoffe: 20, 40 und 60% Reduktion für NO_X, SO_2 und NH_3 in allen Sektoren

► Sektorspezifische Reduktionen: drei Sätze von 20, 40 und 60% Reduktionen aller Emissionen, die aus einem einzelnen Sektor stammen, d.h. Verkehr, Hausbrand und Landwirtschaft

► NEC-Szenario: Wie lauten die Bildungsfaktoren für jeden Sektor unter einem realistischen Emissionsreduktionsszenario?

In jedem Szenario wurde der Kennzeichnungsansatz verwendet, um den Beitrag eines Sektors in diesem Szenario zu verfolgen. Die modellierten Konzentrationsverteilungen wurden zu einem Mittelwert über das ganze Land für das Jahr 2018 gemittelt. Die Emissionsverteilungen wurden über das Land und denselben Zeitraum integriert, um zu den jährlichen Gesamtemissionszahlen zu gelangen.

Die Reduktionszenarien zeigen, dass sich die Verringerung der Vorläuferstoffe vor allem auf ihre jeweiligen Produkte auswirkt (d.h. NO_X zu NO_3^-, SO_2 zu SO_4^{2-}, und NH_3 zu NH_4^+). Die gleiche relative Reduzierung von NO_X und NH_3 hat eine größere Auswirkung als die Reduzierung der SO_2-Emissionen, was die geringere Bedeutung von Sulfat in der gesamten SIA-Masse widerspiegelt. Überraschenderweise wirkt sich die Reduzierung von NO_X und NH_3 fast gleich stark auf die Summe der inländischen SIA-Konzentration aus. Dies scheint ein doppelter Effekt zu sein, da die Reduzierung eines der beiden Stoffe auch den anderen reduziert. Höchstwahrscheinlich ist diese starke Korrelation auf die Flüchtigkeit von Ammoniumnitrat zurückzuführen. Für jedes Reduktionsszenario wurden die FFs für alle Sektoren berechnet und verglichen. Regionen mit hohen Nitratkonzentrationen stimmen mit Regionen mit hohen Ammoniakemissionen überein, da Ammoniumnitrat halbflüchtig ist. Dies und die Tatsache, dass Ammoniumnitrat der wichtigste Bestandteil von SIA in Deutschland ist, erklärt den höheren Bildungsfaktor für SIA/NH_3 (in der Landwirtschaft, die hauptsächlich NH_3 emittiert) im Vergleich zu SIA/ NO_X (im Verkehr, der hauptsächlich NO_X emittiert).

Simulationen, bei denen Reduzierungen für alle Spezies in einem ganzen Sektor vorgenommen werden, bieten die Möglichkeit, die Gesamtwirkung von sektorweiten Reduzierungen zu untersuchen, und sie zeigen die Auswirkungen von Reduzierungen in einem Sektor auf die Konzentrationen von SIA, die in einem anderen Sektor erzeugt werden. Bei der Analyse dieser Daten ist jedoch Vorsicht geboten. Da sich die Reduktionen auf alle in dem Sektor emittierten Spezies auswirken, kann der SIA-Bildungsfaktor für eine einzelne emittierte Spezies irreführend sein, da es sich nicht um die einzige Spezies handelt, die reduziert wird. Eine dritte Möglichkeit, die Konsistenz der Bildungsfaktoren zu untersuchen, besteht darin, die FFs in einem relevanten Zukunftsszenario mit denen zu vergleichen, die für die der heutigen Zeit berechnet wurden. Zu diesem Zweck haben wir bestehende NEC-Szenario-Berechnungen herangezogen, in denen die Emissionen aller europäischen Länder auf ihre jeweilige Obergrenze im Jahr 2030 skaliert wurden. Die FFs von SIA in Bezug auf ihre Vorläufer sind ähnlich wie die Faktoren, die für die Reduktionsszenarien für einzelne Spezies vorgestellt wurden, mit Ausnahme von SIA/SO_2, das etwa doppelt so hoch ist. Dies könnte damit zusammenhängen, dass das NEC-Szenario eine komplexe Kombination aus verschiedenen Reduktionsmaßnahmen für alle Emissionen in vielen Sektoren und den nichtlinearen Auswirkungen des SIA-Bildungsmechanismus ist. Schließlich wurden als Vorstufe zur Untersuchung der gesundheitlichen Auswirkungen der Aufnahme von SIA-Spezies die jährliche Gesamtaufnahme und die Aufnahmefaktoren berechnet. Das Gesamtbild der Aufnahmefaktoren ist, dass sie den Bildungsfaktoren sehr ähnlich sehen. Dies ist höchstwahrscheinlich darauf zurückzuführen, dass für beide Berechnungen die gleichen Konzentrationen verwendet werden, der IF jedoch nach der Bevölkerungsdichte gewichtet wird. Daher werden bei der IF-Berechnung dicht besiedelte Gebiete hervorgehoben.

Die Simulationen des OA zeigen, dass sowohl halbflüchtige POA als auch NMVOC-Emissionen zur anthropogenen OA-Bildung beitragen. Die modellierte jährliche Gesamt-OA-Konzentration in Deutschland beträgt etwa 1 µg m^{-3}. POA macht mit 0,52 µg m^{-3} etwa die Hälfte der OA-Konzentration aus. POA wird hauptsächlich im Winter gebildet, wenn die Emissionen ein Maximum erreichen und die atmosphärische Durchmischung unterdrückt wird. Aus denselben Emissionsquellen wie POA stammt auch siSOA, aber sein Beitrag ist etwa um den Faktor 3 geringer. Dies ist darauf zurückzuführen, dass die meisten POA-Emissionen im Winter stattfinden, wenn die Photochemie langsam ist, was die Oxidation der halbflüchtigen organischen Dämpfe, die zur SOA-Bildung führen, verhindert, und wenn die Temperaturen niedrig sind, was die Verteilung der halbflüchtigen Emissionen in die Partikelphase begünstigt. Anthropogene SOA, die durch die Oxidation von NMVOC gebildet wird, trägt aufgrund der ineffizienten Umwandlung ihrer Vorläufer, der anthropogenen NMVOC, nur einen kleinen Teil der gesamten SOA über Deutschland bei (0,04 µg m^{-3}). Der Beitrag der biogenen SOA ist im Jahresdurchschnitt signifikant (0,26 µg m^{-3}), zeigt aber einen deutlichen Spitzenwert im Sommer, wenn sie den größten Beitrag zur Ozonbildung über Deutschland leistet. Dies deutet darauf hin, dass ein erheblicher Teil der OA nicht (oder nur indirekt) durch Maßnahmen zur Emissionsminderung kontrolliert werden kann. Was die Validierung dieser Ergebnisse betrifft, so zeigt das Modell eine Unterschätzung um den Faktor ~5 im Vergleich zu den Beobachtungen des organischen Kohlenstoffs an den wenigen Messstationen, die für OA und seine Vorläufer verfügbar sind.

Um die Auswirkungen von Emissionsminderungen auf die durchschnittlichen OA-Konzentrationen beurteilen zu können, wurde eine Reihe von Simulationen mit verschiedenen Minderungsszenarien für anthropogene POA- und NMVOC-Emissionen durchgeführt. Darüber hinaus gibt es bestimmte Sektoren, die große Mengen an POA emittieren, so dass die Verringerung der Emissionen aus diesen Sektoren potenziell einen starken Einfluss auf die Verringerung der OA-Konzentration hat. Daher haben wir die folgende Reihe von Simulationen durchgeführt:

Verringerung der Vorläufer: Verringerung der POA- und NMVOC-Emissionen in allen Sektoren um 20, 40 und 60%

Sektorale Reduktionen: 20, 40 und 60 % Reduktion aller Emissionen aus einem einzigen Sektor, d.h. Hausbrand und Verkehr

Die Ergebnisse der Reduktionsszenarien zeigen, dass die Verringerung der POA-Emissionen effektiver zur Senkung der OA-Konzentrationen beiträgt als die Reduzierung der NMVOC-Emissionen. So führt beispielsweise eine Reduzierung der POA-Emissionen um 20% zu einem Rückgang der gesamten OA-Konzentration um 8% (die POA-Konzentration sinkt um 14% und siSOA um 4%). Die Verringerung der NMVOC-Emissionen hat nur einen geringen Einfluss auf die Gesamt-OA-Konzentration (z.B. führt eine Verringerung der Emissionen um 20% zu einer Verringerung der OA-Konzentration um 0,3%), was auf eine geringe Verringerung der aSOA-Konzentration zurückzuführen ist. In den Szenarien zur Reduzierung der Sektoren sind die Auswirkungen der Reduzierung der Emissionen aus dem Hausbrand und aus dem Verkehr sehr ähnlich wie bei den Szenarien zur Reduzierung der Spezies, da die Emissionen aus der Verbrennung in Wohngebäuden hauptsächlich aus POA bestehen und die Emissionen aus dem Verkehr aus NMVOC. Die FF für OA/POA hat einen Wert von über 0,006 µg m^{-3} kt^{-1}, was im Vergleich zu den anderen Spezies hoch ist. Dies ist darauf zurückzuführen, dass die Bildung von POA das Ergebnis eines schnellen physikalischen Prozesses ist, d.h. der Gas-/Partikelverteilung von SVOCs. Die FF von OA/NMVOC ist etwa 2 Größenordnungen niedriger als die von OA/POA. Dies verdeutlicht die begrenzte Rolle, die NMVOC bei der OA-Bildung in Deutschland insgesamt spielen. Die OA/POA-Bildungsfaktoren für die Emissionsminderung bei dem Hausbrand

betragen etwa 0,009 µg m^{-3} kt^{-1}. Im Referenzszenario beträgt die jährliche Gesamtaufnahme von OA etwa 440 kg für die deutsche Bevölkerung insgesamt. Die IFs von OA/POA für die drei POA-Reduktionsszenarien haben Werte von etwa 4,2-4,4 x 10^{-6}.

SIA-Toolkit

Auf der Grundlage dieser Simulationen haben wir ein Toolkit entwickelt, mit dem wir die Sensitivität der SIA-Bildung über Deutschland auf Emissionsminderungen bewerten können. Das Hauptziel dieses Toolkits ist es, Berechnungen der Auswirkungen des gewählten Emissionsreduktionsszenarios auf die PM-Konzentrationen zu ermöglichen, ohne die Ergebnisse des CTM direkt zu verwenden. Darüber hinaus wird in dem Toolkit eine Bewertung der Bedingungen vorgenommen, unter denen die berechneten Faktoren gültig sind.

Schlussfolgerungen und Empfehlungen

Dieser Bericht befasst sich mit dem Beitrag der gasförmigen Emissionen zur Konzentration sekundärer anorganischer und organischer Aerosolpartikel (SIA bzw. OA) über Deutschland. Als Indikator für die Umwandlung von Vorläufersubstanzen in PM haben wir den Bildungsfaktor (FF) und als Indikator für die Exposition der Bevölkerung den Aufnahmefaktor (IF) verwendet. Die Bildung von sekundären (in)organischen Aerosolen wurde untersucht und dokumentiert. Für PPM finden wir einen FF von etwa 0,01 µg m^{-3} kt^{-1}. Für SIA beträgt diese Zahl etwa 0,001 µg m^{-3} kt^{-1} und für OA etwa 0,006 µg m^{-3} kt^{-1}. Die Reduktion der Emissionen aus der Landwirtschaft scheint der effektivste Weg zu sein, um die SIA-Konzentrationen zu senken, während für OA die Reduktion der Emissionen aus dem Hausbrand am effektivsten ist.

Die SIA-Aufnahmefaktoren für alle Vorläufersubstanzen (NO$_X$, SO$_2$ und NH$_3$) liegen bei etwa 0,3 x 10^{-6} kg kg^{-1}. Für OA liegt der Aufnahmefaktor bei etwa 4 x 10^{-6} kg kg^{-1}. Diese Werte liegen in der gleichen Größenordnung wie die Werte in der Literatur.

Zu den Empfehlungen für die künftige Forschung zu diesem Thema gehören eine verbesserte dynamische Emissionsmodellierung für Sektoren wie Landwirtschaft und Verkehr sowie eine Verfeinerung der räumlichen Auflösung für bestimmte Teilsektoren. Außerdem wird eine Validierung der PM-Quellenzuordnung mit experimentellen Daten empfohlen. Sulfatsimulationen könnten von der Einbeziehung neuerer Erkenntnisse über SO$_2$-Oxidationswege in die Modelle profitieren, während bei organischem Aerosol das Prozessverständnis z.B. über halbflüchtige Emissionen und Gasphasenalterung verbessert werden muss. Auch die Knappheit an Beobachtungsdaten stellt eine Herausforderung für die Darstellung der letzteren in Modellen dar. Emissionsdatensätze, die kondensierbare Stoffe enthalten, sind noch nicht für mehrere Jahre verfügbar, was derzeit die Bewertung der interannuellen Variabilität der FF von SIA und OA behindert. Schließlich werden FF und IF hier als landesweite Daten präsentiert. Zur besseren Unterstützung der Politik auf Länderebene werden Simulationen, die die Konzentrationen, FF und IF pro Bundesland ausweisen, dringend empfohlen.

1   Introduction

1.1   General introduction

Particulate matter (as $PM_{2.5}$ or PM_{10}) is the air pollutant that is responsible for the highest burden of disease in Germany as well as in other European countries, ahead of nitrogen dioxide and ozone. Therefore, measures to reduce the ambient concentrations of particulate matter are of particular importance. Such measures usually start on the emission side and are included, for example, in the national air pollution control programme, which is to be drawn up for Germany by 1 April 2019 and serves to implement the new NEC Directive (Directive (EU) 2016/22842) and the 43. BImSchV. Member States should meet the emission reduction commitments set out in this NEC Directive from 2020 to 2029 and from 2030 onwards. It is crucial to reduce emissions in an efficient manner and to optimise the measures in a way that maximises health benefits. A major challenge in prioritizing mitigation options, however, is that a large proportion of PM is not emitted directly, but is formed from gaseous precursors in the atmosphere. Therefore, there is an urgent need to assess the contribution of gaseous emissions to the concentration of secondary inorganic and organic aerosol particles (SIA and SOA, respectively) in Germany. This quantification requires the use of a chemical transport model (CTM), which includes the emissions of all relevant gases, their chemical transformation and mixing in the atmosphere and the removal of these gases and their reaction products. The main objective of this project is to derive factors for the PM formation potential of gaseous emissions in order to assess the consequences of emission reductions, both of gaseous precursors and directly emitted PM, for the atmospheric PM load and for the derived exposure.

To achieve this main objective, it is divided into several research questions that address specific aspects of the main objective:

1. What is the current understanding of the processes that cause the formation and concentration of secondary aerosols in the atmosphere?
2. How well does LOTOS-EUROS capture these processes compared to the state of the process knowledge, and compared to observations and other models?
3. What is the most appropriate indicator of the PM formation potential of gaseous emissions?
4. To what extent do emission reductions of gaseous precursors affect the concentration of particulate matter in the atmosphere over Germany? Do these factors differ depending on the emitting sector and compound? And what effects do these reductions have on PM exposure?
5. A) What effects do spatial variations in emissions have on the PM formation potential (e.g. mixing of urban with rural air masses)?
   B) and how for temporally varying emissions (e.g. contrast between summer and winter/ day and night)?
6. How sensitive are the obtained PM reduction factors to uncertainties in model processes and parameters? How sensitive are the obtained PM reduction factors to meteorological variations? How sensitive are the obtained PM reduction factors to the resolution of the model?
7. What are the requirements for a screening tool that can effectively support the mitigation of PM pollution?

1.2 Background

Exposure to particulate matter is associated with increased mortality from respiratory and cardiovascular diseases, reduced lung function and chronic lung diseases. According to the World Health Organisation (WHO), there is no safe limit for fine concentrations of particulate matter (WHO, 2021). Harmful effects also result from acute and chronic exposure. The EU Commission estimates that around 310,000 deaths occur prematurely in Europe each year as a result of fine dust pollution. According to calculations by the European Environmental Agency (EEA) 53,800 premature deaths in Germany could be attributed to exposure to particulate matter pollution in 2019 (EEA, 2021). Epidemiological studies indicate on average for Germany a reduction in life expectancy of around ten months. Physically speaking, particulate matter is the totality of particles in the air that correspond to a defined size class, irrespective of the chemical or biological species or what mass or particle shape they have. On the basis of their origin, a distinction is made between particles, which are already emitted as particles, and secondary particles, which are formed in the atmosphere from gaseous compounds. The most important natural sources or processes on a global scale that lead to the formation of primary particles are the oceans (sea salt aerosols) and soil erosion. Within Europe, forest fires are also an important natural source of primary particles. Important anthropogenic sources of particles are the combustion of fuels in transport, as well as domestic heating and the process industry. Secondary aerosol particles are formed by chemical reactions of gaseous precursors of natural and anthropogenic origin in the atmosphere. The most important precursors for the formation of secondary particles are sulphur dioxide, ammonia, nitrogen oxides and volatile hydrocarbons. The main sources of anthropogenic precursors are transport, agriculture and energy production.

Secondary inorganic aerosol (SIA) normally contains the components ammonium sulphate and ammonium nitrate. Together, these compounds contribute a large proportion of the particulate mass in Europe (e.g. Schaap et al., 2002 and Schaap et al., 2010). Of these components, ammonium nitrate is the dominant component in western and central Europe. In addition, ammonium nitrate concentrations are particularly high during episodes of increased particulate matter compared to other components (e.g. Putaud et al., 2004). The low-volatility character of ammonium nitrate complicates the formation of SIA levels, as the formation of e.g. chemical regime (due to the availability of ammonia) and weather conditions. In addition, many processes in the formation and removal of sulphate are pH-dependent. This means that the formation of SIA is not linear.

Secondary organic aerosols (SOA) consist of a variety of organic compounds and contribute significantly to the European aerosol mass (Jimenez et al., 2009). Different sources contribute to the total SOA mass, including anthropogenic sources such as transport, wood and coal combustion, as well as natural sources such as emissions from trees. The exact chemical pathways by which volatile organic compounds (VOCs) are processed in the atmosphere determine the SOA formation. Many factors, for example anthropogenic NO_X emissions, have a major influence on these reaction pathways. Due to its complex nature, which involves a multitude of precursors and atmospheric oxidation processes, SOA formation is less well understood than SIA formation.

1.3 Structure of the report

This report is structured as follows: after this introduction section (Chapter 1), we start with a description of the theory that we applied in the calculation of the formation and intake factors of PM, and with a general description of the LOTOS-EUROS model that we used for the calculations in this report (Chapter 2). Then, we discuss the calculations that we performed on the factors for

PPM (Chapter 3), which serves as a basis for the further discussion on SPM. This is followed by chapters on the theory of SIA and OA formation (Chapters 4 and 5), in which we describe the processes of formation, chemical transformation, transport and removal from the atmosphere of inorganic and organic SPM. In Chapter 6, we present the main part of this work: the calculations of the formation and intake factors of SIA and OA over Germany, based on a reference and several scenario runs with the LOTOS-EUROS model. Comparisons with observation data and other models are also part of this chapter. Based on these simulations, we developed a toolkit for the assessment of the sensitivity of SIA formation over Germany to emission reductions (Chapter 7). The report ends with a discussion and conclusion section (Chapter 8), in which we answer the research questions.

2   Theory and methods

In this chapter, we describe the theoretical basis of the formation and intake factors and we give a general description of the LOTOS-EUROS model that we used for our simulations.

2.1   Formation and intake factors

In this section, we review the available definitions in the literature on formation factor (FF) and intake factor (IF) for secondary PM. We also discuss how these indicators will be applied in this project.

2.1.1   Formation factor

The FF is a variable that aims to quantify the relationship between emissions of a pollutant (or pollutant precursor) to the concentration of a pollutant. While for primary PM, this relationship between emission and concentration is linear, this is not the case for secondary PM, because of the role that chemistry and deposition of the precursors play in its formation. We here explore the approaches that are available to account for these interactions.

The first approach is the aerosol formation factor, which is defined by de Leeuw (2002) as the fraction of the primary emitted pollutant which is converted to particles in the atmosphere [mass/mass]. Annual average factors were derived for Europe as a whole for the precursors NO_x, NH_3 and SO_2 with values of 0.88, 0.64 and 0.54, respectively. For primary PM, this factor would be equal to 1, but emission time series of primary PM were not available at the time of that study. It is not explicitly mentioned in this study, but it seems that the integrated PM mass over the European atmospheric domain was used in the calculations of the formation factor.

In a second approach Amann and Wagner (2014) define pollutant exchange rates for the (then) 28 EU member states, which are used to quantify the required additional emission reduction of one pollutant to compensate for the excess emission of another pollutant. They are expressed in PM equivalent factors, allowing for the conversion between secondary and primary emissions (emitted mass/emitted mass). In this approach, 1 ton of emitted primary $PM_{2.5}$ is equivalent to 3.356 tons SO_2, 14.925 tons NO_x, 5.155 tons NH_3 and 111.111 tons VOC, respectively. These numbers are median values for the 28 countries, and it is acknowledged that large spatial differences will occur due to different meteorological and chemical regimes.

The third approach is the most promising one for our purposes, as it aims to link the change in concentration $C_{y,i}$ of pollutant y in grid cell i (mass/volume) over a certain period to the emission E_x of precursor x (mass) over the same period (Van Zelm et al., 2008; Thunis and Clappier, 2014):

$$FF_{x,i} = \frac{\partial C_{y,i}}{\partial E_x}$$

1

This allows for the calculation of spatial and temporal variations in FF from gridded emission and concentration data as obtained from a CTM. FF is integrated over a certain area, over which emission changes lead to representative changes in concentrations.

The concept of the formation factor was further refined by Thunis and Clappier (2014). They developed a framework for the dynamic evaluation of air quality models, i.e. to assess the response of a model to given model input data. They used the concept of potencies, which is similar to the formation factor: a measure of concentration change due to a change in emission. However, their framework allows for the analysis of non-linearities and interacting terms in the formation of secondary pollutants. Their methodology is based on the Stein and Alpert (1993)

approach to decompose an overall impact into single (one emission source) and combined (multiple emissions sources) contributions, by splitting the FF into linear and non-linear terms. The FF can be calculated for individual species, combinations of species or for sectors, and its robustness over a range of emission reductions then depends on whether the non-linear term can be neglected with respect to the linear term.

In those FFs, deviations from the linear response occur when there are:

► non-linearities in the response to a single species/sector,

► interactions between species/sectors,

► combinations of non-linearities and interactions. Non-linearities and interactions between species or sectors can either enhance or dampen each other's individual effects.

2.1.2 Intake factor

Many factors determine the intake of air pollutants by human beings, including the chemical properties of the emitted species, the location of the emissions, receptor locations (e.g. indoors or outdoors) and population characteristics (Bennett et al., 2002). Therefore, the intake of a certain species is context dependent.

Bennett et al. (2002) define the intake *fraction* as the population intake of a pollutant per unit emission (mass/time). However, for secondary species, the pollutant that is taken in is different from the precursor that is emitted. Therefore, we adopt the term intake factor (IF) from Van Zelm et al. (2008), since this accounts for the transformation of the precursor.

The IF of precursor x in grid cell i (dimensionless) is related to the FF as follows:

$$IF_{x,i} = \frac{\partial I_{y,i}}{\partial E_x} = BR \cdot N_i \cdot \frac{\partial C_{y,i}}{\partial E_x}$$

$$\textbf{2}$$

, where $I_{y,i}$ is the intake of pollutant y in grid cell i (g yr^{-1}), E_x the emission of precursor x (g yr^{-1}), BR the average human breath intake rate (13 m^3 day^{-1}), N_i the population number in grid cell i and

$$\frac{\partial C_{y,i}}{\partial E_x}$$

$$\textbf{3}$$

the formation factor (m^{-3}). These numbers are yearly averages or sums.

The IF can be interpreted as the mass inhaled per mass emitted (precursor). The IF forms the basis for further calculation on the health burden of a population due to air pollutant intake (Van Zelm et al., 2008, 2016; Oberschelp et al., 2020).

2.1.3 Application in this work

In this study, annual average factors are calculated for Germany as a whole or for federal states in the unit µg m^{-3} kTon^{-1}. The definition of the formation factor of pollutant x from emitted species y used in this study is:

$$FF_{x,y} = \frac{\overline{C_{x,reference}} - \overline{C_x}}{E_{y,reference} - E_y}$$

$$\textbf{4}$$

Here, $\overline{C_x}$ the concentration of pollutant *x*, averaged over the German domain and over a certain time period (typically one year) and E_y is the sum of emissions of species *y* over that same domain and time period. The subscript *reference* refers to a control case in which no reductions

were applied. Hence, the formation factor in this definition in effect reflects the sensitivity of pollutant concentrations to emission changes due to a certain reduction scenario.

In the case of primary PM, where atmospheric chemistry does not play a role, the concentration is directly proportional to the emissions. In that case, the formation factor can be simplified to

$$FF_{x,y}^{lin} = \frac{\overline{C_x}}{E_y}$$

5

The area weighted mean value of the concentrations and the area integrated total value of the emissions are determined over the German domain according to:

$$\overline{C_j} = \frac{\iint_A C_j(A)dA}{\iint_A dA} \cdot 10^9 \quad [\mu g \, m^{-3}]$$

6

$$E_i = \iint_A e_i(A)dA \cdot 10^{-6} \cdot 365 \cdot 24 \cdot 3600 \quad [kton]$$

7

Here C_j (A) is the concentration of (in)organic aerosol j as a function of the grid cell area A *(kg m^{-3})* the factor 10^9 is a unit conversion factor to µg m^{-3}, e_i (A) is the emission rate per unit area of gaseous pollutant i as a function of the grid cell area *(kg m^{-2} s^{-1})*, the factors 10^{-6}, 365, 24, and 3600 are necessary for the unit conversion to *kTon* for a whole year.

The Intake Factor (IF) is a population exposure indicator, defined as:

$$IF_{x,y} = \frac{I_{x,reference} - I_x}{E_{y,reference} - E_y} \quad [\frac{kg}{kg}]$$

8

The annual total intake of pollutant x by the German population is given by I_x and it is calculated by multiplying the annual average pollutant concentration with an average breathing rate per person and the local population density:

$$I_x = BR \cdot \iint_A p(A) \cdot C_x(A) \, dA \quad [kg]$$

9

BR is the average breathing rate, as recommended by US EPA (1997), established at 4745 *m^3 yr $^{-1}$* and *P(A)* is the population density as a function of grid cell area A *(pers m^{-2}).* For more details, see van Zelm et al. (2016).

The population number used here is based on the Zensus population map for 2011 at 1x1 km^2 resolution (Figure 1), which is interpolated to match the LE grid. The labeling of the state and

country specific sector contributions enables us to calculate above-mentioned factors for Germany.

Figure 1:   Population density for Germany based on Zensus 2011 data
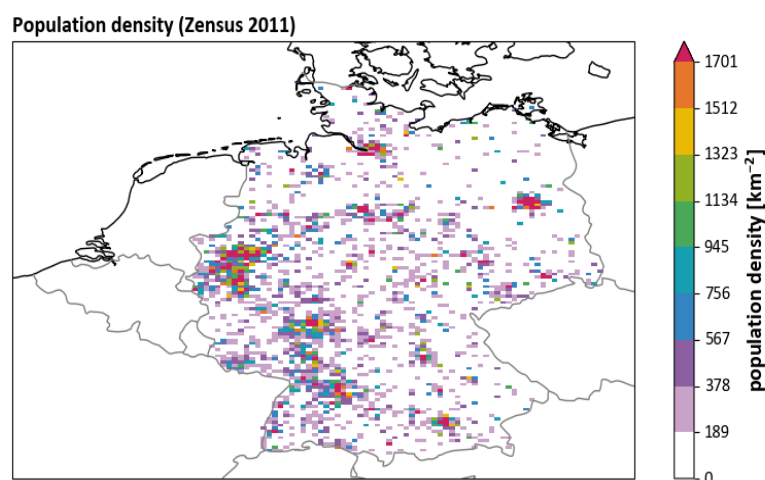
Source: TNO

2.2   LOTOS-EUROS Model description

Our assessment of the formation potential of secondary PM is based on simulation with the LOTOS-EUROS regional chemistry transport model (CTM). LOTOS-EUROS is an open-source 3D CTM that simulates the processes of emission, concentration and deposition of chemical substances in the lower troposphere. The model was developed at TNO in collaboration with partners such as RIVM and the Free University of Berlin. The model is widely used, both in scientific research and for regulatory assessments, for example, air quality forecasts or scenario calculations in climate studies. The model is part of the regional ensemble Copernicus Atmospheric Monitoring Service (CAMS), which provides operational forecasts and analyses for the whole of Europe. In this context, the model is regularly updated and validated using data from ground and satellite observations. For a detailed description of the LOTOS-EUROS model, its history and applications, we refer to Manders et al. (2017) and references given therein.

The LOTOS-EUROS model simulates air pollutant concentrations in the troposphere on a regular Euler grid with variable resolution over Europe. The original vertical grid is based on terrain-following coordinates and extends up to 5 km above sea level in this application. The model uses dynamic boundary layer heights to determine the vertical structure, meaning that the vertical layers vary in space and time. This structure makes the model less computationally intensive and is a realistic approach for horizontal resolution in the 5-25 km range. A relatively recent development is that the model can also be computed on the vertical layers of the driving meteorology. This allows a better representation of the vertical exchange of matter, which is especially important when higher horizontal resolution is desired (2-5 km).

The model is of medium complexity in the sense that the process descriptions are optimized to the computational requirements. This allows the emission, concentration, and deposition contents to be computed at an hourly frequency over several years in acceptable computational

time. In the Euler grid, the concentration changes due to advection, vertical mixing, chemical transformation, physical aerosol processes, and depletion due to wet and dry deposition are calculated. The process description requires information on anthropogenic emissions, land use, and meteorological conditions. The results of the model are stored in output files containing the modelled concentrations and deposition fluxes.

For particle deposition, the scheme of Zhang et al. (2001) is used. The wet deposition module takes into account the saturation of water troughs (Banzhaf et al., 2012). Horizontal advection of contaminants is calculated using a monotonic advection scheme (Walcek, 2000).

The runs are performed with meteorological data from the ECMWF model (European Centre for Medium-range Weather Forecasts) or from the COSMO model (Consortium for Small-scale Modeling). For COSMO, runs are possible with a higher resolution than with ECMWF meteorology, which allows a more detailed representation of spatial differences. This is especially important with regard to differences between urban and suburban areas and within large cities.

2.2.1 Labelling

The subsection 2.2.1 mainly refers to the publication by Timmermans et al. (2022). As already described in Timmermans et al. (2022), "Within the FP7 project EnerGEO, [TNO has developed] a system to track the impact of emission categories within a LOTOS-EUROS simulation […] based on a labelling technique (Kranenburg et al., 2013). [In addition to] species concentrations, the contributions of pre-defined source categories are calculated. The labelling routine is performed for primary, inert aerosol tracers as well as for chemically active tracers with a C, N (reduced and oxidized), or S atom, as these are conserved and traceable. The source attribution module for LOTOS-EUROS provides source attribution valid for current atmospheric conditions", since all chemical transformations occur at the same concentrations of oxidants. "For details and validation of this source attribution module, we refer to (Kranenburg et al., 2013). The source [attribution] technique has been previously used to investigate the origin of particulate matter (episodes) (Hendriks et al., 2013; Timmermans et al., 2017) and nitrogen dioxide (Schaap et al., 2013)."

2.2.2 Time and height profiles of emissions

In LOTOS-EUROS, the emissions from an emission inventory need to be distributed in space and time. Figure 2 show the time and height profiles for the GNFR sectors as applied in the LOTOS-EUROS simulations in this work. The spatial distribution is given by the base emission file, which consists of a map with the spatial distribution of emissions from all sectors. Time profiles are then applied to the emissions from each sector to generate hourly distributions of these emissions, which depend on the month, the day of the week and the time of day. The figures show hourly factors as averages over all weeks, with a mean time factor of 1. Emission fraction indicates the fraction of the emission between height levels. For instance, an emission fraction of 0.5 for 324 m means that 50% of the emissions are between 184 and 324 m.

Emissions from some sectors like residential combustion and road transport are all located close to the surface, while for others, like industry and public power, they take place from high stacks and contain enough heat for the emission plume to rise above the stack height. The latter is reflected in the height profiles that account for typical stack height and plume rise for a specific sector.

Figure 2: **Monthly and hourly emission factors, and emission fraction for different heights of point and area sources for indicated sectors.**
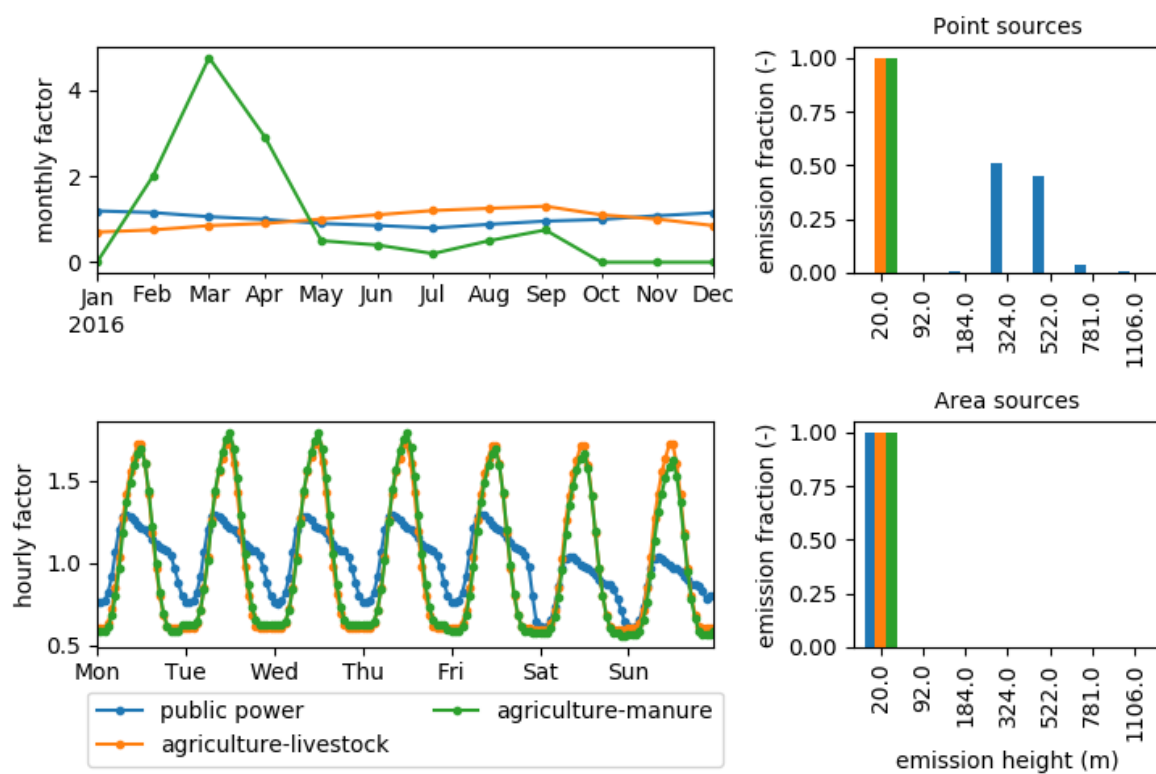
Source: TNO

Figure 3: As Figure 2; note that time factors for shipping and aviation are equal
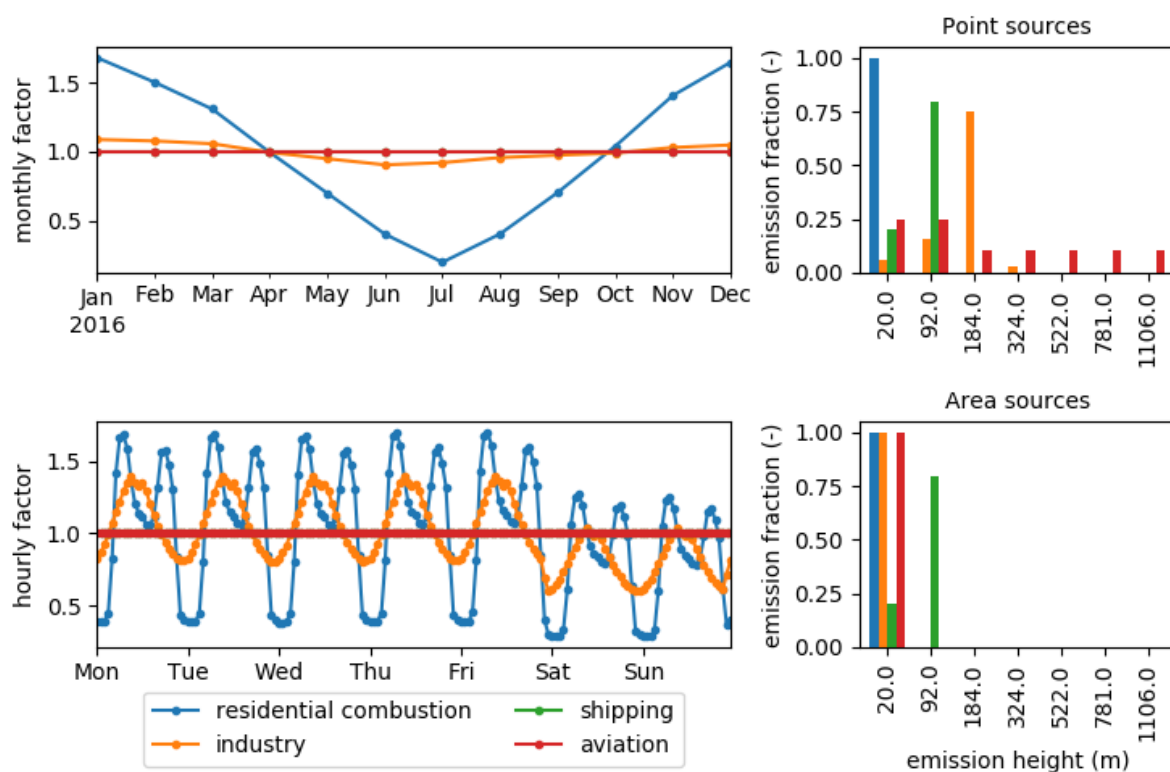
Source: TNO

Figure 4: As Figure 2; Note that time factors for road transport exhaust and road transport non-exhaust are equal
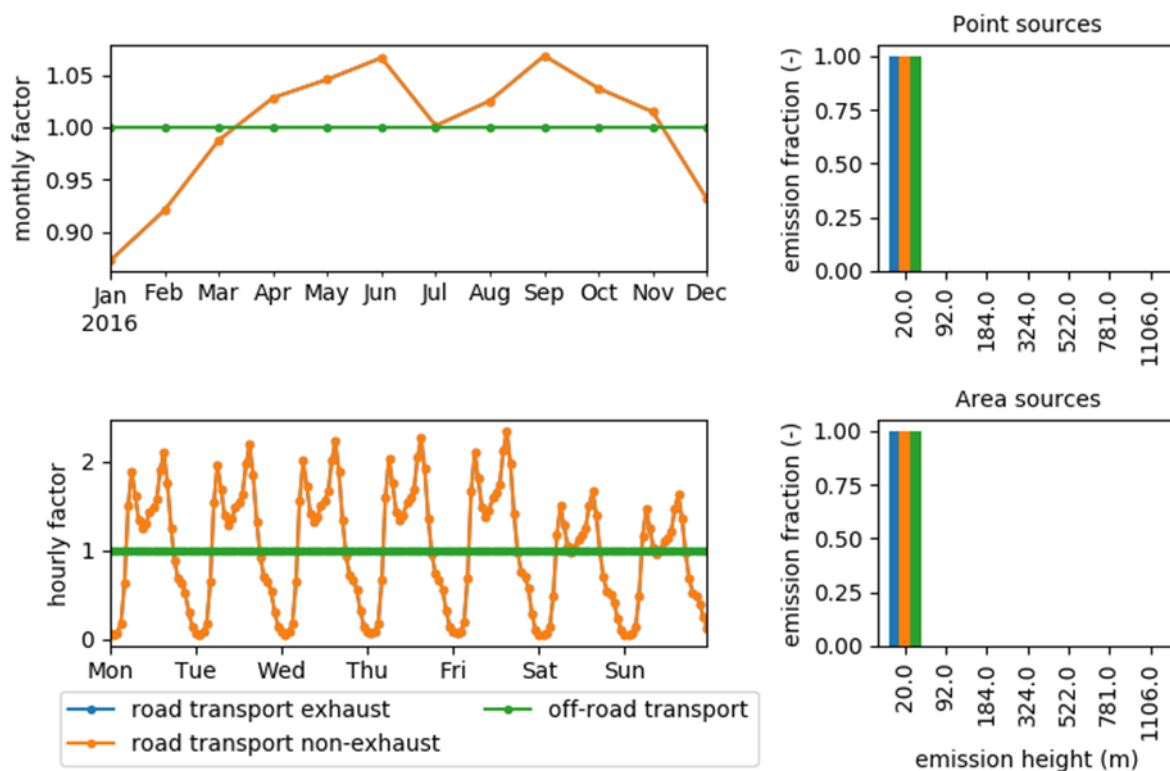
Source: TNO

3 Formation and intake factors for primary particulate matter

In this chapter, we explore the formation factors (FF) and intake factors (IF) for primary particulate matter (PPM). The FF is an indicator for the relation between emission of an atmospheric tracer or its precursor and the concentration of that tracer. The IF is a measure for the exposure of the population resulting from the emission of a certain tracer or its precursor. The FFs for a region and/or sector depend a number of factors including the emission height, temporal emission variability, meteorological conditions, as well as the location with respect to the region border. The IF is further affected by the degree of spatial co-location of population centres and emission density. The central questions to be answered in this WP are:

► In how far do the formation factors vary between sectors and regions?

► How do these formation factors translate into the population intake factor?

We answer these questions through labelled simulations in which the emissions of 30 sectors and regions (or combinations thereof) are traced. The results of this labelling exercise will give insight in how FF and IF vary between sources.

In this work package we analysed the results of simulations of the primary PM concentration over a period of 4 years (2015-2018) at a resolution of 7x7 km^2, and in addition a simulation for a 1year period (2015) at a high resolution of 2x2 km^2. The simulations over 4 year period are used to make sure that the calculated FF and IF are robust, especially when looking into seasonal differences: instead of only a 3-month period for each season of the year, we will have 12 months of output available for each season. The high-resolution simulation is aimed to assess the influence of grid size on the calculated FF and IF.

3.1 LOTOS-EUROS simulations to facilitate label selection

3.1.1 Introduction

In WP 1 the influence of dispersion, emission height, regional climate and temporal emission variability on concentration and exposure factors for primary particulate matter (PM) was explored through labelled simulations in which up to 30 sectors and regions can be traced.

To facilitate the choice of these labels, a number of test simulations was performed. These simulations provided the opportunity for UBA to indicate sectors and/or activities that are of particular interest. The ten most important sectors (NFR) as well as sectors with distinctly different temporal variability (e.g. residential combustion emissions vs land management in agriculture) were quantified.

In the kick-off meeting, it was decided that the following federal states will be labeled to address spatial variability in PM formation factors:

► Nordrhein-Westfalen

► Thüringen

► Niedersachsen

► Bayern

► Brandenburg

► Baden-Württemberg

This selection covers Germany geographically well, includes the largest states and includes regions with different precipitation amounts.

The selection of labeled sectors is described in the following chapters.

3.1.2 LOTOS-EUROS simulations

For the selection of labels, three simulations with the LOTOS-EUROS chemical transport model were performed:

1. A simulation in which primary PM emissions and the resulting concentrations for the various sectors are labeled at NFR level
2. A simulation in which the federal states are labeled.
3. A simulation with combinations of sectors and federal states.

The simulations were performed for the year 2016 for two domains: an outer domain that encompasses Europe and an inner domain that represents Germany at a higher spatial resolution. The model settings for each domain are given in Table 1. The number of vertical levels in each simulation was set to 15, to ensure that the model represents vertical variations of meteorology and pollutant concentrations well.

Table 1 : **Settings for LOTOS-EUROS test simulations**

Simulation area	Emissions	Domain	Resolution
Europe	CAMS v2.2	-15-35 °W, 35-70 °N	0.5x0.25°
Germany	CAMS v2.2	2-16 °W, 47-56 °N	0.1x0.05°

3.1.3 Results

In this section the results of the labelled runs for sectors, federal states, and combinations thereof are described and discussed.

3.1.3.1 Sector PM formation factors

Figure 5 and Figure 6 show the fine primary PM ($PPM_{2.5}$) emissions from one sector (residential combustion) and the resulting $PPM_{2.5}$ concentrations. Labeling enables us to plot German emissions only (foreign sources were not labelled), and the concentrations over Germany were selected by applying a mask to the calculated concentrations. Therefore, the factors are calculated for the German domain only.

Figure 5: **Total residential combustion emissions of PPM₂.₅ over Germany in 2016**
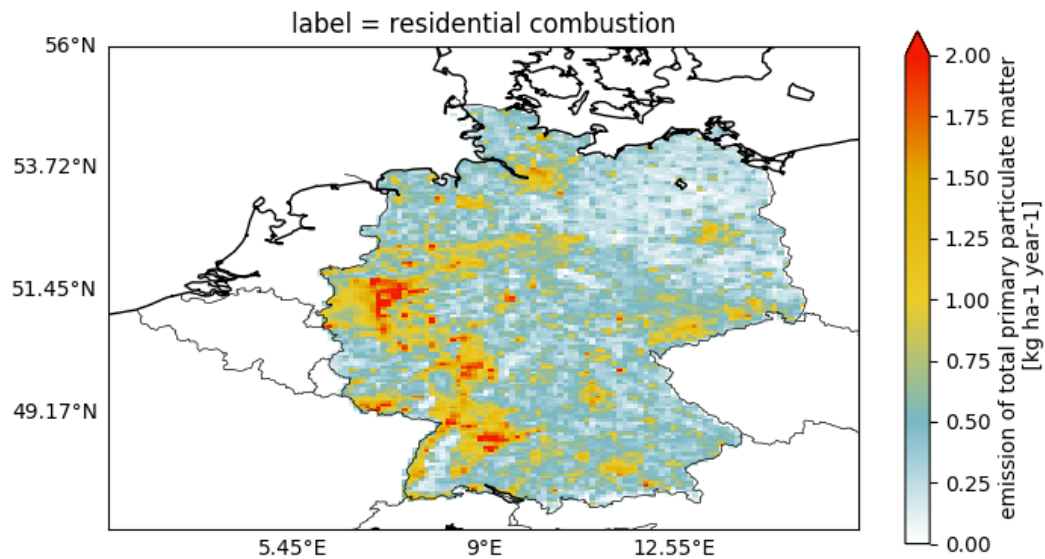
Source: TNO

Figure 6: **Annual mean concentration of PPM₂.₅ from residential combustion over Germany in 2016**
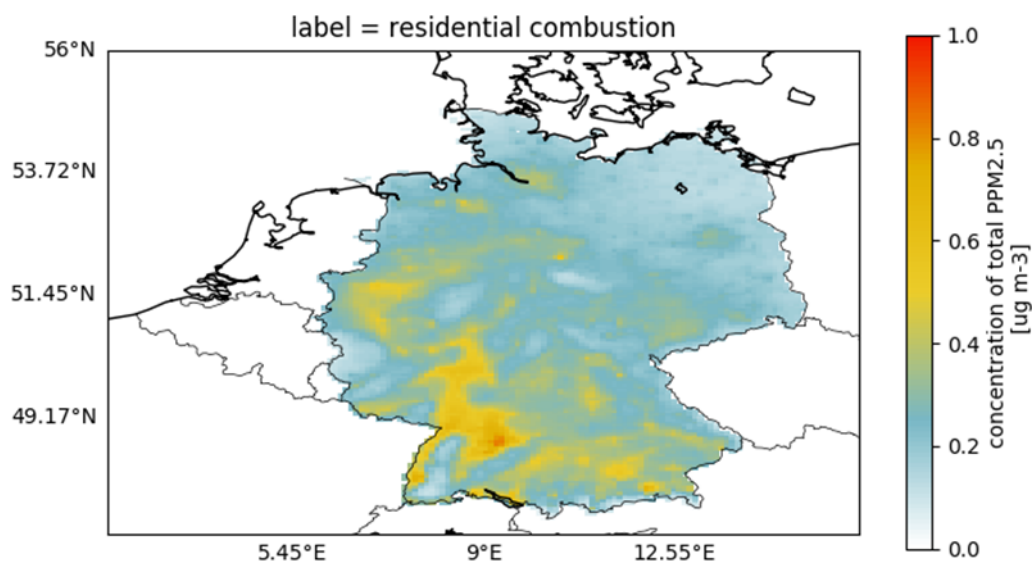
Source: TNO

By dividing the annual mean concentration resulting from the emission of a specific sector Figure 8) by the total annual emission of that sector (Figure 7), we calculated the PPM₂.₅ factor for each sector (Figure 9).

Figure 7:   Total fine primary PM emission from each sector over Germany in 2016
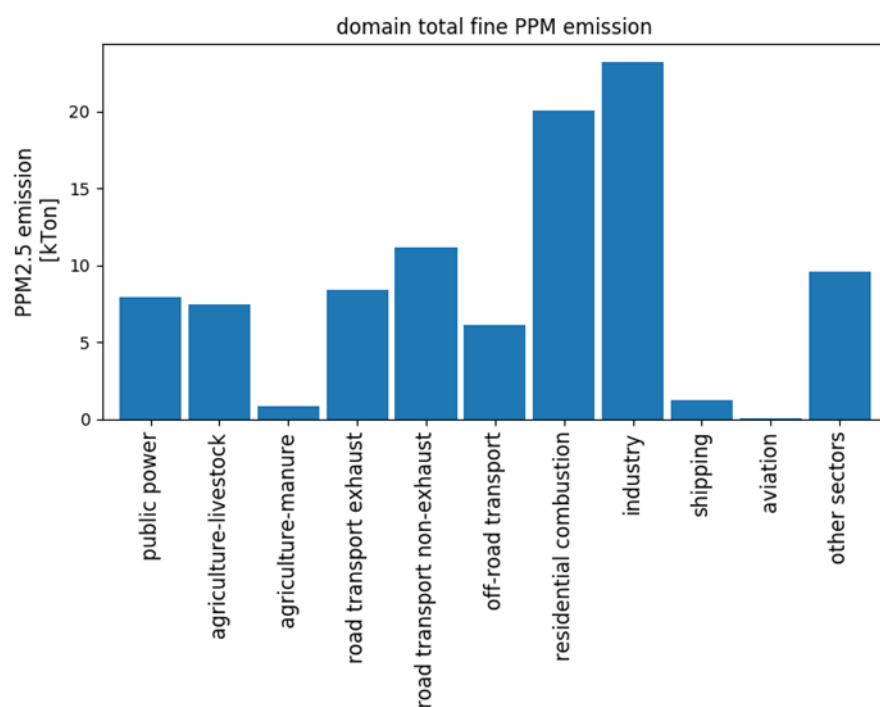
Source: TNO

Figure 8:   Average fine primary PM concentration from each sector over Germany in 2016
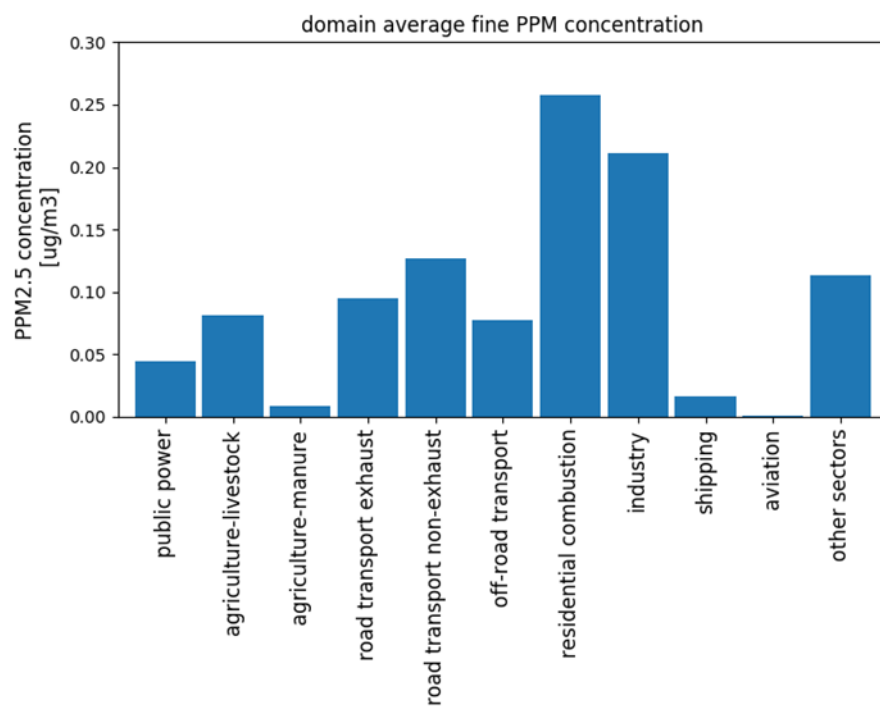
Source: TNO

Figure 9:   **Average fine primary PM formation factor from each sector over Germany in 2016**
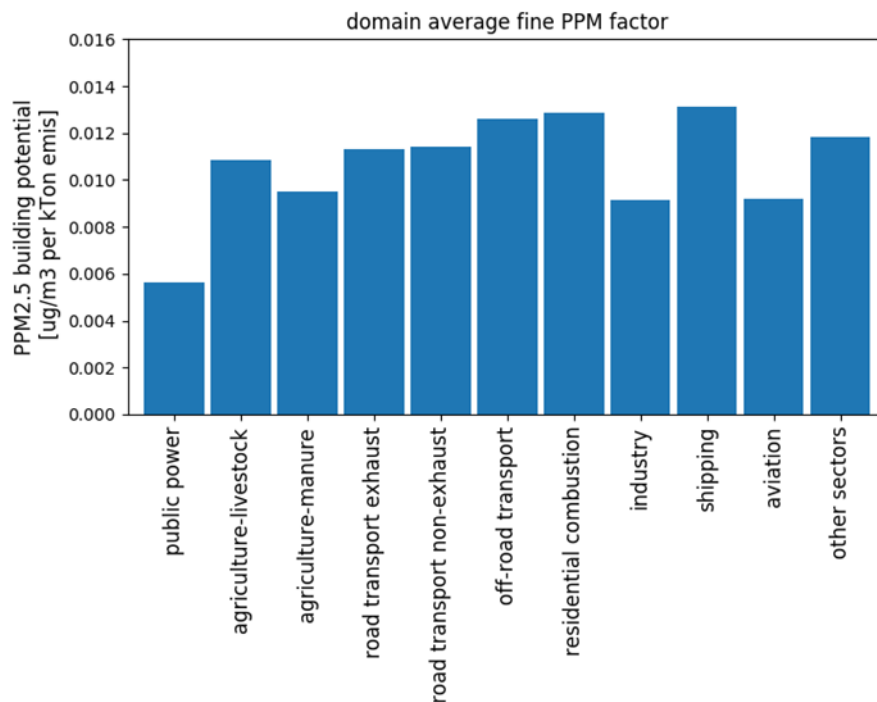
Source: TNO

PPM$_{2.5}$ formation factors vary considerably between sectors: for public power it is less than half of the value of that for residential combustion or shipping.

From Figure 7 and Figure 9 it can furthermore be seen that some sectors have very similar factors (for instance residential combustion and shipping), although they result from very different total sector emissions. Residential combustion emissions are spread out quite evenly over the country (with some hotspots in Nordrhein-Westfalen and Baden-Württemberg), while most shipping emissions result from a few hotspots along the river Rhine.

Based on the results presented above we proposed to track at least the following sectors:

► residential combustion

► industry

► road transport exhaust

► road transport non-exhaust

► and agriculture-livestock

Except for industry, all of these sectors have low emission heights, which explains the high formation factor.

To evaluate the influence of the timing of the emissions on the PM formation factor, we calculated the formation factors for a summer period (June - August) and a winter period (January - March).

Figure 10 shows that the differences between the two periods are rather small. Even for residential combustion, which has a much higher absolute emission in winter, the formation

factor does not vary much between the seasons. This suggests that emission height is more important than emission timing in determining the FF of $PPM_{2.5}$. Moreover, we found that the FF for several sectors (for instance, public power and residential combustion) was somewhat higher in summer than in winter. This is in contrast with our initial hypothesis that emissions into a shallower boundary layer during winter would lead to higher FF. We suspect that this is due to a faster removal of PM by wet deposition, which may be higher in winter than in summer.

Figure 10: Fine primary PM formation factor from each sector over Germany in winter (left) and in summer (right)
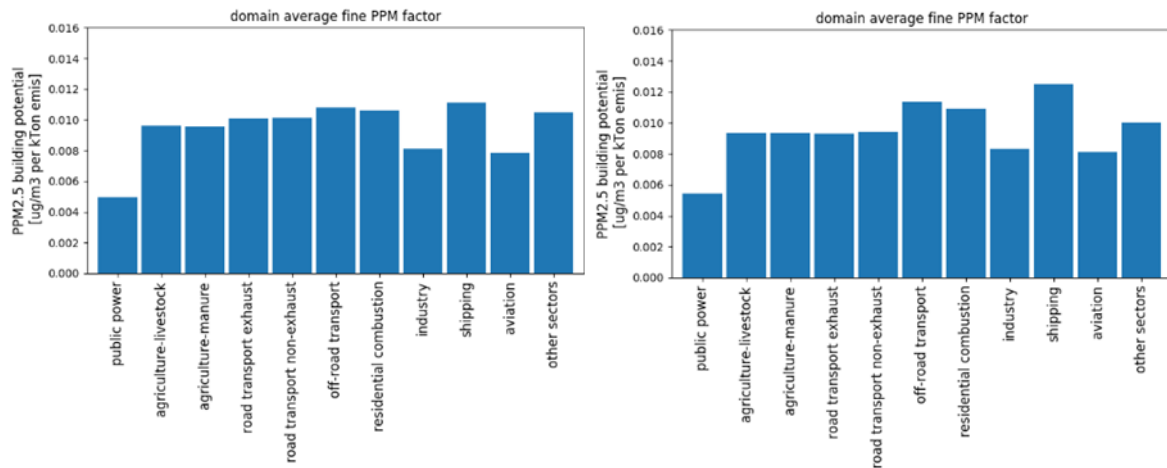
Source: TNO

3.1.3.2 Federal state PM formation factors

To get a better picture of the geographical differences in PM formation factors, the contribution of emissions from each federal state to the fine primary PM loading is analyzed. Figure 11 and Figure 12 show PPM emissions and concentration over Germany of $PPM_{2.5}$ for the state of Nordrhein-Westfalen as an example.

Figure 11:   **Total annual fine primary PM emission for Nordrhein-Westfalen for 2016**
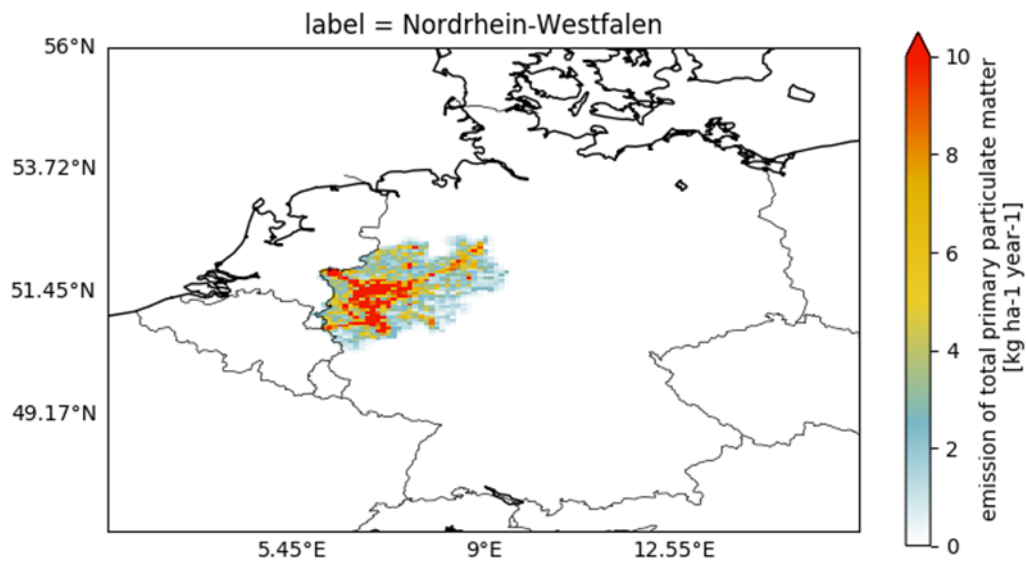
Source: TNO

Figure 12:   **Annual average fine primary PM concentration for Nordrhein-Westfalen for 2016**
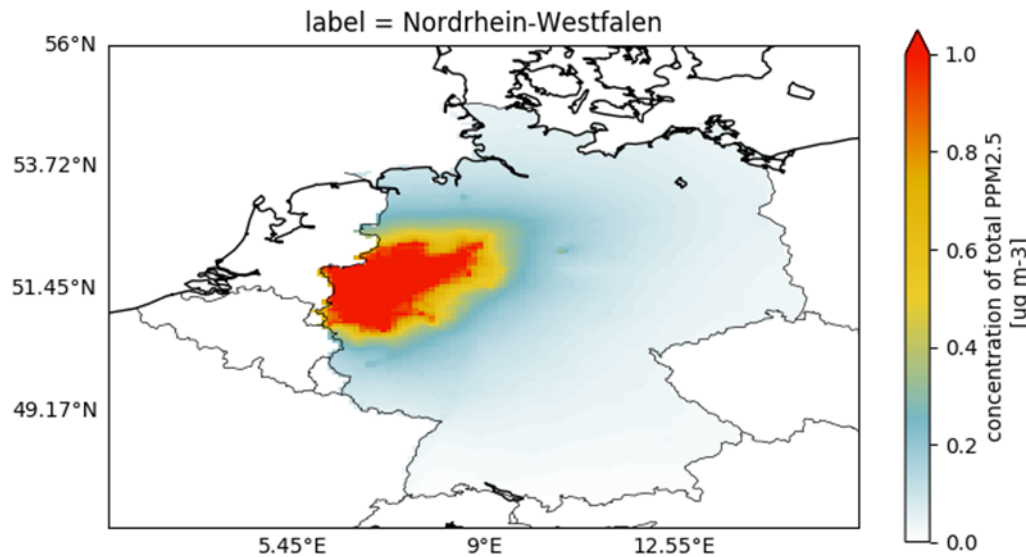
Source: TNO

When we look at the total primary PM emission per state (Figure 13), it is clear that there are large differences, due to the size and economic activities in each state. For instance the emissions in Nordrhein-Westfalen are 20 times as much as those in Berlin. However, the FFs of $PPM_{2.5}$ differ less between states (Figure 15). Schleswig-Holstein and Mecklenburg-Vorpommern have the lowest factors (<0.008 µg m^{-3} kTon^{-1}), but the other states all have factors around 0.01

µg m^{-3} kTon^{-1}. Likely, geographical and meteorological factors play an important role in this behavior.

Figure 13: **Total fine primary PM emission from each federal state over Germany in 2016**
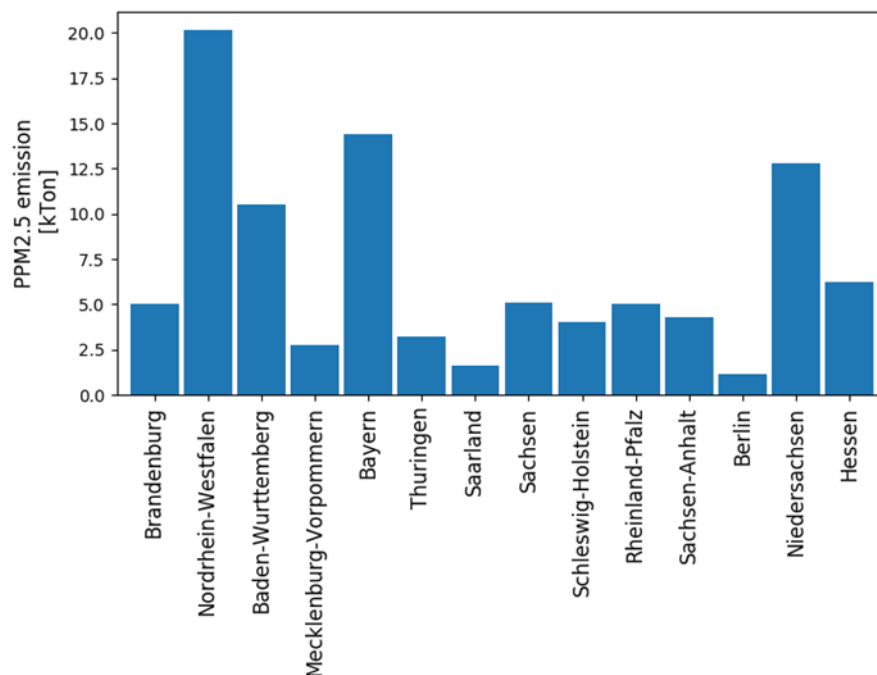
Source: TNO

Figure 14: **Total PPM$_{2.5}$ concentration from each federal state over Germany in 2016**
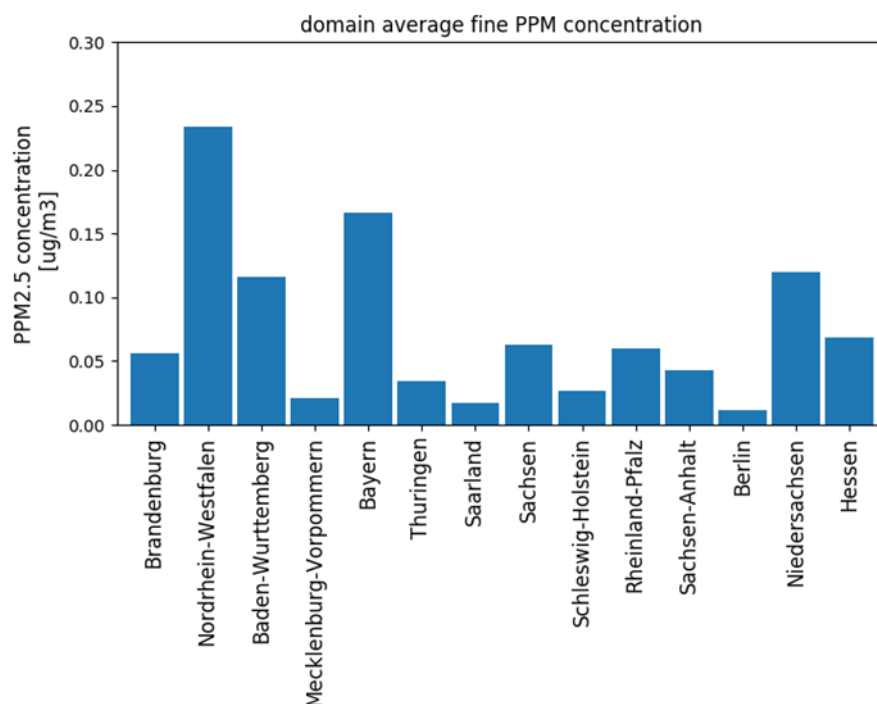
Source: TNO

Figure 15: **Average PPM$_{2.5}$ formation factor for each federal state in 2016 (concentration in each state divided by emission in each state)**
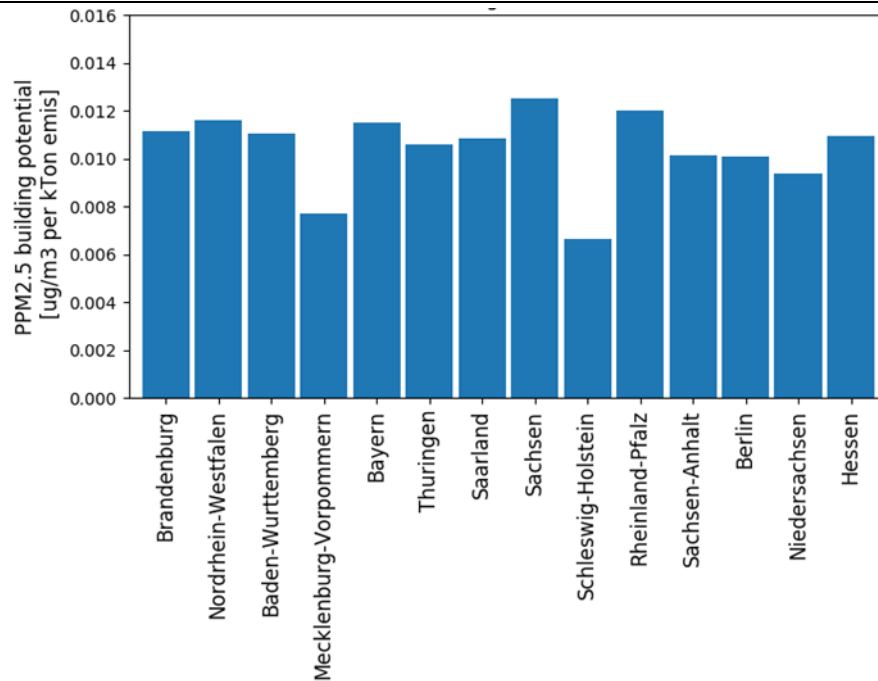
Source: TNO

Figure 16: **Average PPM$_{2.5}$ intake factor for each federal state in 2016**
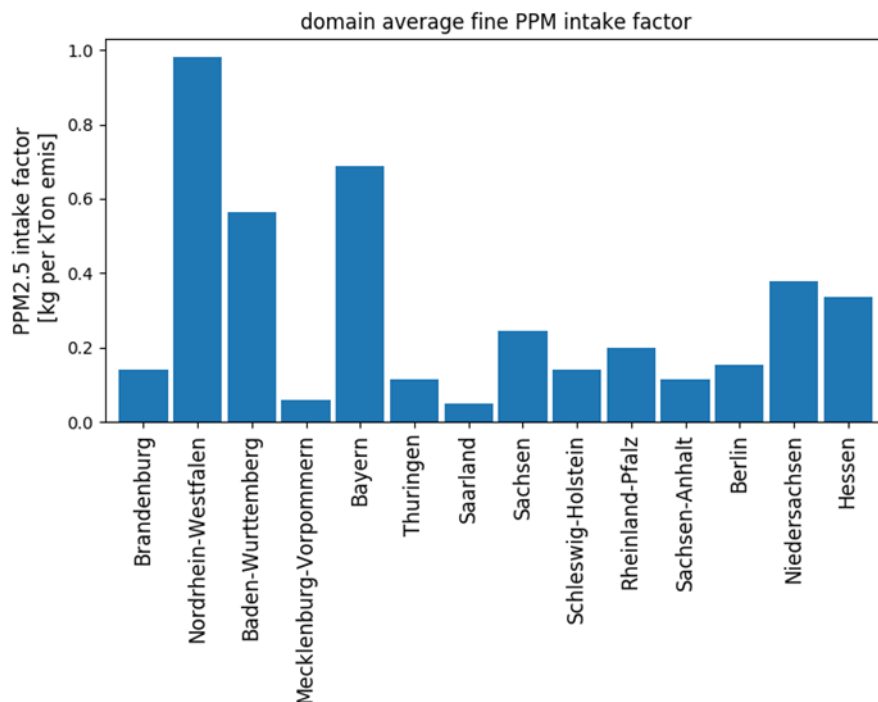
Source: TNO

However, to be able to assess the exposure of people to PPM$_{2.5}$, and how this differs per federal state, we need to take the population density into account. Therefore, we calculated the intake factor as defined by Van Zelm et al. (2016).

50

Due to the differences in population density, large differences are now visible between the federal states (Figure 17). The most populated states (Nordrhein-Westfalen, Bayern and Baden-Wurttemberg) have total intake factors between 0.56 and 0.98 kg kTon^{-1}, while for the least populated states (Saarland, Mecklenburg-Vorpommern and Thüringen) the factors range between 0.05 and 0.11 kg kTon^{-1}.

In other words, a reduction of emissions by a kTon in Nordrhein-Westfalen would lead to a 20 times larger modeled reduction in PM uptake than the same emission reduction in Saarland. Compared to Rheinland-Pfalz, which has a very similar FF as Nordrhein-Westfalen (Figure 15), this reduction is still 5 times larger, due to the higher population number. This indicates that to optimize the reduction of primary PM intake, it may be worth to focus on the 3 most populated states.

It should be noted here that in these calculations, we have not taken the spatial distribution of emissions and population within the states into account. This could lead to an overestimation of

the IF in states where population centers and emission activities (agriculture for instance) are separated in space. These effects will be subject to further investigation.

In addition, calculating the IF per sector would give insight in how the intake factors of emissions that occur close to population centers (e.g. traffic) differ from those that are farther away (e.g. agriculture).

3.1.3.3 Combined sector-state PM formation factors

We also run a simulation with labels for combinations of federal states (Baden-Württemberg, Brandenburg, Niedersachsen and Nordrhein-Westfalen) and sectors (public power, residential combustion, industry, road transport-exhaust and agriculture-livestock). Also, labels for other federal states and other sectors were included.

Figure 17:   **Average fine primary PM formation factor (here building potential) for federal state-sector combinations for 2016**
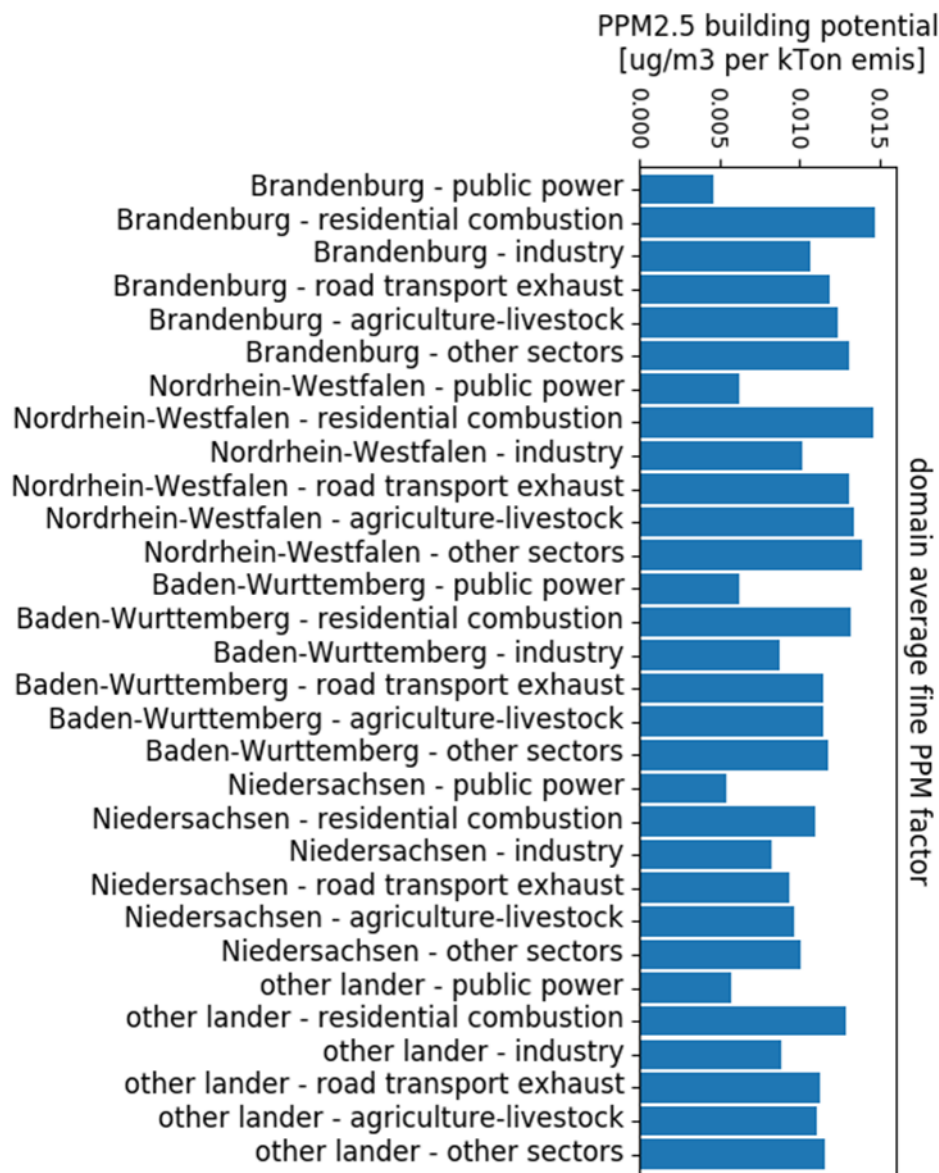
Source: TNO

Figure 17 confirms that the variations in primary PM concentration factor between sectors are larger than those between federal states: for each state, residential combustion, road transport-exhaust and the combined other sectors have the highest factors, while public power and industry have the lowest factors.

3.1.3.4   Conclusions

To support the selection of labels for the assessment of the PM formation potential over Germany, we ran a set of simulations with the LOTOS-EUROS chemical transport model. Annual average formation factors were determined per sector and per federal state. This showed that the differences between sectors are larger than those between states. However, the intake factor, which account for the population number in each state, differs strongly between states.

Our analysis further shows that summer vs. winter differences in primary PM formation potential are small, and that public power and industry have the lowest PM formation factors for each selected state in the simulation in which states and sectors are combined.

3.2 LOTOS-EUROS simulations: production runs for Primary PM

In this section, we describe the LOTOS-EUROS (LE) setup for the final set of simulations to derive the primary PM factors. In summary, LE is run for 3 different domains (see Table 2) using CAMS v4.1 (Kuenen et al., 2018) emissions for Europe, GRETA emissions for Germany and ER emissions for the Netherlands, in simulations that track source contributions to PM with 30 different labels (Table 3).

The CAMS v4.1 dataset and the specific improvements for that version are described in Kuenen et al. (2018). The GRETA emissions for Germany is the 2015 version that we received earlier in 2020 and is based on inventory submission 2019. Point sources are taken from the GRETA grid and height distribution of the point sources is assigned per GNFR category. Over the Netherlands, we have applied the Dutch Emission Registration (ER; http://www.emissieregistratie.nl/erpubliek/bumper.en.aspx) dataset at 1x1 km². The spatial distribution of the emissions is given by the base emission maps for each emission inventory.

Table 2 :   Model simulations, input data and emissions

Zielregion	Eingangsdaten	Emissionen
Europa D1 0.5x0.25° circa 30x30 km²	ECMWF Meteorologie 9x9 Km²	CAMS 4.1, year of submission: 2019 CAMS 4.1 International shipping
Nordwest Europa D2 0.1x0.05° circa 7x8 km²	ECMWF Meteorologie 9x9 Km² Randbedingung von D1	CAMS 4.1, year of submission: 2019 CAMS 4.1 International shipping GRETA 2015, submission 2019 ER 2015, submission 2019
Deutschland D3 0.03125x0.015625° circa 2x2 km²	ECMWF Meteorologie 9x9 Km² Randbedingung von D2	CAMS 4.1, year of submission: 2019 CAMS 4.1 International shipping GRETA 2015, submission 2019 ER 2015, submission 2019

Based on the findings in Section 3.1.3, a set of labels was proposed which consist of combinations of federal states and sectors (Table 3). To accommodate both the federal states with the highest intake factors and all sectors of interest, we have included labels for combinations of federal states and important sectors (road transport – light duty vehicles, agriculture-livestock and residential combustion) for these states, and included labels for sectors only for the whole of Germany. Further, labels are included for other states and other sectors to see their combined contribution.

Table 3: **Overview of label definitions for LOTOS-EUROS simulations**

Labelnr.	Label name	Federal state	Sector
1	NRW_RT_HDV	Nordrhein-Westfalen	Road Transport (NFR 1A3b) - heavy duty
2	NRW_RT_LDV	Nordrhein-Westfalen	Road Transport (NFR 1A3b) - light duty (incl. passenger cars)
3	NRW_ResComb	Nordrhein-Westfalen	Residential and commercial stationary small combustion
4	Bay_RT_HDV	Bayern	Road Transport (NFR 1A3b) - heavy duty
5	Bay_RT_LDV	Bayern	Road Transport (NFR 1A3b) - light duty (incl. passenger cars)
6	Bay_ResComb	Bayern	Residential and commercial stationary small combustion
7	Bay_AgrLive	Bayern	Emissions from manure Management (housing and storage, incl. storage of energy crop digestates)
8	Bay_AgrManu	Bayern	Emissions from Agricultural Soils (Organic and Anorganic Fertilizer Application, Grazing, etc.)
9	BW_RT_HDV	Baden-Wurttemberg	Road Transport (NFR 1A3b) - heavy duty
10	BW_RT_LDV	Baden-Wurttemberg	Road Transport (NFR 1A3b) - light duty (incl. passenger cars)
11	BW_ResComb	Baden-Wurttemberg	Residential and commercial stationary small combustion
12	Nie_AgrLive	Niedersachsen	Emissions from manure Management (housing and storage, incl. Storage of energy crop digestates)
13	Nie_AgrManu	Niedersachsen	Emissions from Agricultural Soils (Organic and Anorganic Fertilizer, Application, Grazing, etc.)
14	OthLand_RT_HDV	other states	Road Transport (NFR 1A3b) - heavy duty
15	OthLand_RT_LDV	other states	Road Transport (NFR 1A3b) - light duty (incl. passenger cars)
16	OthLand_ResComb	other states	Residential and commercial stationary small combustion
17	OthLand_AgrLive	other states	Emissions from manure Management (housing and storage, incl. Storage of energy crop digestates)
18	OthLand_AgrManu	other states	Emissions from Agricultural Soils (Organic and Anorganic Fertilizer, Application, Grazing, etc.)
19	DEU_PP_Coal	all	public power - coal

Labelnr.	Label name	Federal state	Sector
20	DEU_PP_Oth	all	public power - other
21	DEU_Ind	all	Emissions from Industry (incl. stationary combustion in 1A2)
22	DEU_Rail	all	Emissions from Rail Transport (incl. Abrasion)
23	DEU_Ship	all	Emissions from national navigation (domestic shipping)
24	DEU_OffRoad	all	Emissions from Offroad Traffic / Mobile Machinery
25	DEU_Ind_Diff	all	Emissions from handling of bulk products as well as diffuse emissions from industrial establishments
26	DEU_Waste	all	Emissions from registered bonfires as well as building and car fires
27	DEU_Other	all	all other sectors (not labelled with the labels 1-26)
28	IntShip	European incl. Germany	Emissions from international shipping
29	Natural	Natural Emissions	Natural Emissions (as default settings)
30	OtherCountries	European emissions	If possible, all PPM and precursors from boundary conditions for the German nest

3.2.1 Meteorology-dependent emission profiles

To distribute the emissions in time and height, we applied the profiles as presented in Figure 2-Figure 4. In the runs for secondary PM in WP2 we adapted these profiles and made them dependent on meteorology for a number of sectors. This is included for NH_3 emissions from agriculture, cold start emissions from traffic and residential combustion.

An example of a meteorology-dependent emission profile is give in Figure 18. It shows the default emission time profile for the Residential combustion sector, as well as time profiles that reflects how the heating demands and subsequent emissions vary with temperature, expressed in heating degree days, for Germany and France (Mues et al., 2014).

Figure 18:   **Comparison between the meteorology-dependent and the default seasonal (daily) emission factors for sector Residential combustion.**
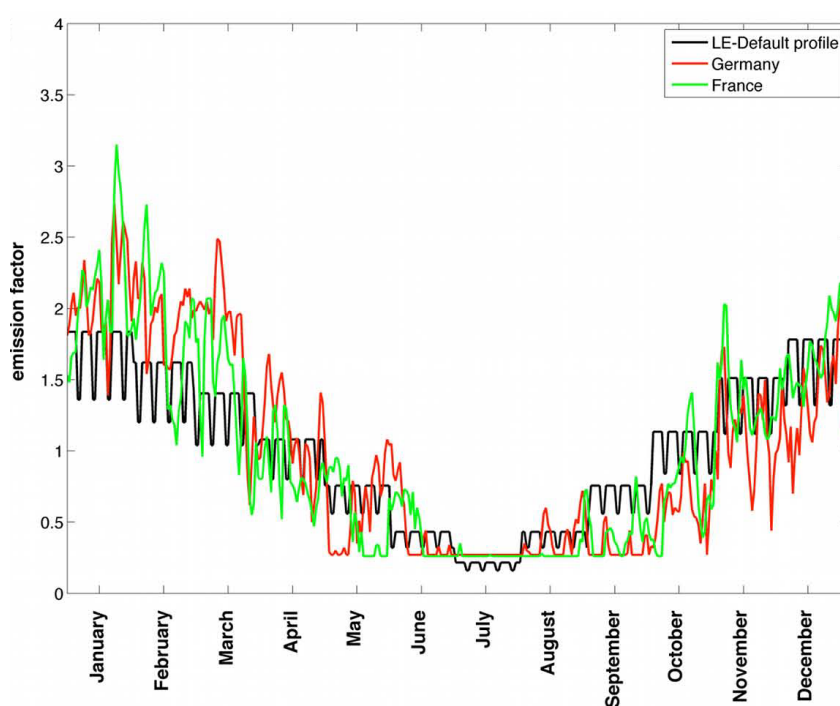
Source: Mues et al ,2014

3.3   Results

An overview over all labels, including emissions, concentrations, formation factors (FF) and intake factors (IF) for fine primary PM (PPM$_{2.5}$) is given in Figure 19 . The bars represent the mean values over the years 2015-2018 and the error bars represent the standard deviation between the mean values for each year.

It shows that for all federal states, the contribution of residential combustion to PPM$_{2.5}$ concentrations is high, both when looking at the absolute concentrations and when looking at the FF and IF.

Light and heavy duty vehicle road transport (LDV, which include passenger cars in this study and HDV respectively) show high FF and IF too, but whereas the FF is higher for HDV than for LDV, the IF is lower for HDV than for LDV.

Two other labels that stand out are International Shipping (IntShip) and Other Countries. They differ from the other labels in the sense that they do not have emissions over Germany; instead they are calculated by dividing the average concentration over Germany by the emissions in the non-German part of the model domain. The chosen domain size thus influences which emissions are included in this calculation and consequently the values of these factors. We still include them here as a reference, although they cannot be compared directly to the factors for the German labels for this reason.

3.3.1 Emissions and concentrations per label

Figure 19 shows the total PPM$_{2.5}$ emissions over 2015-2018 for each label. Clearly, emissions from residential combustion are the highest for all federal states that are labeled. They are followed by the emissions from road transport – light duty vehicles for the labeled federal states. Over Germany as a whole, industrial emissions are large, both from industrial stacks and from diffuse sources. Absolute numbers of emissions are lowest for both agricultural labels, as well as for road transport – heavy duty vehicles and German shipping.

Figure 19: **Total emission, average concentration, FF and IF of PPM$_{2.5}$ for each label over the German domain. Other Countries emission is 250 kTon and concentration 1.9 µg/ m³**
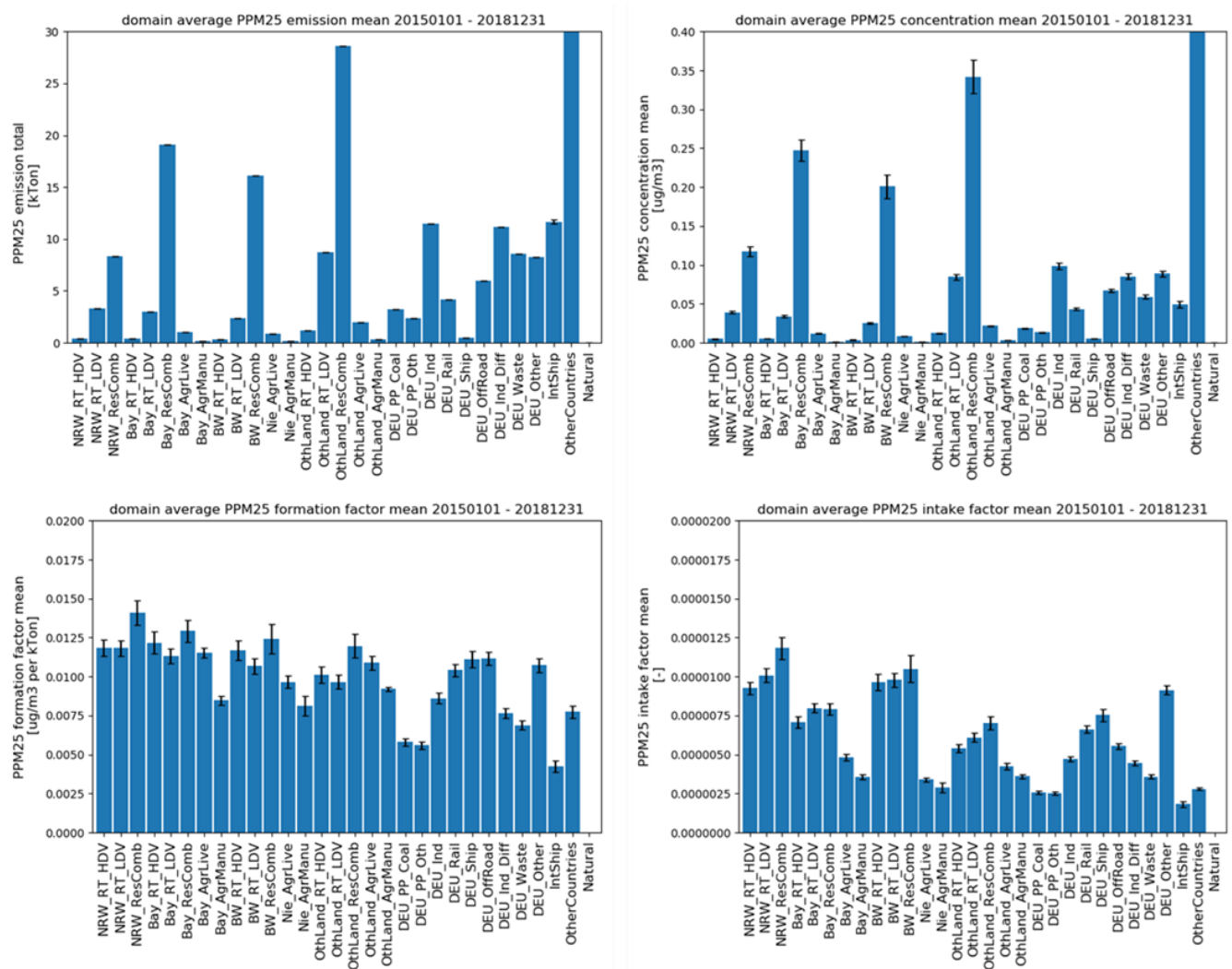
Source: TNO

The resulting contribution of domestic emissions to the PPM$_{2.5}$ concentrations over Germany is highest for residential combustion. Emissions from Other Countries show the highest contribution overall, with 1.9 µg m^{-3}. There are no natural emission sources of PPM$_{2.5}$ (sea salt and dust are not included in the simulations). For the other labels, the concentrations generally follow a similar pattern as the emissions. However, there are some deviations from this pattern too, which are discussed in the following section.

Since the base emissions for 2015 are used for the simulations for all years, there are no differences between the total emissions per label per year. Concentration differences between the individual years are consequently small, and solely caused by the differing meteorology between the years. Since the emissions are the same for each year, the interannual differences in FF and IF are caused by the differences in concentrations only.

3.3.2   Formation factor per label

Although the absolute emissions and source contributions vary largely between sectors, the formation factor shows a relatively even distribution between the labels (Figure 19).

Residential combustion has the highest FF, which can be attributed to the above average emissions during cold and stable conditions in winter which do not favor dilution. For Nordrhein-Westfalen it is higher than for the other states that are situated in the south and the east, which is likely the consequence of transport patterns driven by differences in wind direction and speed. Other sectors that show high FF for the different federal states are road transport – heavy duty traffic, road transport – light duty and agriculture-livestock, which all have emissions close to ground level. There are a couple of Germany-wide sectors that show high FFs too: rail, shipping and off-road transport.

The FFs for large plants in the industrial and power sectors are systematically lower than those of the surface emission source sectors. The reason is that the emissions occur above the mixing layer for a substantial part of the year, which dilutes the pollutants much more and favors large range transport (and thus export outside Germany) above the boundary layer.

3.3.3   Intake factor per label

The IFs in Figure 19 show similar patterns for the different federal states as the FFs: the IF for residential combustion is the highest, followed by road transport – light duty vehicles. Both emissions take place close to where people live, which leads to these high IFs. Compared to the FF, the positions of road transport – light duty vehicles and road transport – heavy duty vehicles have flipped: the IF of light-duty vehicles is higher than or equal to that of heavy-duty vehicles, while for the FF it was the other way around, which is related to the emission in populated areas. Domestic shipping and rail transport show high IFs too.

In contrast, the IFs for the agriculture-related labels are low. For AgrManu, we have already seen that the FFs were low, which explains the low IF to some extent. In addition, for agriculture-livestock, the low IF can be explained by the livestock being kept in rural locations, away from population centers.

Overall the IFs show that there are clear differences in exposure of the population to $PPM_{2.5}$, that cannot be explained by looking at the FF only.

3.3.4   High resolution simulation

To assess the influence of grid resolution on the calculated factors, we compared the results for the year 2015 from the control run at 7x7 km^2 (referred to as D2, Table 2) to a high resolution run at 2x2 km^2 (referred to as D3).

Figure 20 shows that the differences between the D2 and the D3 results are small: the bars represent the mean values over the D2 and the D3 run for 2015 and the error bars represent the standard deviation between the mean values for each run.

Figure 20:   **Total emission, average concentration, FF and IF for each label for PPM$_{2.5}$ over the German domain.**
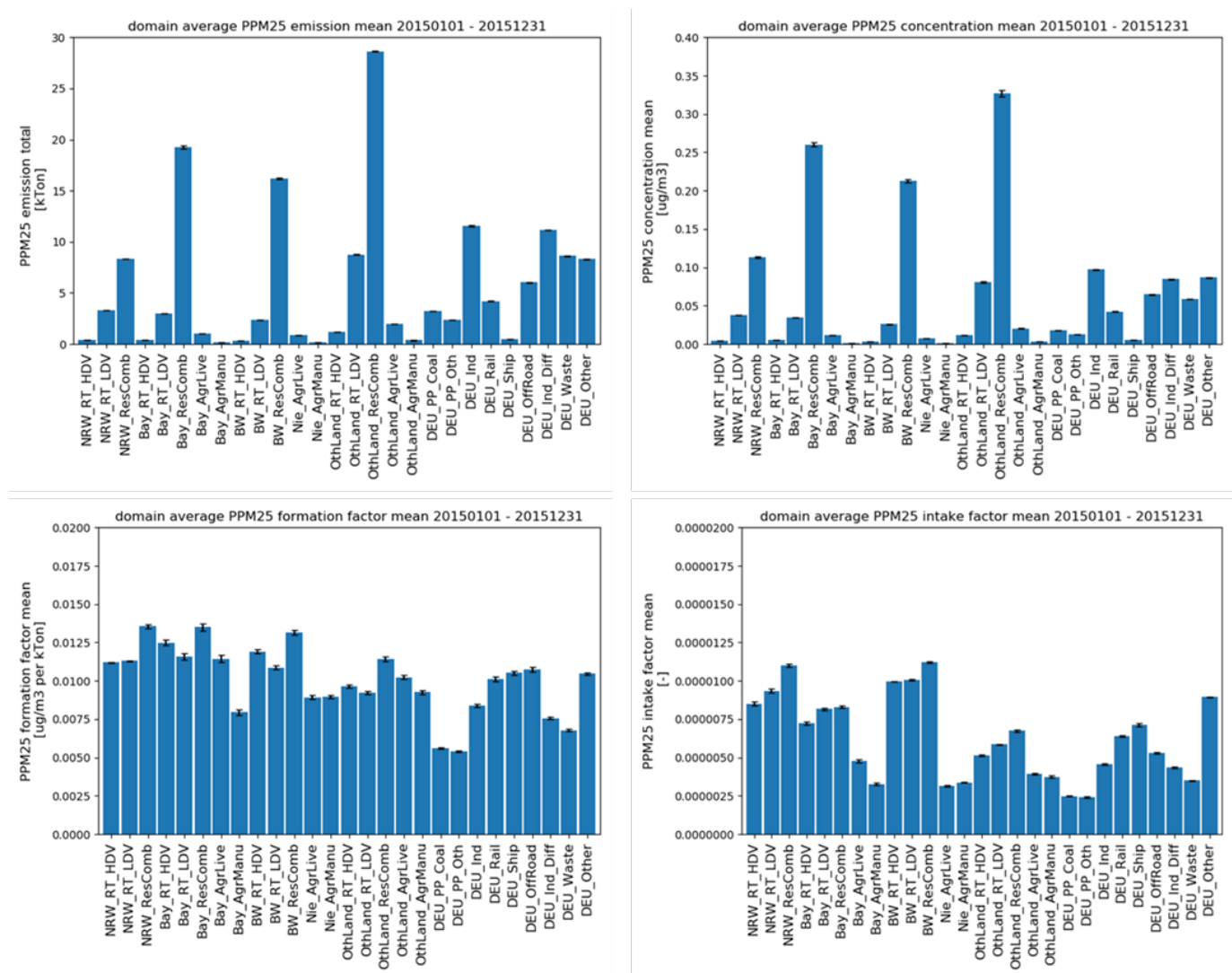
Source: TNO

The error bars show that the differences for any label are lower than 5%. These are due to boundary effects: we use shape files to retrieve the borders of federal states. These shape files are then combined with the model grid to assign emissions to a certain state. At a higher model resolution, boundaries between federal states or between Germany and its neighboring countries are resolved in more detail than at the coarse resolution, which affects the attribution of a calculated concentration to a grid cell.

3.3.5   Spatial distribution of emissions, concentration and intake

We further illustrate and explain these factors by looking at maps for a few labels, all for the year 2015. First, we selected a label that covers the whole of Germany: Offroad Transport. Figure 21 shows that peaks in emissions occur near population centers like the Ruhrgebiet, Hamburg, Berlin, Munich and Frankfurt. The concentration is spread out more evenly over the country, with some peak concentrations in the southeast. The intake, however, peaks in the large cities, where the population density is high.

Figure 21:   Emission, concentration, and intake for Off Road Transport for 2015
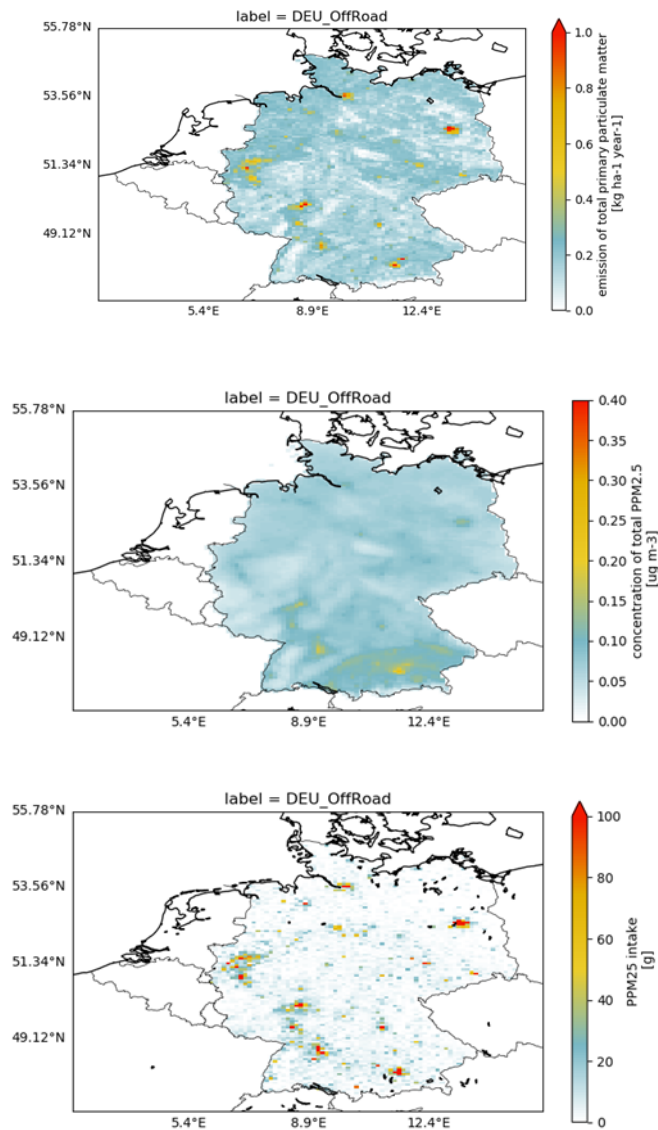
Source: TNO

Then, we have a look at a label for a single federal state: Residential Combustion in Nordrhein-Westfalen. Since Residential Combustion emissions take place in populated areas (Figure 22), the IF is the highest for all labelled sources in Germany (Figure 20). The concentrations peak around the source regions, because these emissions are released close to the surface and mainly during stable atmospheric conditions in winter, so they are not transported away efficiently. Consequently, the intake is highest too around the source regions. However, also the main population centres (e.g. Berlin, Hamburg, Frankfurt) are visible in the intake map, which reflects the cumulative volume of air breathed in by people living there, which leads to significant intake even at relatively low concentrations.

Figure 22:   **Emission, concentration, and intake for Nordrhein-Westfalen - Residential Combustion for 2015**
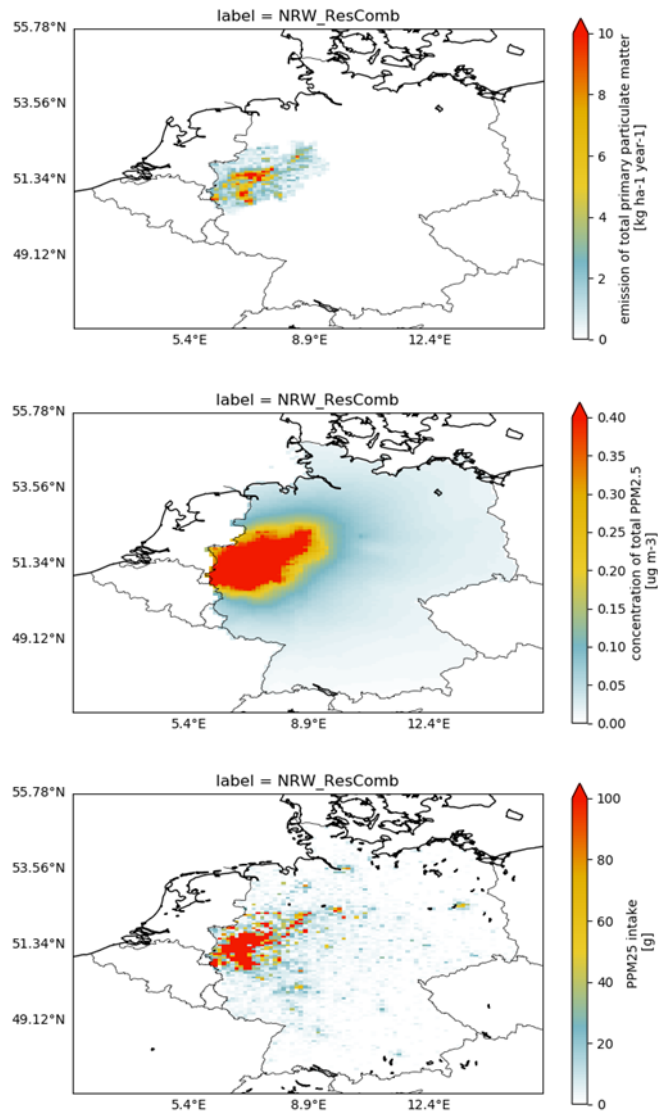
Source: TNO

A source for which emissions take place away from population centers is the agricultural sector. Figure 23 shows results for the label Niedersachsen – Agriculture-livestock. Most emissions are concentrated in the western part of Niedersachsen, which leads to concentration maxima in that area. Consequently, the FF for this label is moderately high (Figure 20). However, the IF is among the lowest for all labels, since the population density in the area is low, so most of the intake occurs in a few cities in the northwest of Germany.

Figure 23: **Emission, concentration, and intake for Niedersachsen – Agriculture-livestock for 2015 (note the difference in scale with Figure 22)**
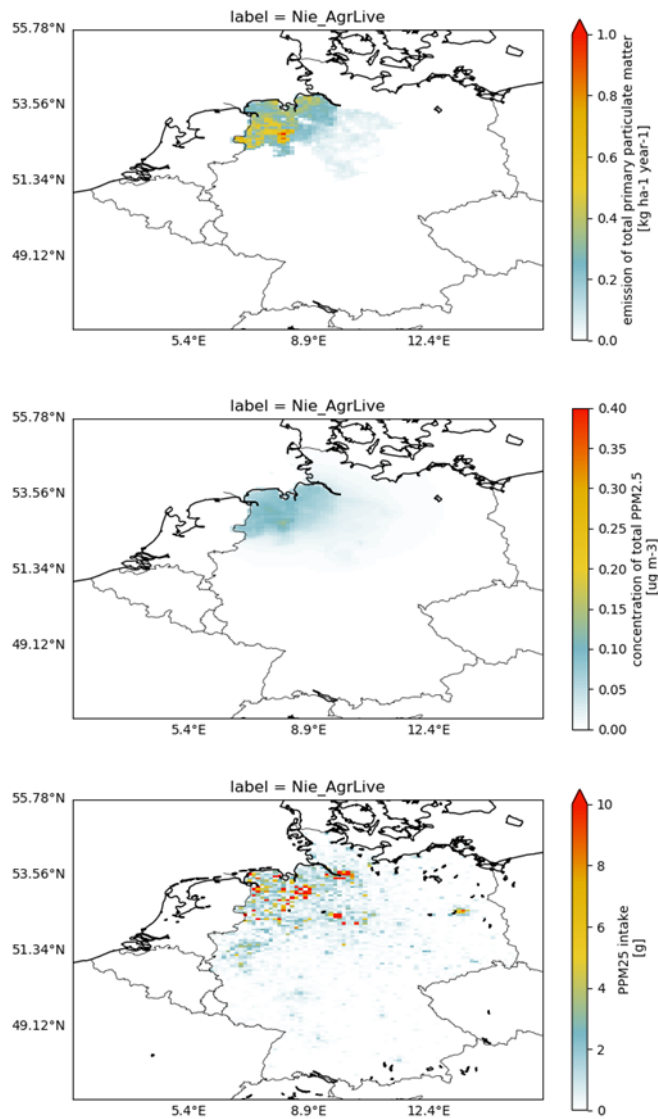
Source: TNO

Finally, to illustrate the issues in determining FF and IF for foreign sources, we show emissions from Other Countries and the resulting concentrations over Germany in Figure 24. These emissions cause higher concentrations over Germany than those from any other labelled source. The maps illustrate the difficulty in calculating the FF and IF for emissions from other countries as included in Figure 20 the choice of the domain boundaries determines which (part of) emissions in foreign countries are included, and thereby affects those calculations. Therefore, these factors should be seen as indicative only.

Figure 24:   **Emission, concentration, and intake for Other Countries for 2015 (note the difference in scale with Figure 22 and Figure 23)**
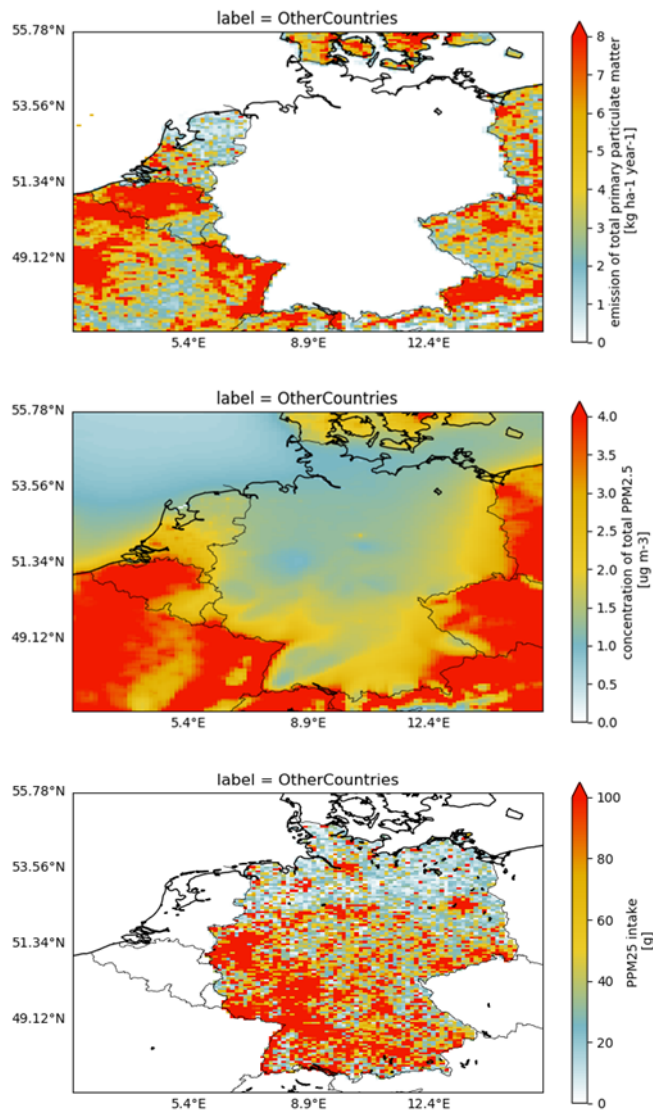
Source: TNO

For International Shipping, something similar applies. Most emissions take place over the North Sea and the Baltic Sea, and these lead to concentrations over Germany that gradually decrease from the Northwest to the South (Figure 25). Because of its proximity to emissions and large population density, the intake from International Shipping is highest in the Hamburg area.

Figure 25:   **Emission, concentration, and intake for International Shipping for 2015 (note the difference in scale with Figure 22 and Figure 23)**
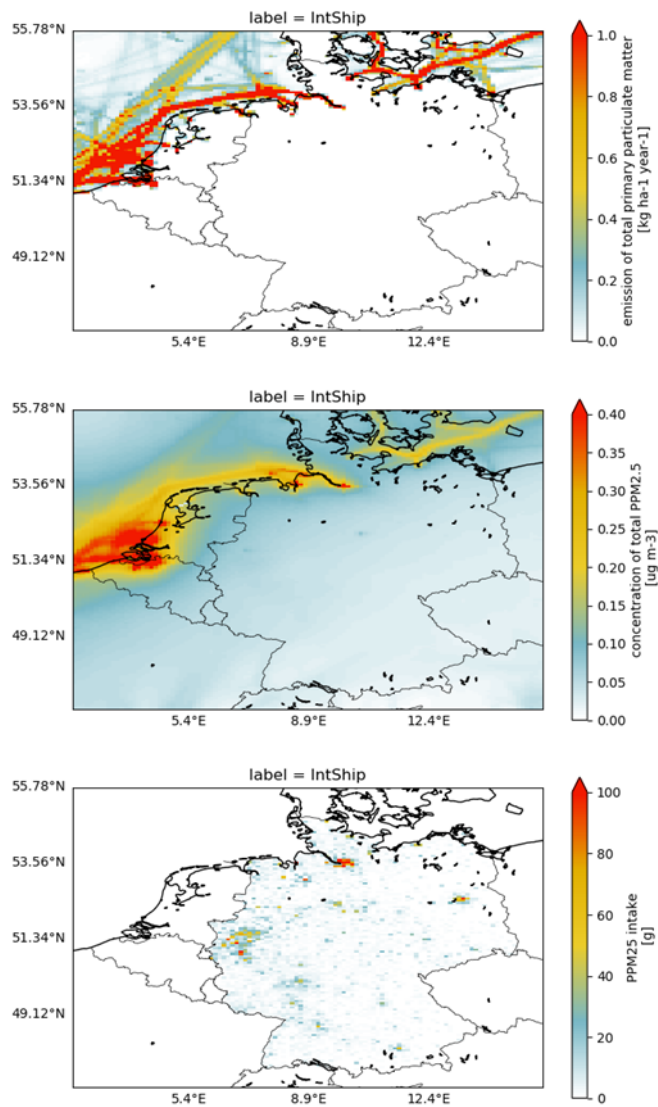
Source: TNO

3.3.6   Coarse primary PM

For coarse primary PM (PPM$_{10}$), the overall picture is similar to that of PPM$_{2.5}$, with a few notable differences (Figure 26), the bars represent the mean values over the years 2015-2018 and the error bars represent the standard deviation): there are no PPM$_{10}$ emissions for road transport – heavy duty and for international shipping. Emissions from transport are mostly coming from fuel combustion, which contributes mainly to fine PM (OC and EC). This explains why the PPM$_{10}$ emissions from domestic and international shipping are (close to) 0. For road transport, PPM$_{10}$ emissions are mostly from road, tyre and brake wear. In the GRETA emission dataset, these are much higher for LDV (incl. passenger cars) than for HDV.

German PPM$_{10}$ emissions are highest for both labels related to Industry, which is reflected in the concentrations. The highest FFs are similar as for PPM$_{2.5}$, with residential combustion followed by road transport – light duty traffic and agriculture – livestock. For the German-wide labels, domestic shipping stands out. Domestic shipping has a small PPM$_{10}$ emission (0.03 kTon), so it is

hard to see in the figure. Combined with a low concentration (2×10^{-4} µg m^{-3}) for this sector, this still gives a high FF.

Figure 26:   **Total emission, average concentration, FF and IF of PPM$_{10}$ for each label over the German domain. Other Countries emission is 92 kTon.**
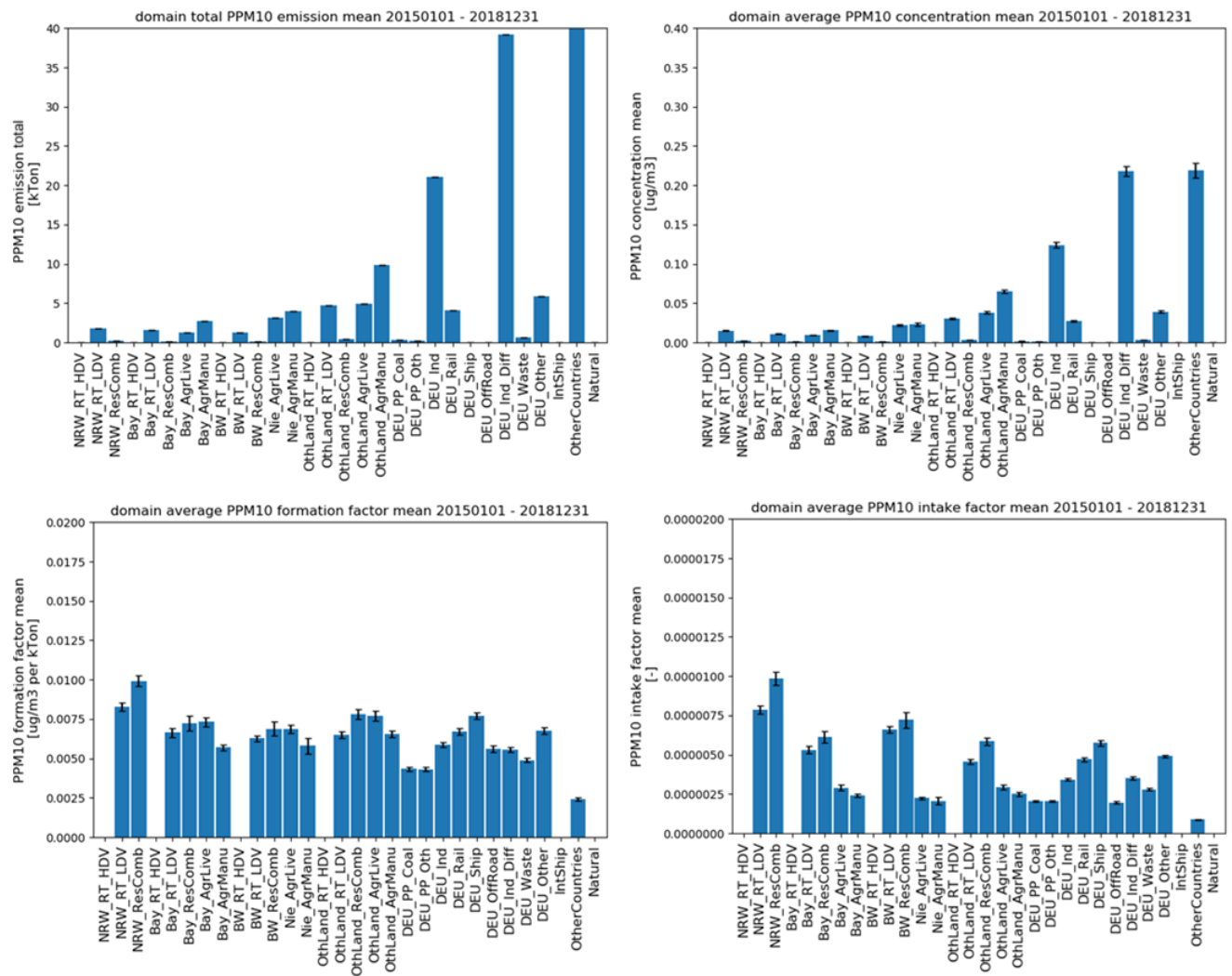
Source: TNO

The IFs for residential combustion and road transport – light duty traffic are much higher than those for agriculture – livestock, due to the emissions close to population centers. In addition, PPM$_{10}$ is removed more efficiently from the atmosphere by dry and wet deposition than PPM$_{2.5}$, which leads to shorter travel distances for the former. Shipping and rail transport have high IFs as well, which reflects their FFs. Note, however, that emission and concentration are very low for domestic shipping.

Also for PPM$_{10}$, the differences between the factors for the D2 and D3 run are small (Figure 27).

Figure 27: **Total emission, average concentration, FF and IF for each label for PPM$_{10}$ over the German domain.**
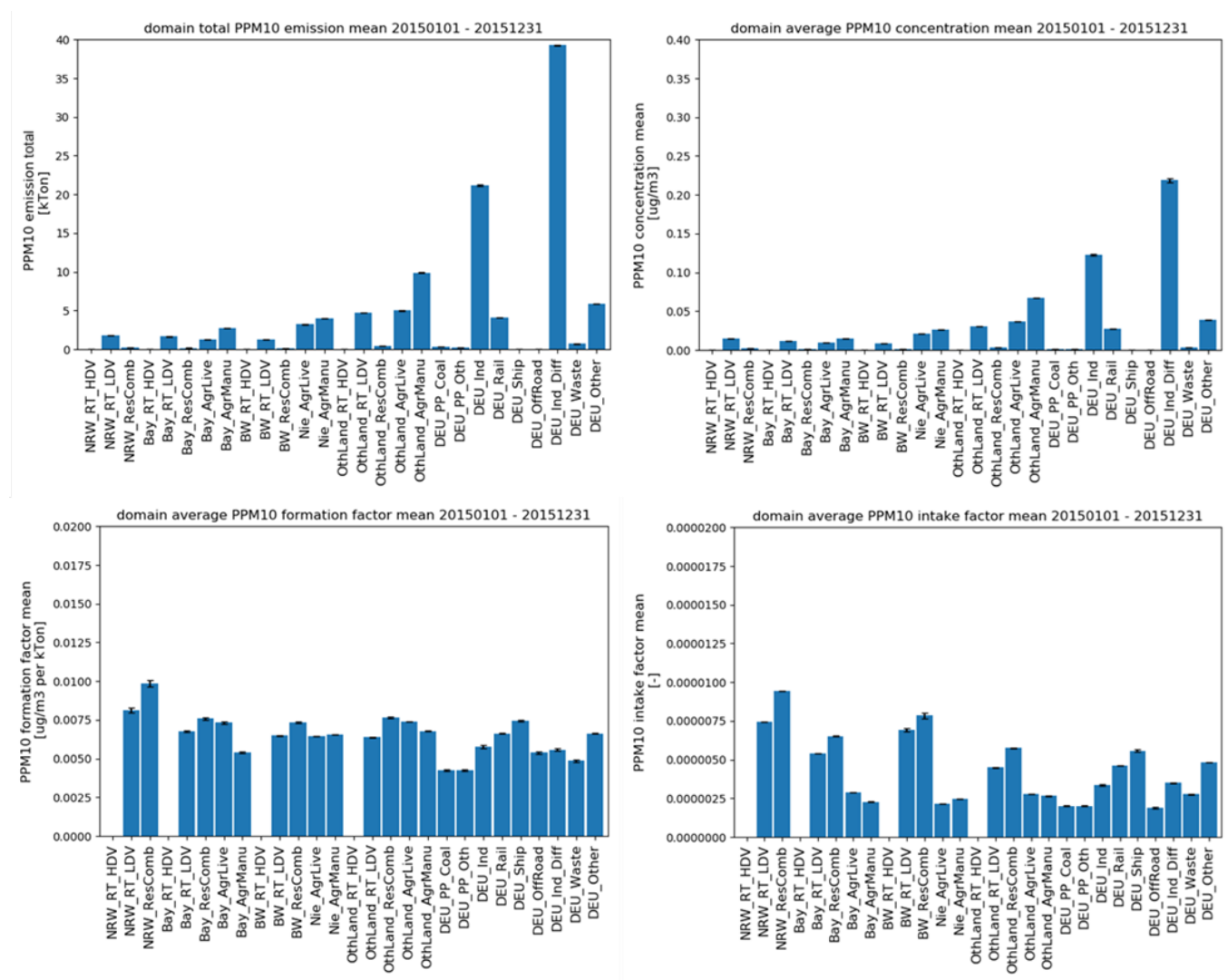
Source: TNO

3.4 Conclusions

► Total emissions and the resulting PPM$_{2.5}$ concentrations show large differences between labels. The variations in formation factors are much smaller, but clear patterns are visible in intake factors as these factors take population density into account.

► Residential combustion has a high FF and IF compared to other sectors due to its low emission height and the proximity of sources to population centers.

► Road transport – LDV (incl. passenger cars) and road transport – HDV show contrasting results for FF and IF, due to the proximity of LDV emissions to population centers. Together with Residential combustion, these labels show the highest FF and IF.

► The FF for Agriculture-Livestock is among the highest for the federal states in which this sector was labeled. However, the IF for this source is among the lowest for all labels, due to the distance between these sources and areas with high population density.

► For OtherCountries and IntShip, FF and IF over Germany can only be approximated, but both sectors contribute significantly to PPM concentrations over Germany.

► The interannual variability in FF and IF is low over all labels, and caused by differences in meteorology. For PPM, the model resolution does not have a significant influence on the calculated annual average factors.

► For PPM_{10}, the FFs and IFs are similar to those of $PPM_{2.5}$, with some difference due to faster removal from the atmosphere and hence shorter transport distances.

► These results show how FF and IF for primary PM differ per label, and how meteorology, emission timing and height, and population distributions affect these factors. This information will form the basis for the assessment of the secondary PM factors, in which the influence of (non-linear) chemistry plays a role on top of these influences.

4   Secondary inorganic aerosol formation and removal

Secondary inorganic aerosols are aerosols that are produced in the atmosphere from reactions involving primary or secondary inorganic gases (Ansari and Pandis, 1998, Dimitris and al, 2005). Salts of ammonium (NH_4^+), nitrates (NO_3^-) and sulfates (SO_4^{2-}), form the major part of SIA composition (Putaud et al., 2010). They are formed by oxidation of NO_x and SO_2 to nitric and sulfuric acid, respectively, and subsequent neutralization by ammonia. The ammonium salts generally have particle diameters (D_p) < 2.5 μm. In case ammonia is absent, nitrate and sulfate may significantly contribute to coarse ($2.5 < D_p < 10$ μm) particle mass. As the figure below illustrates, several reaction pathways in both gas and aqueous phases contribute to the formation of the acids. The efficiency of the reaction pathways is controlled by the availability of the reactants, temperature and relative humidity, as well as pH for aqueous phase reactions. The pH dependency leads to a system in which co-dependencies exist.

Figure 28:   **Important interactions of sulfate, nitrate, ammonium and their precursors in the formation of SIA (Shah et al., 2018)**
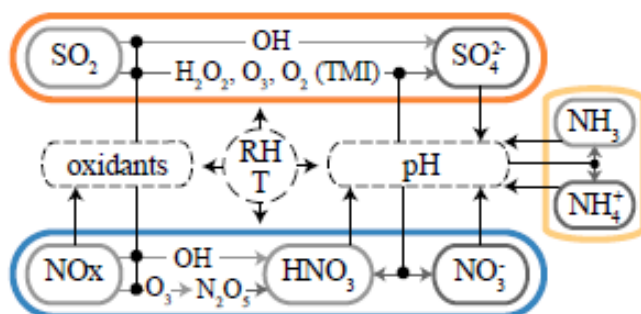
Source: Shah et al., 2018

Below, we will describe the main formation pathways of secondary inorganic aerosol (SIA) in more detail. The focus will be on understanding how emissions of NH_3, NO_x and SO_2 contribute to SIA formation, and how reducing emissions of these species affects the amount of SIA formed.

4.1   Emissions of SIA-precursors in Germany

In the table below, reported emission totals are given for precursors of SIA-formation: NO_x, NH_3, and SO_2. For ammonia agriculture is by far (>90%) the most important emission source. Minor contributions come from traffic and industry. For sulfur dioxide the combustion of sulfur containing fuels (hard and brown coal) in the energy production and industrial sectors are two main emitting sectors (together 90%). Minor contributions come from residential combustion and other sources. Note that international shipping is not included in the German national inventory, meaning that the shipping emissions in German harbors and the Kiel canal are not included in the table. Although for NO_x road transport (42%) is the most important sector, there are several sectors with important contributions. The latter include electricity and heat (energy) production as well as industrial combustion and agricultural soils.

Table 4: **Reported emissions for SIA-precursors in 2015 in kTon, based on 2019 reporting**

	NO$_x$	NH$_3$	SO$_2$
Energy	297.48	1.35	197.78
Industry	175.96	13.21	108.88
Residential combustion	56.78	1.47	15.60
Road Transport	573.32	10.77	0.81
Other Transport	49.49	0.13	1.33
Agriculture	132.98	653.13	0.0
Others	78.08	4.06	11.37
Totals	1364.08	684.12	335.77

In Figure 29, reported trends of precursor emissions are shown for different years and different reporting years. For example, NO$_x$ emissions show a declining trend from 2010 up to 2019, with a reduction of 20% over the whole period. But also a clear shift in reporting can be found from 2019 to 2020, between both reporting cycles. Emission estimates in the latest report have increased with ~10% for total NO$_x$. The main reason for the upward revision of the emission estimates for road transport was the inclusion of a temperature dependency in the NO$_X$ emissions showing increasing hot engine emissions at low temperatures. Inventoried NH$_3$ emissions are estimated to be fairly constant over the last years. Differences between reporting years due to methodological changes can also be observed for this species. Finally, SO$_2$ emissions have decreased due to the declined use of coal firing in energy plants.

Figure 29: **Reported emission totals (NO$_x$: upper left, NH$_3$: upper right, SO$_2$: lower) for Germany for different years, based on different reporting cycles**
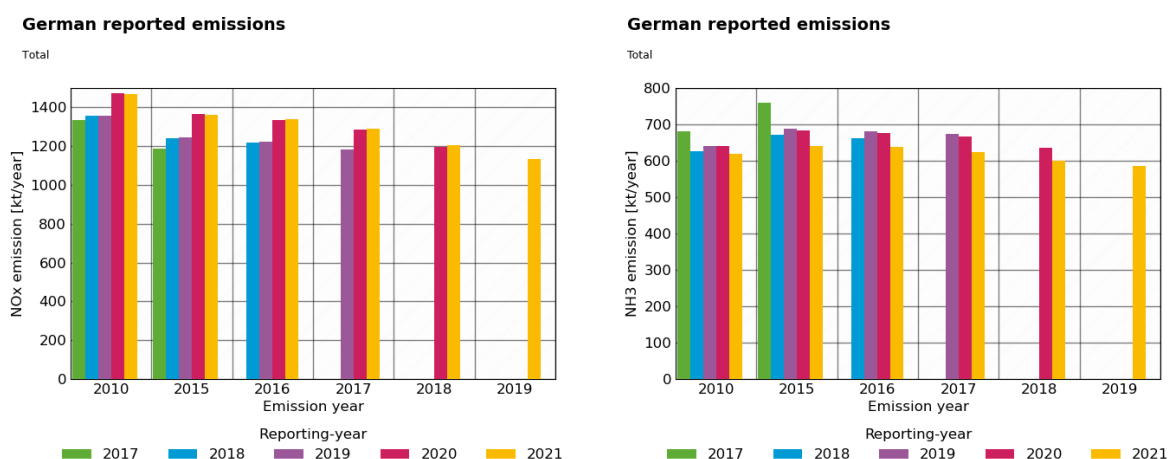
German reported emissions

Total
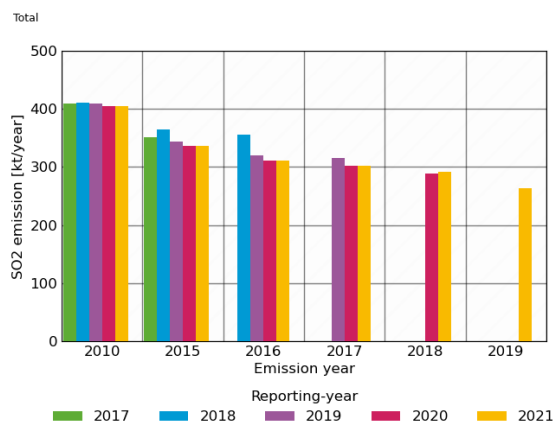
Source: TNO

After emission these species will induce the formation of SIA. The mechanism involved are discussed in the following sections.

4.2 Sulphate formation

After release in the troposphere, sulphur dioxide may be oxidised to sulphate or removed by wet and dry deposition. Traditional understanding is that the oxidation may take place in the gas phase as well as in the aqueous phase.

Gas phase

In the gas phase, SO_2 can be oxidised by the OH radical, after which it is hydrated to sulphuric acid:

$$SO_2 + OH\cdot \rightarrow HSO_3\cdot$$

$$HSO_3\cdot + O2 \rightarrow HO_2\cdot + SO_3$$

$$SO_3 + H_2O \rightarrow H_2SO_4$$
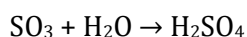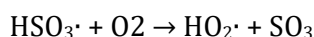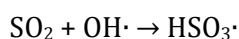
The first step in this reaction is rate limiting and the lifetime of SO_2 with respect to OH oxidation is about 1 week. The vapor pressure of sulphuric acid (H_2SO_4) is so low that its gas phase concentration is negligible. Hence, sulphuric acid will directly condense on pre-existing aerosol. This occurs where the aerosol surface area is the largest, which, under moderately polluted conditions, is in the fine mode. This explains why sulphate is normally present in the fine mode and that coarse mode sulphate is only found in environments where desert dust or marine sea salt dominate the aerosol load (by far). Under pristine conditions sulphuric acid does not have a seed to condense on and its formation may cause particle nucleation events. These nuclei grow into fine mode aerosol and thus provide a surface for condensation.

Aqueous phase

Sulphur dioxide is moderately soluble in water. After dissolution hydrated SO_2 ($SO_2\cdot H_2O$) is formed, which is an acid (sulpherous acid) and is subject to acid-base equilibria forming bisulphite and sulphite ions:

$$SO_2\cdot H_2O \rightleftharpoons H^+ + HSO_3^-$$

$$HSO_3^- \rightleftharpoons H^+ + SO_3^{2-}$$

70
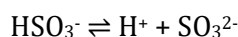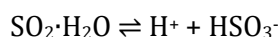
All these compounds have an oxidation state of 4 (S[IV]). The total sum of S[IV] in solution depends strongly on the (cloud) water pH, as with increasing pH the shift towards sulphite stimulates the uptake of SO_2.

Several aqueous phase chemical pathways have been identified for the conversion of S[IV] into sulphate with oxidation state 6 (S[VI]). As shown in Sarwar et al. (2013) "these pathways include the aqueous-phase oxidation of S[IV] by hydrogen peroxide (H_2O_2), ozone (O_3), oxygen catalysed by iron (Fe[III]) and manganese (Mn[II]), nitrogen dioxide (NO_2), [and] other oxidants. In environments where clouds or fogs are present, the production of SO_4^{2-} is often dominated by aqueous phase oxidation of S[IV] by H_2O_2 or O_3."

The oxidation by hydrogen peroxide is fast and not pH dependent. Moreover, the reaction rate is so fast that H_2O_2 and S[IV] in cloud water rarely co-exist, as experimental data show. Hence, the availability of either one of these compounds is rate limiting. In many models it is assumed that all H_2O_2 in solution instantaneously oxidises an equivalent amount of S[IV], when available.

The aqueous phase oxidation of S[IV] by ozone is highly dependent on pH. The reason is that the reaction rate of ozone with sulphite is four orders of magnitude faster than that of bisulphate. This oxidation pathway becomes important above pH = 5, when sulphite starts to appear in the solution. Hence, to include this formation process a variable cloud water pH in a model system is of key importance (Banzhaf et al., 2012).

Traditionally, sulphate formation mechanisms primarily include the abovementioned gas phase oxidation of SO_2 by OH radicals and the aqueous oxidation of S[IV] by H_2O_2 and O_3 (Sarwar et al., 2013). A few models also include the cloud phase production by oxidation of S[IV] by organic peroxides, and O_2 catalysed by transition metal ions (TMIs), e.g., Fe[III] and Mn[II], in cloud water droplets. The latter is considered to provide a contribution of about 15% of the total global sulphate production, which may reach values of up to 30% at higher latitudes (Alexander et al., 2009). S[IV] oxidation by oxygen in cloud water is known to be catalysed by Iron (Fe[III]) and Manganese (Mn[II]). The reaction simply reads:

$HSO_3^- + ½ O_2 \rightarrow SO_4^{2-} + H^+$

$SO_3^{2-} + ½ O_2 \rightarrow SO_4^{2-}$
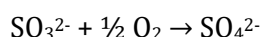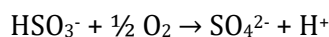
Although the reaction kinetics are not well understood, it appears the reaction rate is most important between pH 5 and 6. There are indications that organic molecules may inhibit the catalysed reactions, leading to the hypothesis that the reaction could be severely suppressed in polluted air (Brandt and van Eldik, 1995).

Although current models differ in complexity and the number of oxidation pathways they describe, almost every modelling system (CAMx, CMAQ, WRF-Chem, LOTOS-EUROS, EMEP, …) reports an underestimation of observed particulate sulphate concentrations in Europe, China and North-America. A recent comparison of the CAMS ensemble shows that sulphate is systematically underestimated (20-50%, but variable) for all models for the monitoring stations in almost all countries of Europe (see Figure 30). In comparison with the station data from Germany, the models show quite different behavior in terms of seasonality. For example, LOTOS-EUROS shows a maximum in winter and a minimum in summer, whereas for EURAD it is the other way around. The biases clearly illustrate the current state of model performances for sulphate.

Realizing this systematic underestimation, some authors assumed a first order oxidation reaction rate with a SO_2 life time of a few days to account for missing oxidation pathways (e.g. Tarrasón and Iversen, 1998; Schaap et al., 2004). The results using these simple approaches compared better with observational data than results calculated using a reaction scheme that

considers explicit cloud chemistry (Schaap et al., 2004; Renner and Wolke, 2010). The main explanation was that such a constant oxidation rate also formed sulphate during episode conditions which are normally associated with prolonged periods of cloud free conditions in Europe. In a similar direction, Zheng et al. (2015) identified heterogeneous chemistry as a potential mechanism to close the gap between observed and modelled sulphate levels in China.

Figure 30: **Overview of evaluation results for sulphate for the CAMS ensemble for 2018. The upper panel shows the seasonal cycle average over all observation sites in Germany. The lower panel shows the normalised mean bias per model and country**
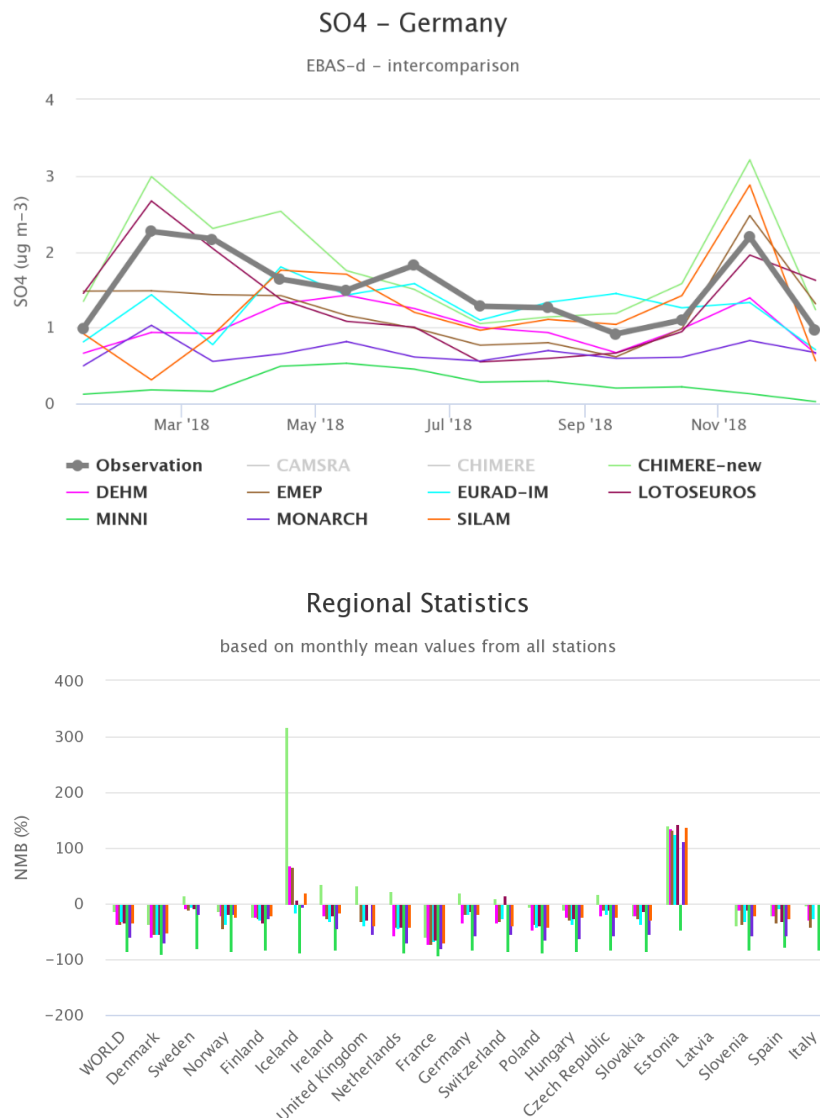
Source: Copernicus atmospheric monitoring service

Recently, a long known pathway for oxidation of S[IV] in water by NO_2 has gotten more attention:

$$2\ NO_2 + HSO_3^- + H_2O \rightarrow 3H^+ + 2\ NO_2^- + SO_4^{2-}$$
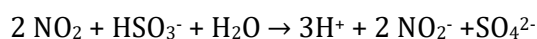
The following is mainly taken from the publication by Sarwar et al. (2013). "In many models, the aqueous-phase oxidation of S[IV] by NO_2 is generally overlooked due to the limited water solubility of NO_2. [...] There have been several studies of this reaction that indicate a range of

rate constants that differ by [several] orders of magnitude depending on experimental conditions (Lee and Schwartz, 1983; Huie and Neta, 1987; Clifton et al., 1988). [...] Littlejohn et al. (1993) adopted the higher reaction rate by Clifton et al. (1988) and suggested SO_4 production from the reaction of S[IV] with dissolved NO_2 could be comparable to the contributions from the S[IV] + H_2O_2 reaction over a range of atmospheric conditions with high NO_2 concentrations and high aqueous phase pH." Sarwar et al. (2013) explored the reaction pathway for the US and showed that the modelled aqueous-phase oxidation of S[IV] by NO_2 increases mean winter sulphate by 4-20%, but does not increase summer sulphate (Sarwar et al., 2013). They explained their findings by the "higher NO_2 concentration and lower temperature in winter which promotes partitioning of more NO_2 into liquid cloud water, combined with the low availability of H_2O_2 and ozone in winter." They postulated that at "high NO_2 concentration, the aqueous-phase oxidation of S[IV] by NO_2 can compete with the metal catalysed oxidation pathway to affect wintertime SO_4^{2-}-production." Pandis and Seinfeld (1989) studied acid deposition for a winter episode in 1985 and suggested that "the reaction contributes considerably to the sulphate production in San Joaquin Valley of California." Sarwar et al. (2013) postulate that "the reaction may significantly affect SO_4^{2-}-production in plumes with elevated NO_x and SO_2 levels in cold weather regions [and] recommend that the reaction be included in air quality models with the lower rate constant until better experimental results become available."

Wang et al. (2016) elaborated on this and postulated that "the aqueous oxidation of SO_2 by NO_2 is key to efficient sulphate formation, but is only feasible under two atmospheric conditions: on fine aerosols with high relative humidity and NH_3 neutralisation or under cloud conditions." Hence, in polluted environments, this SO_2 oxidation process may lead to amplified sulphate production rates and result in severe haze development. With respect to the aerosol pathway, other authors argued that aerosol pH never increases above 5, making this route improbable and limiting the potential impact only through cloud chemistry. Unfortunately, as far as we know, there is no study on the potential importance of this reaction pathway for European conditions.

Several authors suggested other oxidation mechanisms in aerosol water involving H_2O_2 (Liu et al., 2020) and formaldehyde (Song et al., 2019). However, the amount of aerosol water usually ranges from tens to hundreds of micrograms per cubic meter in heavy smog, which is still several orders of magnitude lower than typical cloud liquid water content (0.05–3 g m^{-3}). Hence, the volume for aqueous reactions is considered too small to produce sulphate (Wang et al., 2021). In addition, the dissolution of SO_2 in aerosol water is limited by low aerosol water pH values. Also, these reactions consume a large amount of photochemical oxidants which are often not available during winter smog events. These smog events often occur during stagnant weather conditions with stable boundary layers and weak turbulent diffusion (Seinfeld and Pandis, 2006). Consequently, near surface precursors are not transported upward into cloud layers, and oxidants and aerosols produced in clouds at higher altitudes are not transported downward. These considerations were shown by Zheng et al. (2015), who identified heterogeneous chemistry as a potential mechanism to close the gap between observed and modelled sulphate levels in China.

Wang et al. (2021) relate the SO_2 from coal combustion to the co-emitted amounts of Manganese. They "show that the manganese-catalyzed oxidation of SO_2 on aerosol surfaces dominates sulfate formation during haze events. The mechanism [was] identified via chamber experiments, and the sulfate formation rate of this mechanism is approximately one to two orders of magnitude larger than previously known routes. In-field observations [in China] show similar temporal variations, size distributions and internal mixing state of Mn and sulfate. Furthermore, chemical transport model simulations show[ed] that the manganese-catalyzed oxidation of SO_2

on aerosol surfaces dominates sulfate formation and contributes 92.5 ± 3.9% of the sulphate (69.2 ± 5.0% of the particulate sulfur) production during haze events."

This very recent hypothesis in Wang et al. (2021) could be relevant for Germany as well, as coal combustion remains the major source for SO_2 and sulphate during smog conditions with transport from eastern Europe. It is during these conditions that model evaluations severely underestimate sulphate in central Europe (Banzhaf et al., 2015).

Furthermore, new field observations and chamber experiments have recently revealed a photochemical in-particle formation of H_2O_2, driven by illumination of transition metal ions (TMIs) and humic-like substances (HULIS). Hence, the argument of an absence of oxidants in winter may not be true which could also lead to effective sulphate production. Hence, both hypotheses need to be tested for Europe.

4.3   Nitric acid formation

After release in the troposphere, nitrogen oxides play a key role in atmospheric chemistry. As NO and NO_2 are poorly soluble, dry and wet deposition are a relatively small sink for these species. The most important removal process of NO_x is chemical transformation, mostly through the formation of nitric acid (HNO_3). The oxidation of NO_x to nitric acid occurs via several chemical pathways (Schaap, 2003).

During the day the main pathway is the reaction of NO_2 with the OH radical:

$NO_2 + \cdot OH \rightarrow HNO_3$

During the night, another important formation pathway occurs via N_2O_5 and involves the following reactions:

$NO_2 + O_3 \rightarrow NO_3 \cdot + O_2$

$NO_3 \cdot + NO_2 \rightleftharpoons N_2O_5$

$N_2O_5 + H_2O \rightarrow 2\ HNO_3$
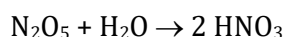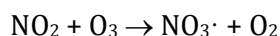
Hydrolysis of N_2O_5 takes place on the surface of aerosols and yields two equivalents of nitric acid. This pathway is not important during the day, since the NO_3 radical and N_2O_5 are readily photo-dissociated:

$NO_3 \cdot + h\nu \rightarrow NO \cdot + O_2$

$NO_3 \cdot + h\nu \rightarrow NO_2 + O \cdot$

$N_2O_5 + h\nu \rightarrow NO \cdot + NO_3 \cdot$
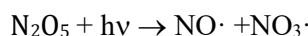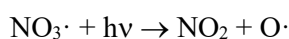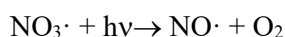
Additional pathways as the reaction of the nitrate radical with organic compounds may also yield nitric acid and/or organic nitrates during night time.

Abovementioned mechanisms are the primary pathways to nitric acid. Previous modelling studies have shown that the heterogeneous pathway dominates in winter and during nighttime, whereas the daytime reaction is important in summer (Schaap et al., 2004). The variability is mainly driven by daylight length.

A simplified overview of nitrogen oxide chemistry is presented in Figure 31. The schematic highlights the presence of two so-called reservoir species (HONO and PAN), relevant for the total budget. They are called reservoir species as the formation of these compounds "stores" NO_x, which may be released when these compounds are photolysed again. As their lifetime is relatively long, they provide a means to transport NO_x into remote areas. Note that also nitric

acid may be photolysed during daytime to reproduce NO_x. However, the reaction is so slow that most nitric acid is removed by wet and dry deposition or transferred to the particulate phase.

Figure 31: **Schematic overview of the oxidised nitrogen chemistry in the troposphere.**
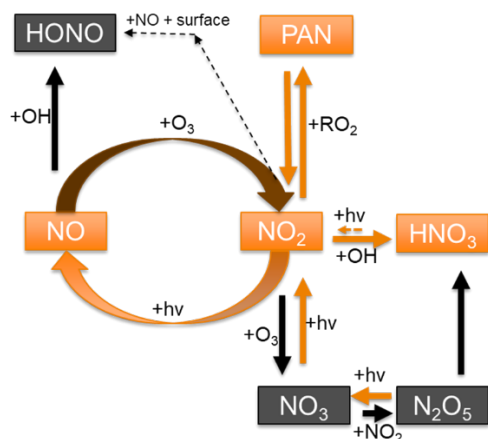
Source: TNO

4.4 SIA formation

Ammonium sulphate and ammonium nitrate are formed when H_2SO_4 and HNO_3 are neutralised by NH_3. Due to its very low saturation vapor pressure sulphuric acid directly condenses to existing particles or nucleates as new particles. Hence, virtually no sulphuric acid in the atmosphere is found in the gas phase. As sulphuric acid is a strong acid, it is readily neutralised by ammonia:

$H_2SO_4 + NH_3 \rightarrow NH_4HSO_4$

$NH_4HSO_4 + NH_3 \rightarrow (NH4)_2SO_4$
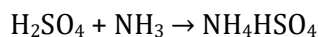
If NH_3 is available in excess, ammonium nitrate may form:

$HNO_3 + NH_3 \leftrightarrow NH_4NO_3$
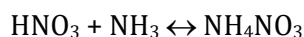
In contrast to ammonium sulphate, ammonium nitrate is a semi-volatile component (Nenes et al., 1999), "which will maintain an equilibrium with its gaseous counterparts" as showed in Schaap (2003). Furthermore, he wrote: "Due to its low vapor pressure, ammonium nitrate will condense on pre-existing aerosol, where the largest surface is available. Ammonium nitrate is therefore predominantly found in the sub-micron size fraction. Under atmospheric conditions aerosols most likely [consist of] liquid droplet[s]. In such aerosols ammonium nitrate is dissolved as a mixture of components, such as ammonium sulphate. Dissolution of nitric acid and ammonia in such highly concentrated solutions is complex and a strong function of the composition, relative humidity and temperature (Mozurkewich, 1993; Ansari and Pandis, 1998). Nitric acid, for example, will hardly dissolve in a solution of sulphuric acid. Only when ammonia neutralises the sulphuric acid, nitric acid can dissolve into the aerosol. [Hence,] Ammonium nitrate is only efficiently formed when the ammonia to sulphate ratio exceeds 2, e.g. all the sulphate is present as ammonium sulphate. This behavior of ammonium nitrate is illustrated in Figure [32], where the amount of nitrate in an aerosol is shown as a function of temperature and ammonia availability." The results have been calculated with the thermodynamic equilibrium module ISORROPIA. "At high temperatures, i.e. in summer, much more ammonia is needed to arrive at a certain ammonium nitrate concentration as compared to the winter. Therefore,

ammonium nitrate concentrations [show] a strong seasonal signature" in most regions, including Germany.

Figure 32:   Ammonium nitrate formation as a function of the molar ratio between the total available ammonia over sulphate at different temperatures (RH = 80%).
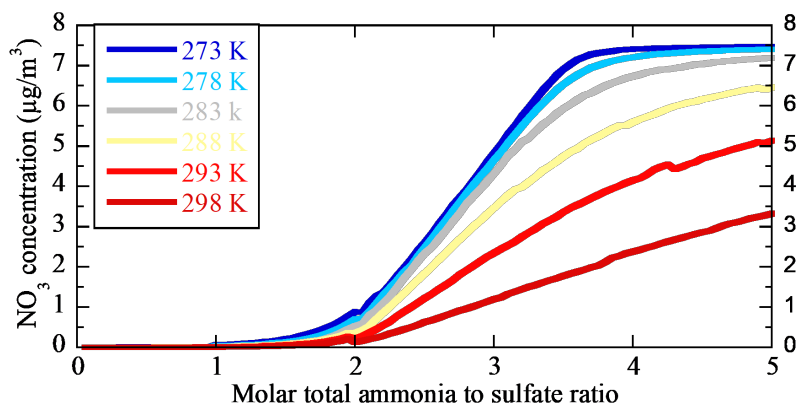
Source: Schaap, 2003

The competition for ammonia leads to a non-linear response in total SIA mass when precursor emissions and their ratios change. At low temperatures, ammonium nitrate is stable and the formation is limited by the availability of either nitric acid or ammonia. At higher temperatures the formation efficiency is highly sensitive to both precursors. This means that the SIA formation can be limited by both precursor emissions. In reality, the dependencies shift through time as the meteorological conditions and emission situation changes within a day and from day to day. Hence, the equilibrium conditions vary from region to region and from season to season.

Coarse mode nitrate and sulphate

As already written in Schaap (2003), "Sea salt acts as a sink for nitric acid and [sulphuric acid and] may provide a surface on which N_2O_5 may hydrolyse. Reaction with nitric acid causes HCl to be liberated:

$NaCl + HNO_3 \rightarrow NaNO_3 + HCl$
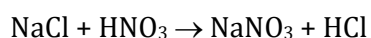
In contrast to ammonium nitrate, sodium nitrate is a non-volatile compound under atmospheric conditions. Partitioning of nitric acid into sea salt is therefore irreversible. Most of the sea salt mass and surface, and therefore the resulting nitrate, is located in the coarse aerosol mode (Vignati et al., 1999). Reaction of nitric acid with mineral dust also yields a stable product, e.g. $Ca(NO_3)_2$, which is also mostly found in the coarse aerosol fraction. [Hence], nitrate may be present in the fine and coarse aerosol mode, where it is associated with ammonium, and sea salt and dust, respectively. […] The size distribution of nitrate is a complex function of the ambient conditions and the concentrations of bases involved. This may result in a seasonal variation in the size of the nitrate [with fine mode ammonium nitrate prevailing in winter and coarse mode nitrate prevailing in summer], as has been observed in Spain (Rodríguez et al., 2002)".

4.5   Deposition processes

Secondary aerosols and their precursors are removed by both wet and dry deposition, albeit with considerable variability in effectiveness, depending on the properties of the compounds. Below the main processes are outlined shortly, along with the controlling parameters and interactions between pollutants for both processes.

Wet deposition

76

Wet deposition is the removal of atmospheric gases and particles by precipitation events. The two main wet deposition processes are in-cloud and below-cloud scavenging. In-cloud scavenging, also called rain-out, is the process where condensation of humid air forms cloud droplets on aerosol particles. Subsequently, water soluble gases may dissolve in the cloud water. In case cloud droplets rain out, the material is lost to the surface. While falling through the air column below the clouds, further gases and particles may be incorporated into droplets due to impaction (particles) or dissolution (gases). This process is called below-cloud scavenging, or wash-out (Banzhaf et al., 2012). The removal of particles depends mostly on their size, as impaction and diffusion are the main mechanisms for the particles to be "caught" by the falling droplets. Below-cloud scavenging is an effective way to remove water soluble gases from the atmosphere, as the removal efficiency is governed by their water solubility (Henry constant). Hence, the efficiency with which the highly soluble ammonia and nitric acid are removed is much larger than those of medium solubility. Low soluble gases like NO and NO_2 are hardly removed by wet deposition. Note that the solubility of gases like ammonia and sulphur dioxide depends on the pH of the solution. Hence, the effectivity of removal between these compounds is connected and some models include pH dependent wet removal as well as saturation effects in their process descriptions.

A third type of wet deposition is the removal of gases or particles via early morning dew or fog. Direct deposition of wind-driven cloud water on mountain ridges known as occult deposition is also included in this process. Normally the description of this process is neglected in CTMs as there is no good process description and no information is available for the direct water deposition from meteorological models. National assessments within PINETI show that this process is of minor importance and that neglecting it will not impact the results for modelling SIA much.

Dry deposition

Dry deposition is the direct removal of atmospheric gases and particles by vegetation, soils, or surface waters (Fowler et al., 2007). The dry deposition flux of trace gases depends on the surface concentrations and the dry deposition velocity. A common way to parameterize the dry deposition velocity is the use of a resistance analogy. In a resistance model, the most important pathways along which trace gases are taken up by the surface are parameterized. The dry deposition velocity can be represented as the reciprocal sum of the aerodynamic resistance, the quasi-laminar resistance and the canopy resistance (Van Zanten et al., 2010). Here, the aerodynamic resistance describes the resistance for the turbulent transport from a given height to the surface. This resistance is lower for an instable atmosphere than for a stable one and it is lower for rough surfaces than for smooth surfaces. Hence, the aerodynamic resistances induce diurnal cycles and seasonal cycles in the dry deposition effectivity, as well as a strong dependence on surface type. This term in the deposition process affects all compounds equally. The quasi-laminar resistance accounts for transport by molecular diffusion through the laminar layer close to the surface. Although it depends on the molecular weight of the gases and particle size, this term is mostly a small part of the total resistance. Lastly, the canopy resistance accounts for the uptake at the surface itself. The surface can be a soil or a water surface, but in case of vegetation the leaves and their stomata play a key role. In principle, the efficiency of removal is determined by the reactivity and solubility of the pollutants combined with the phenology and behavior of the stomata. Stomata opening is controlled by sunlight and temperature conditions. In darkness and at extreme temperatures stomata close and this deposition pathway is shut. The same happens when plants are in drought stress. Hence, the pathway is mostly effective during daytime during the growing season (as the presence of leaves is of course a prerequisite). Given an air flux into the stomata, the water solubility determines

whether a gas is taken up by the plant. The pollutants may also stick to external surface area of a plant or tree, which is especially effective for reactive compounds like nitric acid. In case the canopy is wet the droplets in the plants may take up gases like ammonia and SO_2 effectively, although they may be (partially) released into the atmosphere again.

Note that for ammonia the surface-atmosphere exchange is bi-directional, i.e. NH_3 can be re-emitted from surfaces into the atmosphere. The reason is that ammonia has a non-zero vapor pressure over its solution. Plants, for instance, can act as a source of NH_3 when the NH_3 concentrations in their stomata exceed the ambient atmospheric NH_3 concentrations. The direction of the NH_3 flux depends on the so-called compensation point. The compensation point is defined as the NH_3 concentration at which no net NH_3 exchange takes place between the surface and the atmosphere (Nemitz et al., 2000; Wichink Kruit et al., 2012b). For plants, the compensation point is determined by the temperature, pH, and the ammonium concentration inside the stomata (Massad et al., 2008).

Finally, the dry deposition velocities of NH_3 and SO_2 are connected (Fowler et al., 2001). Again, the pH of the fluids in the system determine the rate in which either gas is dissolved. Hence, in conditions with an excess of ammonia, the SO_2 has a larger deposition velocity than in a situation with an excess of sulphur dioxide. This effect is known as co-deposition.

4.6   Understanding the budget

Understanding the concentrations and variability of secondary inorganic aerosol thus requires a good representation of the emissions, dispersion, chemistry and removal of nitrogen oxides, sulphur dioxide and ammonia and of their interactions. All abovementioned processes take place at the same time and the concentrations of precursors and SIA are resultants of these processes. For example, episodes with high ammonium nitrate concentrations in Northwestern Europe mostly occur during anticyclonic conditions in spring time. In this period, ammonia concentrations are often enhanced due to manure applications to fields prior to the growing season and relatively low mixing layers. The latter also causes enhanced levels of nitrogen oxides. During these conditions temperatures are modest, making ammonium nitrate a relatively stable compound. Combined with the absence of rain and low effectivity of the dry deposition process, the nitric acid produced reacts largely with ammonia and ammonium nitrate levels can build up very effectively.

4.7   Response of SIA concentrations to precursor emissions

Emission reductions of precursor gases may lead to shifts in the chemical regimes which affect the formation, residence time and removal of sulphur and nitrogen compounds (Banzhaf et al., 2013). This can result in a non-linear response of the SIA concentrations in the atmosphere (Fagerli and Aas, 2008). The impact of the complex interactions varies seasonally and regionally over Europe with changing emission regime. Among emission changes of SO_2, NO_x and NH_3, responses to NH_3 emission changes show the largest non-linear behavior (Tarrasón et al., 2005). Erisman and Schaap (2004) were among the first to indicate that a decrease in NH_3 emissions may entail the largest reduction potential for SIA (and therewith PM) concentrations in Europe. Several authors confirmed this reduction potential (e.g. Matejko et al., 2009; Derwent et al., 2009; Redington et al., 2009), although others indicated that other regions could have SO_2- and HNO_3-limited SIA regimes (Pay et al., 2012; de Meij et al., 2009). For example, Renner and Wolke (2010) ran modelling scenarios with changing NH_3 emissions for the SNAP-code "agriculture". They concluded that, if NH_3 levels in the air are very high, NH_3 emission reductions have only a limited effect on SIA concentrations. According to these authors, the formation of SIA in the considered modelling domain (in Germany) was limited by the precursors SO_2 and NO_x.

Bessagnet et al. (2014) studied the effects of NH_3 emission reductions on PM daily limit value exceedances over Europe. They found that the reduction of NH_3 emissions is the most effective control strategy to mitigate $PM_{2.5}$ in both summer and winter, mainly due to a significant decrease of ammonium nitrate. Moreover, the impact of ammonia emissions reduction is significantly more efficient when the emission reduction rises. These contrasting results are indicative for the complexity of modelling the formation of SIA.

A few studies have been conducted that explicitly take the role of aerosol pH on SIA formation into account. Nenes et al. (2020) developed a new conceptual framework to determine the chemical regime of PM sensitivity to NH_3 and HNO_3. In that framework, aerosol pH and associated liquid water content emerge as previously ignored parameters that drive PM formation. However, we feel that earlier work based on thermodynamic equilibrium models already accounted for these aspects. Guo et al. (2018) studied the sensitivity of NH_4NO_3 aerosol to gas-phase NH_3 and NO_x controls for a number of contrasting locations, including Europe, the United States, and China. They found that at all locations, NH_3 reduction leads to effective response in PM mass only when pH is low enough (<3).

Figure 33:   **Impact in total SIA concentration across Germany due to different ammonia emission reductions considering pH dependent cloud chemistry and pH-independent cloud chemistry.**
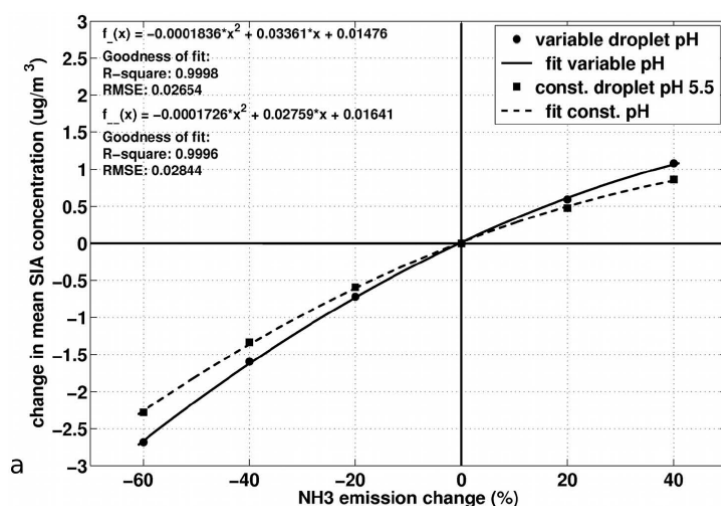
Source: Banzhaf et al. (2013)

Much of the recent literature focuses on the effect of acidity on SIA formation. Overall, these studies confirm that aerosol pH is an important driver for processes leading to PM formation, but that much remains to be learned about the exact conditions under which this influence is most relevant. In a review on the importance of acidity of cloud droplets and aerosols, Pye et al. (2020) discuss the ability of CTMs to simulate particle pH and its effect on partitioning of semi-volatile species. They find that there are large differences between models, mainly due to the differences in the composition of the mixture of species that enters the thermodynamic calculations. In addition, they note that observations of aerosol pH are sparse, due to a lack of direct measurement techniques. They conclude that cloud and aerosol pH is an area where fundamental research is needed, because their representation in CTMs has the potential to influence a wide range of predictions, including relationships between emissions and concentrations of secondary PM and its precursors.

Banzhaf et al. (2013) showed that the modelled sulphate formation increases the non-linear response to ammonia emission reductions (Figure 33) and the formation efficiency in general, while accounting for variable cloud water pH. Afterwards, they showed that the formation potential has significantly changed in the period 1990-2010, due to a sharp decline in sulphur dioxide emissions, while ammonia levels remained relatively stable. They showed that the LOTOS-EUROS model reflected a large part of the non-linear response in SO_2-SO_4 ratios observed in the EMEP network in Europe. Moreover, they showed that the amount of ammonia transferred to ammonium per unit emission declined, driven by a lower availability of sulphuric acid, while the NO_x to nitrate conversion increased for eastern European countries due to a higher availability of ammonia.

The results above call for a detailed assessment of the sensitivity of SIA to reductions in precursor emissions for Germany.

5   Organic aerosol formation and removal

In this chapter, we will review the current state of knowledge on organic aerosol (OA) formation and its removal from the atmosphere. We will also discuss the emission of the (semi-volatile) precursors that lead to it formation, with a focus on Germany, and discuss the literature that deals with the sensitivity of OA formation to its precursor emissions.

5.1   Definition of OA

Organic aerosol comprises all particulate matter (either in the liquid or the solid phase) in the atmosphere that consists of organic molecules. There is a large variety of organic compounds in the earth's atmosphere (thousands of unique species; Goldstein and Galbally, 2007), each of which can reside in the gas-phase, in the particle phase or can partition between these phases. Because of this chemical complexity, clear definitions are required for a systematic discussion on the origin and fate of these compounds in the atmosphere.

The most commonly used definitions of classes of organic compounds are based on their volatility. For the definition of non-methane volatile organic compounds (NMVOC), semi-volatile organic compounds (SVOC) and intermediate volatility organic compounds (IVOC), we refer to the naming convention for atmospheric organic aerosol as suggested by Murphy et al. (2014). These definitions are based on the saturation vapour concentrations of the organic compounds. It is possible to derive the saturation vapour concentration for individual compounds, but since in the atmosphere, there will always be a mixture of many different compounds, the saturation vapour concentration is best regarded as the empirical property of a combination of organic compounds with similar volatilities (Donahue et al., 2006). A typical schematic of the emission and chemical evaluation of organic compounds defined below is given in Figure 34.

NMVOC: non-methane volatile organic compound, with a saturation vapour concentration[1] at 298 K (C^*) $>3.2 \times 10^6$ μg m^{-3}. This includes many primary VOCs that are emitted from fossil fuel combustion and evaporation (e.g. single-ring aromatics like benzene and toluene) or from vegetation (e.g. isoprene, monoterpenes).

IVOC: intermediate volatility organic compound, with a saturation vapour concentration 320 μg m^{-3} < C^* < 3.2×10^6 μg m^{-3}. IVOCS can be primary (directly emitted) and secondary (formed from a NMVOC). Ambient IVOCs are therefore a complex mixture of organics contributed by both primary emissions and photochemical oxidation of gas-phase organics. At atmospheric conditions, they will mostly reside in the gas phase.

SVOC: semi-volatile organic compound, with a saturation vapour concentration (at 298 K) of 0.32 μg m^{-3} < C^* < 320 μg m^{-3}. These compounds partition significantly between the gas and the aerosol phase at atmospheric conditions. They can be formed by oxidation of a NMVOC or from evaporation of primary OA emissions.

Traditionally, OA has been described by just two classes: primary organic aerosol (POA) and secondary organic aerosol (SOA). In this classification, POA consisted of non-volatile organic compounds that were emitted in the particle phase, and which would not experience atmospheric processing other than dilution and deposition. Respectively, SOA included all OA that was formed in the atmosphere by oxidation and subsequent condensation of gaseous precursors (NMVOCs).

---

[1] The saturation vapour concentration is defined as the pressure of a vapour which is in equilibrium with its liquid. For organic vapours, various methods with different degrees of complexity exist for its estimation, usually based on molecular structure.

Figure 34: **Schematic of the emission and chemical evaluation of organic compounds in the atmosphere. Compounds in the particulate phase are denoted with green shading (source: Fuzzi et al., 2015)**
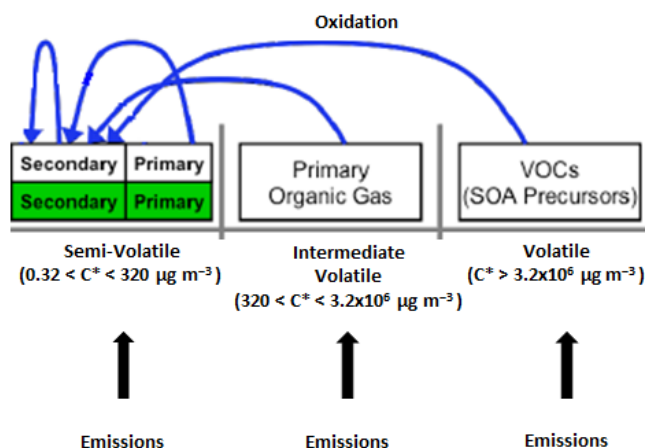
Source: Fuzzi et al., 2015

Currently, POA is defined as organic material that is emitted as aerosol under atmospheric conditions and either stays in the particle phase, or condenses back to the particle phase immediately after evaporation before any chemical transformations have taken place. To put a quantitative constraint on the POA definition, Murphy et al. (2014) defines it as "material emitted in the particle phase at an OA concentration equal to or below 320 $\mu g\ m^{-3}$ and T=298 K", although they acknowledge that this limit is somewhat arbitrary. Note that by this definition, the amount of POA formed from a certain amount of emission depends on atmospheric conditions, and will be lower, for instance, for summer than for winter conditions. So POA is semi-volatile, but how much of it will evaporate depends on the atmospheric conditions.

SOA, in contrast, is the organic aerosol that is formed in the atmosphere from a VOC after one or more generations of oxidation. Therefore, it includes OA formed from both the NMVOCs, such as toluene and monoterpenes, which have traditionally been seen as SOA precursors, as the SVOC and IVOC that originate from the evaporation of POA.

5.2 Emissions of OA(-precursors) over Germany

In general, three categories of precursors contribute to OA formation: semi-volatile POA, NMVOC from anthropogenic sources and NMVOC from biogenic sources. The latter are thought to be the most important OA precursor in Europe in summer (Jiang et al., 2019b; Bergström et al., 2012), although their emissions are quite uncertain (Jiang et al., 2019a). Concerning the emissions of the first two categories, emission inventories traditionally include POA (as a fraction of the total $PM_{2.5}$ emissions) and NMVOC emissions. Based on the literature study in the UBA Kondensaten report (Einfluss von Kondensaten auf die Partikelkonzentration, FKZ 3718 51 241 0; Coenen et al., 2022) we have a list of relevant potential sources of condensable PM including:

► Combustion of wood and coal in households

► Preparation of food (e.g. heating of fat and oil)

► Transport activities

► Specific industrial activities

The emissions of condensables are included in the emission inventories that we use in the final simulations in this project. For the sources for which additional emissions were estimated, it was determined that a total of 51.8 kTon of $PM_{2.5}$ emissions should be added to the German emission inventory for 2018 to fully account for condensable substances. Of the total 51.8 kTon, 31.2 kTon are accounted for by organic components and 20.5 kTon by inorganic components. This means that emissions would increase by 49% compared to the 104.7 kTon in the 2018 (submission 2020) inventory. Figure 35 shows the additionally suggested $PM_{2.5}$ emissions for Germany due to condensables, split between organic and inorganic part. It is found that generally the largest contributors to the organic share of additional $PM_{2.5}$ is small scale heat generation (especially wood but also coal), whereas for the inorganic $PM_{2.5}$ the picture is mixed but mostly of industrial origin. Many industrial sources are found to contribute to the inorganic fraction of condensables, the most important being power and large scale heat generation, metals production and associated processes.

Since estimates of condensable emissions are based on ratio condensable PM/ filterable PM for identified sectors, trends in estimated POA and condensable emissions follow primary PM trends.

Figure 35: **Additional PM$_{2.5}$ emissions for the main sources, split between organic and inorganic particles**
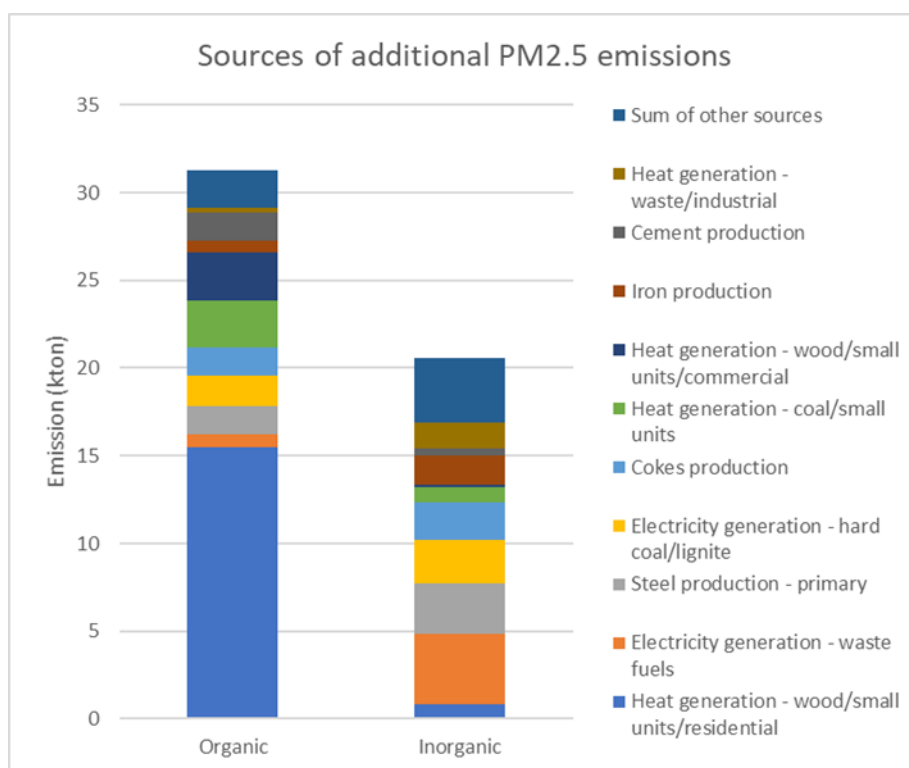
Source : Einfluss von Kondensaten auf die Partikelkonzentration, FKZ 3718 51 241 0; (Coenen et al., 2022)

5.3   Formation pathways of OA in the atmosphere

The formation of POA and SOA in the atmosphere are tightly coupled through the emission of semi-volatile POA. Before discussing the various formation pathways of SOA, it is therefore instructive to first discuss how POA is formed.

As defined in Section 5.1, POA is the semi-volatile organic material that stays in the particulate phase after emission or condenses immediately upon emission (so it includes both filterable and

condensable PM). Note, however, that the amount of POA formed from a given amount of emitted organic material depends on ambient conditions, such as temperature, dilution and the available mass of pre-existing organic aerosol in the atmosphere, since these factors determine the partitioning of the SVOC between the gas and the particulate phase. Concerning the latter, it should be noted that partitioning of semi-volatile organics is an absorptive process, which means that when a larger pre-existing mass of organic aerosol is present, more mass is available for the SVOCs to absorb into.

SOA is formed from two main categories of organic compounds that are separate species in emission inventories: 1) the part of the POA emissions (which themselves are a fraction of $PM_{2.5}$ emissions) that enters the gas phase after emission as primary SVOC, 2) NMVOC, which are completely in the gas phase just after emission. Both SVOC and NMVOC are subject to oxidation in the atmosphere and subsequently form products with lower volatilities. These secondary S/IVOC species will then partition between the gas and the particulate phase, depending on atmospheric conditions, as described above for POA. Figure 36 presents an illustrative example of the organic aerosol formation framework as included in LOTOS-EUROS, which shows the formation pathways of both POA and SOA.

Figure 36:   **Schematic representation of the VBS approach in LOTOS-EUROS. It includes the POA (brown rectangle) and SOA (orange rectangle) formation from semi-volatile OA emissions and the formation of SOA from anthropogenic (blue rectangle) and biogenic NMVOC emissions. (Source: Sturm, 2021).**
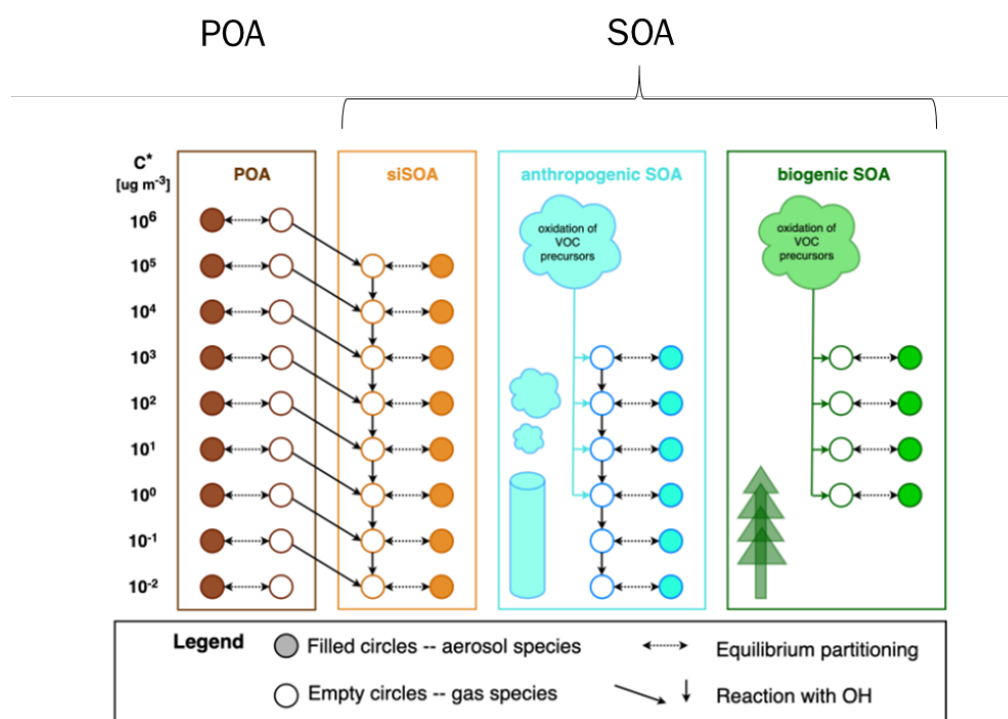
Source : Sturm,2021

5.4   Understanding the budget

The behavior of organic compounds in the atmosphere is very dynamic: they can occur in the gas and in the particle phase and move from one phase to the other due to several chemical and physical processes (Safieddine et al., 2017). Their atmospheric lifetime typically ranges between days and weeks. In the following, we will give an overview of the main processes that drive their atmospheric life cycle.

The fate of the S/IVOC depends on the phase to which it partitions. First, we will describe what happens when it stays in the gas phase after emission. If it stays in the gas-phase, it will be subject to oxidation, mainly by the OH radical (Ma et al., 2017; Shrivastava et al., 2008). Multiple generations of oxidation are possible and the competition between two processes determines the volatility of the S/IVOC: functionalization and fragmentation. Functionalization (the addition of functional groups to the carbon backbone of the molecule) moves the reaction product to a lower volatility, while fragmentation (the breaking up of the carbon backbone of the molecule) results in two or more products with higher volatilities than the parent S/IVOC (Jimenez et al., 2009). The net result of these processes will determine whether the reaction product(s) stay in the gas phase, where they can be further oxidized (ultimately down to CO and CO_2) or whether their volatility has become sufficiently low to condensate and form aerosol.

Figure 37:   **Schematic of gasSOA and aqSOA formation pathways in the gas and aqueous phases of the atmosphere. Dashed arrows denote oxidation reactions. Source: (Ervens et al., 2011)**
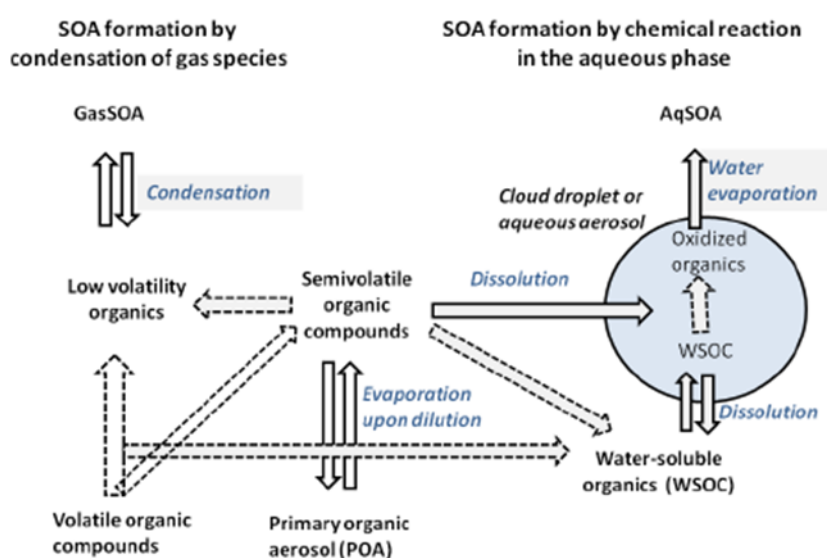
Source : Ervens et al., 2011

Dry and wet deposition are other important loss processes for SVOC. Because of their high solubility and 'stickiness' they are easily taken up by rain droplets and vegetation surfaces (Hodzic et al., 2014; Nguyen et al., 2015). Knote et al. (2015) used a chemical transport model to estimate that dry and wet deposition of SVOC result in a decrease of annual average anthropogenic SOA concentrations over the US by 48%, with the majority (~60%) removed by dry deposition.

SVOC can also dissolve into cloud droplets or aqueous aerosol and in that way form an important source of SOA (Ervens et al., 2011). However, process understanding of aqueous SOA formation pathways is still limited, and therefore its representation in CTMs is incomplete (if it is included at all; McNeill, 2015). Figure 37 shows a schematic picture of SOA formation in the gas and in the aqueous phase.

After entering the particle phase, several chemical and physical processes determine the further behavior of the organic molecule. Further oxidation of the organic compounds can take place on

the surface of the aerosol particle (heterogeneous oxidation) or within the particle (Kroll et al., 2015). How this affects the amount, composition and other properties of SOA is open to scientific investigation.

Removal of particle-phase organic compounds occurs through chemical breakdown of the aerosol or through its deposition to the land surface by wet or dry deposition. Heterogeneous oxidation occurs on aerosol particles with the competition between functionalization and fragmentation determining the net effect (Kroll et al., 2015). Fragmentation can produce high volatile compounds that consequently move back to the gas phase. Loss of organic compounds from particles also occurs through photolysis (Hodzic et al., 2016). Wet deposition is the most efficient deposition mechanism for SOA particles (Knote et al., 2015). Dry deposition only has a minor effect on OA concentrations, since most OA is contained within particles with a diameter less than 1 micron (PM1) (Jimenez et al., 2009), which is in a size range that is not very susceptible to dry deposition (Zhang et al., 2001).

5.5   Response of OA concentrations to precursor emissions

The level of scientific understanding of OA formation is lower than that of SIA, due to the complexity of the formation process and the large uncertainties in the precursor emissions. Therefore, the sensitivity of OA concentrations to emission changes has not been studied extensively.

Ridley et al. (2018) studied the trend of OA concentrations over the United States over a 23-year period (1990-2012). They attributed most of the observed decrease in OA concentration by 25-50% to decreasing anthropogenic emissions from vehicles and residential wood combustion (RWC). For Europe, Ciarelli et al. (2019) studied the trend of OA and its precursors over a 21 year period (1990-2010) by comparing outcomes of several models. Over this period, SOA from anthropogenic NMVOC decreased by 60% in these models, due to emission reductions resulting from improved emission standard for cars, among others. However, a big omission in this study is the fact that none of the applied models included semi-volatile POA emissions. All models in this study strongly underestimated OA concentrations compared to observations, due to this missing source of e.g. RWC emissions.

In addition to these trend studies, there are a number of studies that aim to quantify the contributions of different sources to OA concentrations in Europe, which give an indication of the most important emission sources and how changes in these sources may translate to concentration changes. Bergström et al. (2012) performed a number of sensitivity studies with the EMEP CTM and found that in summer, biogenic SOA and OA from anthropogenic sources and wildfires are important contributors to OA concentrations over Europe. However, the anthropogenic contribution depended strongly on the assumptions regarding the ageing of semi-volatile POA emissions, and the high uncertainty in the biogenic emissions resulted in a contribution from this source which is not well constrained. Further, they could not reproduce high OA levels in Europe in winter, and suggested that a large RWC source was missing from inventories. Subsequently, a revised emission inventory for RWC that accounts for the semi-volatile component of these emissions resulted in RWC emissions that are a factor 2-3 higher than in previous inventories (Denier van der Gon et al., 2015). Inclusion of these emissions in CTMs led to a substantially improved model-measurement agreement for OA.

The first to apply a source apportionment module to modelled OA concentrations over Europe were Skyllakou et al. (2017). For the 3 months in 2008 and 2009 that they included in their simulations, they found that in February RWC dominated, while in May the main source was biogenic and in September wildfires. Road transport was found to be a minor source (8% or less

during all 3 months). Jiang et al. (2019) applied source apportionment of OA over Europe over the whole year 2011 with the CAMx model. With their model that included an updated VBS scheme with source-specific basis sets for wood burning and diesel vehicle, they were able to capture the observed OA concentrations with a lower bias than with previous VBS versions. They found that RWC emissions dominated in winter, contributing about 60% of OA, while in summer biogenic emissions contributed 55% on average. The contribution of road traffic was small on averaged (~5%), but higher in urban areas. Other anthropogenic sources (shipping, energy production, industry, etc.) contributed 9 and 19% in winter and summer, respectively. These studies suggest that RWC is the main anthropogenic source, and that the semi-volatile POA emissions from this source thus dominate over the contribution of anthropogenic NMVOC emissions. This finding is confirmed by (Janssen et al., 2017; Thunis et al., 2021), who found that POA and SOA concentrations resulting from primary emissions are much larger than SOA from anthropogenic NMVOC in a suburb of Paris and in the Po valley, respectively.

Additionally, in a study for the Greater Paris region, Fountoukis et al. (2016) suggested that semi-volatile POA emissions from cooking can form a significant OA source over urban areas. However, these emissions are poorly quantified and their inclusion in emission inventories deserves more attention. A similar conclusion was drawn by McDonald et al. (2018), who found that NMVOC emissions from volatile chemical products, like pesticides and coatings, are overtaking transportation-related emissions as the main source of OA from fossil sources in urban areas in the United States and Europe. However, these emissions are not regularly included in emission inventories either, so quantification of their actual contribution remains a challenge.

In addition to the emission of semi-volatile POA and NMVOC, SOA formation can be sensitive to NO_X chemistry, because it affects oxidant concentrations and SOA yields from biogenic and anthropogenic NMVOC (Lane et al., 2008). This effect has not received much attention in studies over Europe, and the only study that addresses it suggests that the effect may be limited: in a study for the Po valley, Thunis et al. (2021) found that a NO_x emission reduction by 50% leads to a modelled total OA increase by about 6% (in large part due to 50% increase in SOA from anthropogenic NMVOC). This was found to be mainly through the effect that NO_x has on O_3 concentrations.

So the picture that emerges from the literature is that biogenic and RWC emissions are the main sources of OA over Europe in summer and winter, respectively. Road transport forms a minor contribution overall, but may be important in urban areas. Sources such as cooking and volatile chemical products may be important over urban areas as well, but are not well-quantified. In terms of the potential for reducing OA concentrations over Europe, the semi-volatile POA emissions seem the most promising, especially those from RWC.

6   Modelling secondary PM with LOTOS-EUROS

6.1   Model description

The 3-D regional chemistry transport model LOTOS-EUROS is aimed at the simulation of air pollution in the lower troposphere. The model (developed at TNO) is of intermediate complexity in the sense that the relevant processes are parameterized in such a way that the computational demands are modest enabling hour-by-hour calculations over extended periods of several years within acceptable computational time. The model is a so-called Eulerian grid model, which means that the calculations are performed on a fixed three dimensional grid. On this grid the concentration changes due to advection, vertical mixing, chemical transformations and removal by wet and dry deposition are performed. A sketch of such a model system is given in Figure 38. The process calculations require information about anthropogenic emissions, land use and meteorological conditions, which have to be prescribed to the model system. In this study, the model run with a horizontal resolution of approx. 7x7 km^2 over Germany. To get an adequate representation of this high resolution, 12 vertical layers will be used to get more detail in the meteorological boundary layer. The results of the model are stored in output files that contain modelled air pollutant concentrations and deposition fluxes.

Numerous applications of LOTOS-EUROS are described in literature and we refer to Manders et al (2017) for an extended overview. Apart from our own validations, LOTOS-EUROS participates as much as possible in model comparison studies in which the model performance is assessed in comparison to its peers. These exercises (EURODELTA, Mircea et al. (2019), AQMEII, Im et al. (2015), CAMS) have increased the interaction with colleagues through dedicated discussions and exchange of experiences and have contributed to the detection of model flaws and subsequent improvement.

Figure 38:   General sketch of LOTOS-EUROS CTM
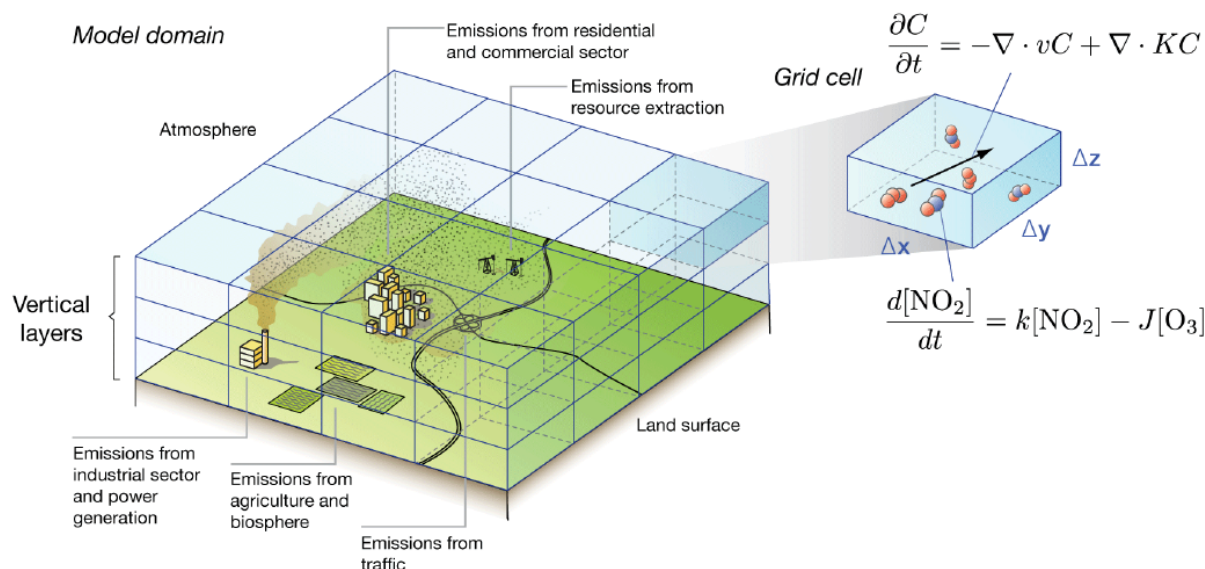
Source: TNO

The model version applied in this study follows a bulk approach for the fine (f) and coarse (c) aerosol (a) modes. The total particulate matter mass is computed from the individual model compounds:

$$PM_{2.5} = SO_{4_{af}} + NH_{4_{af}} + NO_{3_{af}} + EC_f + POM_f + PPM_f + SOA_f + SeaSalt_f + Dust_f \quad (1)$$

$$PM_{10} = PM_{2.5} + NO_{3_{ac}} + POM_c + PPM_c + 3.26 * SeaSalt_c + Dust_c \quad\quad\quad (2)$$

$$SIA = SO_{4_{af}} + NH_{4_{af}} + NO_{3_{af}} \quad\quad\quad\quad\quad\quad\quad\quad\quad\quad (3)$$

Below we describe how the model system describes the relevant processes for SIA formation and removal.

6.1.1   Emissions

The modelling of air pollution starts with the prescription of the source strengths. In this section, we describe the emissions that are used in the default version of the model. Project-specific emission datasets are described in Section 6.3.1. In the model calculations hourly emissions are required for the full modelling domain. The model either takes the emission information from an inventory or calculates them using parametrizations. The latter occurs mostly for (semi-) natural emissions.

LOTOS-EUROS contains a module that is able to process quite a number of different emission inventories. To transform the annual totals of the inventory, the model allows for different methodologies to prescribe the temporal variability. The easiest option is to use the standard time profiles specifying the variability across the month of the year, the day of the week and the hour of the day. In case more information is available, time profiles can be prescribed per country or as a dynamic grid. For a number of compounds (e.g. NMVOC, PPM) the composition of these containers are prescribed with so-called split profiles. The specification for the emissions is always different per project and goal, and are described in more detail below.

Natural emissions are required to correctly describe the ozone and oxidant formation in the gas phase chemistry and provide the natural particulate matter compounds. Biogenic NMVOC emissions are derived from the CORINE land use database which is combined with the distribution maps of 115 tree species over Europe (Köble and Seufert, 2001). During each simulation time step, biogenic isoprene and monoterpene emissions are calculated as a function of the biomass density and standard emission factor of the species or land use class (Hendriks et al., 2016. (see Table 5 for most important types; full table see Schaap et al. (2009)). Local temperature and photo-synthetically active radiation are used to calculate the hourly biogenic emissions (Beltman et al., 2013) by following the empirically designed algorithms proposed by Guenther et al. (1993) and Tingey et al. (1980). Our implementation of biogenic VOC emissions is very similar to the simultaneously developed approach by Steinbrecher et al. (2009). Alternatively, biogenic trace gas emissions can be calculated online using the MEGAN model (Guenther et al., 2006), which is operationally applied for studies outside Europe.

Emissions of NO from soils is included using the parameterization depending on soil type and soil temperature from Novak and Pierce (1993). Emissions of mineral dust (wind-blown dust and resuspension caused by traffic and agricultural practices) and sea salt are calculated on-line using meteorology-dependent relations described in Schaap et al. (2009). Sea salt emissions are calculated according to Mårtensson et al. (2003); Monahan et al. (1986) based on 10m wind speed and sea surface temperature. Hourly emissions from forest fires are taken from the CAMS global fire assimilation system (Kaiser et al., 2012).

Table 5:   **Biogenic emission factors for most important vegetation types**

Name	Biomass (g /m²)	Isoprene c oeff. (µg/g$_{DM}$/h)	Terpene coeff. (light) (µg/g$_{DM}$/h)	Terpene coeff. (mass) (µg/g$_{DM}$/h)	Reference
Arable land	1067.5	0.5	-	0.5	Karl[a]
Permanent crops	251	0.5	-	0.5	Karl[b]
Grassland	400	0.1	-	0.1	Simpson
Deciduous forest	300	10	0.2	0.2	Simpson[c]
Abies alba	1400	0.1	-	3.0	Simpson
Acer sp.	320	0.1	-	3.0	Simpson
Betula pubescens	320	0.1	-	0.2	Simpson
Eucalyptus sp.	400	20	-	3.0	Simpson
Fagus sylvatica	320	0.1	-	0.7	Simpson
Populus alba	320	60	-	-	Simpson
Pinus pinea	700	0.1	-	6.0	Simpson
Prunus avium	300	0.1	-	-	Simpson
Quercus robur	320	60	-	0.2	Simpson
Salix sp.	150	34	-	-	Simpson
Ulmus minor	320	0.1	-	0.2	Simpson

Source: Schaap et al. (2009)

6.1.2   Meteorology and transport

The standard datasets to prescribe meteorological fields and chemical boundary conditions in LOTOS-EUROS are derived from the ECMWF-IFS system. In addition, interfaces are available to drive the model using meteorology from COSMO, ICON, WRF and RACMO.

The meteorological fields are used in all process descriptions. Stability parameters are derived for each land use class separately to be able to calculate land use dependent aerodynamic resistances. The schemes used are the IFS schemes when using ECMWF meteorology. For the other systems friction velocity and Obukhov length are calculated on-line based on the land use parameters (roughness length) of LOTOS-EUROS and wind speed, solar zenith angle and cloud cover.

The advection in all directions is handled with a monotonic advection scheme (Walcek, 2000). In addition, an extended horizontal diffusion scheme is implemented to get a better representation of the concentrations at a high spatial resolution. Vertical exchange is modelled using eddy diffusivity (Kz) theory.

6.1.3   Chemistry

The gas-phase chemistry is a condensed version of CBM-IV (Gery et al., 1988), with some modifications in reaction rates and can be found in (Manders et al., 2017). A kinetic pre-processor is used which makes it relatively straightforward to add or modify chemical reactions. In the current version of the model 38 chemical active tracers are calculated with 96 reactions. Photolysis rates are used in the CBM-IV chemistry scheme. Rates are calculated for each grid cell based on solar angle, radiation and cloud coverage. For 14 different tracers in the CBM-IV scheme: O_3, NO_2, N_2O_5, HONO, H_2O_2, HNO_3, NO_3 (2x), HCHO (2x), ALD, MGLY, OPEN and ISPD, off-line derived rates are used. Those rates are based on IUPAC (Atkinson, 1997; 1999) recommendations for different wavelengths. This gas phase mechanism also describes the photochemical gas phase formation of sulfuric acid and nitric acid.

The following heterogeneous chemistry process are included: sulphate production on wet aerosol surface (Wichink Kruit et al., 2012a), in-cloud oxidation leading to formation of SO_4 from SO_2, while accounting for the pH of cloud droplets (Banzhaf et al., 2012), heterogeneous H_2O_5 chemistry, and coarse mode nitrate formation on dust and sea salt particles. These processes are all calculated using mass transfer kinetics.

The thermodynamic SIA module implemented in LOTOS-EUROS is ISORROPIA-II (Fountoukis and Nenes, 2007) scheme. It is applied to calculate the temperature and relative humidity dependent thermodynamic equilibrium between gaseous nitric acid, sulphuric acid, ammonia and particulate ammonium nitrate and ammonium sulphate and aerosol water. Equilibrium between the aerosol and gas phase is assumed at all times. Note that the module is not applied to the coarse mode aerosol as these are externally mixed. Assuming an internal mixture would erroneously transfer a lot of the nitrate to the sea salt and mineral dust fractions.

LOTOS-EUROS has recently been updated (Manders et al., 2021) to include the Volatility Basis Set (VBS; Donahue et al., 2006), which describes the formation of OA. It accounts for the formation of SOA from NMVOCs and semi-volatile POA as described in Section 5.3. The VBS in LOTOS-EUROS consists of 4 basis sets, which describe the formation and aging of primary organic aerosol (POA), secondary organic aerosol from S/IVOC (siSOA), SOA from anthropogenic NMVOC (aSOA) and SOA from biogenic NMVOC (bSOA), respectively (Figure 36).

6.1.4   Deposition of gases and aerosols

For dry deposition, a resistance approach is taken. The size dependent parameterization by Zhang et al. (2001) is implemented for particles, and for gases the DEPAC module is used (Van Zanten et al., 2010). Dry deposition velocities are not only used for the calculation of removal of species, but also to translate concentrations in the surface layer to concentrations at observations height (2.5 m) by using a constant flux approach in the lowest layer.

In DEPAC, the deposition process considers three main resistances: the aerodynamical resistance (ra), the resistance of the quasi-laminar sublayer (rb), and the bulk surface resistance (rc). The aerodynamic resistance depends on the surface roughness and friction velocity (u*), whereas quasi-laminar sublayer is also species dependent. The surface resistance can be further classified into four specific resistances: the stomata-mesophyll resistance, cuticle resistance, in-canopy resistance, and ground resistance. The ground and external resistance depend on

wetness of the surface and are temperature dependent for those compounds that deposit to snow (SO_2, NH_3). The calculation of the stomatal leaf conductance, g_sto (in nmol/m^2/s) starts with given values for the maximum stomatal leaf conductance, which then is multiplied with (reduction) factors which are a function of the phenomenological status of the plant, the light intensity, the air temperature, the water vapor deficit and the soil water content (Emberson et al., 2000). Hence, the stomata opening depends on environmental conditions and close under conditions of darkness, freezing, high temperature and drought conditions. The final calculation of the stomatal uptake also accounts for the sunlit and shaded leaf area.

For NH_3 a compensation point approach is implemented (Wichink Kruit et al., 2012b). In addition, the surface resistances for SO_2 and NH_3 are connected as a simple representation of the co-deposition effect is implemented.

Aerosol particles and trace gases are also removed from the atmosphere by wet deposition, which is distinguished between in-cloud and below-cloud scavenging. Both processes are parameterised in terms of size-dependent scavenging and collection efficiencies for particles and corresponding uptake coefficients for gases. The uptake of gases is constrained by pH dependent saturation effects as described in Banzhaf et al. (2012).

6.2   Comparison to other models

The determination of the contributions of specific emitter groups to NO_2, PM_{10}, $PM_{2.5}$, ozone and NH_3 concentrations requires the application of a chemical transport model (CTM), as NO_2 and especially ozone are predominantly formed via chemical processes. Particulate emissions are not only caused by direct emissions, but to a large extent by secondary aerosol formation, in which gaseous precursors such as NO_2, SO_2, NH_3 and NMVOC give rise to secondary particles such as sulphates, nitrates, ammonium and organic aerosol.

For the selection of one or more suitable CTMs for the dispersion calculations required in this project, an overview of CTMs commonly used in Europe was first compiled and reviewed with regard to their model properties. This comparison of process representations of secondary PM formation in 4 other CTMs includes:

► EMEP (Simpson et al., 2012)

► EURAD (Hass et al., 1995) http://www.eurad.uni-koeln.de/17224.html?&L=0

► COSMO-MUSCAT (Renner and Wolke, 2010; Wolke et al., 2012) https://cosmo-muscat.tropos.de/

► RCG (Beekmann et al., 2007; Stern, 2009)

We compared the above-mentioned models on a large number of characteristics (Table 6). When looking at the components that are most relevant for SIA-formation, we see that LOTOS-EUROS is the only one that uses the version 2 of ISORROPIA, while the other models apply version 1 of ISORROPIA or an alternative thermodynamic model. The main difference between version 1 and 2 of ISORROPIA is that the latter includes the elements calcium, potassium and magnesium, which improves the modeled partitioning of ammonium and nitrate, especially in the presence of dust. Additionally, the inclusion of the Banzhaf et al. (2012) cloud chemistry scheme in LOTOS-EUROS makes sure that the pH-dependence of sulphate formation is taken into account.

The models also employ different schemes for OA formation. LOTOS-EUROS and EMEP/MSC-W use the VBS scheme, which represents the coupled ageing, dilution and partitioning of semi-

volatile organic compounds. This enables these models to simulate the formation of POA and SOA from semi-volatile emissions in a consistent and physically realistic way, in addition to the formation of SOA from NMVOCs. In contrast, the SORGAM module, which is applied in the other models, only accounts for the formation of SOA from NMVOC. In these models, POA is considered to be non-volatile.

Table 6:   **Technical overview CTMs**

	LOTOS-EUROS	EMEP/MSC-W	EURAD/-IM	RCG	COSMO-MUSCAT
Version	2.2.002	rv4.17	NA	3.0	NA
Model-documentation	Yes	Yes	NA	Yes	Yes
Horizontal resolution	variable, lower limit about 1000m	variable, lower limit about 5000m	lower limit about 5000m	variable, lower limit ca. 500m	variable, lower limit at least 7000m
Vertical resolution	From meteorological inputs	20 sigma-Level	23 sigma-Level	variable, from ca. 4000m height	Variable, 20-60 m
Nesting	One way	One way	One way	One way	One way
Dry Deposition	Gas: DEPAC (Zanten et al., 2010) Aerosol: Zhang et al. (2001);	Simpson et al. (2012)	Zhang et al. (2003), Petroff & Zhang (2010)	Following DEPAC model (Zanten et al., 2010)	Resistance approach after Seinfeld and Pandis (2006)
Wet Deposition	Banzhaf et al. (2012), Parametrization with washout coefficients (in-cloud, subcloud)	Berge and Jakobsen, (1998), Parametrization with washout coefficients	Roselle and Binkowski (1999)	Parametrization with simple washout coefficients	Simpson et al., (2012),Parametrization with washout coefficients
Gasphase Chemistry	TNO-CBM-IV	CRI v2, CRI v2 R5, CBM_iV, CB-05, OSRM, EMEP_EmChem03, EMEP_EmChem09, EMEP_EmChem09s a.o	RACM-MIM	Carbon Bond-IV (CBM-IV) (Gipson & Young, 1999)	RACM-MIM2
Cloud chemistry	Banzhaf et al., 2012	Simpson et al., 2012	NA	Beekmann et al., 2007	Schrödner et al. 2014
Aerosol	Inorganic aerosol: ISORROPIA II; Organic aerosol: VBS	Inorganic aerosol: MARS (Binkowski & Shankar, 1995); Organic aerosol: VBS-NPAS	Inorganic aerosol: Friese and Ebel (2010); Organic aerosol:	Inorganic aerosol: ISORROPIA; Organic aerosol: SORGAM	Inorganic aerosol: ISORROPIA; Organic

	LOTOS-EUROS	EMEP/MSC-W	EURAD/-IM	RCG	COSMO-MUSCAT
		(Simpson et al., 2012)	SORGAM (Li et al., 2013)		aerosol: SORGAM
Source geometry	Point; Grid	Grid	Grid	Point; Grid	Point; Grid
Source attribution	Source Apportionment for $PM_{2.5}$ und PM_{10} (Kranenburg et al., 2013)	Through scenario runs	Through scenario runs	Through scenario runs	Marker tracer for source regions
Scenarios	Reduction factors for emissions can be specified for any country or sector (SNAP)	Possibly change of emission dataset	Reduction factors for emissions can be specified for any country or sector (SNAP)	Reduction factors for emissions can be specified for any country or sector (SNAP)	Change of emission dataset
Simulation time	1 Year	1 Year	1 Year (assumed)	1 Year	1 Year

Further, we looked into the available model intercomparison studies for SIA and OA formation, with a focus on Europe, to get a picture of how well different CTMs are capable of simulating concentrations of these aerosol components.

In the AQMEI-II model intercomparison, which included LOTOS-EUROS and COSMO-MUSCAT, Im et al. (2015) found that, sulphate was underestimated over the continental EU while nitrate and ammonium (with the exception of southern Europe) were overestimated by a majority of the models. Based on these results, they suggest that modeled ammonium nitrate formation dominates over ammonium sulphate formation, while heterogeneous sulphate formation may be underestimated in models.

Prank et al. (2016) evaluated the ability of four CTMs (including EMEP/MSC-W and LOTOS-EUROS) to reproduce the total and speciated PM mass over Europe over the year 2005 in the TRANSPHORM project. According to Prank et al. (2016) the model ensemble predicted "the highest contribution [to PM] from the summed secondary inorganic species, nitrate being [most] important in central Europe and sulfate contributing mostly in southern and eastern regions. The models adequately reproduce the observed seasonal variation of SIA and its precursors, [with the exception of HNO_3 and NH_3 concentrations]. EMEP and LOTOS-EUROS [overestimated]" the seasonal variability of HNO_3. Compared to observations, nitrate was on average overestimated, whereas ammonium and sulphate were underestimated, but much less than total PM. EMEP/MSC-W (the only model which included the VBS parameterisation) simulated the highest contribution of OC to $PM_{2.5}$ and PM_{10} of all models in the comparison, but still underestimated the contribution of OC compared to observations. Also the seasonal variations were not captured well by the model. Over all models, underestimations in simulated OC in $PM_{2.5}$ ranged from 40-80%.

As part of the EURODELTA III exercise, Mircea et al. (2019) compared 6 models for OA, including EMEP and RCG (LOTOS-EUROS was part of this study, but only participated in the model

comparison of elemental carbon). Even though only two models used the VBS approach, most CTMs predicted similar levels of total OA, irrespective of which SOA formation approach was used. This suggests that processes other than the SOA formation mechanism, such as missing IVOC emissions and heterogeneous chemistry, are the reason for this. Highest concentrations (over 6 µg m^{-3}) were simulated during cold periods with intense anthropogenic emissions. Simulated POA concentrations were highest during cold seasons. All models, except CAMx, simulated anthropogenic SOA concentrations less than 0.5 µg m^{-3}, with maxima close to sources like the Po Valley (Italy). The EMEP/MSC-W and CAMx models simulated higher contributions of anthropogenic SOA than the other models, due to the inclusion of IVOC emissions. Biogenic SOA contribution were highest during summer and autumn for all models, although large differences in absolute values exist due to different biogenic VOC emission models and land-use maps.

A comparison against aerosol mass spectrometer observations at 14 locations during two periods showed that all models underestimate SOA concentrations (measurements ranging from 2.0-2.6 µg m^{-3} between periods), while most overestimate POA concentrations (0.6-0.8 µg m^{-3}), leading to a net underestimation of total OA levels.

6.3 Model setup

In this study we first apply LOTOS-EUROS on a European domain (D1) with a horizontal resolution of 0.5° (longitude) and 0.25° (latitude) corresponding to about 28 x 32 km^2 (Table 7). An increased resolution is then obtained for a nested domain (D2) covering Germany with 0.125° (longitude) and 0.0625° (latitude), approximately 7 x 8 km^2. The nested approach is taken to account for the long range transport of air pollution from important source regions outside our domain of interest.

6.3.1 Description of emission sets used in final LOTOS-EUROS runs

In the final set of simulations that we run with LOTOS-EUROS, we applied a set of more advanced emission datasets than in the simulation that we used for the primary PM (Section 3.2). Here we describe these datasets and the reasons for choosing them.

The main reason for using new emission datasets is the availability of datasets that include the emission of condensable species, which can form a significant contribution to modelled (in)organic aerosol. We refer to the UBA Kondensaten project (Coenen et al., 2022) for a detailed description of how the emissions of condensables were developed.

In organic aerosol modeling, traditionally separate sources of POA and SOA were assumed. The former were assumed to be emitted in the particle phase directly, to be non-volatile and chemically inert. SOA was assumed to be formed by the partitioning between the gas and the particle phase of the semi-volatile oxidation products of anthropogenic and biogenic NMVOC.

However, this view has changed over the last 15 years, and we now know that emitted POA consists of semi-volatile organic compounds (SVOC), meaning that they can (partly) evaporate upon emission, be oxidized in the atmosphere and subsequently lead to the formation of SOA. The remaining part of the SVOC either stays in the particle phase or condensates directly after cooling down, thus forming POA. Moreover, it was found that in addition to the semi-volatile POA emissions, large amounts of intermediate volatility organic compounds (IVOC) are emitted, which were not included in traditional emission inventories.

This means that to be able to accurately model POA and SOA concentrations in the atmosphere, both the semi-volatile nature of emitted POA (SVOC) and the emissions of IVOC need to be taken into account. To date, no emission datasets for the European and German domain exist which

include S/IVOC emissions in a consistent way. However, emission datasets that include SVOC emission in a consistent way have been developed lately, both for the European domain (CAMS v5.1 REF2) and the German domain (as specified in the UBA Kondensaten project; (Coenen et al., 2022)).

Therefore, we are using the following emission datasets in this project:

► EU emissions: SVOC

- CAMS v5.1 REF2

- Available for the year 2018

- Includes SVOC (condensable) emissions from Residential Wood Combustion

- Does not include inorganic condensables

► German emissions: SVOC

- Emissions developed in the UBA Kondensaten project (Coenen et al., 2022)(Figure 39 and Figure 40)

- Available for the year 2018

- Includes emissions of SVOC and inorganic condensables in $PM_{2.5}$ and PM_{10} for relevant sectors

► IVOC emissions

- Not included in inventories yet

- Default approach: for each kTon of SVOC emissions from a sector, 1.5 kTon of IVOC emissions are added (Robinson et al., 2007)

► Volatility distribution of the emissions

- In the LOTOS-EUROS simulations, the emissions of SVOC and IVOC are then distributed over the 9 volatility bins that are applied in the VBS module. These bins span saturation concentrations over 9 orders of magnitude, encompassing the full range of volatilities of SVOC and IVOC.

In conclusion, emission inventories including SVOC emissions are available for the European and the German domain, but from 2018 onwards. IVOC emissions will have to be added to that, using an approach that is commonly used in CTM calculations of SOA formation: by assuming that IVOC scale with SVOC emissions by a factor 1.5 for all sectors.

For Germany, the GRETA (2018, sub 2022) emission dataset is provided by UBA on a high-resolution (1/60x1/120° lon-lat). For the remainder of the European domain the CAMS emission dataset (v5.1 REF2, available for 2018) is used to prescribe the anthropogenic emissions of NO_x, SO_2, CH_4, CO, NMVOC, NH_3, $PM_{2.5}$ and PM_{10} for all European countries on a resolution of 0.1x0.05° lon-lat. The CAMS dataset is based on the 2020 official country reporting of national emissions to UNECE and the EU. Within CAMS these have been disaggregated spatially using actual point source locations and strengths as well as several proxy maps for area sources (Kuenen et al., 2022).

In Figure 39, maps are shown of the annual emission totals for NH_3, NO_x, SO_2 and NMVOC. Emission totals of $PM_{2.5}$, PM_{10} and POA are presented in Figure 40. In those figures, the higher spatial resolution over Germany and the Netherlands is visible with respect to other countries. Note that the spatial distribution is distinctly different for individual compounds and sectors. For example, in the NO_x emissions the large cities, industrial areas and transport corridors are clearly visible. For ammonia the distribution shows the largest emissions in those areas with the largest animal number densities such as lower Saxony, Schleswig-Holstein, southern Baden-Württemberg and Bavaria, and abroad in the Netherlands. The sulphur dioxide and NMVOC emissions are mainly due to point source emissions for power and heat production. For sulphur dioxide, an artefact can be seen in the North Sea (top left corner), where a shipping route appears to be abruptly cut short. This was caused by the replacement of the CAMS emissions by the GRETA emissions for the region around the Kiel canal. However, this is not a problem, since this study only considers emissions on land in Germany. $PM_{2.5}$ and POM emissions have the same spatial pattern: highest emissions are found in urban areas (e.g., Berlin, Hamburg, Frankfurt) and industrial areas (e.g., Ruhrgebiet). In addition, there are elevated emissions in some rural areas (e.g., Scharzwald, Bavaria). PM_{10} emissions show maxima in the Ruhrgebiet, Niedersachsen and in urban areas in general.

For the vertical distribution of the emissions, height profiles per GNFR code are used, following the GRETA information for Germany and the approach of EURODELTA (Thunis et al., 2008) for CAMS emissions. The temporal disaggregation of emissions is done using sector-specific monthly, daily and hourly time factors. For several sectors (Households, traffic, agriculture) scientific approaches exist to improve the static emission profiles. Here, we replaced the standard emission profiles for households by a heating-degree-day approach and we replaced the standard emission profiles for traffic for an approach that account for cold starts.

Table 7:   **Settings for LOTOS-EUROS production simulations**

Simulation area	Emissions	Domain	Resolution
Europe	CAMS v5.1 REF2	-15-35 °W, 35-70 °N	0.5x0.25°
Germany	GRETA year 2018, sub. 2022 CAMS v5.1 REF2	2-16 °W, 47-56 °N	0.1x0.05°

Figure 39:   **Annual emissions for NH₃ (upper left), NOₓ (upper right), SO₂ (lower left) and NMVOC (lower right) over North west European domain**
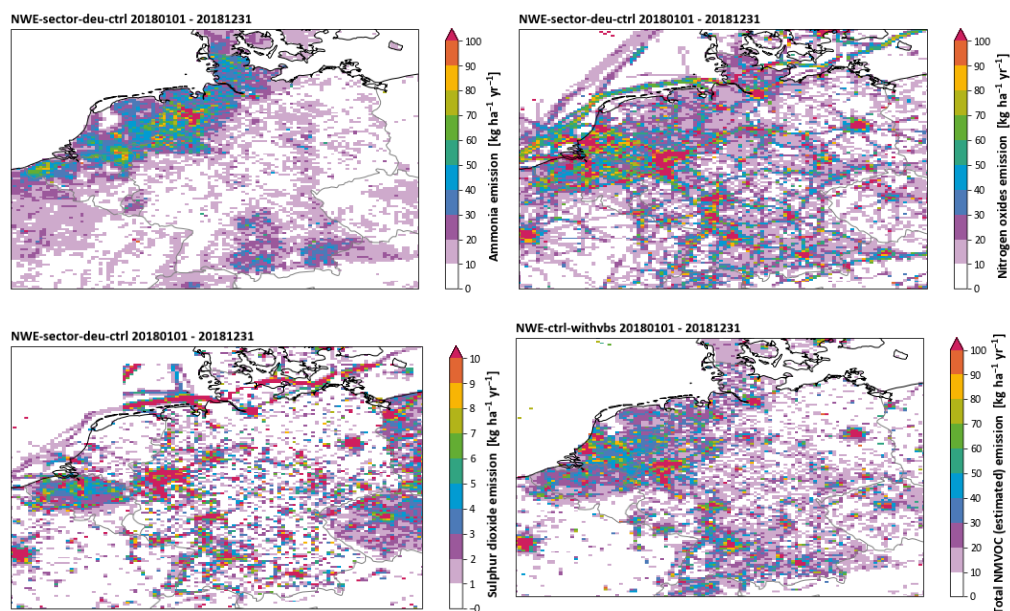
Source: TNO

Figure 40:   **Annual emissions for PM₂.₅ (upper left), PM₁₀ (upper right), and POA (lower left) over North west European domain**
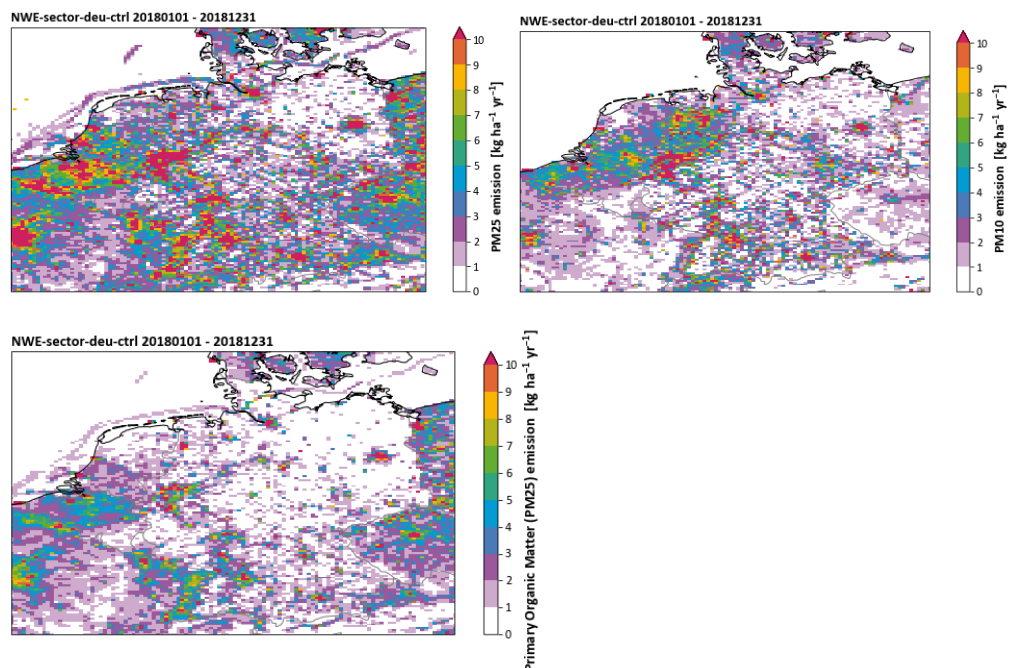
Source: TNO

To properly assess the effect of NO$_x$, SO$_2$, and NH$_3$ emissions on the concentrations of pollutants NO$_3^-$, SO$_4^{2-}$, and NH$_4^+$, a source apportionment technique is applied in the SIA simulations described below. A concise description of this technique can be found in Section 2.2.1. To be able to quantify the formation factors the contribution of all main source categories were tracked for

those located in Germany and abroad. For agriculture, a split in housing and application emissions was made and for traffic the light and heavy duty contributions were tracked separately. The labelling enabled to link the modelled concentration contributions to the corresponding emission strengths.

6.4 SIA: Base case results and validation

The results presented in this section refer to simulations performed with LOTOS-EUROS for Germany in the year 2018. The analyses are based on annual averaged values of concentrations of NO_3^-, SO_4^{2-}, and NH_4^+ over Germany during that year and total emissions of NO_x, SO_2, and NH_3 integrated over the country and the year.

6.4.1 Modelled distributions

Figure 41 presents the annual mean modelled concentrations of sulfate, nitrate and ammonium and its precursors across Germany in 2018. A general feature is that the gradients of the secondary inorganic aerosol compounds are much smaller than those of their primary emitted precursors. This is explained by the effect of atmospheric chemistry and the time scale at which this takes place.

For sulfur dioxide background concentrations of about 1.5 µg m^{-3} are modelled across most of the countries. Around regions with a high number of power plants and industrial activities (i.e. Ruhrgebiet) annual mean concentrations are well above 5 µg m^{-3}. Increased concentrations are also modelled along the Kiel canal and Saxony. Furthermore, the impact of individual power plants can be recognized in the modelled distribution. Annual mean sulphate concentrations show maxima in the Ruhr area and the Czech Republic, due to concentrated industrialized zones. Across large parts of the country the modelled values are on average between 1 and 1.5 µg m^{-3}.

In case of NO_2, modelled background concentrations range between 8 and 14 µg m^{-3}. Large concentrations are modelled for all populated and industrialized regions in the country. In fact, also some transport corridors can be recognized. Urban areas including Berlin, Stuttgart, Munich and the Main-Rhein areas as well as the Ruhrgebiet stand out as maxima. The regions with high nitrogen oxide levels do not correspond do those with the largest annual mean ammonia concentrations, because their predominant emission sources are different.

Figure 41:   **Modelled annual mean concentrations of SO₄, NO₃, NH₄ aerosol and their precursors across Germany**

Sulphur dioxide   Sulphate PM$_{2.5}$

Nitrogen dioxide   Nitrate PM$_{2.5}$

Ammonia   Ammonium PM$_{2.5}$
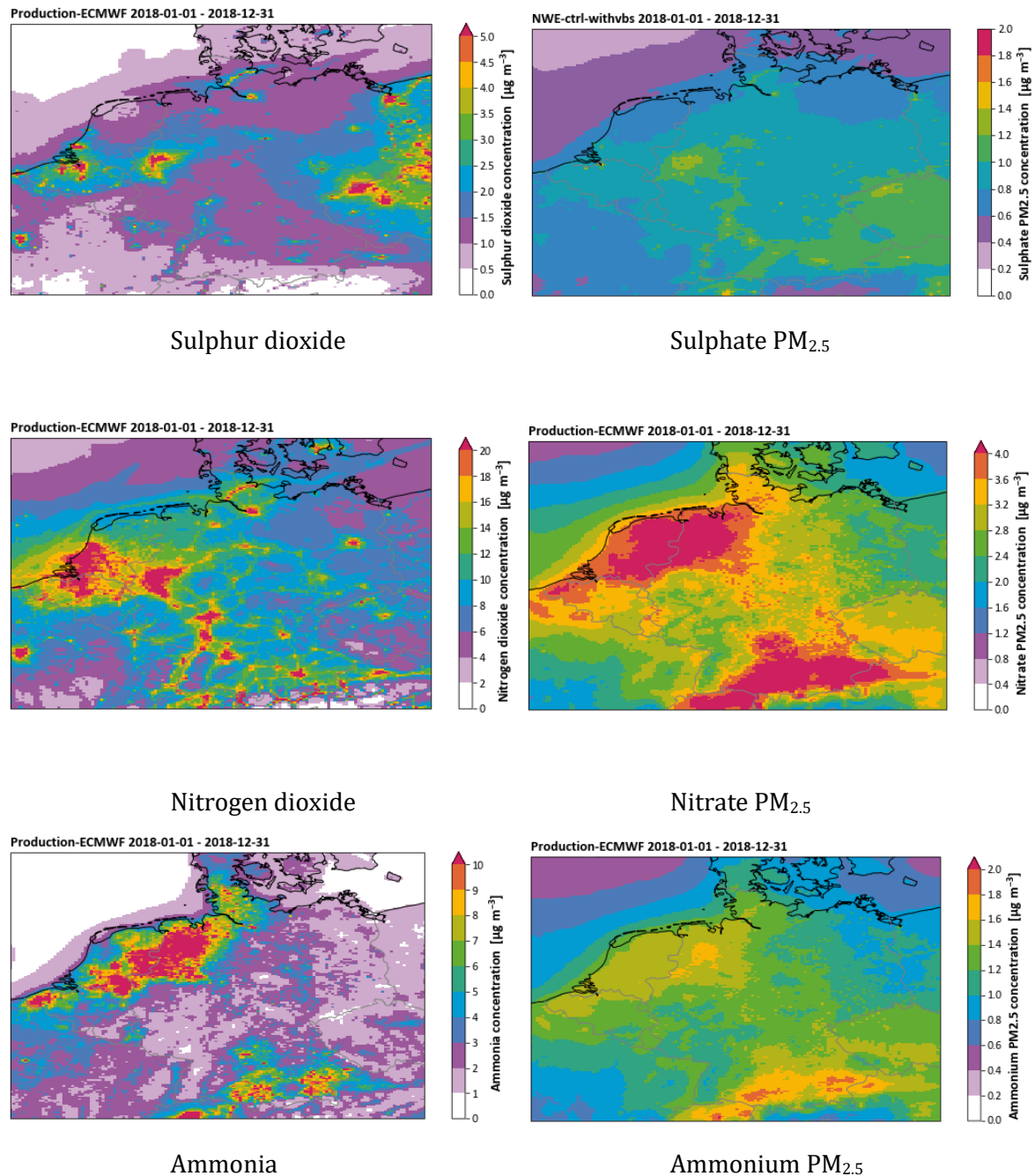
Source: TNO

Largest simulated ammonia concentrations can be found in the region with the largest animal density. The western half of lower Saxony and the northern part of North-Rhein-Westphalia are characterized with modelled ammonia levels above 8 µg m⁻³. Similar values are only modelled in small regions in the southeast of Baden-Wurttemberg and in Bavaria. In most of Germany concentrations between 1 and 3 µg m⁻³ are modelled as regional background.

Nitrate contributes the largest mass fraction to SIA levels across Germany. It might be counter-intuitive that the nitrate concentrations do not peak in the regions with the largest NO$_x$ emissions, but in those with the largest ammonia concentrations. The reason is found in the semi-volatile nature of ammonium nitrate. With a larger ammonia concentration a larger

amount of nitric acid is driven into the aerosol phase. Ammonium neutralizes both sulfate and nitrate leading to a field that shows a large correspondence with the nitrate concentration levels, albeit with less distinct gradients.

6.4.2 Comparison with observations

For the precursors NO_x and SO_2 a large network of monitoring stations exists in Germany. Measuring sulphate is a straightforward procedure. As written in Schaap (2003) "measuring sulphate [is] a straightforward procedure. Measurements of particulate nitrate are [more difficult as] most methods are not reliable because of artefacts associated with the volatility of ammonium nitrate, and the reactivity of nitric acid (Schaap, 2003). Schaap et al. (2002) made a compilation of available aerosol nitrate measurements in Europe and critically assessed their quality. Shortly, reliable data are only obtained with devices that remove nitric acid prior to aerosol sampling and stabilize the collected ammonium nitrate against evaporation, e.g. denuder filter combinations." Unfortunately, such devices are not used in Germany for monitoring purposes. Field campaigns in Europe indicate that evaporation from quartz filters is significant at temperatures higher than 20°C (Schaap et al., 2004). Hence, the obtained data from these widely used filter types in Germany for nitrate (and ammonium) are likely to represent lower limits. Positive artefacts may occur by adsorption of nitric acid on a cellulose filter or on preloaded alkaline aerosols. "In winter both evaporation and adsorption of nitric acid is thought to be small due to low ambient temperatures and low nitric acid concentrations. Hence, summertime data were found to be more uncertain than those acquired during winter" (Schaap, 2003).

Elevated stations above 700 m have been excluded for the model to measurement comparison because 1) the orography and therefore the representation of the mixing layer height in these areas are strongly parameterised in the model which makes it difficult to correctly assess in which model layer the station is located, [and 2)] the measurements may be strongly influenced by sub-grid meteorological phenomena" (Schaap et al., 2004). Furthermore, we excluded traffic stations in the evaluation of nitrogen oxides and ozone.

6.4.3 Evaluation results

In this section we provide an overview of the model evaluation results for the precursor gases SO_2, NO_x and NH_3 and the SIA components sulphate, nitrate and ammonium. The simulations are evaluated over 2018. Only data from stations that met the following criteria were included in the evaluation: at least 50% of observations should be available, the height of the stations should not exceed 700 m and for the gas-phase species the stations of the type 'traffic' were excluded, because stations close to roads may show concentration peaks that are not representative of the grid cell in which it is situated.

The scatter plots in Figure 42 compare the annual mean modelled concentrations to the observed ones for different species. The modelled mean concentrations for SO_2 are larger than those observed for most stations. This is not only the case for the higher concentration levels but also for baseline values. Inspection of the observed values on top of the modelled map shows that a large part of the variability is captured, but that the values at some stations relatively close to the Ruhr area show the largest overestimation. This is further illustrated by the time series presented in Figure 43 at station Waldhof. A systematic difference between model and observations is found throughout the year.

Figure 42: **Mean modelled and measured SO$_2$ concentration over Germany in 2018 in a scatterplot (left) and on a map (right)**
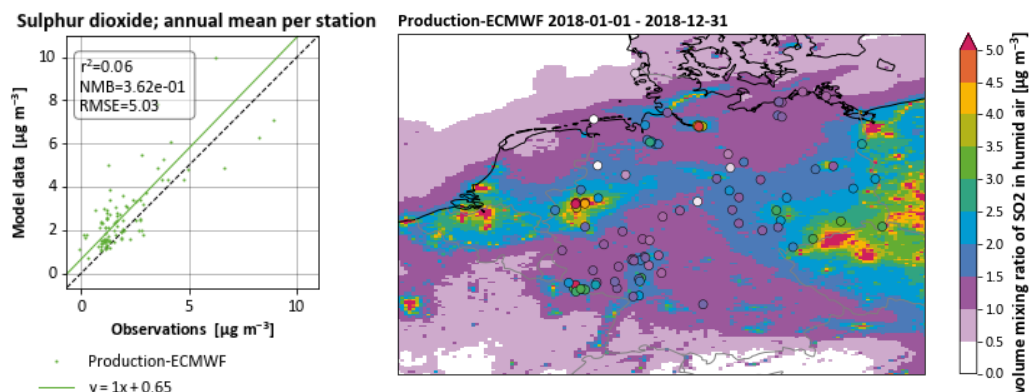
Source: TNO

Figure 43: **Time series of sulphur dioxide and sulphate concentration at station Waldhof.**
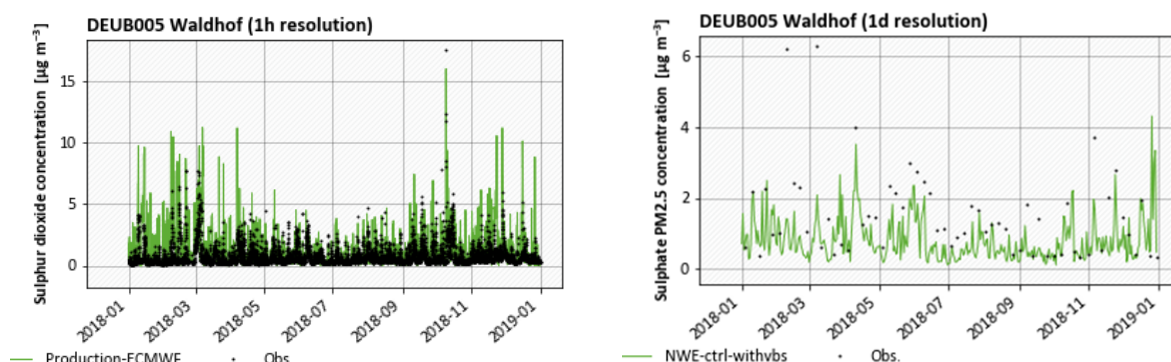
Source: TNO

Observed mean nitrogen dioxide concentrations tend to be slightly underestimated by the model. The fit line indicates that on average the underestimation is about one-eighth. Inspection of the observed values on top of the modelled map shows that many sites show concentration levels above 20 µg m^{-3} where the model only predicts half and where nearby stations indicate substantially lower observed concentrations. Hence, it may be that especially the concentrations in the urban background of small sized cities and towns are not captured as the model smears these emissions out across a 7x7 km^2 area or several of these when the grid cell boundary cuts through such a city. As is illustrated by the time series at Eisenhüttenstadt (Figure 45) in an industrial area, both NO$_2$ and particulate nitrate show a strong seasonal cycle with a summer minimum, which is captured well in the model. For both compounds an overestimation in the April months is apparent at many stations, the reason is yet unclear.

Figure 44: **Mean modelled and measured NO₂ concentration over Germany in 2018 in scatterplot (left) and on a map (right)**

Source: TNO

Figure 45: **Time series of nitrogen dioxide and nitrate concentrations at station Eisenhüttenstadt.**
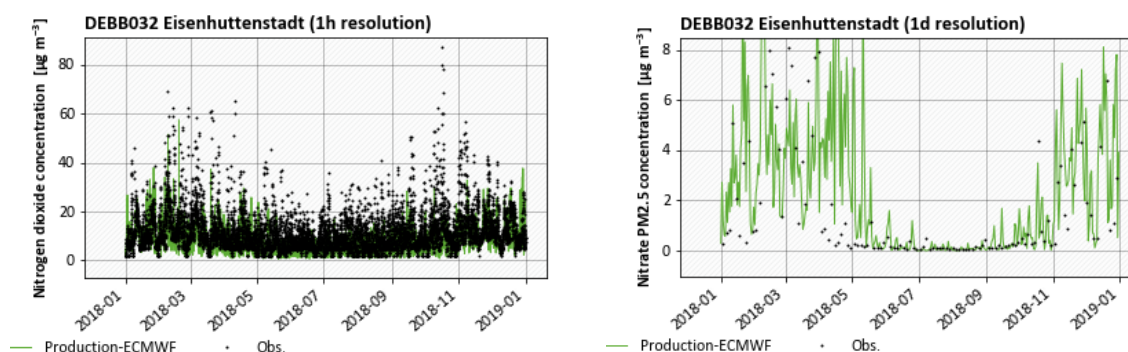
Source: TNO

Ammonia concentrations are relatively well represented by the model, with the caveat that there are only a few stations with reliable observation data. Regional background concentrations are found between 1 and 4 μg m⁻³. The highest simulated concentrations can be found in the northwest and the southeast, but these high concentrations are only reflected in lower Saxony.

The station at Zierenberg (Figure 47) shows an overestimation in early summer. This may be caused by the fact that measurement stations are commonly placed at a distance from the sources. Inspection of the seasonal cycle shows an overestimation of ammonia in spring time, and a slight tendency to underestimate summer concentration levels. Hence, it seems that the application emissions are too strongly appointed to the start of the growing season. The modelled ammonium concentrations tend to be close to the observed ones (example shown at Waldhof, Figure 47).

Figure 46: **Mean modelled and measured NH₃ concentration over Germany in 2018 in scatterplot (left) and on a map (right)**
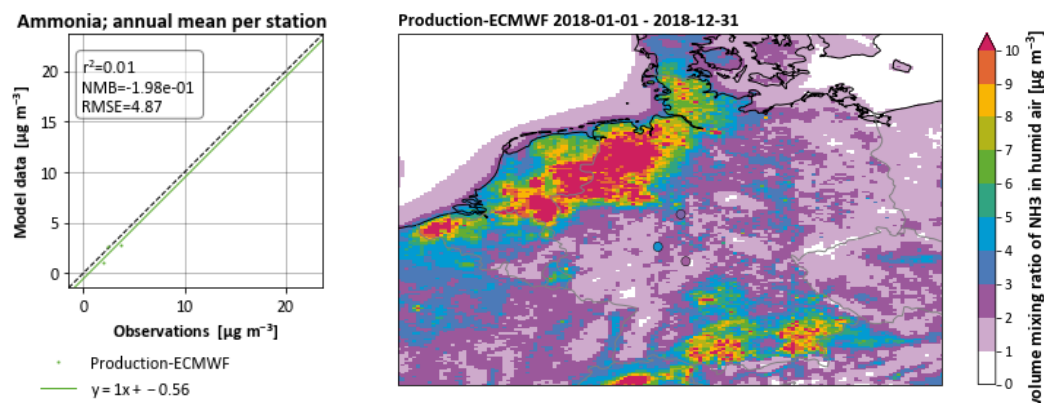
Source: TNO

Figure 47: **Time series of ammonia concentration at station Zierenberg and ammonium PM₂.₅ at Waldhof.**
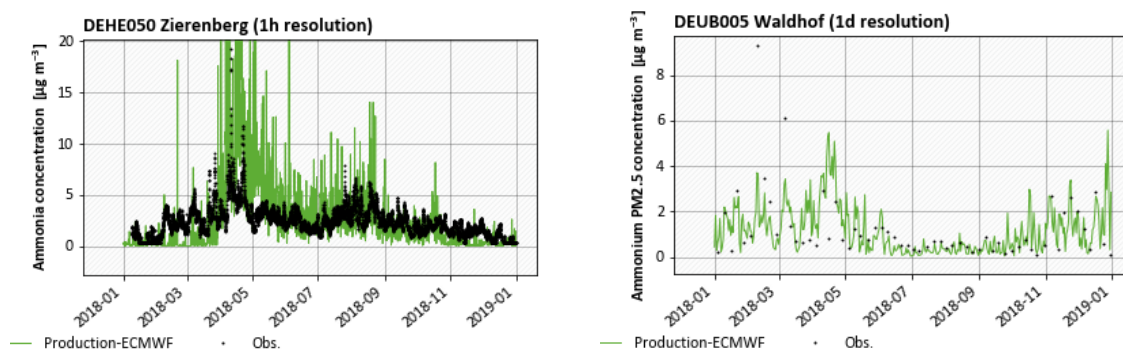
Source: TNO

The ozone predictions by the model (see Figure 48) fit the observations very well in general. The map shows higher ozone levels in the more rural areas. For instance, levels are low around the Ruhr area and the other industrial areas around the Rhine and in the south of Bavaria. The map of ozone concentrations almost looks like the inverse of the ammonium, sulphate and nitrate maps. This can be explained by the formation mechanism of ozone from nitrogen dioxide and oxygen in the presence of solar radiation and heat. This reaction is an equilibrium of which the backreaction (breakdown of ozone) is stimulated by the presence of nitrogen monoxide. NO is usually present in higher concentrations in urban areas – zones with more traffic – explaining the lower ozone levels in cities and industrial areas.

The role of solar radiation in this equilibrium is further emphasized by the time series shown in Figure 49. A clear seasonal pattern can be seen with higher values in summertime and lower in wintertime.

Figure 48:   **Mean modelled and measured O₃ concentration over Germany in 2018 in scatterplot (left) and on a map (right)**
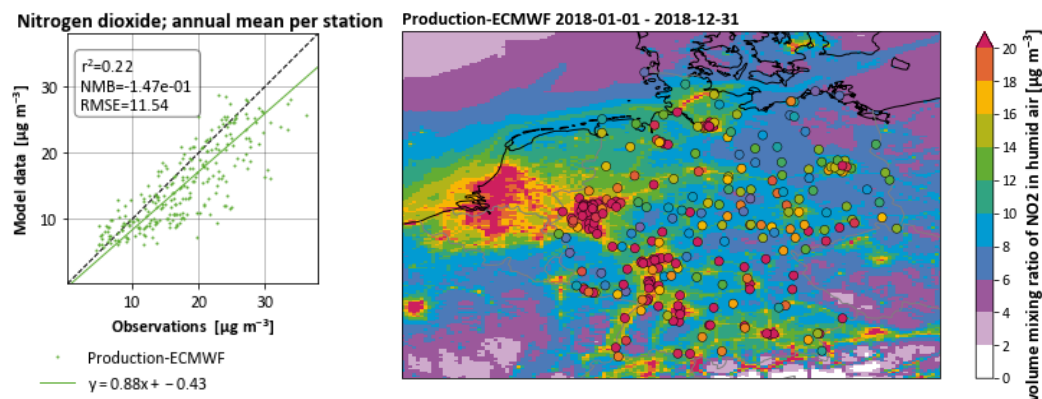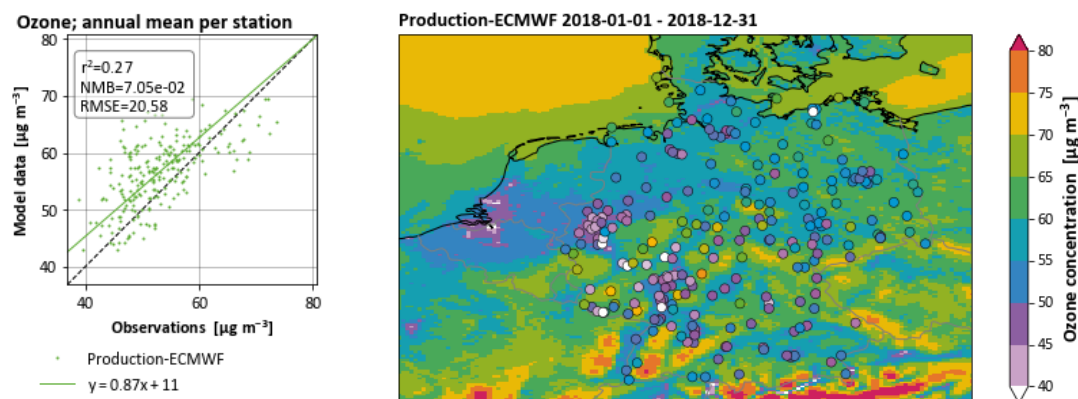

Source: TNO

Figure 49:   **Time series of ozone concentration at station Waldhof.**
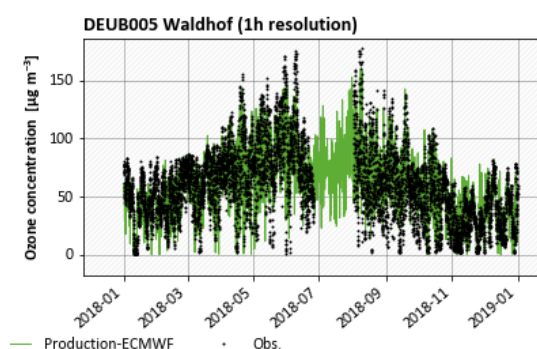
Source: TNO

Finally, we show here the evaluation of the SIA components.

Sulphate concentrations are underestimated by the model at all available stations by about a factor of 2 (Figure 50). Underestimation of sulphate formation is a topic of current scientific debate. As discussed in Section 4.2, cloud-phase oxidation mechanism which are currently missing in most models may partly explain this underestimation.

Figure 50:   **Mean modelled and measured sulphate concentration over Germany in 2018 in scatterplot (left) and on a map (right)**
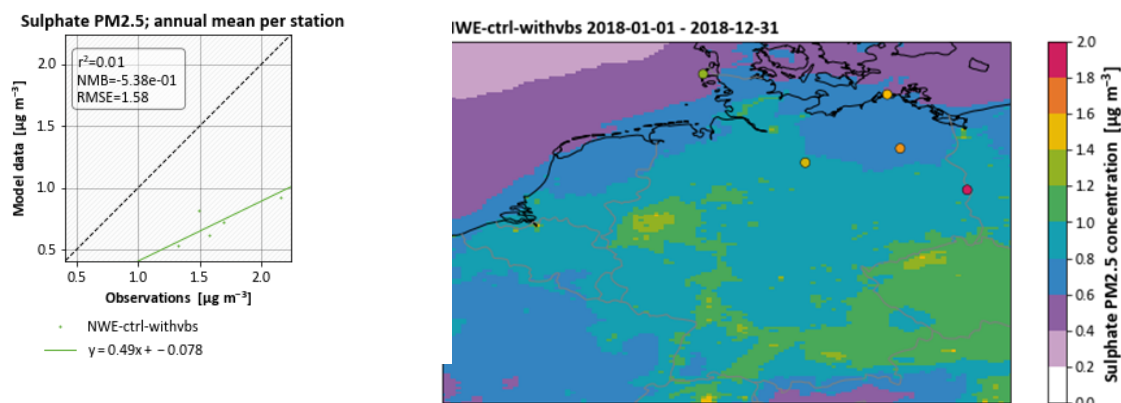
Source: TNO

Observed concentrations are between 1.3 – 1.7 µg m^{-3}, except for one station which is located near an industrial site. Unfortunately, all stations for sulphate and other SIA species are located in the north of Germany, which prohibits the evaluation of the ability of the model to simulate spatial gradients of these components. At least the gradient from coast to inland seems to be present in both model and measurement.

Overall, the modeled nitrate concentrations show a small overestimation (Figure 51). It also shows that the model is able to capture the west-east gradient in nitrate concentrations to some extent.

Figure 51:   **Mean modelled and measured nitrate concentration over Germany in 2018 in scatterplot (left) and on a map (right)**
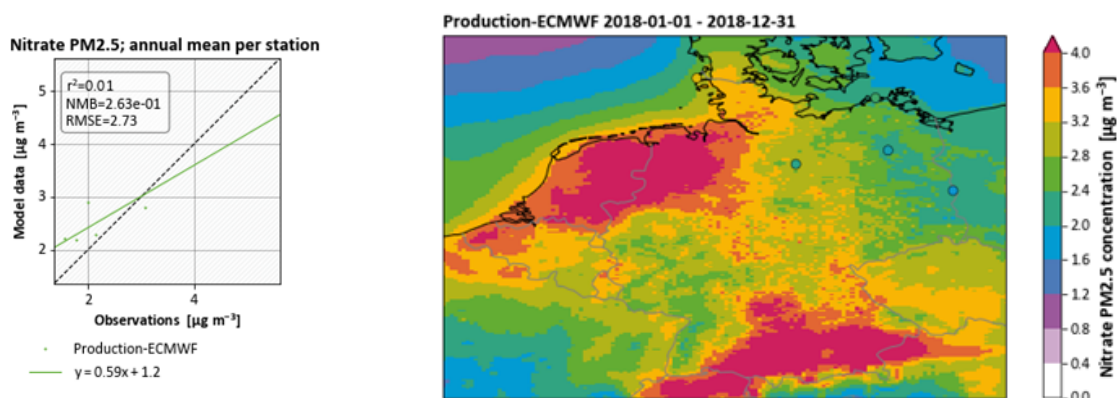
Source: TNO

Ammonium shows a similar spatial pattern as nitrate, but is underestimated at all stations (Figure 52).

Figure 52:   **Mean modelled and measured ammonium concentration over Germany in 2018 in scatterplot (left) and on a map (right)**
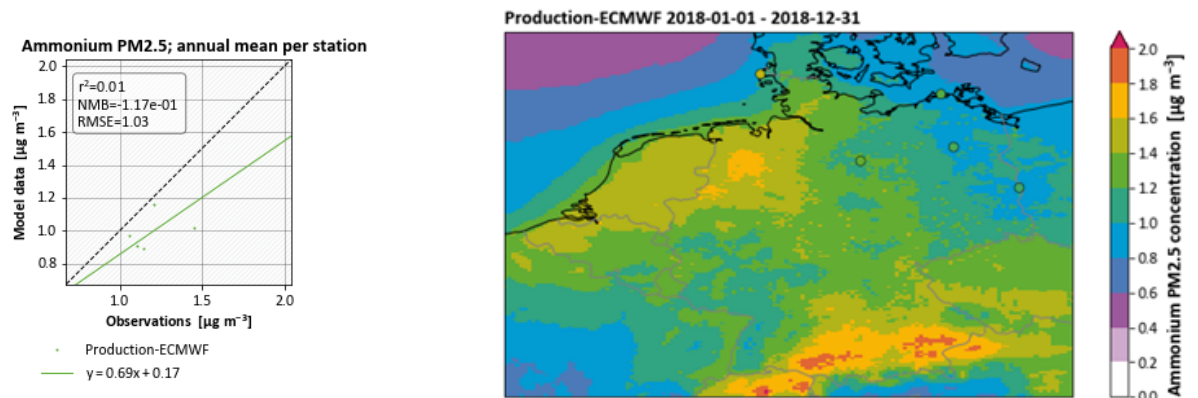
Source: TNO

6.5   SIA Sensitivity analysis and model strategy development

To enable assessment of the effects of emission reductions on the average concentrations of SIA, a number of simulations were performed for different reduction scenarios. Emission reductions in a single sector may impact the formation of SIA in another sector. For example, when agricultural ammonia emissions are reduced by 40%, the pH dependencies in the formation of sulfate may change, impacting the amount of SO_2 converted into sulphate from the energy sector. Hence, to investigate the sensitivity of the SIA concentrations, the sector dependent formation factors and the cross sector dependencies the following scenarios were performed:

► Precursor reductions: 20, 40 and 60% reduction for NO_x, SO_2, and NH_3 in all sectors

► Sector reductions: three sets of 20, 40, 60% reductions of all emissions originating from a single sector, i.e. Traffic, Residential combustion and Agriculture

► NEC scenario: what are the formation factors for each sector under a realistic emission reduction scenario?

In each scenario the labelling system was used to track the contribution of a sector in that scenario. The modelled concentration distributions were averaged to a mean value over the whole country for the year 2018. The emission distributions were integrated over the country and the same period to arrive at total annual emission numbers.

6.5.1   Base case

Figure 53 shows the total annual emissions and mean concentrations over Germany in 2018 of the control run to which no reduction scenario was applied. Sulphur dioxide emissions are dominated by the Energy and Industry sectors, whereas ammonia is almost exclusively emitted by the Agriculture sector. Nitrogen dioxide has a broader set of sources, including Energy, Industry, Agriculture and Residential combustion, but Traffic is the main contributor.

The modelled contribution of German sources is about 2.9 µg m^{-3} of secondary inorganic aerosol in Germany, against 2.6 µg m^{-3} from foreign sources. This indicates the need for international collaboration to reduce the concentrations of SIA in Germany.

SIA consists of an amount of ammonium sulphate and almost 5 times as much ammonium nitrate. Without accounting for interdependencies, sulphate source contributions are dominated by Industry and Energy, nitrate concentrations are attributed to Traffic (~1/3 of the part originating from Germany) and comparable shares from Energy, Industry, Agriculture and Natural sources. Ammonium originates from ammonia, almost exclusively produced in Agriculture as mentioned.

Figure 53:   Total annual emissions of NO$_x$, SO$_2$, and NH$_3$ (left) and mean concentrations of NO$_3$, SO$_4$, NH$_4$ aerosol and SIA across Germany (right) in different sectors in 2018.
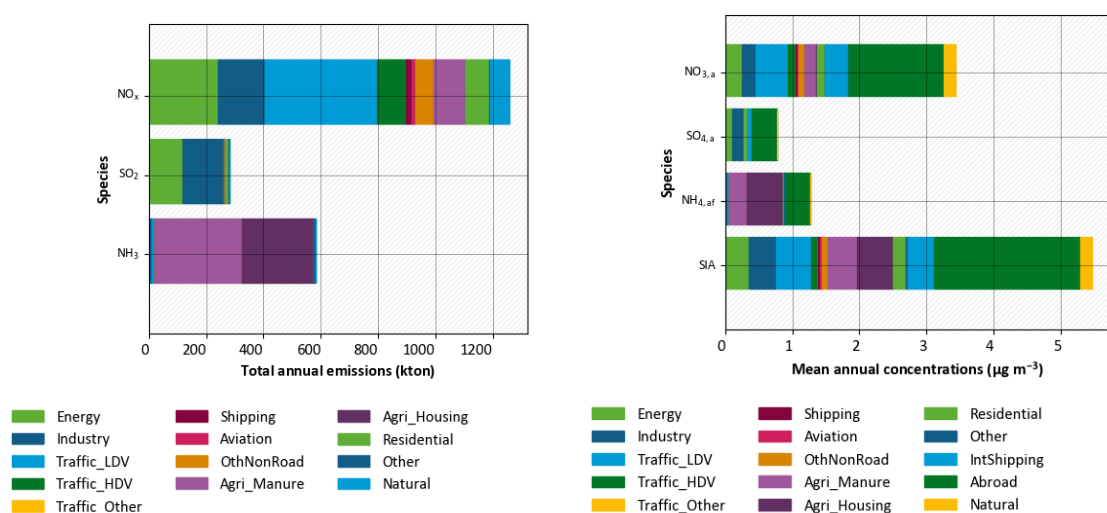
Source: TNO

6.5.2   Effect of precursor reductions scenarios on concentrations of SIA

A set of nine simulations was performed in which the emissions of SO$_2$, NO$_x$, and NH$_3$ were reduced separately by 20, 40 and 60%. These percentage we applied across all sectors equally. The resulting country mean concentrations of the constituent species of SIA are presented as stacked bar charts in Figure 54 for German (left) and non-German source contributions (right).

For the German source contributions, it is immediately apparent that the main effect of reducing the precursor is on their respective products (viz. NO$_x$ to NO$^-_{3,a}$, SO$_2$ to SO$^{2-}_{4,a}$ and NH$_3$ to NH$^+_{4,a\,f}$). The same relative reduction on NO$_x$ and NH$_3$ has a larger impact than the reduction in SO$_2$ emission, which reflects the lower importance of sulphate in the total SIA mass. Surprisingly, the reduction of NO$_x$ and NH$_3$ have an almost equal effect on the sum of the domestic SIA concentration. This seems to be a double effect, since the reduction in either of them also reduces the other. Most likely, this strong correlation is caused by the volatility of ammonium nitrate as explained in Section 4.4.

Figure 54: **Mean concentrations of SIA components for German (left) and non-German (right) source contributions for precursor emission reductions of 20, 40 and 60%.**
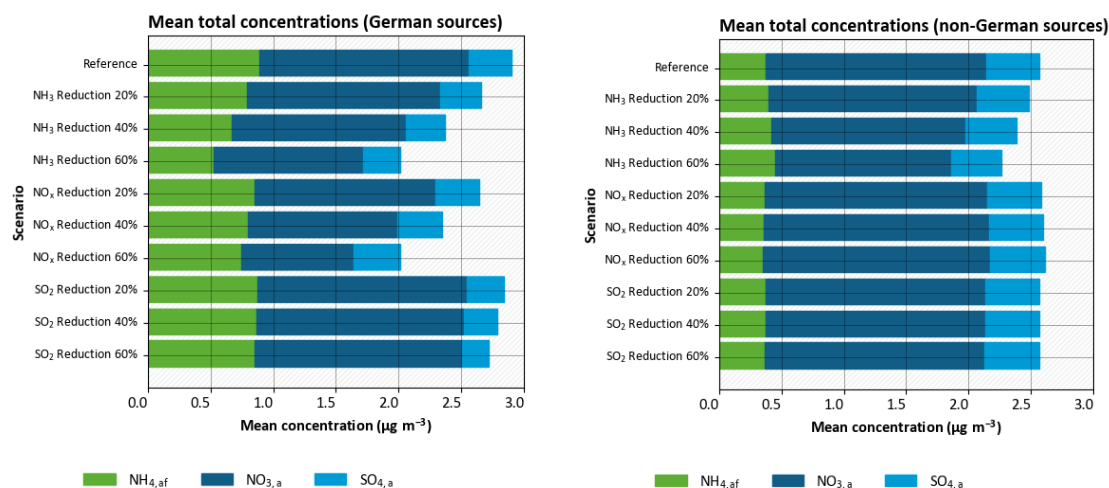
Source: TNO

Table 8: **Mean concentrations of SIA components for German sources for single species reduction scenarios**

	Nitrate µg m^{-3}	Sulphate µg m^{-3}	Ammonium µg m^{-3}	SIA total µg m^{-3}
Reference	1.67	0.342	0.889	2.90
SO$_2$ reduction 20%	1.66	0.302	0.878	2.84
NO$_x$ reduction 20%	1.44	0.350	0.848	2.64
NH$_3$ reduction 20%	1.54	0.326	0.789	2.66

The right bar chart in Figure 54 shows to what extent German emissions impact the levels of SIA attributed to emissions in other countries. There is hardly any influence modelled of independent sulphur or nitrogen oxides emission reductions, as the sulphate and nitrate concentrations from abroad have already largely been formed outside the German domain. However, reducing the ammonia emissions in Germany does have an effect on the thermodynamic equilibrium of ammonium nitrate, leading to a lower contribution of nitrate from abroad when ammonia emissions are reduced.

6.5.2.1   Formation factors

Formation factors have been calculated for three species of interest in the investigation of secondary inorganic aerosols: SIA/SO$_x$, SIA/NO$_x$, and SIA/NH$_3$. As explained in Section 3.3.2, formation factors for SIA will be calculated as the ratio of a mean concentration *change* and a *change* in total emissions. This has the beneficial effect that species that are hardly influenced by changes in emissions of a precursor (for instance sulphate originating from sea salt) are not taken into account.

In the graphs of formation factors presented in this report, data will only be presented if the change in emissions is not near zero. The formation factor does not provide useful information in case of very small emission changes. Extra information is provided in the bar charts regarding the relative importance of the presented formation factors. The bars have an opacity depending

on the change in emissions for the particular reduction scenario. The more opaque the color of the bar, the higher the importance of the formation factor. This technique is also applied for intake factors in a later section.

6.5.2.2   Cross-sensitivities for single species reduction scenarios

For each reduction scenario the formation factors for all sectors were calculated and compared, the most interesting results are shown below per reduction scenario, starting with the reductions in single species. This analysis enables direct visualisation of the effects of one single emitted species on the concentration of SIA species. Reductions of 20, 40, and 60% were calculated, to inspect non-linearities in the resulting concentrations and formation factors.

Effect of sulphur dioxide reduction on SIA formation factor

Overall SIA production per ton of SO_2 is increasing, since reduction of sulphur dioxide emissions causes the pH to rise in aerosol droplets, which stimulates the transformation of SO_2 to sulphate. This has a small moderating effect on the sulphate concentration (reduction).

SO_2 emissions primarily originate from the Energy and Industry sectors, resulting in most representative formation factors in these sectors. The formation factor of Residential combustion is of much less importance, due to its significantly lower SO_2 emissions. In line with the concentration changes shown in Table 8, the effect of more drastic reductions of SO_2 emissions on the formation factor is only mild.

Figure 55:   SIA Formation Factor for reduced SO_2 emission
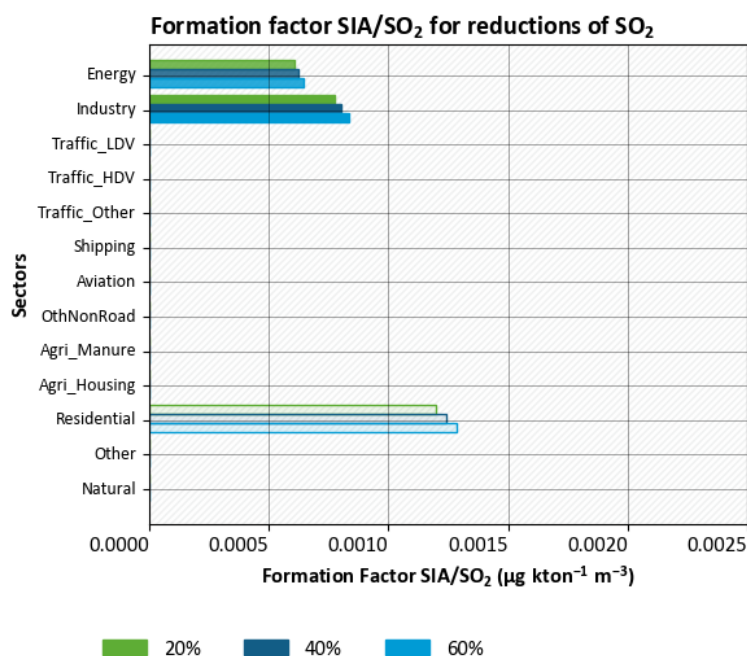
Source: TNO

Effect of nitrogen oxides reduction on SIA formation factor

Nitrogen oxide emissions primarily originate from the Energy, Industry and Traffic sectors, resulting in most representative formation factors in these sectors. The Agriculture Manure

sector shows particularly high values of the formation factor, but due to the relatively low value of the emission difference, the FF is very sensitive to small variation in emissions and therefore less representative. Similar to the SIA formation factor for SO_2 reductions, the nitrate formation factor increases upon NO_x reductions (see Figure 56), but the effect is more pronounced. With a certain amount of ammonia available the fraction of NO_x ending up in ammonium nitrate becomes slightly larger with decreasing emissions.

Figure 56:   **SIA Formation Factor for reduced NO_x emission**
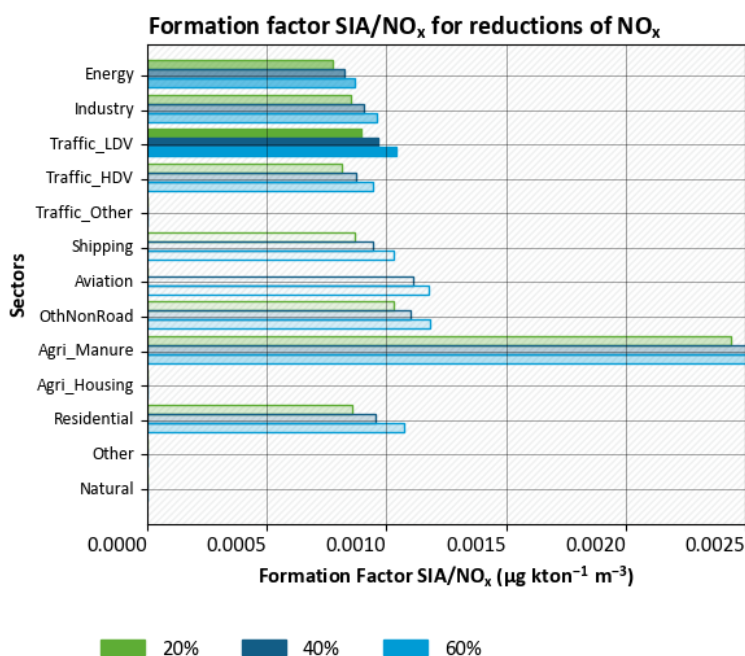
Source: TNO

Effect of ammonia reduction on SIA formation factor

The effect of ammonia reductions on the formation of SIA is presented in Figure 57. It is most prominent in the Agriculture sector, as that is the sector with most ammonia emissions. Similar to the reduction scenario of NO_x presented above, the ammonium formation factor also increases as a result of ammonia emission reduction. This may be attributed to the effect that both ammonium and nitrate decrease when ammonia emissions are decreased.

Figure 57:   **SIA Formation Factor for reduced NH₃ emission**
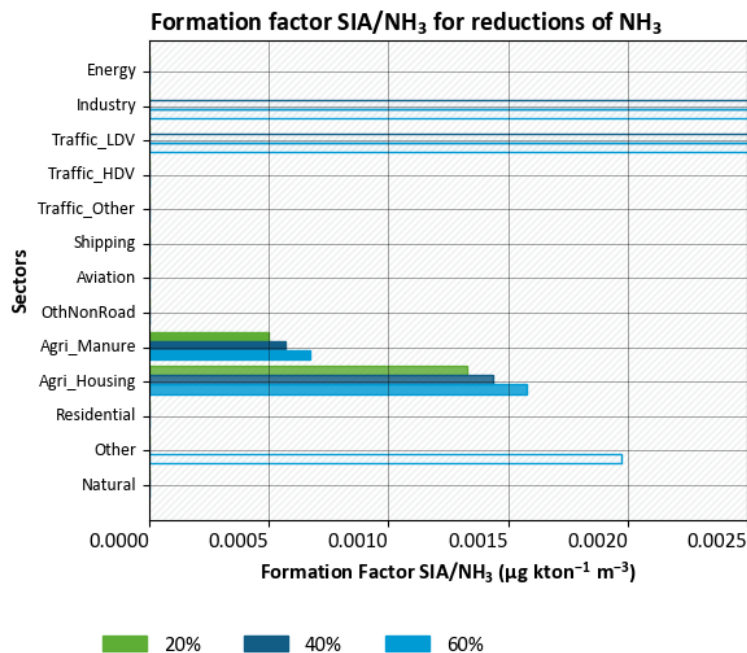
Source: TNO

As was explained in Section 6.4.1, regions of high nitrate concentrations line up with regions of high ammonia emissions due to the semi-volatile nature of ammonium nitrate. This, combined with the fact that ammonium nitrate is the predominant constituent of SIA in Germany, explains the higher formation factor for SIA/NH₃ (in Agriculture, mainly emitting NH₃), compared to SIA/NO$_x$ (in Traffic, mainly emitting NO$_x$).

There will also be a temporal variation of the formation factor. Wintertime has lower temperatures and higher nitrate concentrations than summertime, while the emissions of NO$_x$ does not show a very strong trend throughout the year. Hence, the formation factor for SIA/NO$_x$ is expected to be higher in winter. Since the ammonia emissions are higher in summertime, the sensitivity to changes in emission will be lower in summertime and the formation factor for SIA/NH₃ will also be higher in winter.

6.5.2.3   Cross-sensitivities for sector wide reduction scenarios

Simulations where reductions are effected for all species in a whole sector provide the possibility to investigate the overall effect of sector wide reductions and it shows the effect of reductions in one sector on concentrations of SIA generated in another sector. However, care should be taken in analysing these data. Because the reductions are effected on *all species* emitted in the sector, the formation factor of SIA over a single emitted species can be misleading since it is not the only species that is reduced. For studying the effect of single species reductions, the factors presented in the previous section are more reliable.

The most important results of this analysis are discussed below, per sector.

Effect of reductions in Residential combustion sector on the SIA/NO$_x$ and SIA/SO₂ formation factors

Formation factors for SIA from SO_2 are almost 6 times higher than the factor for SIA from NO_X (Figure 58). Again, this is a demonstration of the sensitivity of the formation factor for low emission values. The sector Residential combustion emits much less SO_2 than NO_x.

Figure 58:   SIA/NO$_x$ and SIA/SO$_2$ Formation Factors for reductions in sector Residential combustion
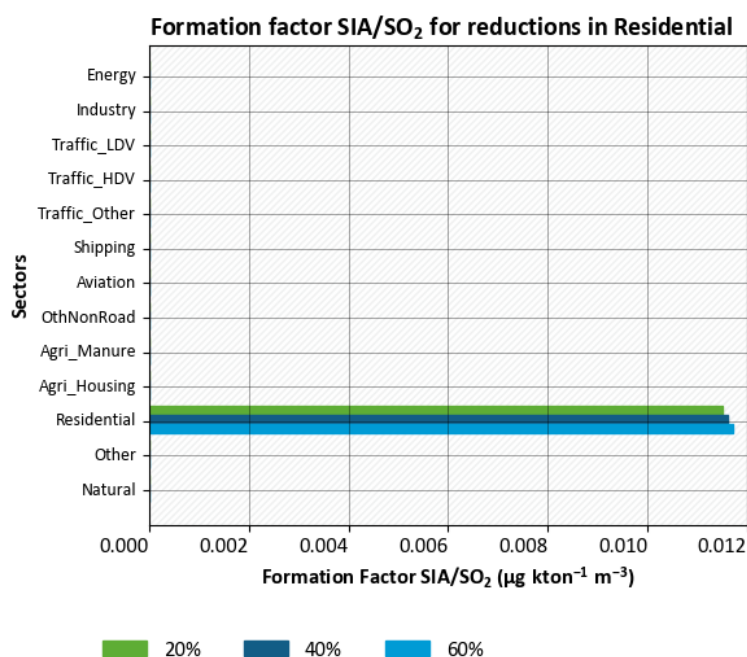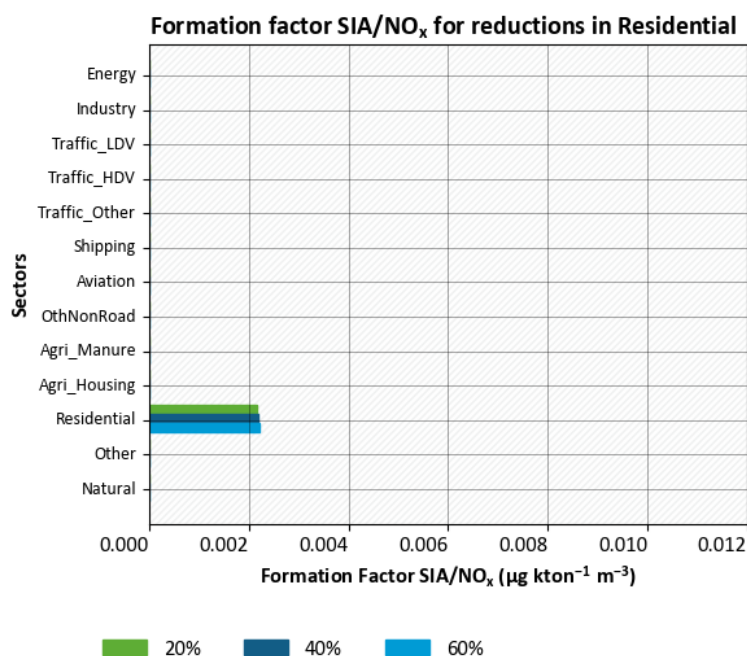
Source: TNO

Effect of reductions in the Traffic sector on the SIA/NO$_x$ and SIA/NH$_3$ formation factors

Reductions in the sector Traffic (both LDV (incl. passenger cars) and HDV) have a similar effect on the formation factors presented (see Figure 59). The NO$_x$ emissions are much stronger than the NH$_3$ emissions in Traffic, hence the huge difference in formation factors. In addition, it appears the formation factor for the 20% reduction scenario is not shown. The reason is that the emission difference is so small that the formation factor would blow up. Hence the algorithm does not show it.

Figure 59:   SIA/NO$_x$ and SIA/NH$_3$ Formation Factors for reductions in sector Traffic
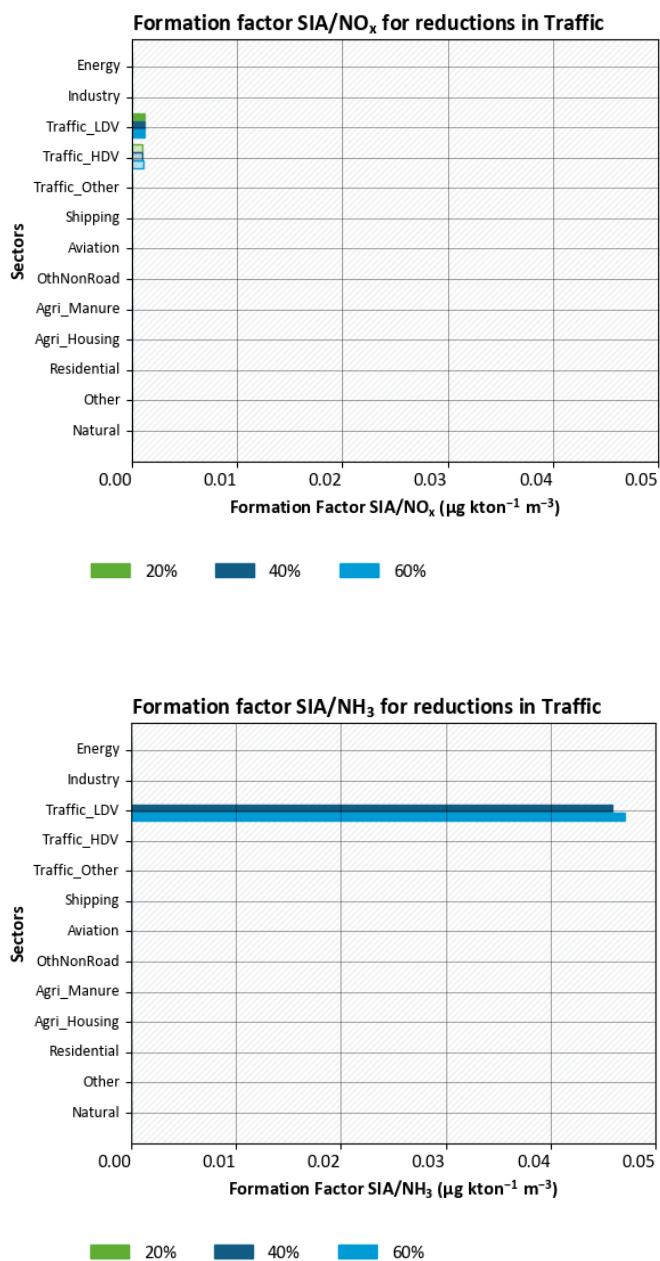
Source: TNO

Effect of reductions in the Agriculture sector on the SIA/NO$_x$ and SIA/NH$_3$ formation factors

The scenarios for reductions in the agricultural sector affect ammonia largely, hence the formation factors are comparable to the ones presented for the ammonia reduction scenarios (Figure 60).

Figure 60:   **SIA/NO$_X$ and SIA/NH$_3$ Formation Factors for reductions in sector Agriculture**
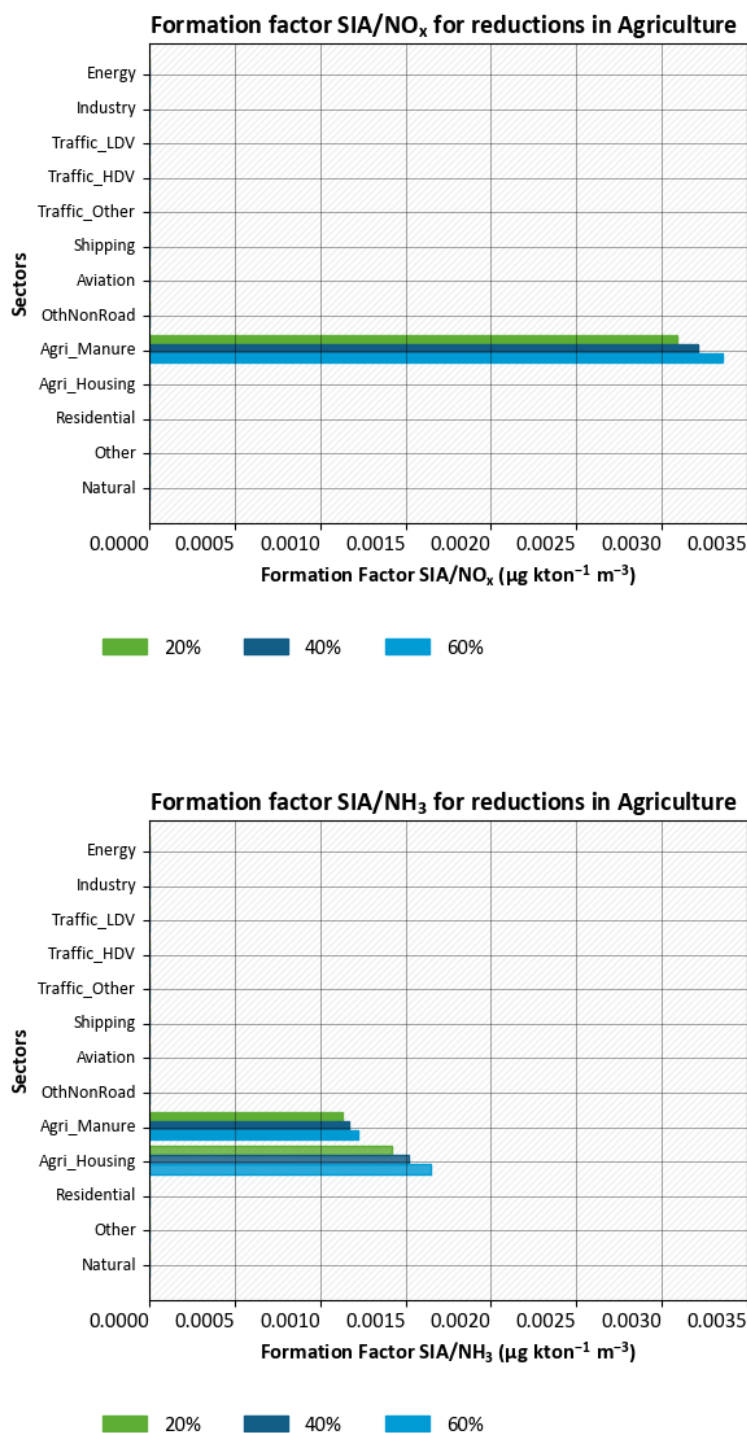
Source: TNO

6.5.2.4   Effect of NEC reduction scenario for Germany

A third way to look at the consistency in formation factors is to compare the formation factors in a relevant future scenario to those calculated for the present day. For this purpose we took existing NEC scenario calculations in which the emissions of all European countries were scaled to their respective ceiling in 2030. LOTOS-EUROS simulations have been performed for Germany for the meteorological year 2015 in which emitted species and pollutant concentrations were labelled per aggregated sector (energy, industry, road traffic, non-road equipment, agriculture and residential combustion) (see Figure 61). Note that these data aggregated slightly differently from the data presented in the previous subsections. The NEC reference and scenario runs were not calculated on the basis of CAMS v5.1 emission, but CAMS v4.1. However, that has most likely only a minor effect on the formation factors. Compared to 2018 for the sectors presented, NO_x emissions are comparable (~1270 kTon), SO_2 is higher (~350 compared to 280 kTon in 2018), but ammonia is higher (~660 compared to 580 in 2018). The NO_3 concentration is lower (~2.8 compared to 3.4 ug/m3 in 2018), SO_4 is slightly higher (~0.9 to 0.8 in 2018), NH_4 is comparable and SIA is lower (~4.9 to 5.5 in 2018). These data serve as a reference case for similar simulations on a NEC reduction scenario for 2030 presented in Figure 62.

Figure 61:   **Annual total emissions of NO_x, SO_x and NH_3, and annual mean concentrations of NO_3^-, SO_4^{2-}, NH_4^+, and SIA estimated for 2015 per sector**
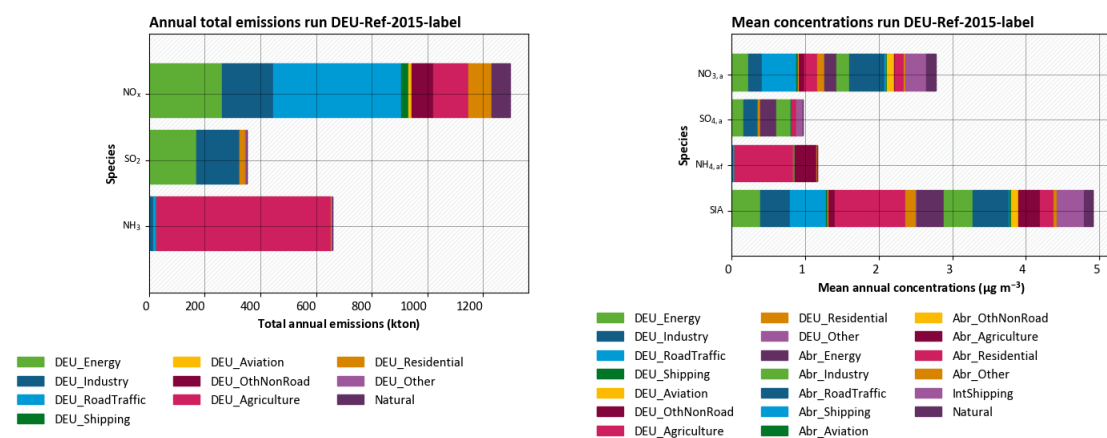
Source: TNO

The NEC scenario for 2030 implies reductions of 47% of NO_x, 56% of SO_2 and about 35% of NH_3 emissions relative to 2015. The reductions are primarily in Energy and Road Traffic for NO_x, in Energy and Industry for SO_2, and in Agriculture for NH_3. This results in a reduction of total SIA concentrations by more than a third.

Figure 62:   **Annual total emissions of NOₓ, SOₓ and NH₃, and annual mean concentrations of NO₃⁻, SO₄²⁻, NH₄⁺, and SIA estimated for 2030 per sector**
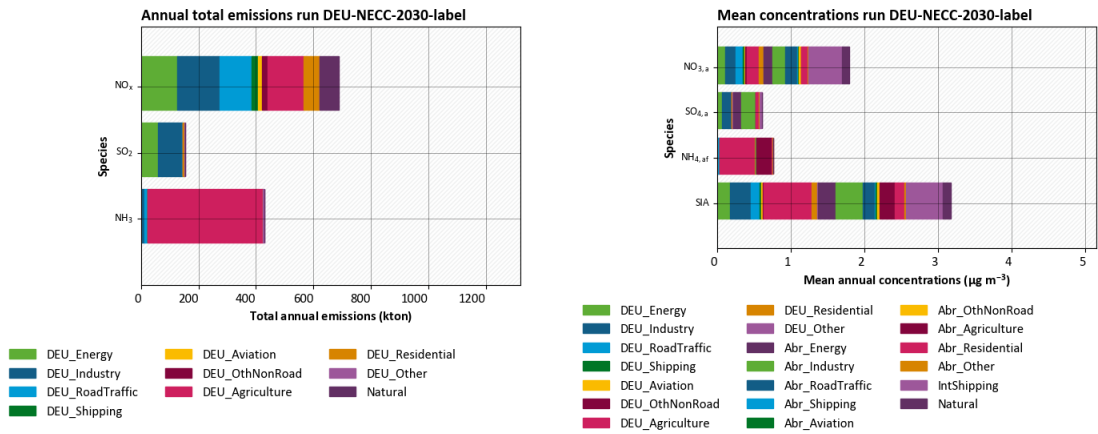
Source: TNO

Figure 63:   **SIA/NOₓ, SIA/NH₃ and SIA/SO₂ Formation Factors for NEC reduction scenario.**

Source: TNO

117
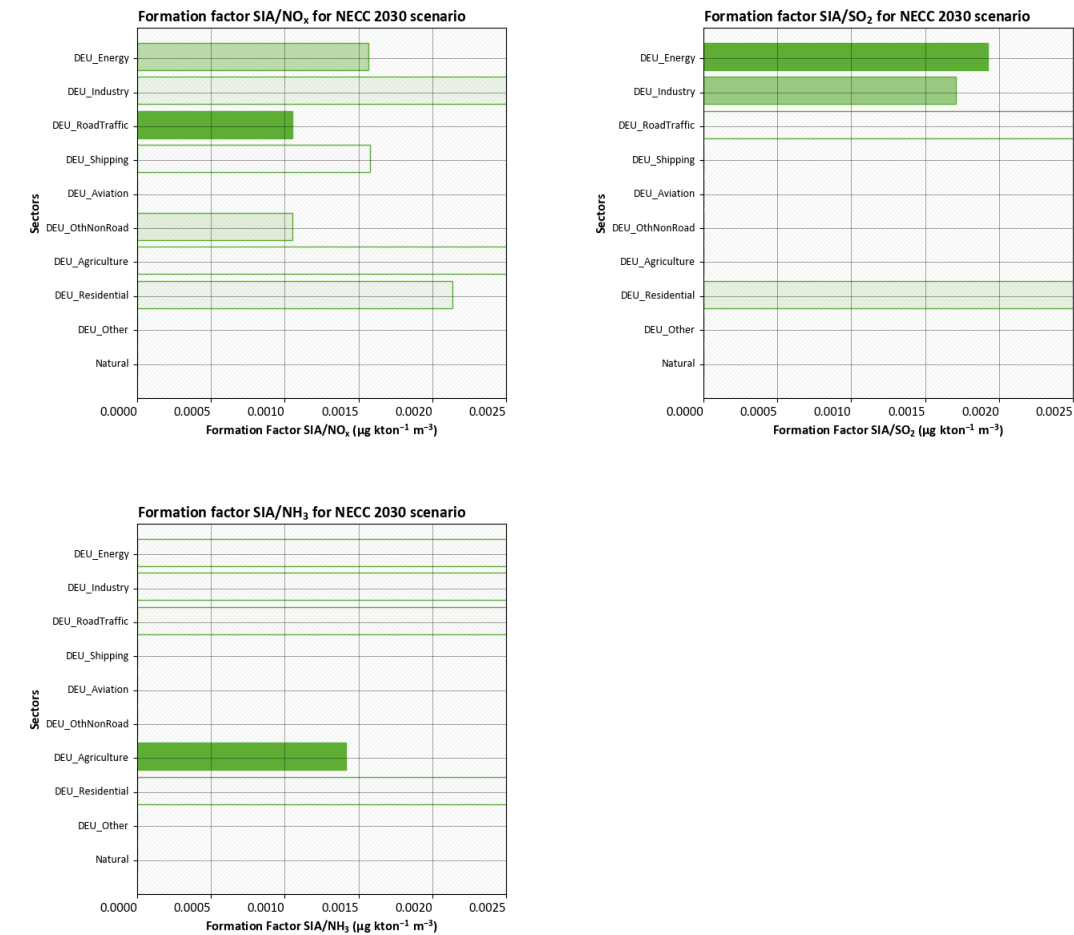
Effect of NEC scenario on SIA Formation factors

As shown in Figure 63 above, the formation factors of SIA on its precursors are similar to the factors presented for the single species reduction scenarios, except for SIA/SO_2 which is approximately twice as high. This may have to do with the fact that the NEC scenario is a complex combination of different reduction measures for all emissions in many sectors and the non-linear effects of the SIA formation mechanism. Hence, the formation factors presented for the NEC scenario need to be regarded with caution, similar to the formation factors of the sector wide reduction scenarios.

6.5.2.5 Total Annual Intake and Intake Factors

As a precursor to the investigation of health effects of the intake of SIA species, the total annual intake and intake factors were calculated. This was performed for the same ratios as the formation factors presented above. For brevity, only the intake factors for single species reductions are shown here, the plots for sectoral reduction scenarios are given in Appendix A.

Figure 64 presents the map of total annual intake of SIA in Germany per unit surface area. It reflects regions of dense population and high industrial and agricultural activity. Specifically, the Ruhr area and larger cities along the Rhine show high values for the intake of SIA, as do Munich, Berlin and Hamburg. In these areas, per hectare over 250 mg of SIA are inhaled during a year.

Figure 64:   Total annual intake of SIA in Germany in 2018.
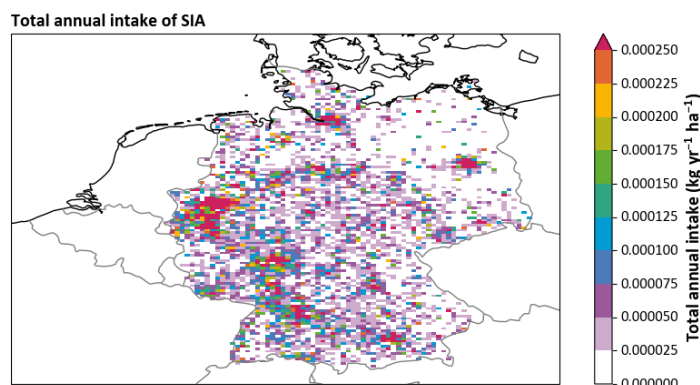
Source: TNO

Similar to the formation factor plots, the bars in the plots have an opacity depending on the difference in emissions between reference case and reduction scenario. The figures show intake factors of SIA

- from NH_3 for NH_3 reduction scenarios
- from SO_2 for SO_2 reduction scenarios
- from NO_x for NO_x reduction scenarios

The overall picture of the intake factors is that they look very similar to the formation factors. This is most likely caused by the fact that the same concentrations are used for both calculations, but the IF is weighted by population density. Hence, in the IF calculation densely populated areas are emphasized. These areas are often also the areas where concentrations are high.

118

Figure 65:   **SIA/NOₓ, SIA/NH₃ and SIA/SO₂ Intake Factors for single species reduction scenarios.**
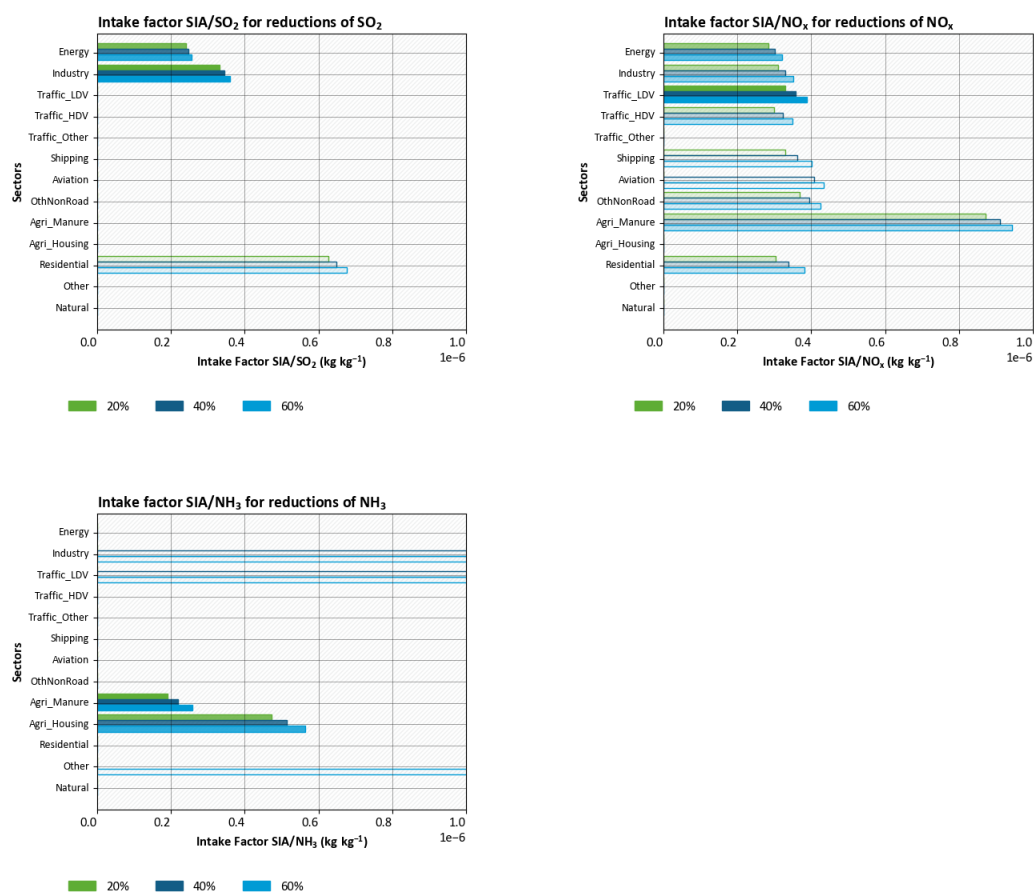
Source: TNO

6.6   OA: Base case results and evaluation

The results presented in this section refer to simulations performed with LOTOS-EUROS for Germany in the year 2018. The analyses are based on annual averaged values of concentrations of POA and SOA over Germany during this year and total emissions of POA and NMVOC integrated over the country and the year.

6.6.1   Modelled distributions

Both semi-volatile POA and NMVOC emissions contribute to anthropogenic OA formation, and the annual total emissions in the Reference simulation are shown in Figure 66. Only the NMVOC that contribute to OA formation in LOTOS-EUROS (i.e. aromatics, alkanes and alkenes) are included in this figure. The POA emissions include the condensables, as discussed in Section 6.3.1, but not the IVOCs, as these are added in the model calculations.

Figure 66:   Annual total POA and NMVOC emissions over Germany in 2018
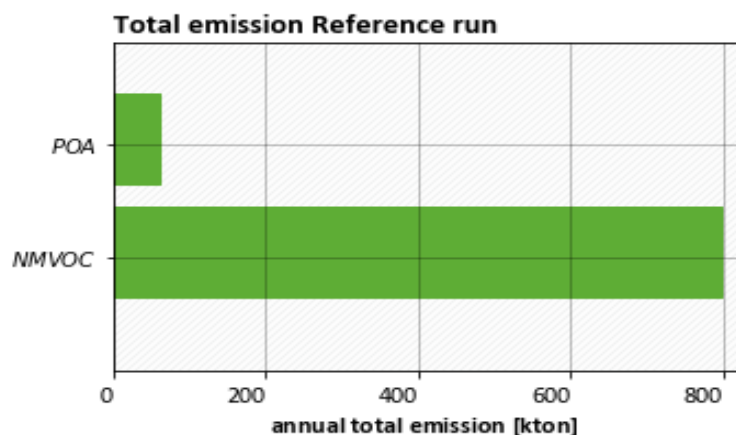
Source: TNO

Figure 67 shows the yearly mean modelled concentrations of total OA across Germany, which is about 1 µg m^{-3}.

Figure 67:   Modeled annual average total organic aerosol concentration in the Reference run
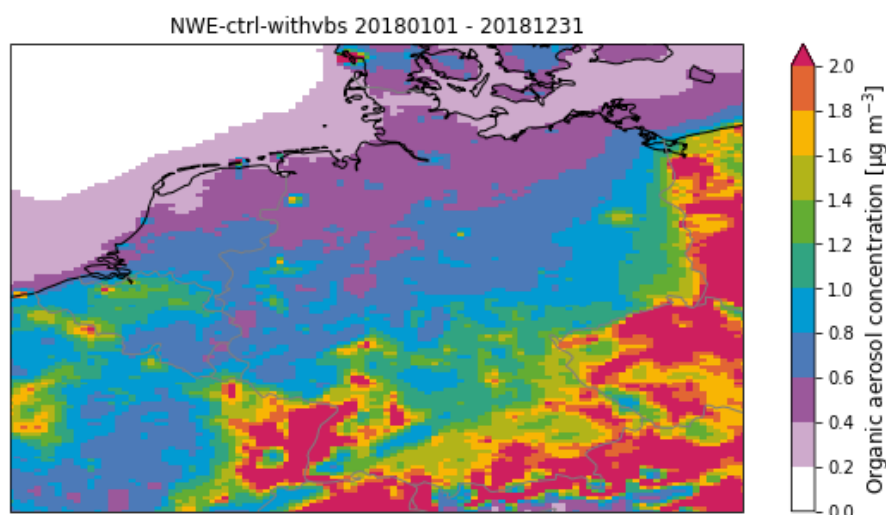
Source: TNO

This concentration shows a strong gradient from northeast to southwest, with some more local maxima in industrial (Ruhrgebiet) and urban areas (e.g. Berlin, Hamburg, Frankfurt). The annual mean concentrations of the OA components is shown in Figure 68.

Figure 68:   Concentrations of the OA components over Germany in 2018
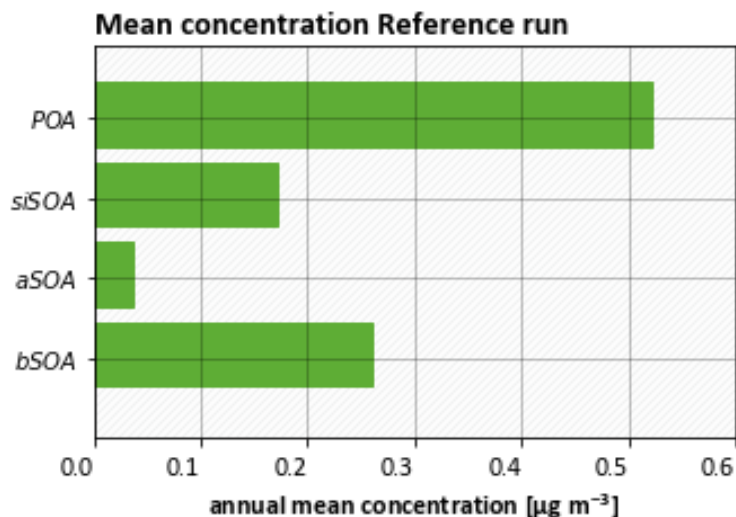
Source: TNO

POA forms about half of the OA concentration with 0.52 µg m^{-3}. POA is formed mainly in winter when its emissions have a maximum and when atmospheric mixing is suppressed. Spatial maxima can be found near populated areas, where most emissions take place. Originating from the same emission sources as POA is siSOA, but its contribution is about a factor of 3 lower (0.17 µg m^{-3}). This is due to the fact that most POA emissions take place in winter when photochemistry is slow, which prohibits the oxidation of the semi-volatile organic vapors which lead to SOA formation, and when temperatures are low, which favors the partitioning of the semi-volatile emissions to the particle phase. The concentrations are more spread out than those of POA and show a strong west to east gradient, which reflects the role of transport.

The third OA component of anthropogenic origin is aSOA, which is formed by the oxidation of NMVOC. aSOA only contributes a small part of the total OA over Germany (0.04 µg m^{-3}), due to the inefficient conversion of its precursors, the anthropogenic NMVOC, to SOA. Highest concentrations can be found in southern half of the country, but nowhere do they exceed 0.01 µg m^{-3}.

The contribution of bSOA is significant on the annual average (0.26 µg m^{-3}), but shows a clear peak in summer when it is the dominant OA contributor over Germany. Its concentration shows spatial maxima in forested areas like the Black Forest and the mountainous areas of Bavaria. This suggests that there is a significant part of OA which cannot (or only indirectly) be controlled by emission reduction policies.

6.6.2   Comparison with observations

Unfortunately, in Germany only a few monitoring stations exist for OA and its precursors. Organic carbon observations are available at a few stations, where they are measured different methods (VDI, TOT, TOR). Here, we only use TOT data (DIN EN 16909:2015-10 (TOT, EUSAAR2)), a thermal method with optical correction (transmission). After excluding stations above 700 m, 3 stations in the Northeast remain, where OC observations are available every 6 days. To be able to compare simulated organic aerosol concentration to measured organic

carbon (OC) concentration, we apply a OM:OC ratio of 1.33 (Aiken et al., 2008) in the conversion from OC to OA.

We find that for these 3 stations, the model shows an underestimation by a factor ~5 (Figure 69).

Figure 69: **Modeled versus observed organic carbon concentrations over Germany in 2018**
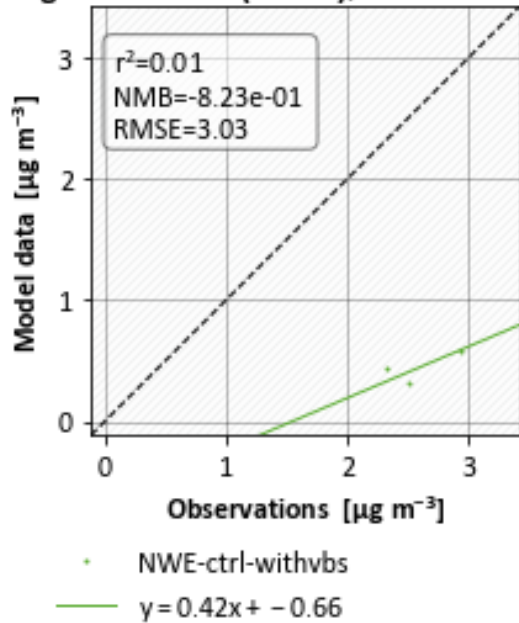
Source: TNO

The seasonal cycle suggests that OC concentrations are underestimated both in summer and in winter. Figure 70 shows an example seasonal cycle for one of the stations. However, no strong conclusions can be drawn from this comparison, because all three stations are located in the same region, where simulated concentrations are low (Figure 67). Therefore, we cannot draw conclusions on whether the model is able to reproduce spatial gradients in OC either.

Figure 70: Time series of organic carbon concentration at station Zingst
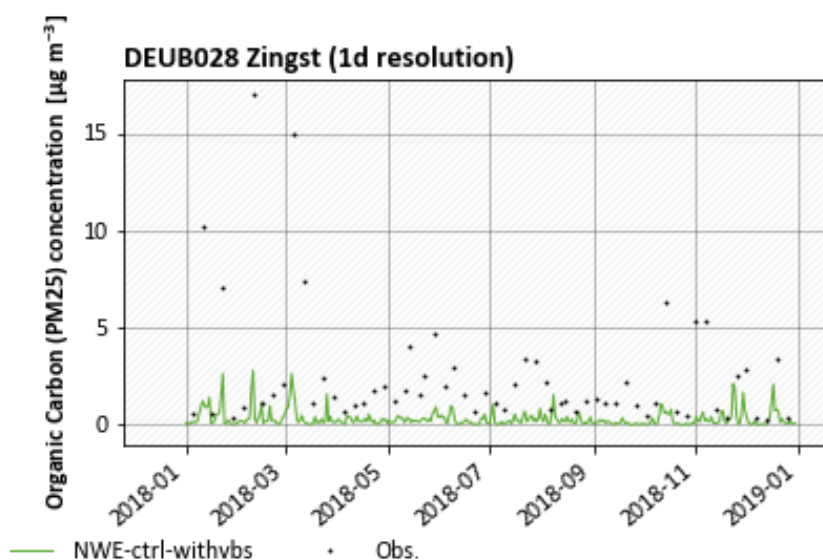
Source: TNO

Figure 71: Modeled and observed annual average organic carbon in PM$_{2.5}$ concentration in the Reference run. The dots indicate the annual mean observations at individual stations.
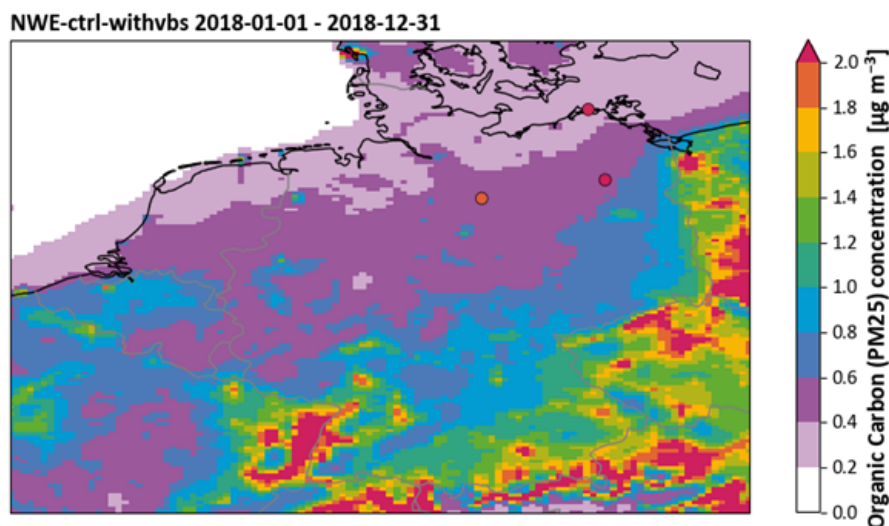
Source: TNO

6.7 OA: Sensitivity analysis

To enable assessment of the effects of emission reductions on the average concentrations of OA, a number of simulations were performed for different reduction scenarios. Total OA concentrations respond to emission reductions in anthropogenic POA and NMVOC emissions, so we included these species in the analysis. Further, there are specific sectors which emit large quantities of POA, so reducing emissions from these sectors has potentially a strong effect on OA concentration reductions. Therefore, we performed the following set of simulations:

► Precursor reductions: 20, 40 and 60% reduction of POA and NMVOC emissions in all sectors

► Sector reductions: 20, 40, 60% reductions of all emissions originating from a single sector, i.e. Residential combustion and Traffic

Figure 72:   **Annual total emissions (top row) and mean concentrations (bottom row) of OA precursors and components in the species reduction scenarios (left column) and the sector reduction scenarios (right column).**
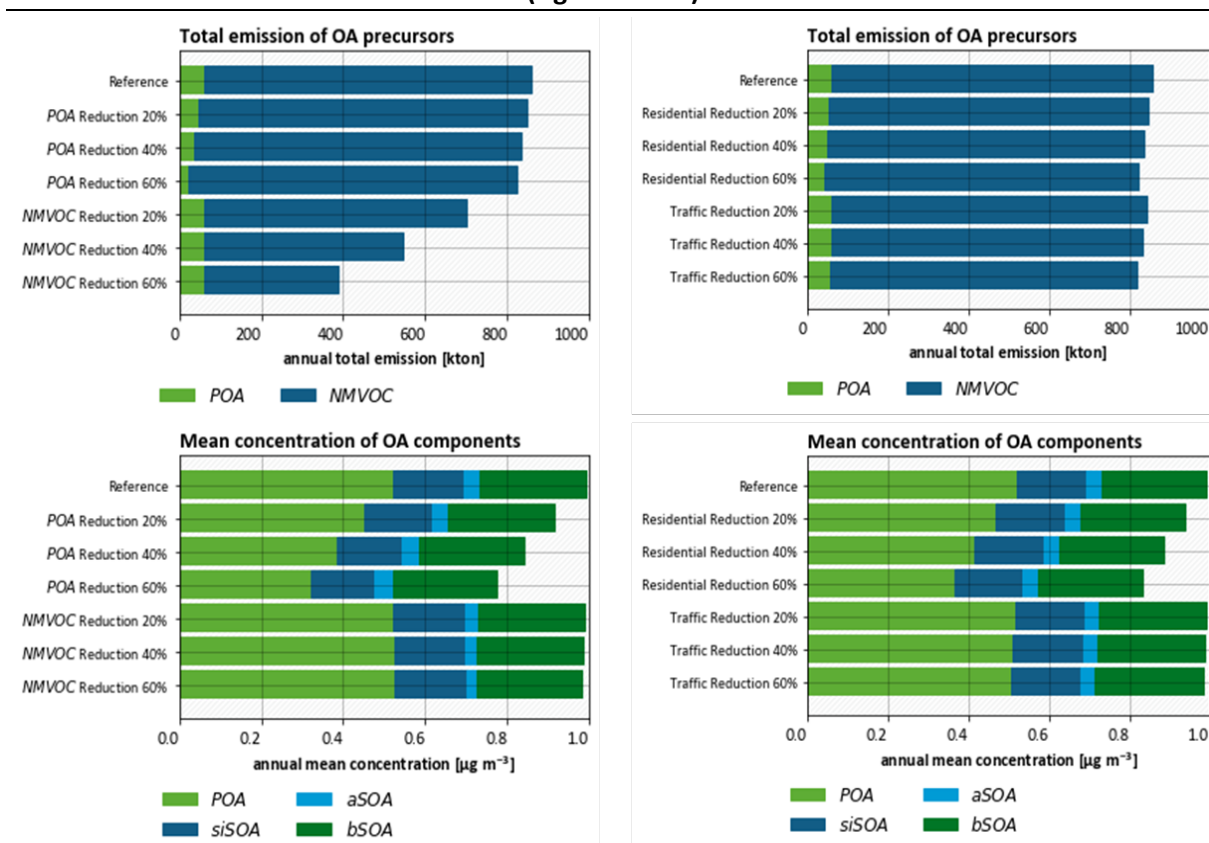
Source: TNO

Since the labelling system cannot be used in combination with OA formation in LOTOS-EUROS, the contribution of single sectors to the total OA concentration can only be assessed through sensitivity runs. The modelled concentration distributions were averaged to a mean value over the whole country. The results discussed below thus focus on the annual mean impacts of these simulations and the quantification of the formation factors.

6.7.1   Effect of precursor reductions scenarios on concentrations of OA

The outcomes of the reduction scenarios show that reducing POA emissions is more effective for reducing OA concentrations than reducing NMVOC emissions (Figure 72). Even though the absolute reduction in POA emissions is much smaller than the absolute reduction in NMVOC emissions, the resulting concentration reductions are much larger. For instance, a POA emission reduction of 20% leads to a decrease of total OA by 8% (POA concentration decreases by 14% and siSOA by 4%). NMVOC reductions only have a minor influence on total OA concentrations (for instance, a 20% emission reduction leads to a 0.3% OA concentration reduction), resulting from a small decrease in aSOA concentration. Concentrations of bSOA are only slightly affected by changes in oxidant concentrations that result from the effect that SVOC and NMVOC have on the gas-phase chemistry.

In the sector reduction scenarios, the effects of reducing Residential combustion and Traffic emissions are very similar to the species reduction scenarios, since Residential combustion emissions mainly consist of POA and Traffic emissions of NMVOC (Figure 72). Consequently, reducing emissions from Residential combustion has a similar effect on OA concentrations as reducing POA emissions over all sectors. The effect is a bit weaker (for instance, a Residential combustion reduction of 20% leads to an OA concentration reduction of 6%), however, since other sectors (e.g. Industry) contribute significantly to POA emissions as well. Reducing emissions from Traffic has only a minor effect on OA concentrations, because most of the reduction concerns NMVOC emissions, which have little effect on total OA production.

6.7.2   Organic aerosol formation and intake factors

From the scenario runs that we discussed in the previous section, we can now calculate the formation factors (FF) and intake factors (IF) of OA. Figure 73 shows the FFs for each POA reduction scenario, relative to the Reference scenario.

Figure 73:   **Formation factor of total OA to POA emissions for various POA reduction scenarios.**
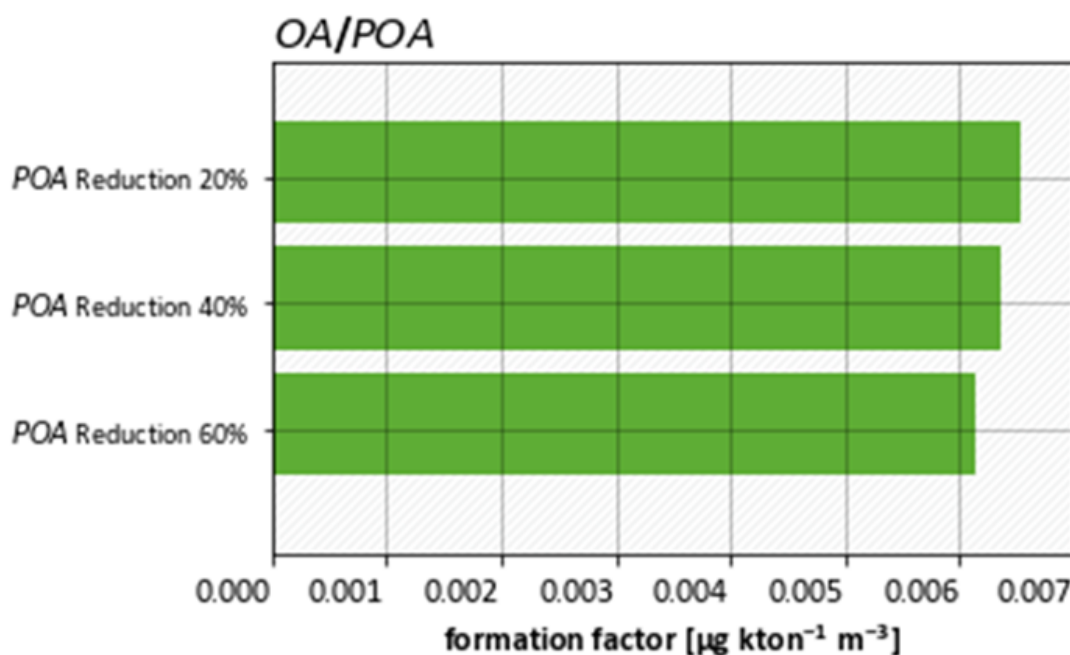
Source: TNO

The FF for OA/POA has a value of over 0.006 µg m^{-3} kTon^{-1}, which is high compared to that of other species. This is caused by the fact that POA formation results from a fast physical process, i.e. gas/particle partitioning of SVOCs. Due to their semi-volatile nature upon emission, a substantial part of POA emissions enter or stay in the particle phase without any intermediate steps. This is further illustrated by comparing the POA/POA and the siSOA/POA formation factors (Figure 74).

Figure 74:   **Formation factor of POA to POA emissions (left) and siSOA to POA emissions (right) for various POA reduction scenarios**
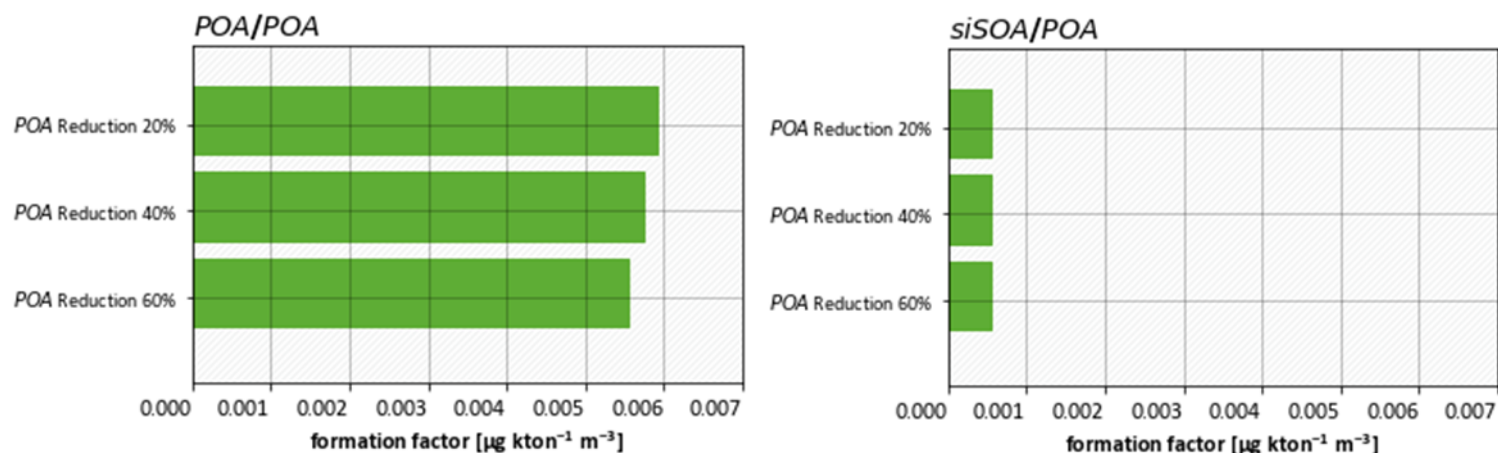
Source: TNO

It shows that the larger part of the OA/POA FF is due to the partitioning of POA emissions to POA, while only a small part is due to the formation of siSOA from the evaporation and subsequent chemical transformation of semi-volatile POA emissions. The fact that siSOA formation is less efficient than POA formation, because of the intermediate steps involved, is exacerbated by the fact that most POA emissions take place in winter, when photochemistry is low.

The POA/POA FF is somewhat dependent on the percentage of POA emission reduction. This is caused by the partitioning between the gas and the particle phase of SVOCs, which depend on the concentration of OA that is present in the atmosphere. This provides the surface onto which the SVOC can be absorbed: there is more OA available when the emission reduction is smaller.

Figure 75:   **Formation factor of total OA to NMVOC emissions for various NMVOC reduction scenarios**
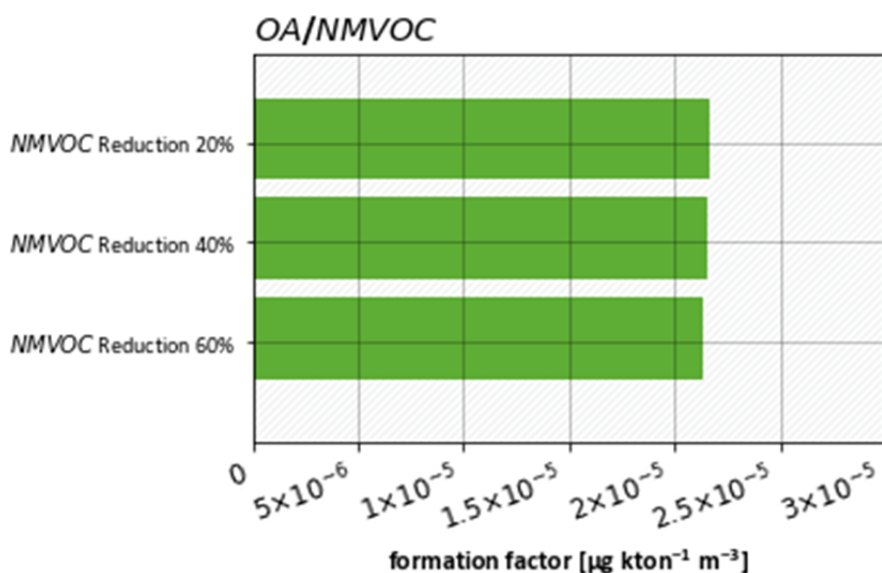
Source: TNO

The FF of OA/NMVOC (Figure 75) is about 2 orders of magnitude lower than that of OA/POA. This further illustrates the limited role that NMVOC play in OA formation over Germany as a whole. Because of their limited relevance, FFs and IFs of OA/NMVOC will not be discussed further. We find that the reduction scenarios per sector is mostly driven by POA reductions (Figure 76).

Figure 76:   Formation factors of OA/POA for the various POA emission reduction scenarios
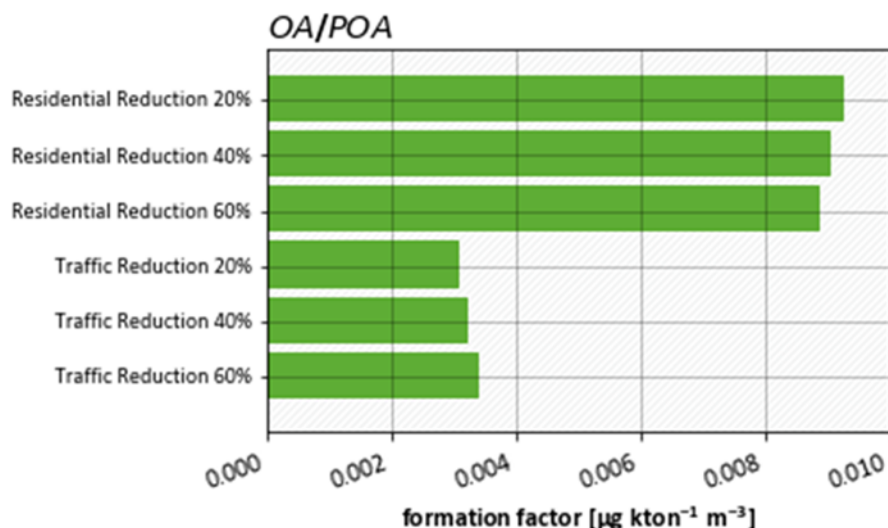
Source: TNO

OA/POA factors for Residential combustion emission reductions are about 0.009 µg m^{-3} kTon^{-1}. For Traffic, they are less than half that number, and it should also be noted that, they are based on a small OA concentration reduction in absolute terms.

The OA/POA FF is highest in winter, because of the lower temperatures and despite lower photochemical activity than in summer: in winter, a smaller fraction of the semi-volatile POA will evaporate, and the SVOC that result from this evaporation will be subject to slower oxidation than in summer. The former effect dominates over the latter (Figure 74), leading to a net more efficient OA formation from POA emissions in winter.

Finally, we discuss here the intake and intake factor of organic aerosol. The intake calculations that we show here are based on the Reference and the POA emission reduction scenarios and are based on Equation 8.

Figure 77:   **Total annual intake of OA in Germany for the Reference and the POA reduction scenarios.**
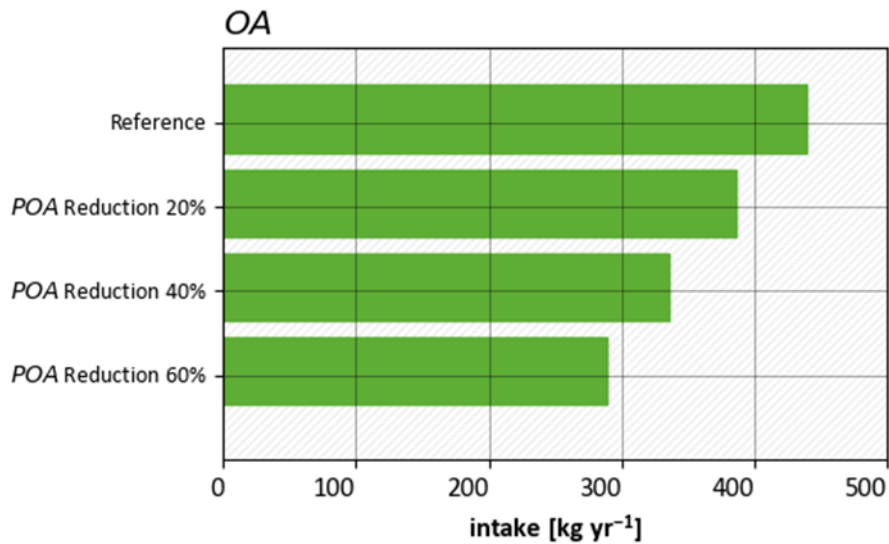
Source: TNO

Figure 77 shows that in the Reference scenario, the total annual intake of OA is about 440 kg for the German population as a whole. This intake decreases steadily, with a rate proportional to the concentration reduction, when emission reductions are increased.

Figure 78:   **Spatial distribution of total annual intake of OA in Germany for the Reference scenario**
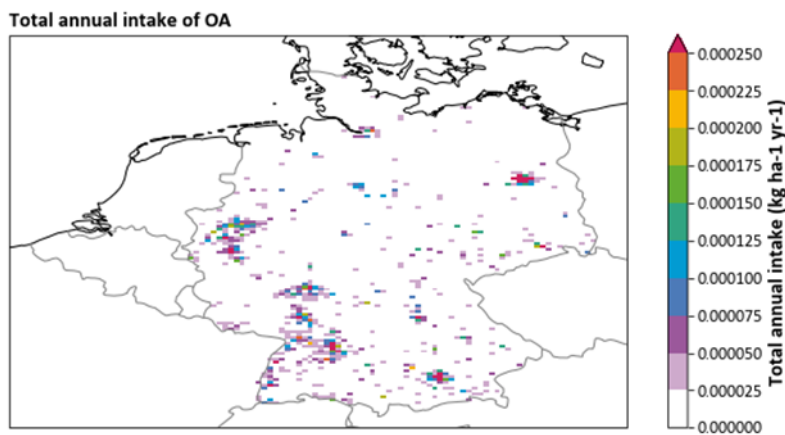
Source: TNO

The spatial distribution of OA intake is closely linked to the population density (Figure 1) because of two reasons: 1) a higher population density translates into a higher total amount of air breathed in in a specific region and 2) the highest OA concentrations are found in places where its main sources (i.e. Residential combustion) are.

Like the FF, the IF of OA can only be calculated from the difference between a Reference and an emission reduction scenario. In Figure 79, we show the IFs of OA/POA for the three POA

reduction scenarios with values of about 4.2-4.4 x 10^{-6}. Similar as the FF (Figure 74), the IF of OA/POA decreases somewhat with increasing emission reduction.

Figure 79: **Intake factors of OA/POA for the various POA emission reduction scenarios**
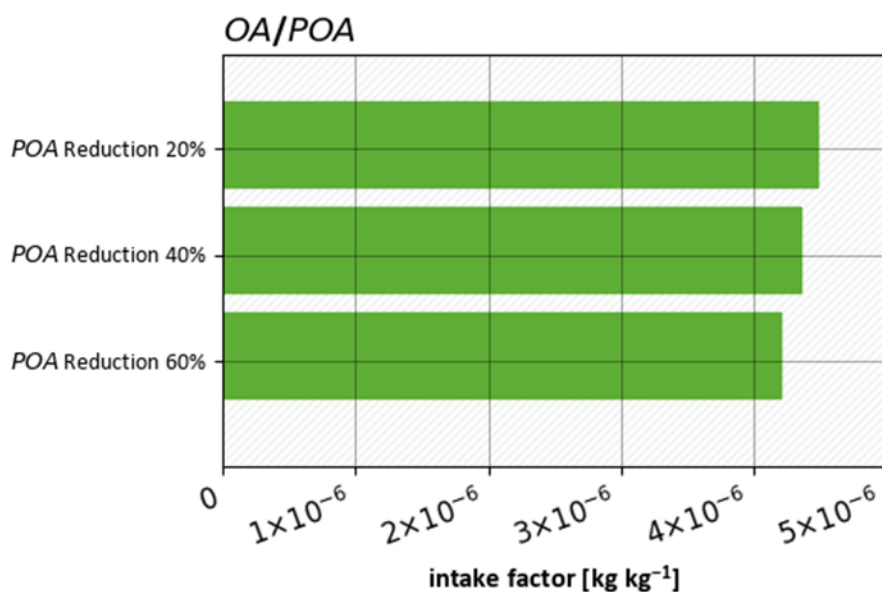
Source: TNO

7   SIA Toolkit

7.1   Introduction

In Work Package 4, a toolkit is developed to derive the PM formation potential and apply it to alternative emission reduction scenarios. The main objective of this WP is to provide tools to calculate the impact of emission reduction scenarios on PM concentrations without using the results of the CTM directly. In addition, an assessment is made of the conditions under which the calculated factors are valid, so that the results can be put into context. For this purpose, factors were first derived using the simulations presented in Chapter 6, by which the PM concentration is reduced for a specific change in emissions.

The PM formation factors are calculated according to the methods described in Section 2.1. In addition, PM intake is assessed as a function of precursor emissions. The toolkit comprises a software package in Python that reads the LOTOS-EUROS output and uses labeled concentrations and emissions to derive this potential from runs with different emission scenarios. The PM formation potential can be directly related to the contribution of individual sectors to emissions and the concentration of a particular PM component. The toolkit is based on a Partial Least Squares Model (PLS, see below) that relates concentration and exposure data to emission data for each run in the calibration set. It provides visual feedback on the effects of reduction scenarios on concentrations, PM formation and intake factors created by the user. Because the toolkit is created in a modular way, it is also possible to use classes and functions from the toolkit for other purposes. For instance, calculating formation and intake factors is possible for emission and concentration/intake data from any source.

7.2   Data preparation

7.2.1   Input data for creation of the PLS model

As presented in Chapter 6, a number of calculations were performed for different emission reduction scenarios. In addition, a control run was performed to obtain results without any reductions. The output of these runs contains, among other fields, daily files with hourly values for concentrations and emissions at ground level at all grid cells in the domain. This data is labeled per GNFR sector in a domain of North-West Europe including Germany. See Appendix B for a short overview of the file formats of all used data.

The first step to prepare calculation of total emissions and mean concentrations is to calculate the annual total of the emission data and the annual mean of the concentration data for the year 2018 in each grid cell. Next, a mask is applied to the data that only keeps the data in the German domain. Finally, the area weighted mean value of the concentrations and the area integrated total emissions are determined over the German domain according to the equations in Section 2.1.3.

7.2.2   The PLS model

In order to predict output data (viz. mean concentration or total intake) from input data (viz. total emissions) for different, user configurable, reduction scenarios, a model is needed that links concentrations to emissions. One approach for this, would be to use multivariate least squares (MLS) modeling. In that case, a relationship is assumed between the output (say concentrations) and emissions, for instance a linear or polynomic relation:

$$\overline{C_j} = \sum_i \alpha_i \cdot E_i + \beta \quad \text{or} \quad \overline{C_j} = \sum_i \sum_{k=0}^{N} \alpha_{i,k} \cdot E_i^k)$$

, and this relation is fitted to the emission and concentration using linear regression. The downside of this approach is that a predetermined model equation is imposed on the data. In addition, there may be interrelations in the input and output data that are not covered by the model. In the current dataset, for instance, the concentrations of nitrate and sulphate will be related to the concentration of ammonium through the deposition mechanism.

If the interrelations are not covered in the model and a predetermined model equation is fitted, the validity of predictions by the model can be negatively affected. A common way to counter this, is to apply Partial Least Squares Regression (PLSR). PLSR was first applied in social sciences and economics, but soon gained huge popularity in chemometrics (computational chemistry, data science applied in chemistry) (Abdi, 2010). PLSR is a method for relating two data matrices, X (emissions in this case) and Y (concentrations or intake, in this case), by a linear multivariate model, but goes beyond traditional regression because it also models the *structure* of X and Y (Wold et al., 2001). PLSR derives its usefulness from its ability to analyze data with many, noisy, collinear (containing interdependencies), and even incomplete variables in both X and Y. PLSR has the desirable property that the precision of the model parameters improves with the increasing number of relevant variables and observations (Wold et al., 2001).

Two PLS models need to be created, one for the prediction of concentrations and one for the prediction of total intake. They are created from a set of emissions, concentrations, and intake values originating from LOTOS-EUROS runs for different reduction scenarios. This is the calibration set. The independent data or predictor variables for both models are the emissions of NO_x, SO_2, $SO_{4\,a,f}$ (fine aerosol sulphate), and NH_3 in each of the following GNFR sectors:

► Energy

► Industry

► Traffic Light and Heavy Duty Vehicles, and Other Traffic

► Shipping

► Aviation

► Other Non-road Transport

► Agriculture Manure and Housing

► Residential combustion

► Other

Natural emissions and emissions from abroad (Abroad & International Shipping) will not be considered here, since they do not constitute German anthropogenic emissions. The emissions form a matrix of n x m elements called the predictor variable matrix, with n the number of runs in the calibration set (i.e., the samples) and m the product of the number of species and the number of sectors.

The dependent data or response variables for the first model are the concentrations of aerosol species NO_3^-, SO_4^{2-} and NH_4^+ for each of the above mentioned sectors. In addition, the sum of these species is taken into account as a fourth variable *SIA*. The responses for the second model are the total intake values of these species. Both models therefore have matrices of response variables of n x p elements called the response variable matrices, with n the number of runs and p the product of the number of aerosol species and the number of sectors.

If one of the variables in either the predictor or response matrices would have significantly larger values than the others, it would automatically dominate the model. Therefore, the values of each variable need to be properly centered and scaled. This is done by subtracting the mean value of each variable (columns in the matrix) and dividing the resulting values by the standard deviation of that variable. That way, each variable is scaled with its own center and range, ensuring they will get equal influence in the model.

In multiple linear regression and other linear regression techniques, a choice needs to be made for the number of fit parameters of the model. Taking *too few* parameters would result in a *very coarse model* that will not represent the calibration set well. Nor will it produce reliable predictions from any input data outside the calibration set. Taking *too many* parameters would result in a *very detailed, but rigid, model* that represents the calibration set perfectly, but it is incapable of predictions on any input data outside the calibration set. PLSR works in a similar way, in that the number of *latent variables* or *principle* components needs to be chosen[2]. Latent variables represent the interrelations between the predictor variables and the response variables. To find the optimal amount of latent variables the model needs to cover, a series of models with variable amounts of latent variables is tested on the calibration data to see what the effect is on the mean squared error of cross-validation (MSECV). To this end, the calibration set is split into a training set to create the model on and a test set to determine the prediction error. This is done a number of times to calculate MSECV from all values of the prediction error. The process is called cross-validation and it is applied on the calibration data of both the concentration and the intake model. The method of cross-validation applied here is Leave One Out, in which the test set always consists of one sample, while the rest is used to create the model.

Figure 80:   MSECV for the PLS model for prediction concentrations (left) and intake (right).
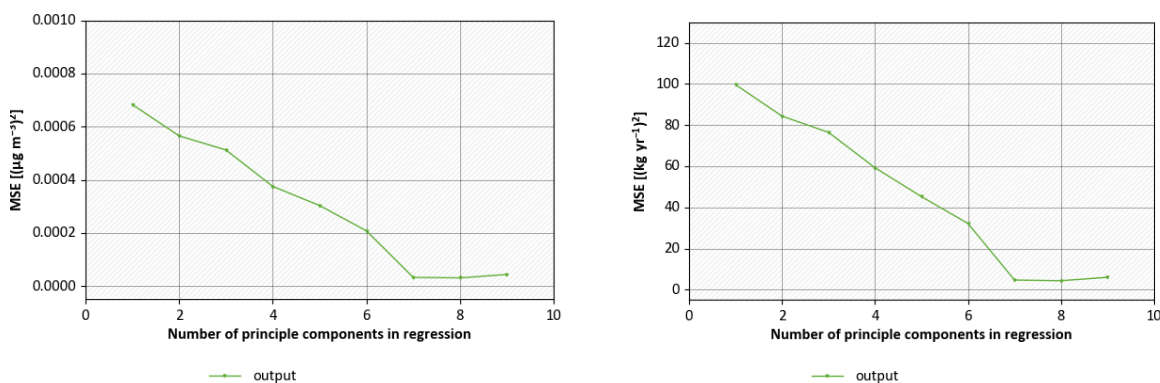
Source: TNO

Figure 80 shows the mean square error of cross-validation for both models. In both cases, there appears to be a cut-off at 7 principle components. Models of more than 8 principle components cause the error to explode. Hence, in both cases 7 principle components will be used. Figure 81

[2] A complete description of the mechanism of PLS model creation is not given here, for more information, the reader is referred to (Wold et al., 2001) or (Abdi, 2010)

shows the cross-validation plots for both models; the models fit the data well with a correlation coefficient of over 0.95.

Figure 81: **Cross-validation plot for the PLS model for prediction concentrations (left) and intake (right).**
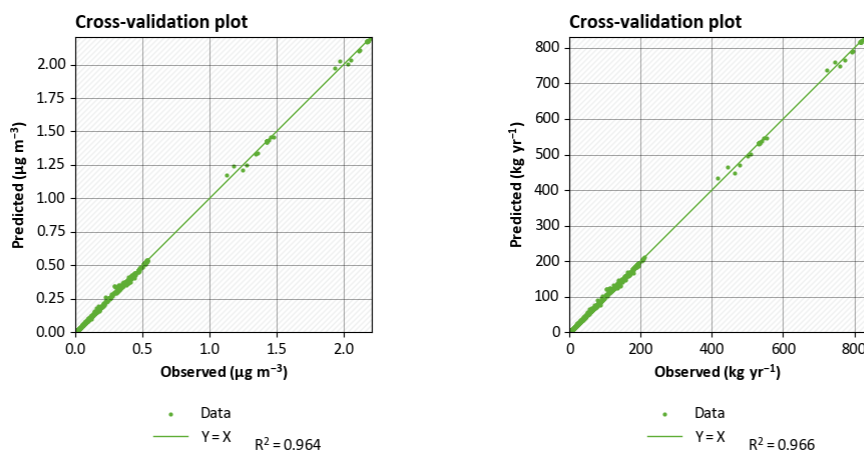
Source: TNO

The PLS models can now be used to predict the concentrations or intake of the above mentioned aerosol species in the above mentioned sectors on the basis of a set of emission data supplied by the user. However, any emission dataset will result in a concentration/intake dataset, regardless whether the emission dataset strongly deviates from the emissions in the calibration dataset or not. Therefore, a metric is needed to provide feedback on the validity of the predictions. Leverage is such a metric applied widely in regression modeling. This is a number that signifies the 'distance' between a sample and the calibration dataset: high leverage signifies a strong deviation of the sample from the calibration set. For a full explanation on leverage, see Zhang and Garcia-Munoz (2009). The leverage can be used to estimate a prediction error, but for PLS this is not as straightforward as it is for other linear regression techniques. Hence, the approach followed here is to compare the leverage with a maximum value to say something about the validity of a prediction. The maximum leverage $h_{l, max}$ is given by

$$h_{i,max} = \frac{2n_{comp}}{n_{samples}}$$

10

In this equation, n_{comp} is the number of principle components in the model and $n_{samples}$ is the number of samples in the calibration set. For emission datasets of which the leverage exceeds this maximum, the validity of the prediction may be compromised. This is not a hard boundary, but it does give an idea about the trustworthiness of the prediction.

The PLS Regression model on which the toolkit is based, is made with Python library SciKit Learn (Pedregosa et al., 2012).

7.2.3 Calculation of formation factors and intake factors

Once the models produce concentration and intake data for user defined reduction scenarios, the formation (FF) and intake factors (IF) can be calculated using the definitions given in Section 2.1.3. The toolkit also offers the possibility to calculate FF and IF for emission and concentration/intake data from other sources. For this purpose, the data should have the format described in Appendix B. The documentation of the toolkit describes the procedure to be followed.

7.3   Visualisation

A screen shot of the frontpage of the visualisation tool is shown in Figure 82. The visualisation of data in the toolkit is based on the Python libraries Param (https://param.holoviz.org/), Panel (https://panel.holoviz.org/), Matplotlib (https://matplotlib.org/) and Bokeh (http://docs.bokeh.org/en/latest/).

Figure 82:   Screen shot of the front page of the visualisation tool
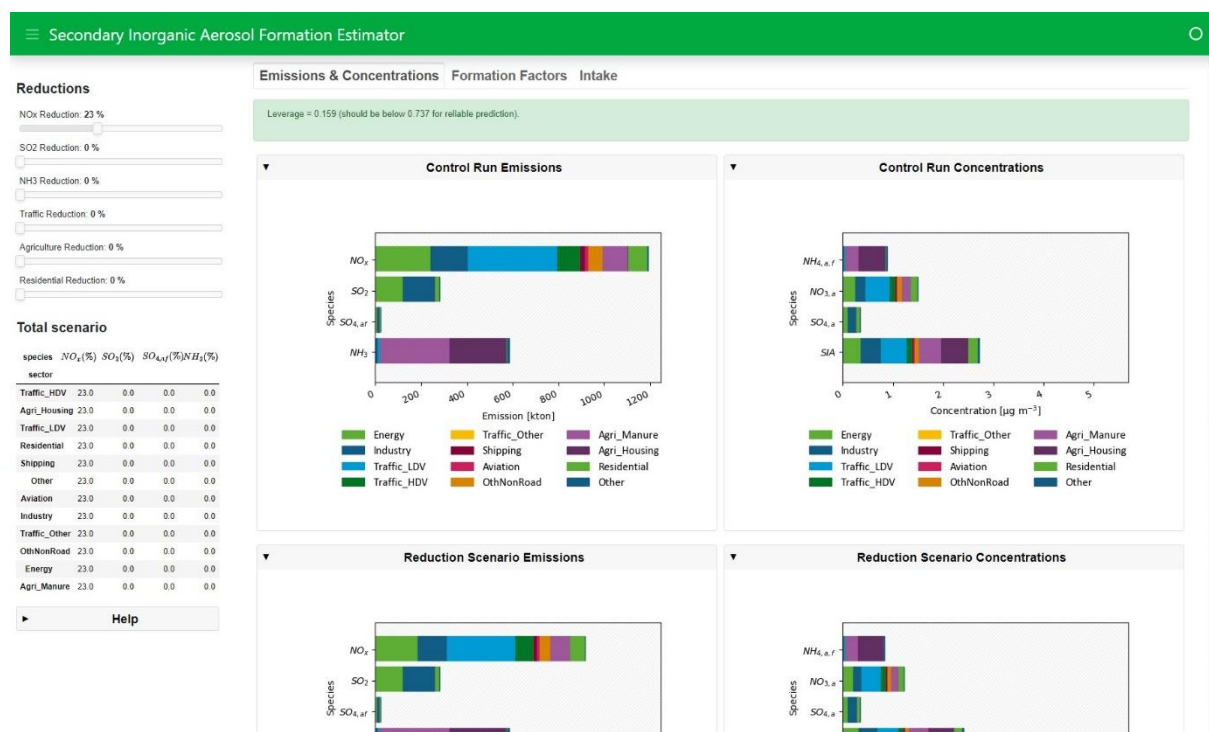
The visualisation tool runs as a web server that creates an interactive web page of the user interface in a browser window. It consists of a left panel and a main page containing three tabs: Emissions & Concentrations, Formation Factors and Intake. In the left panel, the user can configure a reduction scenario by means of the sliders. Reductions are possible for the main SIA precursors – NO_x, SO_2 and NH_3 – and for three sectors – Traffic (LDV & HDV combined), Agriculture (Manure & Housing combined), and Residential combustion. Since the current calibration set only includes data from LOTOS-EUROS runs with max. 60% reductions of these six categories, the sliders have been limited to 60%.

Changes in the reduction scenario are shown in the Total Scenario table and they directly affect the figures in the tabs of the main page. The Emissions and Concentrations tab shows 6 graphs. The top two present stacked bar graphs of the total emissions and average concentrations for the relevant species and sectors originating from the control run (i.e. no reductions applied). Below that are the graphs with the emissions and predicted concentrations for the reduction scenario the user has specified and the difference between the control and reduction scenario is shown in the bottom two graphs (not visible in the screenshot).

The second tab on the main page contains a panel with a description of the calculation of formation factors and a panel with a graph of the formation factor (see Figure 83, description panel not shown). The dropdown menu can be used to select a particular formation factor from a list containing $NO_{3,a}/NO_x$, $SO_{4,a}/SO_2$, $NO_{3,a}/NH_3$, $SO_{4,a}/NH_3$, $NH_{4,a}/NH_3$, SIA/NO_x, SIA/SO_2, and SIA/NH_3. The green alert bar on top shows the leverage and maximum leverage of the chosen reduction scenario as feedback on the validity of the model prediction. For reduction scenarios

134

where the leverage exceeds the maximum value, the bar turns red and a warning appears that the scenario deviates too much from the calibration set for a reliable prediction.

Figure 83: **Screen shot of the Formation Factors panel.**
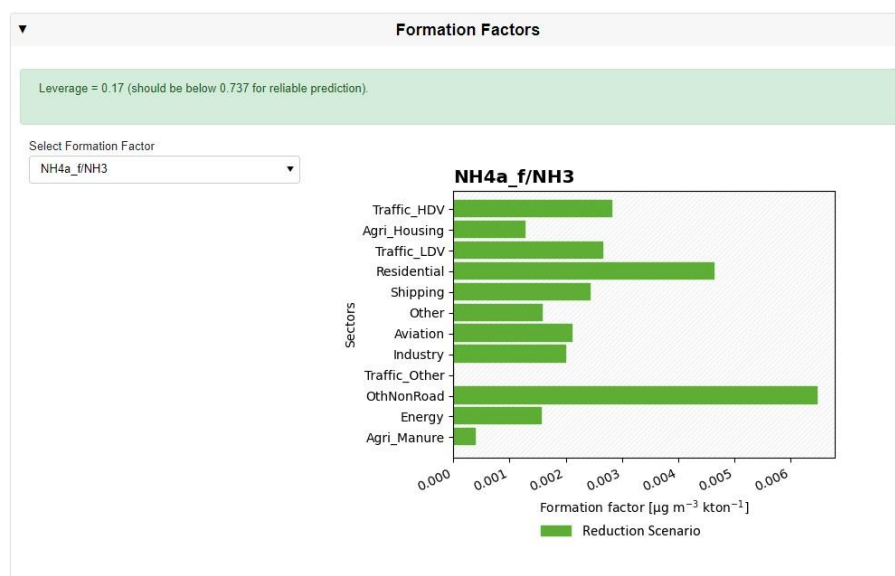
The third tab contains a stacked bar graph of the total intake for the chosen scenario and bar graphs for the intake factors (Figure 84), the latter of which only displays the intake factor selected from a dropdown menu. Similar to the formation factor panel, both display the leverage alert.

Figure 84:   Screen shot of the total intake (top) and intake factors (bottom) panels.
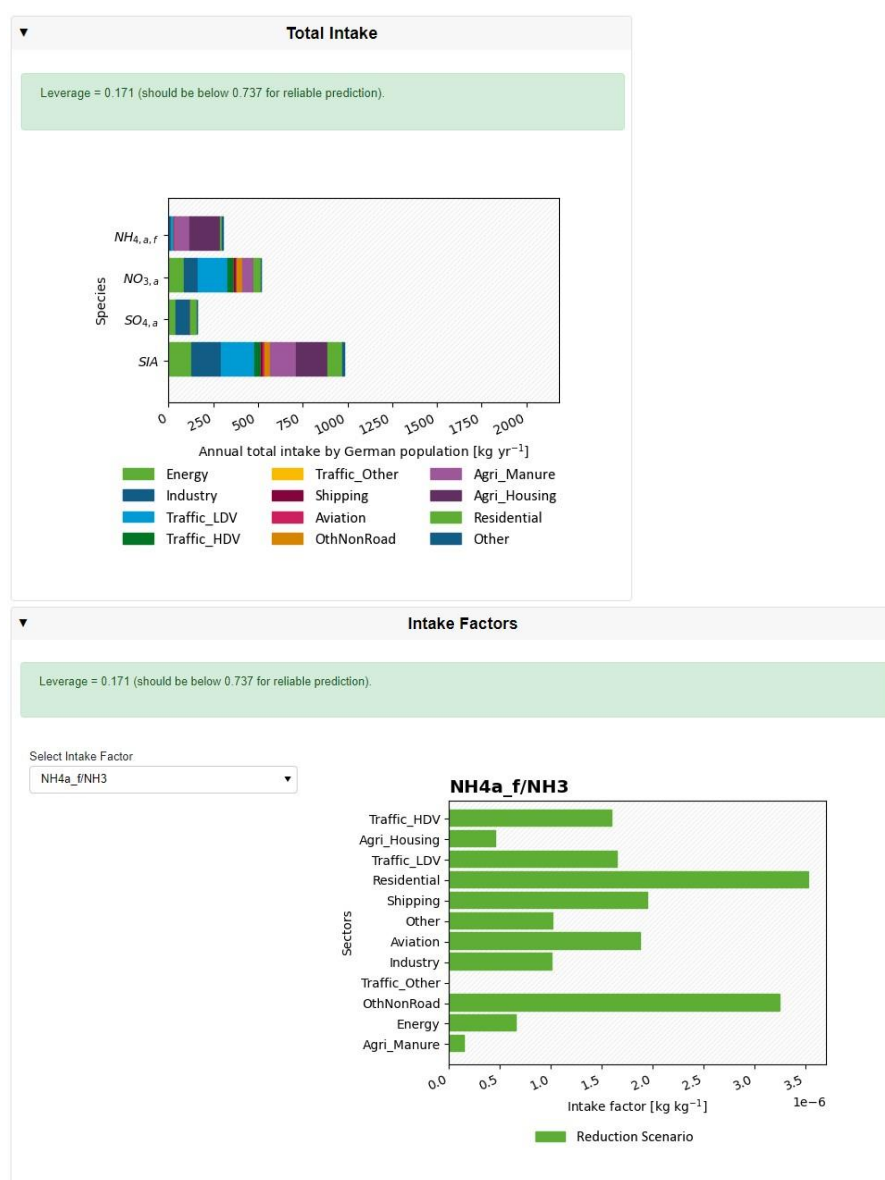
8   Discussion, conclusions and recommendations

This report deals with the contribution of gaseous emissions to the concentration of secondary inorganic and organic aerosol particles (SIA and OA, respectively) in Germany. In this section, we discuss the main findings of our work in relation to the research objectives in the introduction.

8.1   Current understanding of secondary PM formation

Level of process understanding

The formation of secondary inorganic aerosols has been thoroughly investigated and documented (research question 1). The most important pathways of formation and the most important interactions between the SIA precursors are known, including their pH and temperature dependence. The volatility of ammonium nitrate is shown to have a significant effect on the concentrations of the SIA forming species and their deposition and intake. Seasonal and diurnal cycles of species concentrations and their effect on SIA formation can be explained, though sulphate concentrations are systematically underestimated. The kinetics of some reaction pathways towards sulphate are not well understood yet (viz. metal catalyzed reactions), as well as the role of organic molecules in these reactions. These processes are the subject of ongoing scientific research. We recommend the implementation of these new insights on sulphate formation from SO_2 in LE to assess whether they lead to improvements in modelled sulphate concentrations.

For organic aerosol, the level of process understanding is relatively low, although a lot of progress has been made over the last 15 years. Significant uncertainties in the model representation of semi-volatile emissions and gas-phase aging remain, as well as a lack of understanding of and robust parametrizations for processes such as SVOC dry deposition, aqueous phase SOA production and photolytic breakdown of OA. In addition, the availability of observational data for organic aerosols needs to be improved to assess the validity of model results.

Indicators

As indicator of the conversion of precursors to PM, we applied the formation factor, which indicates the change in concentration of a certain PM component that results from a change in its (precursor) emission (research question 3). Further, the intake factor was applied to assess the change of population exposure of a certain PM component resulting from changes in its (precursor) emission. Both factors represent the effect of a change in emissions on concentrations and intake, comparing a reduction scenario with a reference case. The factors are calculated by dividing a change in concentration/intake by the change in emissions. Therefore, any background values cancel out, so the factors give insight in the *sensitivity* of concentrations and intake on emission changes with bias.

Representation of processes in LE (research question 2)

LOTOS-EUROS was used to describe the interactions between different species that form particulate matter, as well as their transport trough and removal from the atmosphere. Simulated gradients of the SIA compounds are much smaller than those of their primary emitted precursors, due to the effect of atmospheric chemistry and the time scale at which this takes place.

The regions with high nitrogen oxide levels do not correspond to those with the largest annual mean ammonia concentrations, because their predominant emission sources are different (research question 5). Largest simulated ammonia concentrations can be found in the region

with the largest animal density, whereas nitrogen oxides are predominantly present for all populated and industrialized regions in the country.

Nitrate contributes the largest mass fraction to SIA levels across Germany. Its concentration peaks in regions with the largest ammonia concentrations, due to the semi-volatile nature of ammonium nitrate: with a larger ammonia concentration a larger amount of nitric acid is driven into the aerosol phase. Ammonium neutralizes both sulfate and nitrate leading to a field that shows a large correspondence with the nitrate concentration levels.

Organic aerosol formation over Germany was simulated for the first time with LOTOS-EUROS. Its concentration shows a gradient from northwest to southeast. Despite including additional condensables in the POA emissions and accounting for IVOC emissions, the model underestimates annual average OC concentrations compared to the few available measurements. There are many possible factors that may contribute to this, including missing emissions and processes in the model. Since these underestimations seem to happen both in summer and in winter, it is likely that there is not a single cause for this underestimation. The implementation of the organic aerosol model with condensables needs to be developed further in upcoming projects to address these underestimations.

8.2   Influence of emission reductions on secondary PM concentrations over Germany

To assess the sensitivity of SPM concentrations to emission reductions (research question 4), we first established Reference simulations for SIA and OA. These simulations yielded annual mean SIA concentration of 5.5 µg m^{-3} and annual mean OA concentration of 1 µg m^{-3} OA over Germany in 2018. These reference runs were used as a basis for emission reduction scenarios, which were done for (precursor) species and for specific sectors. The species reduction scenarios gave an FF for SIA of about 0.001 µg m^{-3} kTon^{-1}, while for OA this number is about 0.006 µg m^{-3} kTon^{-1}. This is due to the fact that most of the OA formation is a rapid physical process (i.e. gas/particle partitioning), while SIA formation involves intermediate (chemistry) steps. For PPM, we found an FF of about 0.01 µg m^{-3} kTon^{-1}, which indicates that the efficiency of OA formation over Germany resembles that of PPM formation more than that of SIA formation. Based on the reduction scenarios for individual sectors, we conclude that reducing emissions from Agriculture appears the most effective pathway to reduce SIA concentrations, while for OA the reduction of emissions from the Residential combustion sector is the most effective.

Regarding the effect of emission reductions on the total intake of secondary PM, intake factors were calculated for different precursors. From single species reduction scenarios it was found that SIA intake factors for all precursors (NO_x, SO_2, and NH_3) were around 0.3 x 10^{-6} kg/kg. For OA/POA the intake factor is around 4 x 10^{-6} kg/kg. These values are in the same order of magnitude as those from Van Zelm (2016), who published values between 0.5 x 10^{-6} and 1.6 x 10^{-6} kg/kg for the intake of PM$_{2.5}$ in Germany for the mentioned precursors, while for primary PM they found an IF of 4.6 x 10^{-6}.

8.3   Spatio-temporal variations in formation factors

For SIA, it was shown that regions of high nitrate concentrations line up with regions of high ammonia emissions due to the semi-volatile nature of ammonium nitrate. This, combined with the fact that ammonium nitrate is the predominant constituent of SIA in Germany, explains the higher formation factor for SIA/NH$_3$ (in Agriculture, mainly emitting NH$_3$), compared to SIA/NO$_x$ (in Traffic, mainly emitting NO$_x$). Regarding temporal variations, wintertime has lower temperatures and higher nitrate concentrations than summertime, while the emissions of NO$_x$

does not show a very strong trend throughout the year. Hence, the formation factor for SIA/NO$_x$ is expected to be higher in winter. Since the ammonia emissions are higher in summertime, the sensitivity to changes in emission will be lower in summertime and the formation factor for SIA/NH$_3$ will also be higher in winter. Improved dynamic emission modelling for sectors including agriculture and traffic is recommended to capture the temporal variations in NH$_3$ and NO$_x$ emissions better and hence the timing of the SIA formation from these sources.

For OA, spatial variations in emissions do not play a major role, because mixing of different OA precursors is not directly relevant for the OA formation (only secondary effects on SOA formation through oxidant concentrations). Temporal variations do play a role: in winter, the POA/POA formation factor will be higher than in summer, because of the lower temperatures. In summer, the siSOA/POA formation factor will be higher than in winter because of stronger photochemistry. However, the former effect dominates over the latter.

8.4 Sensitivity of FF and IF to uncertainty in model processes

This section answers research question 6.

Interannual variability

The simulations on which the FF calculation for PPM are based ran from 2015 through 2018. Since the same emission dataset was used for each of these years, the interannual variability in calculated FFs is due to meteorology only. We found that for all sectors, interannual variability in calculated FF was 10% or less. From this, we conclude that for OA, the interannual variability would likely be similar to that of PPM, although there is the additional effect that temperature and atmospheric mixing has on gas/particle partitioning. For SIA, temperature and radiation may also play a role, but in addition also a potential difference in chemical regime could play a role. However, with emissions -including condensables- only available for the year 2018, we were not able to explicitly test this. Once multi-year emission datasets including condensables become available, interannual variability of the formation factor of SIA and OA can be properly investigated.

Model resolution

We assessed the influence of model resolution on the FF of PPM by comparing results from two model runs over Germany: one at a 7x7 km^2 resolution and one at a 2x2 km^2 resolution (research question 6). This comparison showed that the difference in calculated FFs were less than 5%, so we can conclude that FFs of PPM are not very sensitive to the chosen model resolution. Based on this, we argue that also for SPM, model resolution is not a critical factor: if anything, the sensitivity of SPM formation should be lower than that of PPM, since SPM generally shows smoother gradients than PPM. This is due to the fact that SPM formation involves intermediate steps, such as chemistry, which take some time (in contrast to PPM formation which is instantaneous upon emission, i.e. in the same model time step), allowing the spreading out of the precursors and intermediate reaction products by horizontal and vertical transport.

This discussion applies to the resolution of 7x7 km^2 of most simulations in this study, which is sufficiently fine to capture gradients in concentrations and population densities good enough to yield robust annual average FF and IF. For model runs at a coarser resolutions (e.g. 50x50 km^2), these gradients may not be captured that well. This may lead to higher calculated FF and IF for secondary PM since the atmosphere is considered well-mixed over larger horizontal areas.

In this work, results for formation and intake factors of SIA and OA are presented as countrywide data. For certain subsectors, it may be worthwhile to investigate whether spatial

resolution needs refinement. For better support of state-level policies, it is recommended to calculate concentrations, FF and IF per state, applying the labelling technique.

Biogenic emissions

Emissions of NO from soils (136 kTon in NO_2-equivalents) are small compared to anthropogenic NO_x emissions (1270 kTon NO_2-equivalents) over Germany. This indicates that biogenic emissions likely constitute a small but non-negligible precursor for nitrate formation, especially in areas with relatively small anthropogenic NO_x sources, like Mecklenburg-Vorpommern.

There is a significant contribution of biogenic VOCs to the total OA concentration in the Reference run. This finding is in line with the literature, but it is hard to assess its validity and the associated uncertainty because no observational data is available for the evaluation of simulated biogenic VOC and bSOA concentrations, at least not for the region and period studied here. Therefore, this needs further investigation in future projects dealing with biogenic emissions.

8.5   Toolkit

A toolkit is developed (research question 7) to derive the PM formation potential and apply it to alternative emission reduction scenarios. The main objective of this WP is to provide tools to calculate the impact of emission reduction scenarios on PM concentrations without using the results of the CTM directly. The toolkit shows a visualization of the effect of user definable reduction scenarios on the concentrations of SIA components and their formation and intake factors. Since the toolkit is provided as open source Python code, the user can freely use the functionality the toolkit provides, for instance to calculate intake and formation factors of data from the user. The toolkit is fully documented; it provides usage information of the visualization tool, but also of the application programming interface (API).

9   List of References

Abdi, H.: Partial least squares regression and projection on latent structure regression (PLS Regression), WIREs Comput. Stat., 2, 97–106, https://doi.org/10.1002/wics.51, 2010.

Aiken, A. C., DeCarlo, P. F., Kroll, J. H., Worsnop, D. R., Huffman, J. A., Docherty, K. S., Ulbrich, I. M., Mohr, C., Kimmel, J. R., Sueper, D., Sun, Y., Zhang, Q., Trimborn, A., Northway, M., Ziemann, P. J., Canagaratna, M. R., Onasch, T. B., Alfarra, M. R., Prevot, A. S. H., Dommen, J., Duplissy, J., Metzger, A., Baltensperger, U., and Jimenez, J. L.: O/C and OM/OC Ratios of Primary, Secondary, and Ambient Organic Aerosols with High-Resolution Time-of-Flight Aerosol Mass Spectrometry, Environ. Sci. Technol., 42, 4478–4485, https://doi.org/10.1021/es703009q, 2008.

Alexander, B., Park, R. J., Jacob, D. J., and Gong, S.: Transition metal-catalyzed oxidation of atmospheric sulfur: Global implications for the sulfur budget, J. Geophys. Res. Atmospheres, 114, https://doi.org/10.1029/2008JD010486, 2009.

Amann, M. and Wagner, F.: A Flexibility Mechanism for Complying with National Emission Ceilings for Air Pollutants, InternationalInstituteforAppliedSystemsAnalysis(IIASA), Laxenburg,Austria, 2014.

Ansari, A. S. and Pandis, S. N.: Response of Inorganic PM to Precursor Concentrations, Environ. Sci. Technol., 32, 2706–2714, https://doi.org/10.1021/es971130j, 1998.

Atkinson, R.: Gas-Phase Tropospheric Chemistry of Volatile Organic Compounds: 1. Alkanes and Alkenes, J. Phys. Chem. Ref. Data, 26, 215–290, https://doi.org/10.1063/1.556012, 1997.

Banzhaf, S., Schaap, M., Kerschbaumer, A., Reimer, E., Stern, R., van der Swaluw, E., and Builtjes, P.: Implementation and evaluation of pH-dependent cloud chemistry and wet deposition in the chemical transport model REM-Calgrid, Atmos. Environ., 49, 378–390, https://doi.org/10.1016/j.atmosenv.2011.10.069, 2012.

Banzhaf, S., Schaap, M., Wichink Kruit, R. J., Denier van der Gon, H. a. C., Stern, R., and Builtjes, P. J. H.: Impact of emission changes on secondary inorganic aerosol episodes across Germany, Atmospheric Chem. Phys., 13, 11675–11693, https://doi.org/10.5194/acp-13-11675-2013, 2013.

Banzhaf, S., Schaap, M., Kranenburg, R., Manders, A. M. M., Segers, A. J., Visschedijk, A. J. H., Denier van der Gon, H. a. C., Kuenen, J. J. P., van Meijgaard, E., van Ulft, L. H., Cofala, J., and Builtjes, P. J. H.: Dynamic model evaluation for secondary inorganic aerosol and its precursors over Europe between 1990 and 2009, Geosci. Model Dev., 8, 1047–1070, https://doi.org/10.5194/gmd-8-1047-2015, 2015.

Beekmann, M., Kerschbaumer, A., Reimer, E., Stern, R., and Möller, D.: PM measurement campaign HOVERT in the Greater Berlin area: model evaluation with chemically specified particulate matter observations for a one year period, Atmospheric Chem. Phys., 7, 55–68, https://doi.org/10.5194/acp-7-55-2007, 2007.

Beltman, J.,Hendriks, C., Tum, B., Schaap, M. : The impact of large scale biomass production on ozone air pollution in Europe, Atmospheric Environment 71 352-363, 2013.

Bennett, D. H., McKone, T. E., Evans, J. S., Nazaroff, W. W., Margni, M. D., Jolliet, O., and Smith, K. R.: Defining Intake Fraction, Environ. Sci. Technol., 36, 206A-211A, https://doi.org/10.1021/es0222770, 2002.

Bergström, R., Denier van der Gon, H. a. C., Prévôt, A. S. H., Yttri, K. E., and Simpson, D.: Modelling of organic aerosols over Europe (2002-2007) using a volatility basis set (VBS) framework: application of different assumptions regarding the formation of secondary organic aerosol, Atmospheric Chem. Phys., 12, 8499–8527, https://doi.org/10.5194/acp-12-8499-2012, 2012.

Bessagnet, B., Beauchamp, M., Guerreiro, C., de Leeuw, F., Tsyro, S., Colette, A., Meleux, F., Rouïl, L., Ruyssenaars, P., Sauter, F., Velders, G. J. M., Foltescu, V. L., and van Aardenne, J.: Can further mitigation of ammonia emissions reduce exceedances of particulate matter air quality standards?, Environ. Sci. Policy, 44, 149–163, https://doi.org/10.1016/j.envsci.2014.07.011, 2014.

Brandt, C. and van Eldik, R.: Transition Metal-Catalyzed Oxidation of Sulfur(IV) Oxides. Atmospheric-Relevant Processes and Mechanisms, Chem. Rev., 95, 119–190, https://doi.org/10.1021/cr00033a006, 1995.

Ciarelli, G., Theobald, M. R., Vivanco, M. G., Beekmann, M., Aas, W., Andersson, C., Bergström, R., Manders-Groot, A., Couvidat, F., Mircea, M., Tsyro, S., Fagerli, H., Mar, K., Raffort, V., Roustan, Y., Pay, M.-T., Schaap, M., Kranenburg, R., Adani, M., Briganti, G., Cappelletti, A., D'Isidoro, M., Cuvelier, C., Cholakian, A., Bessagnet, B., Wind, P., and Colette, A.: Trends of inorganic and organic aerosols and precursor gases in Europe: insights from the EURODELTA multi-model experiment over the 1990–2010 period, Geosci. Model Dev., 12, 4923–4954, https://doi.org/10.5194/gmd-12-4923-2019, 2019.

Clifton, C. L., Altstein, Nisan., and Huie, R. E.: Rate constant for the reaction of nitrogen dioxide with sulfur(IV) over the pH range 5.3-13, Environ. Sci. Technol., 22, 586–589, https://doi.org/10.1021/es00170a018, 1988.

Coenen, P. W. G. H., Kuenen, J. J. P., Visschedijk, A. J. H., Janssen, R. H. H., Diegmann, V., Neunhauserer, L., Latt, C., and Hartmann, U.: UBA FKZ 3718 51 241 0: Einfluss von Kondensaten auf die Partikelkonzentration; Endbericht-Entwurf, 2022.

Dimitris V., Takahama, S., Davidson, C., Pandis, S.: Simulation of the thermodynamics and removal processes in the sulfate-ammonia-nitric acid system during winter: Implications for PM2.5 control strategies, Journal of Geophysical Research, VOL. 110, D07S14, doi:10.1029/2004JD005038, 2005

De Leeuw, F. A. A. M.: A set of emission indicators for long-range transboundary air pollution, Environ. Sci. Policy, 5, 135–145, https://doi.org/10.1016/S1462-9011(01)00042-9, 2002.

Denier van der Gon, H. a. C., Bergström, R., Fountoukis, C., Johansson, C., Pandis, S. N., Simpson, D., and Visschedijk, A. J. H.: Particulate emissions from residential wood combustion in Europe – revised estimates and an evaluation, Atmospheric Chem. Phys., 15, 6503–6519, https://doi.org/10.5194/acp-15-6503-2015, 2015.

Derwent, R., Witham, C., Redington, A., Jenkin, M., Stedman, J., Yardley, R., and Hayman, G.: Particulate matter at a rural location in southern England during 2006: Model sensitivities to precursor emissions, Atmos. Environ., 43, 689–696, https://doi.org/10.1016/j.atmosenv.2008.09.077, 2009.

Donahue, N. M., Robinson, A. L., Stanier, C. O., and Pandis, S. N.: Coupled Partitioning, Dilution, and Chemical Aging of Semivolatile Organics, Environ. Sci. Technol., 40, 2635–2643, https://doi.org/10.1021/es052297c, 2006.

EEA: Health impacts of air pollution in Europe, 2021, 2021.

Emberson, L. D., Ashmore, M. R., Cambridge, H. M., Simpson, D., and Tuovinen, J.-P.: Modelling stomatal ozone flux across Europe, Environ. Pollut., 109, 403–413, https://doi.org/10.1016/S0269-7491(00)00043-9, 2000.

Erisman, J. W. and Schaap, M.: The need for ammonia abatement with respect to secondary PM reductions in Europe, Environ. Pollut., 129, 159–163, https://doi.org/10.1016/j.envpol.2003.08.042, 2004.

Ervens, B., Turpin, B. J., and Weber, R. J.: Secondary organic aerosol formation in cloud droplets and aqueous particles (aqSOA): a review of laboratory, field and model studies, Atmospheric Chem. Phys., 11, 11069–11102, https://doi.org/10.5194/acp-11-11069-2011, 2011.

Fagerli, H. and Aas, W.: Trends of nitrogen in air and precipitation: Model results and observations at EMEP sites in Europe, 1980–2003, Environ. Pollut., 154, 448–461, https://doi.org/10.1016/j.envpol.2008.01.024, 2008.

Fountoukis, C. and Nenes, A.: ISORROPIA II: a computationally efficient thermodynamic equilibrium model for K^+ - Ca^{2+} - Mg^{2+} - NH_4^+ - Na^+ - SO_4^{2-} - NO_3^- - Cl^- - H_2O aerosols, Atmospheric Chem. Phys., 7, 4639–4659, https://doi.org/10.5194/acp-7-4639-2007, 2007.

Fountoukis, C., Megaritis, A. G., Skyllakou, K., Charalampidis, P. E., Denier van der Gon, H. A. C., Crippa, M., Prévôt, A. S. H., Fachinger, F., Wiedensohler, A., Pilinis, C., and Pandis, S. N.: Simulating the formation of carbonaceous aerosol in a European Megacity (Paris) during the MEGAPOLI summer and winter campaigns, Atmospheric Chem. Phys., 16, 3727–3741, https://doi.org/10.5194/acp-16-3727-2016, 2016.

Fowler, D., Sutton, M. A., Flechard, C., Cape, J. N., Storeton-West, R., Coyle, M., and Smith, R. I.: The Control of SO2 Dry Deposition on to Natural Surfaces by NH3 and its Effects on Regional Deposition, Water Air Soil Pollut. Focus, 1, 39–48, https://doi.org/10.1023/A:1013161912231, 2001.

Fowler, D., Smith, R., Muller, J., Cape, J. N., Sutton, M., Erisman, J. W., and Fagerli, H.: Long Term Trends in Sulphur and Nitrogen Deposition in Europe and the Cause of Non-linearities, in: Acid Rain - Deposition to Recovery, edited by: Brimblecombe, P., Hara, H., Houle, D., and Novak, M., Springer Netherlands, Dordrecht, 41–47, https://doi.org/10.1007/978-1-4020-5885-1_5, 2007.

Gery, M. W., Whitten, G. Z., and Killus, J. P.: Development and testing of the CBM-IV (Carbon-Bond Mechanism) for urban and regional modeling. Final report, July 1985-June 1987, Systems Applications, Inc., San Rafael, CA (USA), 1988.

Goldstein, A. H. and Galbally, I. E.: Known and Unexplored Organic Constituents in the Earth's Atmosphere, Environ. Sci. Technol., 41, 1514–1521, https://doi.org/10.1021/es072476p, 2007.

Guenther, A., Karl, T., Harley, P., Wiedinmyer, C., Palmer, P. I., and Geron, C.: Estimates of global terrestrial isoprene emissions using MEGAN (Model of Emissions of Gases and Aerosols from Nature), Atmospheric Chem. Phys., 6, 3181–3210, https://doi.org/10.5194/acp-6-3181-2006, 2006.

Guenther, A. B., Zimmerman, P. R., Harley, P. C., Monson, R. K., and Fall, R.: Isoprene and monoterpene emission rate variability: Model evaluations and sensitivity analyses, J. Geophys. Res. Atmospheres, 98, 12609–12617, https://doi.org/10.1029/93JD00527, 1993.

Guo, H., Otjes, R., Schlag, P., Kiendler-Scharr, A., Nenes, A., and Weber, R. J.: Effectiveness of ammonia reduction on control of fine particle nitrate, Atmospheric Chem. Phys., 18, 12241–12256, https://doi.org/10.5194/acp-18-12241-2018, 2018.

Hass, H., Jakobs, H. J., and Memmesheimer, M.: Analysis of a regional model (EURAD) near surface gas concentration predictions using observations from networks, Meteorol. Atmospheric Phys., 57, 173–200, https://doi.org/10.1007/BF01044160, 1995.

Hendriks, C., Kranenburg, R., Gijlswijk, R., Wichink Kruyt, R., Segers, A., Denier van der Gon, H., and Schaap, M.: The origin of ambient particulate matter concentrations in the Netherlands, Atmospheric Environ. 69, 289-303, https://doi.org/10.1016/j.atmosenv.2012.12.017, 2013.

Hodzic, A., Aumont, B., Knote, C., Lee-Taylor, J., Madronich, S., and Tyndall, G.: Volatility dependence of Henry's law constants of condensable organics: Application to estimate depositional loss of secondary organic aerosols, Geophys. Res. Lett., 41, 4795–4804, https://doi.org/10.1002/2014GL060649, 2014.

Hodzic, A., Kasibhatla, P. S., Jo, D. S., Cappa, C. D., Jimenez, J. L., Madronich, S., and Park, R. J.: Rethinking the global secondary organic aerosol (SOA) budget: stronger production, faster removal, shorter lifetime, Atmospheric Chem. Phys., 16, 7917–7941, https://doi.org/10.5194/acp-16-7917-2016, 2016.

Huie, R. E. and Neta, P.: Rate constants for some oxidations of S(IV) by radicals in aqueous solutions, Atmospheric Environ. 1967, 21, 1743–1747, https://doi.org/10.1016/0004-6981(87)90113-2, 1987.

Im, U., Bianconi, R., Solazzo, E., Kioutsioukis, I., Badia, A., Balzarini, A., Baró, R., Bellasio, R., Brunner, D., Chemel, C., Curci, G., Denier van der Gon, H., Flemming, J., Forkel, R., Giordano, L., Jiménez-Guerrero, P., Hirtl, M., Hodzic, A., Honzak, L., Jorba, O., Knote, C., Makar, P. A., Manders-Groot, A., Neal, L., Pérez, J. L., Pirovano, G., Pouliot, G., San Jose, R., Savage, N., Schroder, W., Sokhi, R. S., Syrakov, D., Torian, A., Tuccella, P., Wang, K., Werhahn, J., Wolke, R., Zabkar, R., Zhang, Y., Zhang, J., Hogrefe, C., and Galmarini, S.: Evaluation of operational online-coupled regional air quality models over Europe and North America in the context of AQMEII phase 2. Part II: Particulate matter, Atmos. Environ., 115, 421–441, https://doi.org/10.1016/j.atmosenv.2014.08.072, 2015.

Janssen, R. H. H., Tsimpidi, A. P., Karydis, V. A., Pozzer, A., Lelieveld, J., Crippa, M., Prévôt, A. S. H., Ait-Helal, W., Borbon, A., Sauvage, S., and Locoge, N.: Influence of local production and vertical transport on the organic aerosol budget over Paris, J. Geophys. Res. Atmospheres, 122, 8276–8296, https://doi.org/10.1002/2016JD026402, 2017.

Jiang, J., Aksoyoglu, S., Ciarelli, G., Oikonomakis, E., El-Haddad, I., Canonaco, F., O'Dowd, C., Ovadnevaite, J., Minguillón, M. C., Baltensperger, U., and Prévôt, A. S. H.: Effects of two different biogenic emission models on modelled ozone and aerosol concentrations in Europe, Atmospheric Chem. Phys., 19, 3747–3768, https://doi.org/10.5194/acp-19-3747-2019, 2019a.

Jiang, J., Aksoyoglu, S., El-Haddad, I., Ciarelli, G., Denier van der Gon, H. A. C., Canonaco, F., Gilardoni, S., Paglione, M., Minguillón, M. C., Favez, O., Zhang, Y., Marchand, N., Hao, L., Virtanen, A., Florou, K., O'Dowd, C., Ovadnevaite, J., Baltensperger, U., and Prévôt, A. S. H.: Sources of organic aerosols in Europe: a modeling study using CAMx with modified volatility basis set scheme, Atmospheric Chem. Phys., 19, 15247–15270, https://doi.org/10.5194/acp-19-15247-2019, 2019b.

Jimenez, J. L., Canagaratna, M. R., Donahue, N. M., Prevot, A. S. H., Zhang, Q., Kroll, J. H., DeCarlo, P. F., Allan, J. D., Coe, H., Ng, N. L., Aiken, A. C., Docherty, K. S., Ulbrich, I. M., Grieshop, A. P., Robinson, A. L., Duplissy, J., Smith, J. D., Wilson, K. R., Lanz, V. A., Hueglin, C., Sun, Y. L., Tian, J., Laaksonen, A., Raatikainen, T., Rautiainen, J., Vaattovaara, P., Ehn, M., Kulmala, M., Tomlinson, J. M., Collins, D. R., Cubison, M. J., E., Dunlea, J., Huffman, J. A., Onasch, T. B., Alfarra, M. R., Williams,

P. I., Bower, K., Kondo, Y., Schneider, J., Drewnick, F., Borrmann, S., Weimer, S., Demerjian, K., Salcedo, D., Cottrell, L., Griffin, R., Takami, A., Miyoshi, T., Hatakeyama, S., Shimono, A., Sun, J. Y., Zhang, Y. M., Dzepina, K., Kimmel, J. R., Sueper, D., Jayne, J. T., Herndon, S. C., Trimborn, A. M., Williams, L. R., Wood, E. C., Middlebrook, A. M., Kolb, C. E., Baltensperger, U., and Worsnop, D. R.: Evolution of Organic Aerosols in the Atmosphere, Science, 326, 1525–1529, https://doi.org/10.1126/science.1180353, 2009.

Kaiser, J. W., Heil, A., Andreae, M. O., Benedetti, A., Chubarova, N., Jones, L., Morcrette, J.-J., Razinger, M., Schultz, M. G., Suttie, M., and van der Werf, G. R.: Biomass burning emissions estimated with a global fire assimilation system based on observed fire radiative power, Biogeosciences, 9, 527–554, https://doi.org/10.5194/bg-9-527-2012, 2012.

Knote, C., Hodzic, A., and Jimenez, J. L.: The effect of dry and wet deposition of condensable vapors on secondary organic aerosols concentrations over the continental US, Atmospheric Chem. Phys., 15, 1–18, https://doi.org/10.5194/acp-15-1-2015, 2015.

Köble, R. and Seufert, G.: Novel Maps for Forest Tree Species in Europe, in: A Changing Atmosphere, 8th European Symposium on the Physico-Chemical Behaviour of Atmospheric Pollutants, Torino, Italy, 7, 2001.

Kranenburg, R., Segers, A. J. J., Hendriks, C., and Schaap, M.: Source apportionment using LOTOS-EUROS: module description and evaluation, Geosci. Model Dev., 6, 721–733, https://doi.org/10.5194/gmd-6-721-2013, 2013.

Kroll, J. H., Lim, C. Y., Kessler, S. H., and Wilson, K. R.: Heterogeneous Oxidation of Atmospheric Organic Aerosol: Kinetics of Changes to the Amount and Oxidation State of Particle-Phase Organic Carbon, J. Phys. Chem. A, 119, 10767–10783, https://doi.org/10.1021/acs.jpca.5b06946, 2015.

Kuenen, J., Dellaert, S., Visschedijk, A., Jalkanen, J.-P., Super, I., and Denier van der Gon, H.: CAMS-REG-v4: a state-of-the-art high-resolution European emission inventory for air quality modelling, Earth Syst. Sci. Data, 14, 491–515, https://doi.org/10.5194/essd-14-491-2022, 2022.

Kuenen, J. J. P., S.N.C. Dellaert, A.J.H. Visschedijk, S. Jonkers, H.A.C. Denier van der Gon, and J.-P. Jalkanen: CAMS_81 – Global and Regional emissions D81.1.1.1 : European emissions dataset (2015), 2018.

Lane, T. E., Donahue, N. M., and Pandis, S. N.: Effect of NOx on Secondary Organic Aerosol Concentrations, Environ. Sci. Technol., 42, 6022–6027, https://doi.org/10.1021/es703225a, 2008.

Lee, Y. and Schwartz, S. E.: Kinetics of oxidation of aqueous sulfur(IV) by nitrogen dioxide, in: Precipitation Scavenging, Dry Deposition, and Resuspension, Elsevier, 31–52, 1983.

Littlejohn, D., Wang, Y., and Chang, S. G.: Oxidation of aqueous sulfite ion by nitrogen dioxide, Environ. Sci. Technol., 27, 2162–2167, https://doi.org/10.1021/es00047a024, 1993.

Liu, T., Clegg, S. L., and Abbatt, J. P. D.: Fast oxidation of sulfur dioxide by hydrogen peroxide in deliquesced aerosol particles, Proc. Natl. Acad. Sci., 117, 1354–1359, https://doi.org/10.1073/pnas.1916401117, 2020.

Ma, P. K., Zhao, Y., Robinson, A. L., Worton, D. R., Goldstein, A. H., Ortega, A. M., Jimenez, J. L., Zotter, P., Prévôt, A. S. H., Szidat, S., and Hayes, P. L.: Evaluating the impact of new observational constraints on P-S/IVOC emissions, multi-generation oxidation, and chamber wall losses on SOA

modeling for Los Angeles, CA, Atmospheric Chem. Phys., 17, 9237–9259, https://doi.org/10.5194/acp-17-9237-2017, 2017.

Manders, A. M. M., Builtjes, P. J. H., Curier, L., Denier van der Gon, H. A. C., Hendriks, C., Jonkers, S., Kranenburg, R., Kuenen, J., Segers, A. J., Timmermans, R. M. A., Visschedijk, A., Wichink Kruit, R. J., Van Pul, W. A. J., Sauter, F. J., van der Swaluw, E., Swart, D. P. J., Douros, J., Eskes, H., van Meijgaard, E., van Ulft, B., van Velthoven, P., Banzhaf, S., Mues, A., Stern, R., Fu, G., Lu, S., Heemink, A., van Velzen, N., and Schaap, M.: Curriculum Vitae of the LOTOS-EUROS (v2.0) chemistry transport model, Geosci. Model Dev. Discuss., 1–53, https://doi.org/10.5194/gmd-2017-88, 2017.

Manders, A. M. M., Segers, A. J., and Jonkers, S.: LOTOS-EUROS v2.2.002 Reference Guide, 2021.

Mårtensson, E. M., Nilsson, E. D., de Leeuw, G., Cohen, L. H., and Hansson, H.-C.: Laboratory simulations and parameterization of the primary marine aerosol production, J. Geophys. Res. Atmospheres, 108, https://doi.org/10.1029/2002JD002263, 2003.

Massad, R. S., Loubet, B., Tuzet, A., and Cellier, P.: Relationship between ammonia stomatal compensation point and nitrogen metabolism in arable crops: Current status of knowledge and potential modelling approaches, Environ. Pollut., 154, 390–403, https://doi.org/10.1016/j.envpol.2008.01.022, 2008.

Matejko, M., Dore, A. J., Hall, J., Dore, C. J., Błaś, M., Kryza, M., Smith, R., and Fowler, D.: The influence of long term trends in pollutant emissions on deposition of sulphur and nitrogen and exceedance of critical loads in the United Kingdom, Environ. Sci. Policy, 12, 882–896, https://doi.org/10.1016/j.envsci.2009.08.005, 2009.

McDonald, B. C., Gouw, J. A. de, Gilman, J. B., Jathar, S. H., Akherati, A., Cappa, C. D., Jimenez, J. L., Lee-Taylor, J., Hayes, P. L., McKeen, S. A., Cui, Y. Y., Kim, S.-W., Gentner, D. R., Isaacman-VanWertz, G., Goldstein, A. H., Harley, R. A., Frost, G. J., Roberts, J. M., Ryerson, T. B., and Trainer, M.: Volatile chemical products emerging as largest petrochemical source of urban organic emissions, Science, 359, 760–764, https://doi.org/10.1126/science.aaq0524, 2018.

McNeill, V. F.: Aqueous Organic Chemistry in the Atmosphere: Sources and Chemical Processing of Organic Aerosols, Environ. Sci. Technol., 49, 1237–1244, https://doi.org/10.1021/es5043707, 2015.

de Meij, A., Thunis, P., Bessagnet, B., and Cuvelier, C.: The sensitivity of the CHIMERE model to emissions reduction scenarios on air quality in Northern Italy, Atmos. Environ., 43, 1897–1907, https://doi.org/10.1016/j.atmosenv.2008.12.036, 2009.

Mircea, M., Bessagnet, B., D'Isidoro, M., Pirovano, G., Aksoyoglu, S., Ciarelli, G., Tsyro, S., Manders, A., Bieser, J., Stern, R., Vivanco, M. G., Cuvelier, C., Aas, W., Prévôt, A. S. H., Aulinger, A., Briganti, G., Calori, G., Cappelletti, A., Colette, A., Couvidat, F., Fagerli, H., Finardi, S., Kranenburg, R., Rouïl, L., Silibello, C., Spindler, G., Poulain, L., Herrmann, H., Jimenez, J. L., Day, D. A., Tiitta, P., and Carbone, S.: EURODELTA III exercise: An evaluation of air quality models' capacity to reproduce the carbonaceous aerosol, Atmospheric Environ. X, 2, 100018, https://doi.org/10.1016/j.aeaoa.2019.100018, 2019.

Monahan, E. C., Spiel, D. E., and Davidson, K. L.: A Model of Marine Aerosol Generation Via Whitecaps and Wave Disruption, in: Oceanic Whitecaps: And Their Role in Air-Sea Exchange Processes, edited by: Monahan, E. C. and Niocaill, G. M., Springer Netherlands, Dordrecht, 167–174, https://doi.org/10.1007/978-94-009-4668-2_16, 1986.

Mozurkewich, M.: The dissociation constant of ammonium nitrate and its dependence on temperature, relative humidity and particle size, Atmospheric Environ. Part Gen. Top., 27, 261–270, https://doi.org/10.1016/0960-1686(93)90356-4, 1993.

Mues, A., Kuenen, J., Hendriks, C., Manders, A., Segers, A., Scholz, Y., Hueglin, C., Builtjes, P., and Schaap, M.: Sensitivity of air pollution simulations with LOTOS-EUROS to the temporal distribution of anthropogenic emissions, Atmospheric Chem. Phys., 14, 939–955, https://doi.org/10.5194/acp-14-939-2014, 2014.

Murphy, B. N., Donahue, N. M., Robinson, A. L., and Pandis, S. N.: A naming convention for atmospheric organic aerosol, Atmospheric Chem. Phys., 14, 5825–5839, https://doi.org/10.5194/acp-14-5825-2014, 2014.

Nemitz, E., Sutton, M. A., Schjoerring, J. K., Husted, S., and Paul Wyers, G.: Resistance modelling of ammonia exchange over oilseed rape, Agric. For. Meteorol., 105, 405–425, https://doi.org/10.1016/S0168-1923(00)00206-9, 2000.

Nenes, A., Pandis, S. N., and Pilinis, C.: Continued development and testing of a new thermodynamic aerosol module for urban and regional air quality models, Atmos. Environ., 33, 1553–1560, https://doi.org/10.1016/S1352-2310(98)00352-5, 1999.

Nenes, A., Pandis, S. N., Weber, R. J., and Russell, A.: Aerosol pH and liquid water content determine when particulate matter is sensitive to ammonia and nitrate availability, Atmospheric Chem. Phys., 20, 3249–3258, https://doi.org/10.5194/acp-20-3249-2020, 2020.

Nguyen, T. B., Crounse, J. D., Teng, A. P., Clair, J. M. S., Paulot, F., Wolfe, G. M., and Wennberg, P. O.: Rapid deposition of oxidized biogenic compounds to a temperate forest, Proc. Natl. Acad. Sci., 112, E392–E401, https://doi.org/10.1073/pnas.1418702112, 2015.

Novak, J. H. and Pierce, T. E.: Natural emissions of oxidant precursors, Water. Air. Soil Pollut., 67, 57–77, https://doi.org/10.1007/BF00480814, 1993.

Oberschelp, C., Pfister, S., and Hellweg, S.: Globally Regionalized Monthly Life Cycle Impact Assessment of Particulate Matter, Environ. Sci. Technol., 54, 16028–16038, https://doi.org/10.1021/acs.est.0c05691, 2020.

Pandis, S. N. and Seinfeld, J. H.: Mathematical modeling of acid deposition due to radiation fog, J. Geophys. Res. Atmospheres, 94, 12911–12923, https://doi.org/10.1029/JD094iD10p12911, 1989.

Pay, M. T., Jiménez-Guerrero, P., and Baldasano, J. M.: Assessing sensitivity regimes of secondary inorganic aerosol formation in Europe with the CALIOPE-EU modeling system, Atmos. Environ., 51, 146–164, https://doi.org/10.1016/j.atmosenv.2012.01.027, 2012.

Pedregosa, F., Varoquaux, G., Gramfort, A., Michel, V., Thirion, B., Grisel, O., Blondel, M., Prettenhofer, P., Weiss, R., Dubourg, V., Vanderplas, J., Passos, A., Cournapeau, D., Brucher, M., Perrot, M., Duchesnay, E., and Louppe, G.: Scikit-learn: Machine Learning in Python, J. Mach. Learn. Res., 12, 2012.

Prank, M., Sofiev, M., Tsyro, S., Hendriks, C., Semeena, V., Vazhappilly Francis, X., Butler, T., Denier van der Gon, H., Friedrich, R., Hendricks, J., Kong, X., Lawrence, M., Righi, M., Samaras, Z., Sausen, R., Kukkonen, J., and Sokhi, R.: Evaluation of the performance of four chemical transport models in predicting the aerosol chemical composition in Europe in 2005, Atmospheric Chem. Phys., 16, 6041–6070, https://doi.org/10.5194/acp-16-6041-2016, 2016.

Putaud, J.-P., Van Dingenen, R., Alastuey, A., Bauer, H., Birmili, W., Cyrys, J., Flentje, H., Fuzzi, S., Gehrig, R., Hansson, H. C., Harrison, R. M., Herrmann, H., Hitzenberger, R., Hüglin, C., Jones, A. M., Kasper-Giebl, A., Kiss, G., Kousa, A., Kuhlbusch, T. A. J., Löschau, G., Maenhaut, W., Molnar, A., Moreno, T., Pekkanen, J., Perrino, C., Pitz, M., Puxbaum, H., Querol, X., Rodriguez, S., Salma, I., Schwarz, J., Smolik, J., Schneider, J., Spindler, G., ten Brink, H., Tursic, J., Viana, M., Wiedensohler, A., and Raes, F.: A European aerosol phenomenology – 3: Physical and chemical characteristics of particulate matter from 60 rural, urban, and kerbside sites across Europe, Atmos. Environ., 44, 1308–1320, https://doi.org/10.1016/j.atmosenv.2009.12.011, 2010.

Pye, H. O. T., Nenes, A., Alexander, B., Ault, A. P., Barth, M. C., Clegg, S. L., Collett Jr., J. L., Fahey, K. M., Hennigan, C. J., Herrmann, H., Kanakidou, M., Kelly, J. T., Ku, I.-T., McNeill, V. F., Riemer, N., Schaefer, T., Shi, G., Tilgner, A., Walker, J. T., Wang, T., Weber, R., Xing, J., Zaveri, R. A., and Zuend, A.: The acidity of atmospheric particles and clouds, Atmospheric Chem. Phys., 20, 4809–4888, https://doi.org/10.5194/acp-20-4809-2020, 2020.

Redington, A. L., Derwent, R. G., Witham, C. S., and Manning, A. J.: Sensitivity of modelled sulphate and nitrate aerosol to cloud, pH and ammonia emissions, Atmos. Environ., 43, 3227–3234, https://doi.org/10.1016/j.atmosenv.2009.03.041, 2009.

Renner, E. and Wolke, R.: Modelling the formation and atmospheric transport of secondary inorganic aerosols with special attention to regions with high ammonia emissions, Atmos. Environ., 44, 1904–1912, https://doi.org/10.1016/j.atmosenv.2010.02.018, 2010.

Ridley, D. A., Heald, C. L., Ridley, K. J., and Kroll, J. H.: Causes and consequences of decreasing atmospheric organic aerosol in the United States, Proc. Natl. Acad. Sci., 115, 290–295, https://doi.org/10.1073/pnas.1700387115, 2018.

Robinson, A. L., Donahue, N. M., Shrivastava, M. K., Weitkamp, E. A., Sage, A. M., Grieshop, A. P., Lane, T. E., Pierce, J. R., and Pandis, S. N.: Rethinking Organic Aerosols: Semivolatile Emissions and Photochemical Aging, Science, 315, 1259–1262, https://doi.org/10.1126/science.1133061, 2007.

Rodríguez, S., Querol, X., Alastuey, A., and Plana, F.: Sources and processes affecting levels and composition of atmospheric aerosol in the western Mediterranean, J. Geophys. Res. Atmospheres, 107, AAC-12, 2002.

Safieddine, S. A., Heald, C. L., and Henderson, B. H.: The global nonmethane reactive organic carbon budget: A modeling perspective, Geophys. Res. Lett., 44, 3897–3906, https://doi.org/10.1002/2017GL072602, 2017.

Sarwar, G., Fahey, K., Kwok, R., Gilliam, R. C., Roselle, S. J., Mathur, R., Xue, J., Yu, J., and Carter, W. P. L.: Potential impacts of two SO2 oxidation pathways on regional sulfate concentrations: Aqueous-phase oxidation by NO2 and gas-phase oxidation by Stabilized Criegee Intermediates, Atmos. Environ., 68, 186–197, https://doi.org/10.1016/j.atmosenv.2012.11.036, 2013.

Sarwar, G., Simon, H., Fahey, K., Mathur, R., Goliff, W. S., and Stockwell, W. R.: Impact of sulfur dioxide oxidation by Stabilized Criegee Intermediate on sulfate, Atmos. Environ., 85, 204–214, https://doi.org/10.1016/j.atmosenv.2013.12.013, 2014.

Schaap, M.: On the importance of aerosol nitrate over Europe: data analysis and modelling, Universiteit Utrecht, Utrecht, the Netherlands, ISBN 90-393-3572-9, 160 pp., 2003.

Schaap, M., Müller, K., and ten Brink, H. M.: Constructing the European aerosol nitrate concentration field from quality analysed data, Atmos. Environ., 36, 1323–1335, https://doi.org/10.1016/S1352-2310(01)00556-8, 2002.

Schaap, M., van Loon, M., ten Brink, H. M., Dentener, F. J., and Builtjes, P. J. H.: Secondary inorganic aerosol simulations for Europe with special attention to nitrate, Atmospheric Chem. Phys., 4, 857–874, https://doi.org/10.5194/acp-4-857-2004, 2004.

Schaap, M., Manders, A., Hendriks, E., Cnossen, J., Segers, A. J., Gon, H., Jozwicka, M., Sauter, F., Velders, G. J. M., Matthijsen, J., and Builtjes, P. J. H.: Regional modelling of particulate matter for the Netherlands, 2009.

Schaap, M., Kranenburg, R., Curier, L., Jozwicka, M., Dammers, E., and Timmermans, R.: Assessing the sensitivity of the OMI-NO2 product to emission changes across europe, Remote Sens., 5, 4187–4208, https://doi.org/10.3390/rs5094187, 2013.

Schaap, M., Otjes, R., Weijers, E.: llustrating the benefit of using hourly monitoring data on secondary inorganic aerosol and its precursors for model evaluation", Copernicus GmbH, 2010

Seinfeld, J. H. and Pandis, S. N.: Atmospheric chemistry and physics: From air pollution to climate change, John Wiley & Sons, Hoboken, NJ, 2006.

Shah, V., Jaeglé, L., Thornton, J. A., Lopez-Hilfiker, F. D., Lee, B. H., Schroder, J. C., Campuzano-Jost, P., Jimenez, J. L., Guo, H., Sullivan, A. P., Weber, R. J., Green, J. R., Fiddler, M. N., Bililign, S., Campos, T. L., Stell, M., Weinheimer, A. J., Montzka, D. D., and Brown, S. S.: Chemical feedbacks weaken the wintertime response of particulate sulfate and nitrate to emissions reductions over the eastern United States, Proc. Natl. Acad. Sci., 115, 8110–8115, https://doi.org/10.1073/pnas.1803295115, 2018.

Shrivastava, M. K., Lane, T. E., Donahue, N. M., Pandis, S. N., and Robinson, A. L.: Effects of gas particle partitioning and aging of primary emissions on urban and regional organic aerosol concentrations, J. Geophys. Res. Atmospheres, 113, https://doi.org/10.1029/2007JD009735, 2008.

Simpson, D., Benedictow, A., Berge, H., Bergström, R., Emberson, L. D., Fagerli, H., Flechard, C. R., Hayman, G. D., Gauss, M., Jonson, J. E., Jenkin, M. E., Nyíri, A., Richter, C., Semeena, V. S., Tsyro, S., Tuovinen, J.-P., Valdebenito, Á., and Wind, P.: The EMEP MSC-W chemical transport model – technical description, Atmospheric Chem. Phys., 12, 7825–7865, https://doi.org/10.5194/acp-12-7825-2012, 2012.

Skyllakou, K., Fountoukis, C., Charalampidis, P., and Pandis, S. N.: Volatility-resolved source apportionment of primary and secondary organic aerosol over Europe, Atmos. Environ., 167, 1–10, https://doi.org/10.1016/j.atmosenv.2017.08.005, 2017.

Song, S., Gao, M., Xu, W., Sun, Y., Worsnop, D. R., Jayne, J. T., Zhang, Y., Zhu, L., Li, M., Zhou, Z., Cheng, C., Lv, Y., Wang, Y., Peng, W., Xu, X., Lin, N., Wang, Y., Wang, S., Munger, J. W., Jacob, D. J., and McElroy, M. B.: Possible heterogeneous chemistry of hydroxymethanesulfonate (HMS) in northern China winter haze, Atmospheric Chem. Phys., 19, 1357–1371, https://doi.org/10.5194/acp-19-1357-2019, 2019.

Stein, U. and Alpert, P.: Factor Separation in Numerical Simulations, J. Atmospheric Sci., 50, 2107–2115, https://doi.org/10.1175/1520-0469(1993)050<2107:FSINS>2.0.CO;2, 1993.

Steinbrecher, R., Smiatek, G., Köble, R., Seufert, G., Theloke, J., Hauff, K., Ciccioli, P., Vautard, R., and Curci, G.: Intra- and inter-annual variability of VOC emissions from natural and semi-natural vegetation in Europe and neighbouring countries, Atmos. Environ., 43, 1380–1391, https://doi.org/10.1016/j.atmosenv.2008.09.072, 2009.

Stern, R.: Entwicklung und Anwendung des chemischen Transportmodells REM/CALGRID, Umweltbundesamt, 2009.

Sturm, O.: Advecting Superspecies: Reduced order modeling of organic aerosols in LOTOS-EUROS using machine learning, 2021.

Tarrasón, L. and Iversen, T.: Modelling intercontinental transport of atmospheric sulphur in the northern hemisphere, Tellus B Chem. Phys. Meteorol., 50, 331–352, https://doi.org/10.3402/tellusb.v50i4.16132, 1998.

Tarrasón, L., Benedictow, A., Fagerli, H., and Jonson, J.E.; Klein, H.; van Loon, M.; Simpson, D.; Tsyro, S.; Vestreng, V.; Wind, P.; Forster, C.; Stohl, A.; Amann, M.; Cofala, J.; Langner, J.; Andersson, C.; Bergström, R.: Transboundary acidification, eutrophication and ground level ozone in Europe in 2003. EMEP status report 2005., 2005.

Thunis, P. and Clappier, A.: Indicators to support the dynamic evaluation of air quality models, Atmos. Environ., 98, 402–409, https://doi.org/10.1016/j.atmosenv.2014.09.016, 2014.

Thunis, P., Cuvelier, C., Roberts, P., White, L., Post, L., Tarrasón, L., Tsyro, S., Stern, R., Kerschbaumer, A., Rouïl, L., Bessagnet, B., Bergström, R., Schaap, M., Boersen, G. A. C., and Builtjes, P. J. H.: EURODELTA – II : evaluation of a sectoral approach to integrated assessment modelling including the Mediterranean Sea, Publications Office, LU, 2008.

Thunis, P., Clappier, A., Beekmann, M., Putaud, J. P., Cuvelier, C., Madrazo, J., and de Meij, A.: Non-linear response of PM2.5 to changes in NO_x and NH_3 emissions in the Po basin (Italy): consequences for air quality plans, Atmospheric Chem. Phys. Discuss., 1–26, https://doi.org/10.5194/acp-2021-65, 2021.

Timmermans, R., van Pinxteren, D., Kranenburg, R., Hendriks, C., Fomba, K. W., Herrmann, H., and Schaap, M.: Evaluation of modelled LOTOS-EUROS with observational based PM10 source attribution, Atmospheric Environ. X, 14, 100173, https://doi.org/10.1016/j.aeaoa.2022.100173, 2022.

Tingey, D. T., Manning, M., Grothaus, L. C., and Burns, W. F.: Influence of Light and Temperature on Monoterpene Emission Rates from Slash Pine, Plant Physiol., 65, 797–801, https://doi.org/10.1104/pp.65.5.797, 1980.

Van Zanten, M. C., Wichink Kruit, R. J., van Jaarsveld, H. A., and van Pul, W. A. J.: Description of the DEPAC module : Dry deposition modelling with DEPAC_GCN2010, Rijksinstituut voor Volksgezondheid en Milieu RIVM, 2010.

Van Zelm, R., Huijbregts, M. A. J., den Hollander, H. A., van Jaarsveld, H. A., Sauter, F. J., Struijs, J., van Wijnen, H. J., and van de Meent, D.: European characterization factors for human health damage of PM10 and ozone in life cycle impact assessment, Atmos. Environ., 42, 441–453, https://doi.org/10.1016/j.atmosenv.2007.09.072, 2008.

Van Zelm, R., Preiss, P., van Goethem, T., Van Dingenen, R., and Huijbregts, M.: Regionalized life cycle impact assessment of air pollution on the global scale: Damage to human health and vegetation, Atmos. Environ., 134, 129–137, https://doi.org/10.1016/j.atmosenv.2016.03.044, 2016.

Vignati, E., de Leeuw, G., Schulz, M., and Plate, E.: Characterization of aerosols at a coastal site near Vindeby (Denmark), J. Geophys. Res. Oceans, 104, 3277–3287, https://doi.org/10.1029/1998JC900019, 1999.

Walcek, C. J.: Minor flux adjustment near mixing ratio extremes for simplified yet highly accurate monotonic calculation of tracer advection, J. Geophys. Res. Atmospheres, 105, 9335–9348, https://doi.org/10.1029/1999JD901142, 2000.

Wang, G., Zhang, R., Gomez, M. E., Yang, L., Levy Zamora, M., Hu, M., Lin, Y., Peng, J., Guo, S., Meng, J., Li, J., Cheng, C., Hu, T., Ren, Y., Wang, Y., Gao, J., Cao, J., An, Z., Zhou, W., Li, G., Wang, J., Tian, P., Marrero-Ortiz, W., Secrest, J., Du, Z., Zheng, J., Shang, D., Zeng, L., Shao, M., Wang, W., Huang, Y., Wang, Y., Zhu, Y., Li, Y., Hu, J., Pan, B., Cai, L., Cheng, Y., Ji, Y., Zhang, F., Rosenfeld, D., Liss, P. S., Duce, R. A., Kolb, C. E., and Molina, M. J.: Persistent sulfate formation from London Fog to Chinese haze, Proc. Natl. Acad. Sci., 113, 13630–13635, https://doi.org/10.1073/pnas.1616540113, 2016.

Wang, W., Liu, M., Wang, T., Song, Y., Zhou, L., Cao, J., Hu, J., Tang, G., Chen, Z., Li, Z., Xu, Z., Peng, C., Lian, C., Chen, Y., Pan, Y., Zhang, Y., Sun, Y., Li, W., Zhu, T., Tian, H., and Ge, M.: Sulfate formation is dominated by manganese-catalyzed oxidation of SO2 on aerosol surfaces during haze events, Nat. Commun., 12, 1993, https://doi.org/10.1038/s41467-021-22091-6, 2021.

WHO: WHO global air quality guidelines: particulate matter (PM2.5 and PM10), ozone, nitrogen dioxide, sulfur dioxide and carbon monoxide, Geneva, 2021.

Wichink Kruit, R. J., Schaap, M., Sauter, F. J., van der Swaluw, E., and Weijers, E.: Improving the understanding of the secondary inorganic aerosol distribution over the Netherlands., Tech. rep. Utrecht, The Netherlands: TNO, report TNO-060-UT-2012-00334., 2012a.

Wichink Kruit, R. J., Schaap, M., Sauter, F. J., van Zanten, M. C., and van Pul, W. a. J.: Modeling the distribution of ammonia across Europe including bi-directional surface–atmosphere exchange, Biogeosciences, 9, 5261–5277, https://doi.org/10.5194/bg-9-5261-2012, 2012b.

Wold, S., Sjöström, M., and Eriksson, L.: PLS-regression: a basic tool of chemometrics, Chemom. Intell. Lab. Syst., 58, 109–130, https://doi.org/10.1016/S0169-7439(01)00155-1, 2001.

Wolke, R., Schröder, W., Schrödner, R., and Renner, E.: Influence of grid resolution and meteorological forcing on simulated European air quality: A sensitivity study with the modeling system COSMO–MUSCAT, Atmos. Environ., 53, 110–130, https://doi.org/10.1016/j.atmosenv.2012.02.085, 2012.

van Zelm, R., Preiss, P., van Goethem, T., Van Dingenen, R., and Huijbregts, M.: Regionalized life cycle impact assessment of air pollution on the global scale: Damage to human health and vegetation, Atmos. Environ., 134, 129–137, https://doi.org/10.1016/j.atmosenv.2016.03.044, 2016.

Zhang, L. and Garcia-Munoz, S.: A comparison of different methods to estimate prediction uncertainty using Partial Least Squares (PLS): A practitioner's perspective, Chemom. Intell. Lab. Syst., 97, 152–158, https://doi.org/10.1016/j.chemolab.2009.03.007, 2009.

Zhang, L., Gong, S., Padro, J., and Barrie, L.: A size-segregated particle dry deposition scheme for an atmospheric aerosol module, Atmos. Environ., 35, 549–560, https://doi.org/10.1016/S1352-2310(00)00326-5, 2001.

Zheng, B., Zhang, Q., Zhang, Y., He, K. B., Wang, K., Zheng, G. J., Duan, F. K., Ma, Y. L., and Kimoto, T.: Heterogeneous chemistry: a mechanism missing in current models to explain secondary inorganic aerosol formation during the January 2013 haze episode in North China, Atmospheric Chem. Phys., 15, 2031–2049, https://doi.org/10.5194/acp-15-2031-2015, 2015.

A   Appendix A: SIA Intake factor plots for sectorwide reduction scenarios

A.1 Reductions in Residential combustion
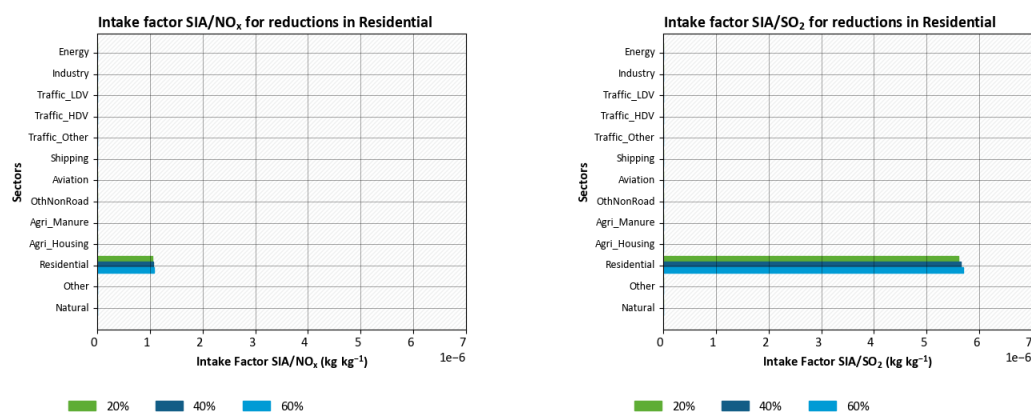
A.2 Reductions in Traffic
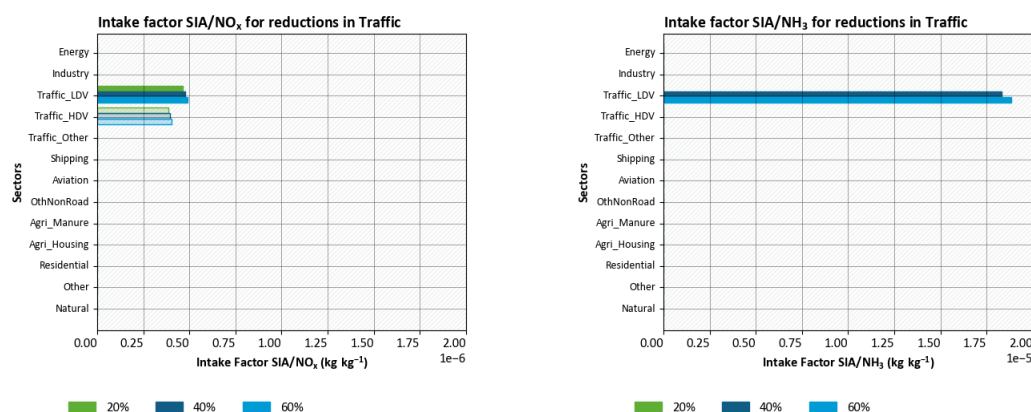
A.3 Reductions in Agriculture

B   Appendix B: File format of data for SIA Toolkit

B.1 Mean concentration and total emissions data files

Format & creation

The output of LOTOS-EUROS consists of a number of different files, among which there are daily files of hourly data on emissions that is labelled per sector (*LE_xxx_emis-label-col_xxx_xxx.nc*) and daily files of hourly concentrations on surface level, labelled per sector (*LE_xxx_labelled-conc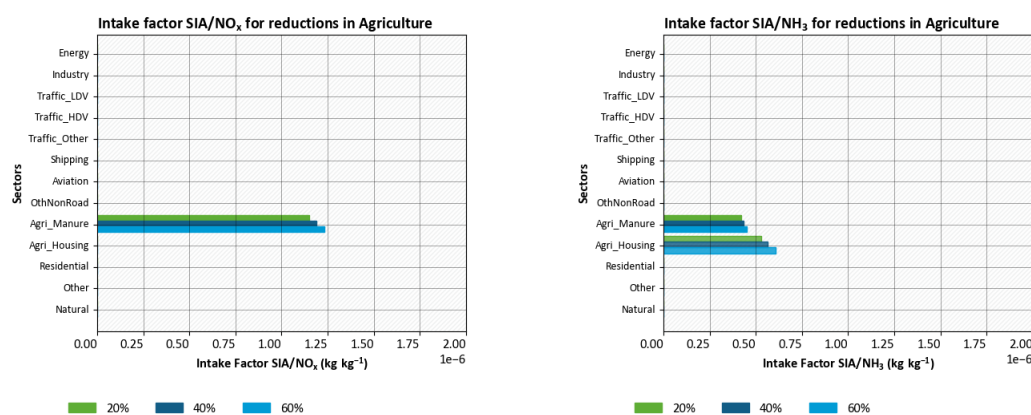-sfc_xxx_xxx.nc*). These are averaged by the NetCDF record averaged *ncra*. This results in files with the following format (example for emission files, shortened for conciseness):

Figure 85:   **Example of an annual averaged emission file.**

```
netcdf LE_NWE-sector-deu-ctrl_emis-label-col_20150101_20151231

{   dimensions:
      longitude = 110 ;
      latitude = 140 ;
      nv = 2 ;
      longitude_crnr = 111 ;
      latitude_crnr = 141 ;
      level = 1 ;
      time = UNLIMITED ; // (1 currently)
      label = 18 ;
      labelname_len = 13 ;
   variables:
      float longitude(longitude) ;
         longitude:standard_name = "longitude" ;
         longitude:units = "degrees_east" ;
         longitude:_CoordinateAxisType = "Lon" ;
         longitude:bounds = "longitude_bnds" ;
      float latitude(latitude) ;
         latitude:standard_name = "latitude" ;
         latitude:units = "degrees_north" ;
         latitude:_CoordinateAxisType = "Lat" ;
         latitude:bounds = "latitude_bnds" ;
      float longitude_bnds(longitude, nv) ;
         longitude_bnds:long_name = "longitude bounds" ;
         longitude_bnds:units = "degrees_east" ;
      float latitude_bnds(latitude, nv) ;
         latitude_bnds:long_name = "latitude bounds" ;
         latitude_bnds:units = "degrees_north" ;
      float longitude_crnr(longitude_crnr) ;
         longitude_crnr:long_name = "longitude corners" ;
         longitude_crnr:units = "degrees_east" ;
      float latitude_crnr(latitude_crnr) ;
         latitude_crnr:long_name = "latitude corners" ;
         latitude_crnr:units = "degrees_north" ;
      int level(level) ;
         level:long_name = "layer" ;
         level:_CoordinateAxisType = "Height" ;
```

```
    double time(time) ;
       time:standard_name = "time" ;
       time:long_name = "time" ;
       time:units = "seconds since 2015-01-01 00:00:00 UTC" ;
       time:calendar = "standard" ;
       time:_CoordinateAxisType = "Time" ;
       time:cell_methods = "time: mean" ;
    char labelnames(label, labelname_len) ;
       labelnames:standard_name = "Names of the label defnitions" ;
    float no(time, label, level, latitude, longitude) ;
       no:standard_name = "emission_of_nitrogen_monoxide_in_air" ;
       no:long_name = "emission_of_nitrogen_monoxide_in_air" ;
       no:units = "kg m-2 s-1" ;
       no:molemass = 0.0300061f ;
       no:molemass_unit = "kg mole-1" ;
       no:cell_methods = "time: mean" ;

    ...
    // global attributes:
       :author = "xxx" ;
       :institution = "xxx" ;
       :version = "v2.2.001" ;
       :model = "LE" ;
       :expid = "NWE-sector-deu-ctrl" ;
       :Conventions = "CF-1.6" ;
       :history = "Wed Aug  4 11:15:15 2021: /usr/bin/ncra ... " ;
       :NCO = "netCDF Operators version 4.7.5 (Homepage = http://nco.sf.net, Code =
  http://github.com/nco/nco)" ;
       :nco_openmp_thread_number = 1 ;
    }
```

The file should at least have dimensions *label*, *latitude*, and *longitude*, and coordinates with the same name. The *latitude* and *longitude* coordinates hold the coordinates of the center of each grid cell. Preferably, *latitude_crnr* and *longitude_crnr* are also present as dimension, as they simplify the calculation of cell area necessary for area integrals. If they are not given, latitude and longitude will be used to calculate the cell boundaries and area.

Each species (see highlighted section for NO) needs to have the dimensions *label*, *latitude*, and *longitude*. In addition, there may be others, as in the shown example, such as *time* and *level*, but these are not used in the calculations of total emissions or mean concentrations over Germany, nor for calculation of formation or intake factors, since they are both of length 1 (due to time averaging).

In addition, each species should contain units and a standard name in its attributes. Emissions should have the unit 'kg m-2 s-1' and concentrations 'kg m-3'. The attributes *molemass* and *molemass unit* are used for calculating summed variables that need to be expressed in terms of a reference species. For instance, NO_x is composed of NO and NO_2. Adding these together would result in the absolute mass (concentration) of NO_x, but it could also be expressed (as usual) in terms of mass of NO_2 equivalents. These are the only attributes used, the rest is ignored.

Finally, a list of names of the sector labels should be present as variable *labelnames* with dimension *label*.

Usage

This type of file is used to prepare the PLS model for the SIA Formation visualization tool (see below). It is also the type of file that is expected by the script *calculate_FF_IF_run.py*, which calculates intake, formation factors and intake factors. The SIA Formation toolkit documentation provides a guide on how to use this script.

B.2 Input data for PLS model

Format & creation

The above described annual averaged emission and concentration files are first processed according to the scheme:

- Summed species are added

    o NO_x emissions as the sum of NO and NO_2 emissions, expressed in NO_2 equivalents

    o SO_{4a} concentrations as the sum of fine and coarse SO_4 aerosol concentrations

    o NO_{3a} concentrations as the sum of fine and coarse NO_3 aerosol concentrations

    o SIA concentrations as the sum of NO_{3a}, SO_{4a} and fine NH_{4a} concentrations

- An area mask is applied to mask all grid cells outside Germany

- Total emissions are calculated for the emission data by integrating over the German domain, mean concentrations are calculated by averaging over the Germain domain, and the total intake is calculated by integrating concentration times breating rate times population density over the German domain.

- The file format of emissions and concentrations is transformed and added together. The result is a file with a variable *emissions* with dimensions *emission_species* and *labelname* and variables *concentrations* and *intake* with dimensions *output_species* and *labelname*.

Figure 86:   Example of data file as input for the PLS model.

netcdf Emission_concentration_deu-all-red20-C_20180101_20181231

```
{ dimensions:
        emission_species = 4 ;
        output_species = 4 ;
        labelname = 18 ;
variables:
        string emission_species(emission_species) ;
        string output_species(output_species) ;
        string labelname(labelname) ;
        double emissions(emission_species, labelname) ;
                emissions:_FillValue = NaN ;
                emissions:standard_name = "area_weighted_sum_of_emissions" ;
                emissions:long_name = "Area weighted sum of emissions" ;
                emissions:units = "kton" ;
        double concentrations(output_species, labelname) ;
                concentrations:_FillValue = NaN ;
                concentrations:standard_name = "area_averaged_mean_concentration" ;
                concentrations:long_name = "Area averaged mean concentration" ;
```

```
                concentrations:units = "ug m-3" ;
        double intake(output_species, labelname) ;
                intake:_FillValue = NaN ;
                intake:standard_name = "total_annual_intake_of_population" ;
                intake:long_name = "Total annual intake of population" ;
                intake:units = "kg yr-1" ;
 }
```

Emissions are expressed in 'kton', concentrations in 'µg m-3' and intake in 'kg yr-1'.

Usage

The emissions, concentrations and intake data are processed as presented above and combined into one big NetCDF file that forms the calibration set of the PLS model. The user does not need to perform the processing, since the SIA toolkit already contains a PLS model with preprocessed calibration data (file *master_input_pls.nc*).